Université de Montréal

Neural correlates of conscious and unconscious visual processing in neurotypical and cortical visually impaired populations assessed with fMRI

par

Michèle W. MacLean

Département de psychologie

Faculté des arts et des sciences

Thèse présentée en vue de l'obtention du grade de

Philosophiæ Doctor (Ph.D.)

en Psychologie

Orientation neuroscience cognitive

31 octobre 2023

Université de Montréal

Faculté des arts et des sciences

Cette thèse intitulée

Neural correlates of conscious and unconscious visual processing in neurotypical and cortical visually impaired populations assessed with fMRI

présentée par

Michèle W. MacLean

a été évaluée par un jury composé des personnes suivantes :

Prof Frédéric Gosselin
(président-rapporteur)

Prof Franco Lepore
(directeur de recherche)

Prof Ian Charest
(membre du jury)

Prof Christopher Pack
(examinateur externe)

Prof Rémy Allard
(représentant du doyen de la FESP)

Résumé

La perception visuelle implique une interaction complexe entre les yeux, le cerveau et les processus cognitifs, transformant les stimuli visuels en une représentation interne de l'environnement. Bien qu'une fraction limitée des informations parviennent à notre conscience visuelle, le cerveau traite une quantité considérable d'informations de manière inconsciente. Des recherches en imagerie par résonance magnétique fonctionnelle (IRMf) ont visé à mieux discerner les corrélats neuronaux associés à la perception consciente et inconsciente. Cependant, l'identification précise des régions cérébrales impliquées dans la génération d'une perception consciente, et leur modulation par l'expérience ou par des lésions cérébrales, demeure un défi. Cette thèse examine le traitement conscient et inconscient de l'information visuelle à l'aide de tâches visuelles et de neuroimagerie, pour comprendre comment ces processus se reflètent dans l'activation cérébrale et l'impact de lésions du cortex visuel.

L'**Article 1** vise à identifier de manière empirique les zones d'activation fonctionnelle associées au traitement visuel conscient et inconscient chez les individus neurotypiques, en menant deux méta-analyses quantitatives de données de neuroimagerie. Les résultats révèlent que le traitement conscient mobilise la jonction fronto-inférieure, le sillon intrapariétal, le cingulum antérieur dorsal, le gyrus angulaire, le cortex temporo-occipital et l'insula antérieure. Le traitement visuel inconscient sollicite davantage les régions postérieures, comme le complexe occipital latéral.

L'**Article 2** traite des processus cognitifs associés à la modulation de l'activation fonctionnelle suite à une lésion du cortex visuel. La déficience visuelle cérébrale (DVC) est caractérisée par une perte des fonctions visuelles due à un dommage cérébral plutôt qu'à une atteinte des yeux. Bien que la majorité des individus ne regagnent pas une vision normale, dans certains cas fascinants une amélioration peut être notée avec le temps en raison de la capacité du cerveau à se réorganiser. La perte visuelle peut s'accompagner du *blindsight*, où les individus sont capables de traiter de l'information visuelle tout en niant l'avoir vue. Cet article novateur utilise un paradigme de détection de mouvement pour évaluer l'activation

des structures corticales et sous-corticales lors d'une performance de blindsight chez un individu avec DVC. Cette contribution significative met en évidence des corrélats neuronaux indépendants des aires visuelles primaires, associés à des structures spécifiques pendant la détection de mouvement en blindsight.

Le **Chapitre 4** présente une base de données d'IRM haute résolution pour la perception du mouvement visuel d'individus neurotypiques et atteints de DVC. Les données incluent des mesures d'IRM structurelles, fonctionnelles, et de diffusion, des évaluations comportementales et de suivi du regard, des mesures électrophysiologiques, en plus de données prétraitées, le code et des métriques de contrôle de la qualité.

L'**Article 3** caractérise les conséquences neurologiques des lésions cérébrales chez les participants DVC, ainsi que l'impact sur leur capacité à traiter divers stimuli de mouvement, comparés à un groupe de contrôles neurotypiques, en utilisant des techniques comportementales et d'IRM fonctionnelle à haute résolution. La détection automatisée des lésions a permis de quantifier de manière fiable l'étendue des dommages cérébraux et les participants ont été catégorisés selon leur capacités visuelles résiduelles. Les résultats confirment que le cerveau peut traiter des informations visuelles malgré l'absence de zones visuelles primaires intactes. Les participants DVC ont présenté des altérations fonctionnelles étendues, contrairement aux participants neurotypiques, qui ont montré une activation focalisée dans des régions spécialisées pour le traitement visuel et de mouvement. L'hémisphère lésé présente une activation plus synergique dans l'aire temporale médiane et le complexe occipital latéral. Dans l'hémisphère intact, ce dernier peut répondre à une stimulation du champ visuel atteint. Le thalamus et le pulvinar ipsilésionnels ont montré une dominance ipsilatérale en réponse au mouvement, contrairement à la dominance controlatérale dans l'hémisphère intact et chez les participants DVC avec des capacités visuelles résiduelles comparables à celles des contrôles.

Cette thèse, par une approche multimodale, étudie les mécanismes neuronaux du traitement visuel chez les individus neurotypiques et atteints de DVC. L'utilisation d'étapes empiriques séquentielles, notamment une étude de cas, des analyses de groupes et des méta-analyses, renforce la fiabilité et l'applicabilité de la recherche, et vise à cartographier l'adaptation cérébrale après une lésion du cortex visuel.

Mots clés : vision, perception visuelle, conscience visuelle, perception visuelle inconsciente, déficience visuelle corticale, neuroplasticité, IRM fonctionnelle

Abstract

Visual perception involves the intricate interplay of the eyes, brain, and cognitive processes, enabling photons of visible light to be captured on the retina, processed through specific pathways in the brain and transformed into a rich internal representation of our surroundings. While only a fraction of information reaches conscious awareness, the brain can process the remaining unconsciously. Functional magnetic resonance imaging studies have sought to understand the neural signals associated with conscious versus unconscious perception. However, comprehensively understanding the core brain regions involved in generating a conscious perception and their modulation through experience or brain damage remains a challenge. In this thesis, we investigate the conscious and unconscious processing of visual information through a series of visual tasks. We aim to understand how these processes are reflected in brain activation and how they can be modulated by damage to the visual cortex.

Article 1 aimed to empirically identify and characterize areas of reliable convergence in functional activation of regions engaged during either conscious or unconscious visual processing in neurotypical participants by conducting two distinct quantitative meta-analyses. The findings reveal that conscious visual processing readily engages a constellation of regions comprising the inferior frontal junction, intraparietal sulcus, dorsal anterior cingulate, angular gyrus, temporo-occipital cortex and anterior insula, whereas unconscious processing recruits posterior regions, mainly the lateral occipital complex.

The aim of **Article 2** was to provide a detailed understanding of cognitive constructs and functional alterations following visual cortex damage. Cerebral visual impairment (CVI) refers to a loss of visual function caused by damage to the brain rather than the eyes. While most individuals do not recover intact vision, some cases have demonstrated improvement over time due to the brain's ability to reorganize itself. In certain instances of visual loss, blindsight can occur, allowing individuals to process visual information without conscious awareness. To our knowledge, this article was the first to propose the use of an event-related

motion detection paradigm to assess functional activation in cortical and subcortical structures, independant of primary visual areas, during a CVI individual's blindsight performance.

Chapter 4 aimed to conceptualize and acquire a unique high-resolution MRI dataset for studying visual motion perception in neurotypical and CVI individuals. This comprehensive dataset encompasses multiple modalities, including structural, functional task-based, resting-state and diffusion MRI, behavioral and evaluations, electrophysiological measures, and eyetracking data, in addition to preprocessed data, code and quality control metrics.

Article 3 aimed to understand the functional consequences of brain damage in CVI individuals and the resulting impact on their ability to process diverse visual motion stimuli, including looming and biological motion, compared to a group of neurotypical controls, using behavioral and high-resolution neuroimaging techniques. Automatic lesion mapping enabled to reliably quantify the extent of brain damage and participants were categorized based on their residual visual ability. The findings demonstrate that the brain can process and represent visual information, without intact primary visual areas. CVI participants exhibited broad functional alterations, contrasting the focused activation in visual and motion processing regions for neurotypical controls. Specifically, the lesioned hemisphere displayed synergistic activation in the middle temporal area and lateral occipital complex, while the intact hemisphere's lateral occipital complex responded to impaired visual field stimulation. The ipsilesional thalamus and pulvinar demonstrated an ipsilateral dominance in response to looming motion, in contrast to the contralateral dominance in the intact hemisphere and among CVI participants with residual visual abilities akin to neurotypical controls.

By employing a multi-modal approach integrating behavioral assessments, structural and functional neuroimaging methods, this thesis comprehensively investigates the neural mechanisms underlying visual processing in both neurotypical individuals and those with CVI. The use of sequential steps in empirical science, namely a case study, group analyses, and meta-analyses, enhances the reliability and applicability of the research, and effectively contributes to help map brain adaptation post visual cortex injury and further inform neurotypical visual information processing.

Keywords: vision, visual perception, visual conscious awareness, unconscious visual perception, cortical visual impairment, neuroplasticity, functional MRI

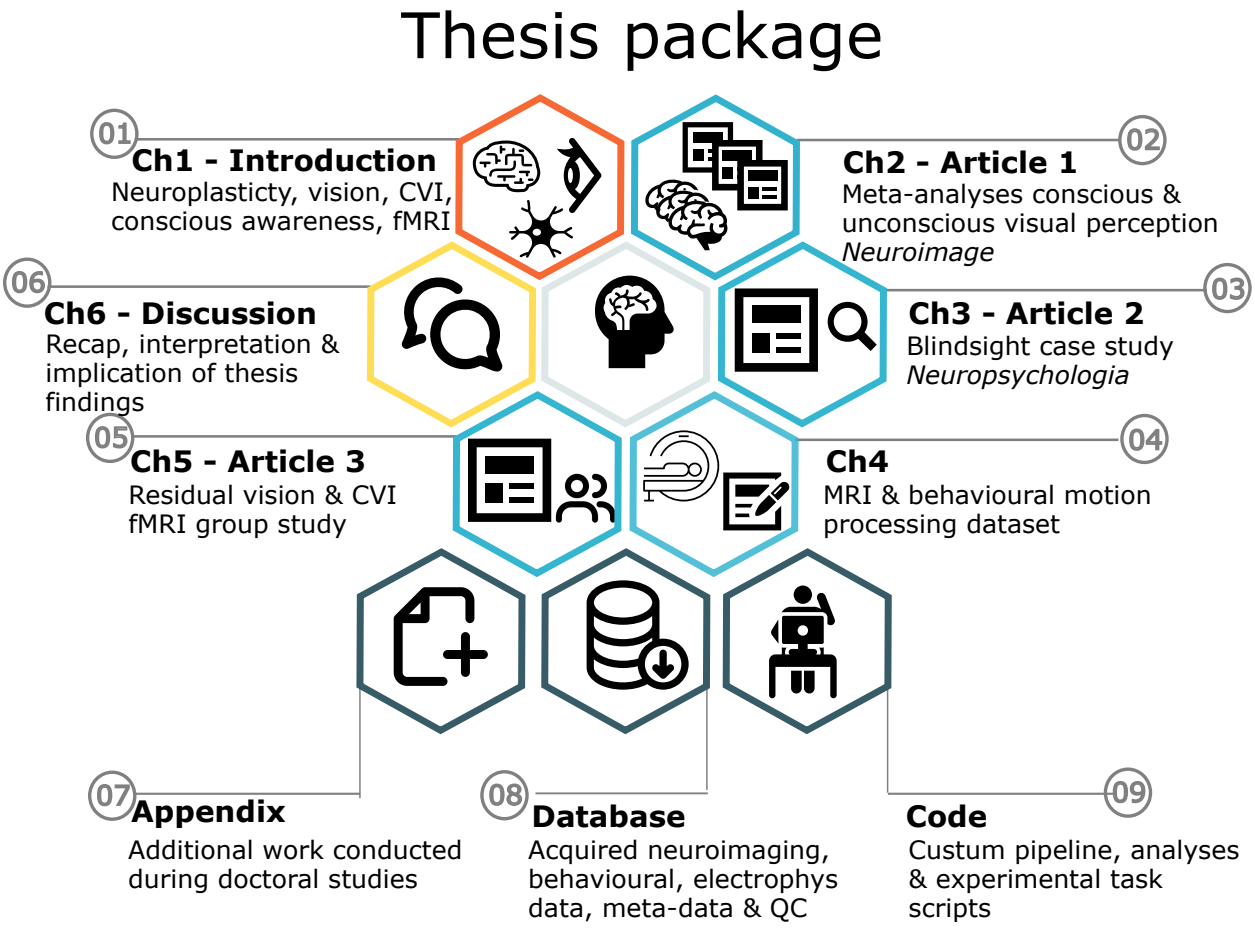

Figure 1 – Visual summary of thesis structure

Contents

List of Tables

List of Figures

List of acronyms

ALE	Activation Likelihood Estimation
ANOVA	Analysis of Variance
BIDS	Brain Imaging Data Structure
BOLD	Blood-Oxygen-Level-Dependent
CVI	Cortical Visual Impairment
DMN	Default Mode Network
DTI	Diffusion Tensor Imagings
DVC	*Déficience Visuelle Corticale*
EEG	Electroencephalography

FC	Functional Connectivity
fMRI	functional Magnetic Resonance Imaging
GLM	General Linear Model
GWT	Global Workspace Theory
HOT	Higher Order Thought Theory
HRF	Haemodynamic Response Function
IIT	Integrated Information Theory
MEG	Magnetoencephalography
MRI	Magnetic Resonance Imaging
RP	Recurrent Processing Theory
ROI	Region of Interest

rsfMRI	resting-state functional Magnetic Resonance Imaging
SD	Standard Deviation
SE	Standard Error
SPM	Statistical Parametric Mapping

List of abbreviations

e.g.	For example
et al.	and colleagues
i.e.	That is

Remerciements

Cette thèse de doctorat a été possible grâce à l'apport et au soutien de nombreuses personnes. Je souhaite adresser en premier lieu mes remerciements à mon directeur de thèse, Franco Lepore. Je suis reconnaissante de l'opportunité que tu m'as offerte de réaliser des études graduées dans ce domaine que j'aime et pour la confiance que tu m'as accordée pour mener à terme ce projet. Merci d'avoir facilité l'accès à plusieurs collaborations, conférences, congrès et formations.

Je remercie également Olivier Collignon de m'avoir accueillie au sein de son équipe à l'UCLouvain en Belgique. Merci à mon ami et collègue Rémi Gau pour les heures innombrables de mentorat, pour ton expertise tant théorique que technique, tes conseils et tes réponses à mes mille questions. Merci pour ton encouragement et ton dévouement à l'avancement de notre projet de recherche.

Merci à tous les collaborateurs et co-auteurs des projets de recherche. Je tiens à exprimer un remerciement particulier à Nathan Spreng pour son soutien envers mon travail, sa capacité à discerner le potentiel d'un projet, sa relecture attentive et ses commentaires pertinents qui ont grandement enrichi la qualité de notre travail.

Un grand merci au *club des membres actifs* du laboratoire, Catherine & Emma. Cette solidarité et entraide que nous avons créée m'ont apporté beaucoup de soutien tout près de la fin. Merci, Catherine, partenaire de bureau, grâce à ta présence et à nos échanges tant sur le plan scientifique que personnel, mes dernières années ont été bien plus agréables. Un merci à tous les membres du laboratoire que j'ai côtoyé, notamment à Marie et Latifa pour leurs conseils lors de mes premières années. Merci à Frédéric Gosselin pour nous avoir ouvert les portes de tes locaux et pour ton inclusivité au sein de ton laboratoire, pour ta disponibilité et le temps consacré à nos échanges. Mes remerciements s'étendent à tous les membres du CPP Lab en Belgique. Merci en particulier à Jeanne avec qui j'ai partagé un bureau et une

passion commune pour la recherche en neuroscience, pour sa compagnie pendant mes séjours de recherche en Belgique. Un merci à toute l'équipe de l'UNF pour leur investissement et leur soutien lors des sessions de neuroimagerie.

Un remerciement spécial est réservé à Alejandra et Carola. Plus que des collègues estimées, vous êtes également devenues pour moi des amies précieuses. Carola, merci d'avoir rendu les premières années au CERNEC tellement plus agréables. Ta présence constante m'a aussi fait sentir que je n'étais jamais seule; merci pour tes conseils et ton écoute chaque fois que je passais par ton bureau et merci pour tous les beaux moments passés à l'extérieur. La détermination avec laquelle tu as obtenu ton PhD a été une grande source d'inspiration pour moi. Alejandra, je suis reconnaissante pour nos nombreuses discussions et échanges d'idées sur la recherche, la vie doctorale et tant d'autres sujets. Traverser les étapes du doctorat en parallèle avec toi - du début des cours jusqu'à la soumission - a nettement enrichi l'expérience. Merci pour la relecture de l'introduction de cette thèse, ta capacité à examiner à la fois les détails minutieux et l'ensemble plus large a permis de préciser ma vision et de renforcer la qualité de ce travail. Je suis profondément reconnaissante pour le temps et l'énergie que tu as investis.

Merci à tous les participants de mes projets de recherche. Un merci particulier s'adresse aux participants ayant subi une blessure au cerveau, pour avoir accepté de prendre part à plusieurs expériences et pour votre patience durant les longues journées d'expérimentation. Cette thèse n'aurait pas été possible sans votre engagement, et je vous en suis reconnaissante. Vos histoires partagées et votre apparente résilience ont renforcé mon désir de poursuivre en recherche.

Merci à ceux qui ont contribué au financement de mon parcours doctoral, notamment la Faculté des Études Supérieures et Postdoctorales (FESP) de l'Université de Montréal, RBIQ, RRSV, Desjardins, FRQS, Mitacs, INLB et mon directeur de thèse Franco. Merci également aux Fonds de Recherche du Québec – Nature et Technologies (FRQNT) pour le soutien financier durant cette thèse.

Merci à ma famille qui me soutient depuis toujours et pour l'encouragement que vous m'avez apporté. Je suis redevable à mes très chers parents, Nadine et Steve, je ne serais

pas arrivé où je suis sans vous. Merci à mon frère, Jean-Philippe, avec qui je partage cette ambition pour l'innovation en recherche. Te voir réussir avec force et dévouement, en plus de tes nombreuses recommendations durant mon parcours, m'a aidé à comprendre que j'en étais également capable. Merci à ma soeur Catherine pour ta joie et ton humanité, tes conseils tant professionnels que personnels, et ton amitié.

Marco, merci pour ton soutien tout au long de ce parcours, pour ta patience, ta stabilité, et ta compréhension des réalités de la conduite d'un projet doctoral. Tu es le premier avec qui j'ai partagé l'idée de réaliser un PhD et, grâce à toi, j'ai eu le courage d'entreprendre cette aventure et de la mener à son terme. Merci pour tes mille relectures, tes conseils, et nos échanges scientifiques. Ton ingéniosité, tes encouragements quotidiens, et ton sens de l'humour ont largement contribué à la réussite de ce projet. Merci à Milo qui nous apporte toujours de la joie et qui nous rappelle souvent qu'il faut sortir dehors pour décrocher. Je suis reconnaissante pour les expériences passées et au plaisir de commencer de nouvelles aventures bientôt.

Enfin, j'ai une pensée toute particulière pour ma grand-mère, Cécile Parent, qui nous a quitté durant cette thèse. Celle qui aurait souhaité de tout son coeur aller à l'université, pour qui la vie ne l'aurait pas permis, tu peux être très fière de bientôt compter la première femme docteure parmi les membres de la famille.

À ma famille.

"Science, for me, gives a partial explanation for life. In so far as it goes, it is based on fact, experience, and experiment."

Rosalind Franklin

"I am among those who think that science has great beauty."

Marie Sklodowska Curie

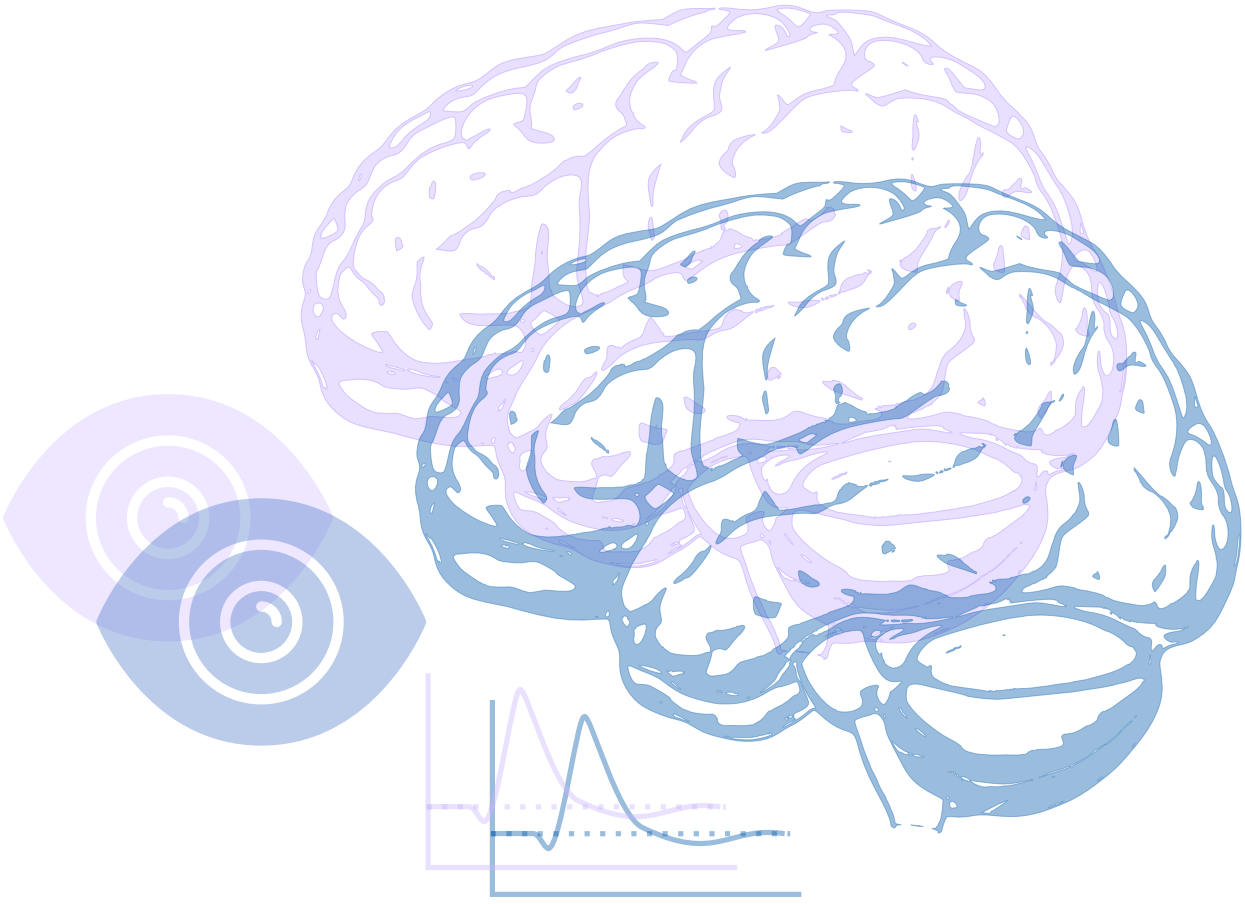

Chapter 1

Introduction

1.1. Rationale

The cognitive processes enabling vision begin with visual information arriving at the retina and traveling through the brain to the visual cortex and beyond, ultimately to construct a conscious visual representation. Multiple factors can modulate our visual perception and impact our sensory visual experience. Cerebral Visual Impairment (CVI) is characterized by a loss of visual function associated with damage to the brain, rather than the eyes. When the brain sustains damage, it undergoes reorganization in response to the new condition, resulting in structural and functional changes. Considering the significance of the visual modality, understanding how the brain processes visual information following an injury and how this information is represented and integrated within the brain becomes critically important.

Although the majority of individuals do not fully regain lost visual function, in some cases, improvement can be noted over time due to the neuroplastic properties of the brain (C. Perez & Chokron, 2014). Hence, residual vision may persist despite a clinical diagnosis of blindness. For example, individuals have been shown to correctly detect, discriminate or point to objects in their blind visual field, with objects in motion arguably providing the most compelling evidence. Understanding at the neurological level why the cerebral reorganization is sometimes beneficial would allow to optimize tools (e.g., neurostimulation) to guide these adaptive changes and recover visual function.

Neuroimaging is a relevant tool to uncover how visual processing is remodeled or reinforced following CVI. Functional magnetic resonance imaging (fMRI) studies can integrate

anatomy, function, and behavioural evidence, along with finely tuned analysis techniques. Previous studies including our work (Celeghin et al., 2018; Tran et al., 2019), demonstrate the intrinsic property of the nervous system to adapt following occipital cortex lesions and propose alternative neuronal pathways enabling residual vision. Brain lesions can help reveal the role of specific regions by assessing how cognitive processes are subsequently modulated. CVI, in particular, can be a valuable model to assess how perception is modulated in the absence of primary occipital brain regions and to what extent the conscious processing of visual information is impacted. The fascination further lies in understanding: what underlying neural mechanisms enable visual processing of information without a state of full conscious visual awareness? However, there is currently limited research linking the extent of brain damage of CVI, with the resulting functional neural substrate, behavioural variables and visual motion processing abilities and comparing to neurotypical controls. In the context of this thesis, "neurotypical" refers to individuals whose information processing, perception, and behavior align with the norm, with their brain-behavior relationships falling within the expected parameters of the general population. This term is applied to characterize individuals without CVI or other neurodevelopmental or neurological conditions. Using an approach that integrates recent advances in neuroimaging, behavioural and analysis techniques, applied both to the CVI model and neurotypical controls, provides an exciting opportunity to help reveal what might be necessary to sustain a conscious visual perception- a long-standing goal of experimental science.

This thesis presents work conducted during my doctoral studies to further our understanding of the neural correlates of both conscious and unconscious visual perception using functional neuroimaging methods, neurotypical groups and clinical populations with CVI. An introductory theoretical background is presented first, as described in more detail in the Chapter overview. The main body of the thesis comprises three empirical studies, in addition to a chapter presenting a new comprehensive MRI and behavioural dataset. In Chapter 2, Article 1 first presents two distinct empirical quantitative meta-analyses to establish a foundation for identifying reliable neural correlates of conscious visual awareness and unconscious visual perception in neurotypical participants across all available functional

neuroimaging studies, published in *NeuroImage* in 2023. In Chapter 3, Article 2 presents a second study to assess conscious and non-conscious visual perception in the context of CVI via behavioural and functional imaging methods. This study, published in *Neuropsychologia*, presents a detailed assessment of the neural plastic functional alterations and residual visual abilities following a unilateral lesion in the primary visual cortex resulting in contralateral blindness in a participant with homonymous hemianopia and blindsight. In Chapter 4, we introduce a new large-scale database, conceptualized and constructed in a standardized format during my doctoral studies, to further tackle these questions. The documentation of the database's structure and specifications as a chapter in this thesis serves multiple purposes: it is an integral part of the doctoral research effort, directly aligns with the thesis's research objectives, enhances scientific transparency and reproducibility, encourages further data exploration and analysis, promotes data sharing and collaboration within the neuroimaging community, and ensures ongoing ethical compliance. In Chapter 5, Article 3 examines the range of modulation in visual processing across various CVI participants following an occipital cortex injury via behavioural paradigms and functional magnetic resonance imaging techniques, accounting for the extent and size of brain damage, with a comparative analysis alongside a group of neurotypical matched controls. Examining multiple subjects advances our understanding of how occipital cortex lesions modulate visual processing pathways, and provides a more nuanced representation of the neural characteristics potentially facilitating spared visual functions, even in the absence of an intact primary visual cortex. Chapter 6 provides a general discussion of the thesis findings, encompassing their interpretation, theoretical and methodological implications, an examination of strengths and limitations, potential future research avenues, and concluding remarks. Finally, additional selected work which were conducted during my doctoral studies and complement this thesis are listed in the appendix. In addition to the studies previously presented, this encompasses my involvement as a co-author in a published systematic review investigating the effects of auditory deprivation on white and gray matter in both auditory and non-auditory regions, highlighting the investigation of various sensory modalities during my studies. Also, this includes contributions to the development of the openly available **bidspm** statistical analyses app.

See Fig.1 presented after the thesis abstract, for the corresponding visual summary of the thesis package.

1.2. Chapter Overview

For the remaining of this thesis chapter, the theoretical background that supports the thesis rationale is provided, including a brief introduction to understanding the principles underlying neuroplasticity in Sec 1.3, followed by an overview of visual processing in Sec 1.4, and the unique case of cortical visual impairment (CVI) in Sec 1.5, with a further focus on conscious and unconscious visual perception in Sec 1.6, and considerations for using neuroimaging for this thesis in Sec 1.7. Finally, the specific thesis objectives and hypotheses are presented in Sec 1.8.

1.3. Understanding the principles underlying neuroplasticity

1.3.1. The role of experience in shaping neuroplasticity

Plasticity, first referring to the potential for modifications in human behaviour as introduced by William James in 1890, was further linked to an anatomical basis in the brain a little over a decade later by Santiago Ramon y Cajal (Pascual-Leone et al., 2005). The brain can modify its structural and functional organization in response to normal development through experiences and learning as well as environmental and physiological changes or following damage. Neuroplasticity, or cerebral reorganization, ranges from cellular or molecular to anatomical and functional changes, potentially involved in resulting simple behavior modifications to modulating our ability to perceive and sense the environment around us.

The brain continuously refines regions responsible for processing sensory afferents during development through learning and adaptation to the surrounding environment or damage to specific regions. Plasticity plays a role across various aspects of human cognition and after central or peripheral lesions (Buonomano & Merzenich, 1998) caused by, for example, strokes

or traumatic brain injuries. Following these injuries, when an initial short-term modulation is sustained, a longer-term modulation of the structure of intracortical and subcortical networks can take place (Pascual-Leone et al., 2005). Within the same population, the degrees of morphological, functional and connectivity changes vary depending on the extent and location of the lesion. From a cellular stand point, studies observed changes in neuronal excitability as well as the synaptic connections between axons and dendrites in order to re-map sensory functions after stroke (Clarkson et al., 2010; Cramer, 2008; Li et al., 2010). These changes in neural circuitry expand across the different structures and compositions of the brain and an impressive number of connections become possible. More specifically, spared pathways can be reinforced or new pathways can be established through dendritic growth or arborization. These new or different neural networks can be recruited to strengthen connections or compensate for the functional loss to be able to carry out a specific task e.g., involving movement or vision (Bridge et al., 2008; Grefkes et al., 2008; Heuninckx et al., 2008; Lotze et al., 2006). This can lead to new or modified functions enabling the individual to cope with new behavioral challenges (de Gelder et al., 2008). Plasticity is a complex process where the effects of a loss of function are likely not localized to one specific area. Thus, multiple brain regions are likely involved contributing and interacting across various neural levels to successfully promote a behavioral goal. For instance, our systematic review, comprising 27 studies and 626 individuals with hearing loss, demonstrates how auditory deprivation can significantly alter white and grey matter in both auditory and non auditory areas via plasticity, such as the superior temporal gyri, inferior fronto-occipital fasciculus, and superior longitudinal fasciculus (Simon et al., 2020).

1.3.2. Neuroplasticity and the visual system

The visual system has been extensively studied to reveal the essential nature and main principles of neuroplasticity. Compelling evidence emerges through the many documented cases of individuals with visual impairment who seem to undergo a series of plastic changes to compensate or adapt to visual damage (Pascual-Leone et al., 2005). On the one hand,

a change in visual input due to ocular impairment can potentially lead to an atypical development of the occipital cortex, known to process vision (Collignon et al., 2011; Hubel & Wiesel, 1970; Wiesel & Hubel, 1963, 1965). Pioneering work in the 1960s showed that early monocular deprivation had drastic consequences on the organization of the visual cortex, whereas deprivation later in life had virtually no effect (Hubel & Wiesel, 1970). Thus, the presence or absence of visual input at a critical developmental period strongly influences the development of the visual cortex (Hubel & Wiesel, 1970; Wiesel & Hubel, 1965). Studies further showed that the age of blindness onset, congenital versus acquired blindness, differentially shape the functional organization of the visual cortex, such that early onset can result to a transfer of functional specialization to a non-visual modality (Collignon et al., 2013). On the other hand, a lesion to a specific region in the occipital cortex can induce a loss of vision and also lead to changes in brain circuitry (Pascual-Leone et al., 2005). Cortical visual impairment (CVI) refers to this brain-based damage resulting in clinical blindness, though the eyes remain intact. In particular, a unilateral post-chiasmatic lesion affecting the primary visual areas and leading to a contraleteral visual loss is a condition referred to as homonymous hemianopia or quadranopia depending on the lesion's extent and resulting visual loss (for review see Goodwin, 2014). Such damage to the visual cortex can prompt a cascade of dynamical, structural and functional neural alterations both at the cortical and subcortical levels. Given the inherent variability among individuals with CVI, understanding specific contributing factors, such as the extent of structural damage and its relationship with neuroplastic functional changes, as well as the resulting residual vision, remains an ongoing challenge. However, gaining insights into these factors could have potential implications for developing strategies or guiding visual rehabilitation efforts to effectively leverage neuroplasticity by strengthening alternative pathways or pre-existing connections.

The second and third studies in this thesis delve into the neurophysiological adaptations occurring within the visual motion system among individuals with cortical visual impairment (CVI) through a combination of behavioral and magnetic resonance imaging techniques. The third study establishes a reliable and reproducible quantification of brain damage to assess its potential impact on the altered processing of visual motion information.

The following sections provide an overview of visual processing, beginning with the functional organization of the visual system in neurotypical individuals, followed by examining the brain's specialization for visual motion processing. Subsequently, the neurofunctional consequences of occipital cortex lesions on visual motion processing will be explored.

1.4. An overview of visual processing

1.4.1. Functional specialization of the visual system

The visual system, arguably one of the most studied systems in humans, processes complex information from the early striate visual cortex (V1) located in the occipital cortex, and then extends to higher-order visual regions to form a coherent perception. This neural architecture involves parallel pathways that converge and integrate in V1, forming multiple parallel output streams (Nassi & Callaway, 2009; S. M. Zeki, 1978a). The transfer of information to V1 begins from single photons of visible light condensed through specific pathways in the brain and transformed into an internal representation of our external visual surroundings. These photons initially reach the retina at the back of the eye where they are absorbed by an array of photoreceptors that then convert them into electrochemical signals, encoding them as function of position, time and wavelength (Nassi & Callaway, 2009). Various retinal cells process and condense this visual information, extracting basic cues such as temporal frequency, spatial contrast and luminance. Ganglion cells, forming the optic nerve, then encode these properties. The visual information is further sent through three main parallel pathways, i.e., the parvocellular, magnocellular and koniocellular pathways, to the lateral geniculate nucleus (LGN) in the thalamus. These pathways are associated with different perceptual processes, for example, the magnocellular pathway is is linked to motion and depth perception, while the parvocellular pathway processes form and colour and the koniocellular pathway is thought to process short wave-length information (Briggs & Usrey, 2011; Nassi & Callaway, 2009). The outputs from the magnocellular and parvocellular layers ultimately project to the primary visual areas (V1) in the brain (Hendrickson et al., 1978; Hubel & Wiesel, 1972; Nassi & Callaway, 2009; Palczewski, 2012; Rodieck, 1998; Weber

et al., 1983). See Fig.1 for visual processing from retinal ganglion cells, through pathways leading to the middle temporal area in accordance with Felleman and Van Essen, 1991, as presented in (Born & Bradley, 2005).

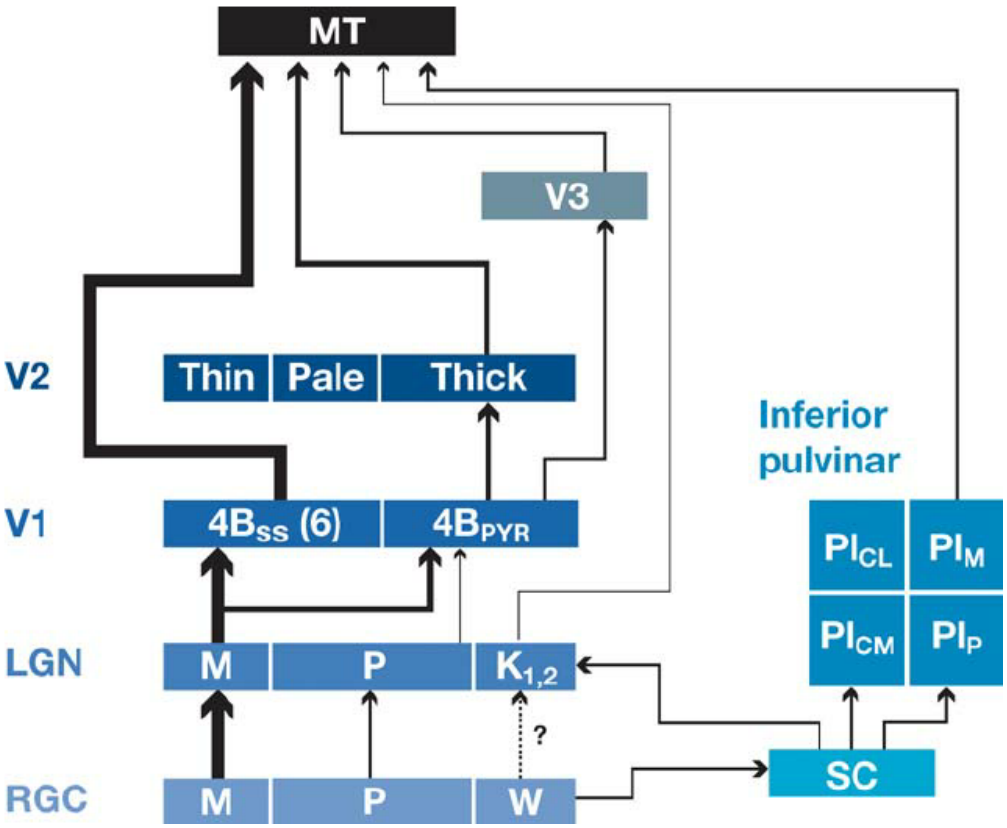

Figure 1 – Visual pathways to MT/V5 according to Felleman and Van Essen, 1991. Line thickness reflects the magnitude of connectivity between brain regions. The most robust connection is the direct cortical pathway from the primary visual area (V1) to the middle temporal area (MT). Weaker connections arrive from subcortical structures such as the Lateral Geniculate Nucleus (LGN), and the superior colliculus (SC) via the inferior pulvinar (PI). Abbreviations: RGC: retinal ganglion cells, M: magnocellular pathway; P: parvocellular pathway; K: koniocellular pathway; SC, superior colliculus; PI: inferior pulvinar (CL: central lateral nucleus, CM: central medial nucleus; M: medial nucleus, P: posterior nucleus); Neuronal types in layer 4B are identified as 4B SS (spiny stellate neurons) and 4B PYR (pyramidal neurons). Figure from (Born & Bradley, 2005).

The system is functionally specialized where different regions are more reliably engaged for specific perceptual and cognitive functions. As demonstrated by Hubel and Wiesel, 1959, neurons in the early visual cortex show a preference for stimuli orientation and location within the visual field. The extrastriate cortex regions also exhibit functional specialization for specific functions, with V4 in the visual cortex primarily involved in color processing (Baker et al., 1981; S. M. Zeki, 1973), and MT (also known as V5) in the middle temporal cortex specializing in motion processing (Dubner & Zeki, 1971; S. M. Zeki, 1974, 1978a). Though much of the original visual input is lost in processing, such as an image's specific spectral composition, the visual system is capable of discriminating highly precise visual information ranging from variations in shape, colour, size, texture, orientations, positions, hue, etc. (Nassi & Callaway, 2009).

Once integrated within the visual cortex, evidence points to a dual-pathway segregation for visual processing, commonly referred to as the what/where pathways, suggesting that visual information is dispatched via two main streams depending on the visual information presented and task demands (Mishkin et al., 1983; Ungerleider & Haxby, 1994). The ventral stream (or "what" pathway) starting from the early visual cortex and projecting to the inferior-temporal cortex is involved in object recognition or identification. The dorsal stream (or "where" pathway) starting from the early visual cortex and projecting to the posterior parietal cortex is involved in spatial localization, motion processing and visually guided actions (E. H. de Haan & Cowey, 2011; Goodale, 2008; Goodale & Milner, 1992; Mishkin et al., 1983). Despite different frames of reference, these pathways work together towards goal-oriented behaviours (Goodale, 2008). Further functional specialization occurs in brain regions dividing labour to process stimuli such as objects, scenes, faces, and motion (Aguirre et al., 1998; Kanwisher et al., 1997; Martin & Solomon, 2011; Schoenfeld et al., 2002). For example, scenes activate the parahippocampal place area (ventral stream) (Epstein & Kanwisher, 1998), faces activate the fusiform face area (ventral stream) (Kanwisher et al., 1997; McCarthy et al., 1997), human body images activate the extrastriate body area (ventral stream) (Downing et al., 2001), and motion activates the middle temporal area (dorsal stream)(S. Zeki et al., 1991).

During visual processing, visual information such as physical features is thought to flow from low-level processing regions to higher-order regions, known as bottom-up processing. Conversely, information flowing from higher-order regions back to lower-level regions is known as top-down processing. Cognitive functions driving top-down processing are notably the observer's attention, expectations, experiences and perceptual demands. These higher-order signals are transmitted via feedback pathways to help interpret the visual scene, with each feed-forward pathway having an equivalent feedback pathway (for review see Gilbert & Li, 2013). These concepts will be integrated throughout this thesis and discussed in the included studies.

The next section will further consider the functional specialization of the brain for visual motion processing and address why studying motion is relevant when investigating cortical visual impairment for this thesis.

1.4.2. The role of the middle temporal area in visual motion processing

Detecting motion in one's environment holds a strong evolutionary significance for survival. The perception of motion guides our actions, from swiftly avoiding oncoming objects to navigating a complex environment. This prompts the fundamental question: how is visual motion represented in the brain? Robust evidence from studies involving animal models, including non-human primates, has identified the extrastriate region as a motion-sensitive region. Electrophysiological research has convincingly demonstrated that area V5 in monkeys contains a high proportion of neurons selective for the direction of movement of a visual stimulus (J. M. Allman & Kaas, 1971; Dubner & Zeki, 1971; Maunsell & Van Essen, 1987; S. M. Zeki, 1978a), in addition to stimulus size, speed and contrast (J. Allman et al., 1985; Maunsell & Van Essen, 1983; Pack et al., 2005). The human homologue (hMT/V5) was identified later and is also known to mediate perception and analysis of visual motion (Born & Bradley, 2005; J. D. Watson et al., 1993; S. Zeki et al., 1991) as well as represent visual motion direction information (Kamitani & Tong, 2006; Tootell et al., 1995b). Lesion studies in both non-human primates and humans have further identified area MT as

a motion-sensitive region (Newsome & Pare, 1988; Zihl et al., 1983) as a damage to this region consequentially leads to impairments in visual motion processing. Furthermore, applying electrical microstimulation of MT neurons or using transcranial magnetic stimulation (TMS) over the MT area causally alters motion processing abilities (Beckers & Zeki, 1995; DeAngelis et al., 1998; Salzman et al., 1992; Zihl et al., 1983). Thus, MT is a functionally specialized region strongly engaged during processing of visual motion information. Once visual information is integrated in MT, it is further sent to the medial superior temporal cortex (MST) for specialized processing such as motion processing of optic flow (Duffy & Wurtz, 1991; Komatsu & Wurtz, 1988b). Therefore, the human MT complex (hMT+/V5) refers to MT as well as other motion selective regions in close proximity, such as MST.

The visual motion information arriving in extrastriate areas such as MT, is thought to mainly travel in the dorsal visual stream from the magnocellular pathway through V1 (Born & Bradley, 2005; Shipp & Zeki, 1989; Yabuta et al., 2001). Studies have also shown a direct connection from the koniocellular cells in LGN to MT for motion processing in the extrastriate cortex (Sincich et al., 2004), though this would represent a small portion of connections. Thus, the brain's motion-sensitive region, MT, receives the majority of its input from the primary visual cortex (V1) through cortico-cortical connections. See Fig.1 for visual input streams to MT. Therefore, if there is damage to V1, it can potentially affect the transmission of visual information that contains motion properties to the MT complex. This raises the question of whether the MT region receives sufficient visual motion information after a V1 lesion and, if so, what are the neural pathways bypassing V1.

Given that processing visual motion information typically triggers a robust functional response in the specialized motion area MT and can be detected through fMRI (Huk et al., 2002; Kolster et al., 2010; Tootell et al., 1995b), the second and third empirical studies in this thesis employed motion-based fMRI designs to explore this activation even in cases of occipital cortex lesions. Moreover, the third article specifically targets this region to assess to what degree the signal in MT may decrease or be modulated following the injury. The following section will explore the case of CVI caused by a V1 lesion and how it impacts the processing of visual motion.

1.5. Exploring the unique case of Cortical Visual Impairment

1.5.1. Epidemiology of Cortical Visual Impairment

The concept that an injury to the occipital lobe can result in cortical blindness has been well-established for over a century (Ajina & Bridge, 2017). However, the extent of cortical visual impairment (CVI) may vary depending on the size and precise location of the lesion. For instance, individuals with a unilateral post-chiasmatic lesion that affects the primary visual cortex in either hemisphere will acquire contralateral cortical blindness, resulting in loss of vision in half their visual field. This condition is known as homonymous hemianopia (see review by Barleben et al., 2015; Goodwin, 2014; Leh et al., 2008). A smaller lesion in the same area may cause quandrantopia, which affects only one fourth of the visual field, either the upper or lower, left or right contralateral quadrant.

CVI is strictly a cortical issue, meaning that the remaining portion of the visual field and the functionality of the eyes remain intact. Homonymous hemianopia represents the primary cause of cortical deficits resulting in visual field loss, affecting more than half a million Americans. The most common cause of this condition is a stroke, followed by a traumatic brain injury or a tumor (Goodwin, 2014). In a matter of seconds these individuals see their quality of life significantly decrease. They frequently report difficulties with reading and driving, in addition to a loss of independence and there is no efficient visual rehabilitation program currently available.

The specific area of a lesion can lead to diverse impairments in aspects of visual processing, reflecting the functions associated with the affected region. Beyond the primary visual area, higher regions in the visual system become more functionally specialized in processing specific visual content. For example, damage to the lateral occipital cortex or fusiform face area can result in difficulties processing objects (visual agnosia) or faces, respectively (Bridge et al., 2013; James et al., 2003; Wada & Yamamoto, 2001). However, these deficits are typically associated with rare cases of bilateral damage (Bridge, 2020). In this thesis, the focus is

on lesions in the primary visual cortex (V1), due to its role as the initial site for processing visual information, effectively acting as a gateway to the visual processing stream. Therefore, investigating the consequences of damage to this region can provide insights into the broader visual processing system and neural plastic alterations. Additionally, unilateral lesions in V1 are known to impact conscious visual perception and are associated with some forms of residual (unconscious) vision (for review see Bridge, 2020; Tong, 2003) (Bridge, 2020), as further introduced below.

1.5.2. Impact of lesions in the primary visual area on visual perception

In the neurotypical organization of the visual system, the early visual cortex and more specifically the primary visual area (V1) is known as the main input of the visual system. Moreover, V1 serves as a platform to integrate and project visual information as well as receive feedback from higher regions. It is plausible to think that a lesion in this region would fundamentally disrupt the brain's ability to process visual information, such as motion related visual information. As mentioned, a unilateral lesion to this area causes a contralateral visual loss. In spite of this clinical blindness, residual visual performances seem to correlate with atypical patterns of functional neural activation resulting from structural and functional neuroplasticity. An increasing amount of studies have proposed various alternative neuronal pathways to explain different residual abilities. Functional MRI studies have started to document the possible relation between residual visual performances and neuronal correlates (for meta-analysis see Celeghin et al., 2018). Blindsight studies have shown that behavioural responses to detecting or discriminating motion are possible without V1. See corresponding Fig. 2 of the introduction showing neurotypical vision in the first panel, followed by a primary visual cortex lesion resulting in contralateral visual loss, and functional modulation of visual pathways in the brain.

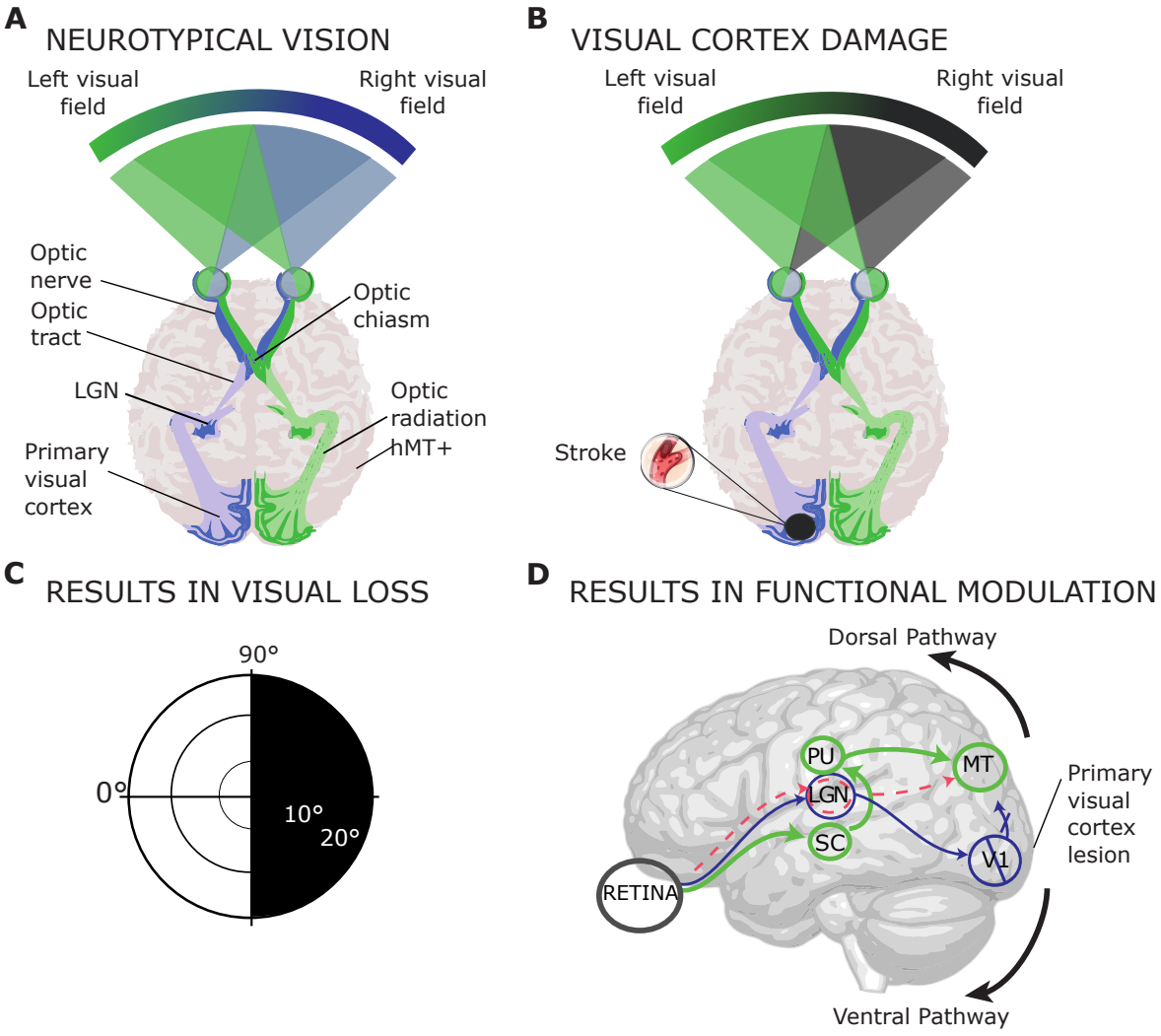

Figure 2 – Visual pathways for motion processing and consequences of a primary visual cortex lesion. (A) Neurotypical visual pathway: from the eyes visual information is transmitted through the optic nerve, optic tract, optic chiasm, LGN, and optic radiation to primary visual areas, with each hemisphere representing the contralateral visual field. (B) Homonymous hemianopia: Unilateral primary visual cortex lesion. The most common cause is stroke, in addition to tumors, hemorrhage or head trauma. (C) Results in contralateral visual loss, consisting of half the visual field. (D) Functional modulation post-lesion: Alternative pathways bypassing V1, involving subcortical structures (superior colliculi and pulvinar) or the LGN. V1: primary visual areas, LGN: lateral geniculate nucleus, hMT+ middle temporal complex, SC: superior colliculi, PU: pulvinar.

Research on animal models has provided a strong foundation for understanding the structural and functional impact of V1-lesions. Studies in non-human primates have shown that even after the removal or inactivation of the striate cortex, MT neuronal populations remain responsive and maintain stimulus selectivity, such as direction selectivity, despite reduced firing rates (Girard et al., 1992; Rodman et al., 1989; Rosa et al., 2000). Thus, sensitivity to motion in the blind field can still be present, though may be weaker compared to intact visual processing, and it appears insufficient to support conscious visual awareness (Goebel et al., 2001; Tong, 2003). Moreover, substantial evidence suggests the posteromedial lateral suprasylvian (PMLS) area, located in the parietal cortex of cats, plays a role in motion processing and may be homologous to the primate area V5/MT+ (Dreher et al., 1996; Payne, 1993; Spear & Baumann, 1975). Earlier observations have suggested that visual pathways passing through the superior colliculus can contribute to and sustain visual activity in macaque area V5 and cat area PMLS, in the absence of primary cortical areas, but their contributions to receptive field properties appear to be minimal in the presence of these cortical areas (Girard et al., 1992; Gross, 1991; Payne, 1993; Rodman et al., 1989; Spear & Baumann, 1979). Despite these significant contributions, blindsight animal models are relatively rare, with exceptions such as macaque monkeys (Yoshida et al., 2017; Yoshida et al., 2008), as studies often rely on the subjective report of participants' experiences with visual stimuli (Overgaard, 2012).

In individuals with CVI, objects in motion presented in their blind visual field have been shown to activate the extrastriate cortex, specifically the human MT complex (Barbur et al., 1993; Bridge et al., 2010). This implies an alternative non-striate pathway carries visual motion information to hMT+ even when V1 is damaged, when visual motion stimuli are presented. Alternative pathways that bypass V1 that notably include cortical and/or subcortical structures have been suggested to play a role in mediating residual vision, without conscious visual awareness. Although, the precise neurological construct and key factors facilitating this form of residual vision remain unknown.

Cortical and subcortical pathways involved in visual motion processing

With regards to cortical structures, studies have shown an intact connection between the

lateral geniculate nucleus (LGN) and MT+/V5 in the absence of V1 (Ajina et al., 2015a; Hervais-Adelman et al., 2015). Intact ipsilateral connections were specifically demonstrarted between LGN and hMT+ in the damaged hemisphere of hemianopic patient GY and a patient with bilateral striate cortex damage, both showing blindsight abilities (Bridge et al., 2010; Bridge et al., 2008). This is also in line with V1-lesion animal models where a pathway connecting LGN neurons to the extrastriate cortex was demonstrated in non-human primates (Yu et al., 2018) with implications of V5/MT+.

Multiple studies have suggested that midbrain structures, such as the superior colliculi and pulvinar, play a vital role in the subcortical pathway that mediate blindsight. Research conducted on hemianopic cats has demonstrated the significant implications of both these structures (Ciaramitaro et al., 1997; H. Jiang et al., 2015; Piche et al., 2015). The retina is thought to project to the superior colliculi, with less than 10% of ganglion cells directly projecting to this region (de Gelder et al., 2008; Leh et al., 2006; Morland et al., 1999; Perry & Cowey, 1984; Tamietto et al., 2010). Indirect projections from the superior colliculi to cortical extrastriate visual areas have been suggested in V1-lesion studies (de Gelder et al., 2008; Tamietto et al., 2010). Direct connections between the superior colliculi and the ventrolateral pulvinar have been observed in non-human primates with V1 lesions performing visually guided saccades (Kinoshita et al., 2019). Studies have also demonstrated a neural pathway from the superior colliculi to MT through pulvinar connections in macaque monkeys (Berman & Wurtz, 2010). The pulvinar is thought to receive visual input directly from the optic tract or via the superior colliculi, and then contribute to relaying visual information to area MT (Ajina & Bridge, 2017; Warner et al., 2010). Therefore, both the superior colliculi and pulvinar are thought to mediate residual vision.

The superior colliculi and pulvinar structures are known to be involved in other aspects of the visual system. The superior colliculi are sensitive to perceptual organization, stimulus configuration, type and specific features (Georgy et al., 2016; Leh et al., 2010; Wessinger et al., 1996). These structures have also been shown to be involved in a rapid route to project facial information bottom up to cortical structures in the monkey (Nguyen et al., 2016). In summary, alternative V1-independant visual pathways have been suggested to connect the

retina to MT and transfer visual motion information that notably include the LGN, superior colliculi and pulvinar regions. The cortical pathway from the retina to the LGN, on to V1 and transmitted to the MT is thought to convey conscious visual information, whereas the alternative subcortical pathway from the retina to the pulvinar and on to MT, bypassing V1, would convey unconscious visual information (Rowe et al., 2023).

Moreover, understanding altered neuronal mechanisms is inherently linked to uncovering the intricacies of the healthy visual system. While primary visual pathways are thought to be fundamental for visual processing, their absence following a V1 lesion may offer a unique opportunity to study alternative visual pathways more effectively. In particular, investigating these non-conscious visual shortcuts can help reveal essential features of brain structures and connections that may be less prominent in the neurotypical state but are likely integral to processing the initial visual input (Ajina & Bridge, 2017; Tamietto & Morrone, 2016). Based on the premise that MT activation is retained even in cases of V1 lesions, the second and third empirical studies of this thesis explore these pathways that might potentially facilitate processing of visual motion information in the absence of this core region of the visual system - without full conscious visual awareness. The role of specialized brain regions in these adaptations is explored along with the degree of reinforcement or remodeling that may support there involvement in residual vision, shedding light on the existence of parallel visual pathways that circumvent damaged primary visual areas, allowing a non-conscious processing of visual information.

1.5.3. Residual visual abilities

The phenomenon allowing one to process visual information while denying having seen it has often been referred to as "blindsight" (Weiskrantz, 1996). Individuals with blindsight or residual vision have been shown to correctly answer to the presentation of an event or object in their blind visual field with no conscious perception of having seen the objects (see reviews by Goodwin, 2014; C. Perez & Chokron, 2014; Urbanski et al., 2014). See corresponding Fig. 3 of the introduction for an illustration of an individual with visual cortex damage correctly processing motion in the blind visual field. This suggests a dissociation between conscious

visual awareness and how these individuals can accurately perform under numerous testing conditions (Berlucchi, 2017; Heeks & Azzopardi, 2015). Almost 50 years have passed since the term blindsight was first coined (Sanders et al., 1974; Weiskrantz et al., 1974) and there has since been an extensive amount of research highlighting the various blindsight abilities, specific characteristics and types. There exists a distinction for two main classifications for blindsight: Type 1, where the subject has no awareness or conscious perception, and Type 2 blindsight, where the subject has awareness of visual presentation in the blindfield without visual qualia (see review by Cowey, 2010; Weiskrantz, 1990, 1998).

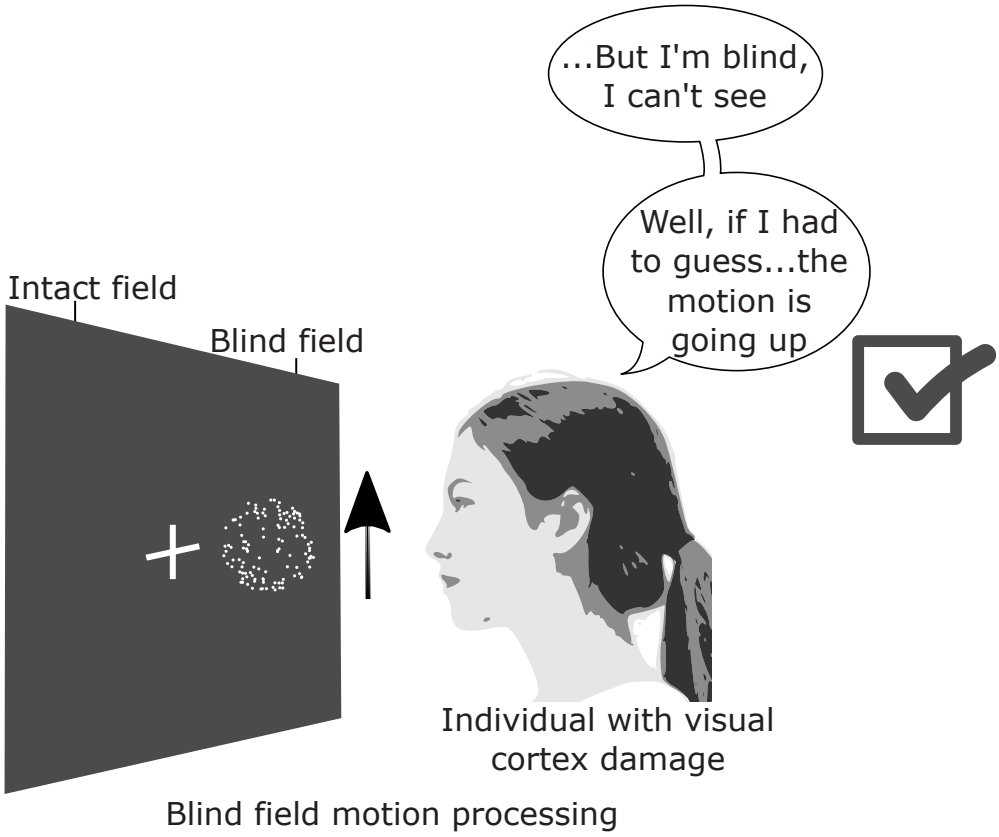

Figure 3 – Altered visual experience post-injury in the clinically blind field. Illustration showing a participant with visual cortex damage tasked with discriminating motion direction. Despite reporting not having consciously perceived the motion, the participant responds correctly, discerning motion direction within the blind field.

A taxonomy of blindsight sub-types has been proposed based on residual functions related to the individual's blind field (Danckert & Rossetti, 2005). These sub-types include action, attention and affective blindsight. Action-blindsight involes the ability to correctly act upon a stimulus in the blind field, demonstrated through visuo-motor abilities, such as saccades, grasping, pointing towards blind field targets and navigating obstacles (Danckert & Rossetti, 2005; de Gelder et al., 2008; Jackson, 1999; Smits et al., 2018; Zihl & Werth, 1984). Attention-blindsight relies on allocating sufficient attention to the blind field, such as detecting or discriminating motion or spatial orienting (Danckert & Rossetti, 2005; Danziger et al., 1997; Gaymard & Pierrot-Deseilligny, 1999; Grasso et al., 2018; Hervais-Adelman et al., 2015; A. Ptito et al., 1991; Walker et al., 2000). These subtypes may intersect, with certain action blindsight abilities relying on attentional processes (Danckert & Rossetti, 2005). Affective-blindsight involves accurate responses to emotionally salient visual stimuli (Celeghin et al., 2015; de Gelder et al., 1999), such as discriminating emotional content or facial emotional recognition (Gerbella et al., 2017; Pegna et al., 2005; Van den Stock et al., 2011). An individual with blindsight (patient TN), after experiencing a complete bilateral destruction of his primary visual cortices, was also able to demonstrate responses to eye contact and perform mental imagery tasks, indicating that V1 is not necessary for these abilities (Burra et al., 2013; de Gelder et al., 2015). The differences in structural damage, specific location or extent of the human V1 lesions may contribute to the different residual visual abilities.

Among the typically spared residual visual abilities, the detection and discrimination of motion were recognized as particularly robust from the early stages of research (Holmes, 1918; Riddoch, 1917; Weiskrantz, 1990), and will serve as the main stimuli in the second and third studies of this thesis. Moreover, the specific choice of motion content becomes crucial in determining their ability to process and represent it within the brain. For instance, research has demonstrated a preference for faster-moving targets, emphasizing their preserved sensitivity to high temporal frequencies (Barbur et al., 1993), aligning with our choice of looming stimuli in the third study.

Given current evidence indicating that V1 damage is associated with a loss of neurotypical conscious visual awareness and results in some forms of these residual visual (unconscious) abilities, further investigating the impact of V1 lesions can potentially provide insights into the neural underpinnings of conscious visual awareness and unconscious perception. Research on individuals with residual vision can help underline what is necessary for conscious visual perception and distinguish from different states of visual processing. The following section will specifically explore conscious visual awareness, unconscious perception, methods for empirical study, and current theories in the field of cognitive neuroscience.

1.6. Conscious and unconscious visual perception

1.6.1. Defining consciousness & standard experimental frameworks

Consciousness can be defined by two primary components: the content of consciousness, which involves awareness of self, the environment, or subjective experience, and the level of consciousness, which pertains to wakefulness (Baars, 1993; Laureys, 2005). In the context of this thesis, the focus is on the neural correlates that underlie varying degrees of awareness of external visual stimuli or environmental content in a state of full wakefulness. See Fig. 4 for a schematic representation of conscious awareness of visual content.

In the experimental context, the question arises: how can studies be designed to investigate the neural correlates of conscious awareness? Several paradigms have been designed to dissociate neural signals pertaining to conscious visual perception from those pertaining to unconscious or preconscious visual perception. The general idea is to observe the difference in the patterns of neural activity between a perceived stimulus and a non-consciously perceived stimulus while keeping the visual input and overall state of the participant as constant as possible. This allows for the observation of changes in phenomenal perception related to the content of consciousness (see review by C. Y. Kim & Blake, 2005).

Standard report-based paradigms for investigating content-specific conscious versus unconscious visual processing include: i) masking techniques, where a "mask" impairs the strength of a target stimulus (Breitmeyer & Ogmen, 2000; Francis, 2000); ii) near perceptual

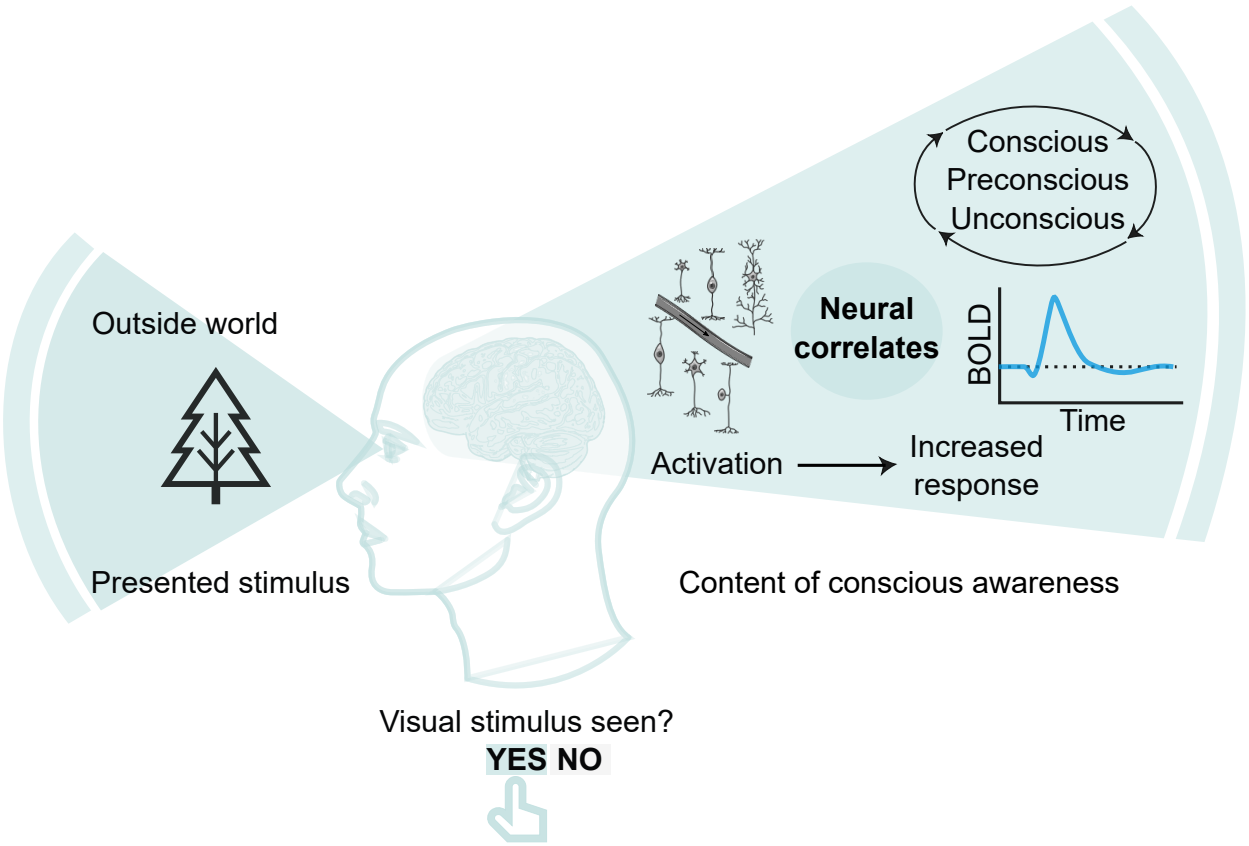

Figure 4 – Representation of conscious awareness of visual content: The brain processes and integrates stimuli from the external world, representing different states of visual awareness—conscious, preconscious, or unconscious. Increased neural activity is associated with higher oxygenation levels, detectable as the BOLD signal in MRI. This signal can be correlated with the observer's response (e.g., visual stimulus seen or no?) regarding the perception of visual stimuli. Original figure inspired by (Koch, 2004).

threshold stimuli (Baria et al., 2017; Podvalny et al., 2019); and iii) interocular or flash suppression, which induces perceptual suppression to render stimuli nonconscious (Tsuchiya & Koch, 2005). Paradigms contrasting conscious versus preconscious visual processing include: i) attentional blink, where attending to a target in a rapid stream of visual stimuli can lead to missing a second target (Kranczioch et al., 2005; Meijs et al., 2018); ii) change

detection, where participants miss detecting a change that occurs during a visual disruption (e.g., a flicker) (Beck et al., 2001); and iii) inattentional blindness, referring to the failure to detect stimuli presented at unattended locations (C. Y. Kim & Blake, 2005; Thakral, 2011). Other designs aim to induce a shift in visual awareness despite constant physical visual input (see review by C. Y. Kim & Blake, 2005). These paradigms typically contrast a first conscious percept versus a second competing percept induced by the same stimulus, which is not currently perceived consciously. Paradigms inducing these transitions between different conscious percepts include: i) bistable perception, which enables perceptual reversals between ambiguous figures such as the Necker cube test, face-vase test, or Mooney images (Flounders et al., 2019; Imamoglu et al., 2012; Kleinschmidt et al., 1998; M. G. Wang et al., 2013); ii) binocular rivalry, where conflicting stimuli are presented between both eyes (Blake & Logothetis, 2002; Lumer et al., 1998); and iii) pop-out paradigms inducing a single perceptual reversal between the two (Eriksson et al., 2007; Portas et al., 2000).

Neuroimaging studies have shown that consciousness is not confined to a particular brain region but instead involves interactions between various structures (Kouider, 2009). Given the vast amount of visual information processed by the brain, not every input can evoke a conscious percept to maintain efficiency (Ajina & Bridge, 2017). In fact, most visual processing is thought to occur without awareness, and non-conscious processing would precede conscious processing (see review by Kouider, 2009). Baars' model of object recognition, suggests that an individual seems to become aware of visual input only once the underlying cortical processes converge onto one interpretation, thus prior to this moment, processing would be unconscious (Baars, 1993). Within unconscious processing, preconscious processing refers to a transient state of activity where information is potentially accessible, yet not accessed (Dehaene et al., 2006). The lack of top-down attentional activity could render a stimulus preconscious as suggested by inattentional blindness and attentional blink paradigms (Hutchinson, 2019). In these paradigms, it is assumed that attention is monopolized by the first presented target, leading to the failure to perceive the second target (Kranczioch et al., 2005). To understand how information reaches conscious awareness or remains at a preconscious or unconscious level, further research is needed.

Lesion studies have demonstrated the important role of the primary visual cortex in conscious visual awareness and revealed that streams of visual processing can occur outside of conscious visual awareness (Kouider, 2009). For instance, as a V1 lesion can result in non-conscious processing of visual information in the blindfield, this implies that V1 might play a role along the visual hierarchy to elicit conscious visual perception. However, it is not yet clear whether the lack of conscious processing in the blind field implies that V1 is an essential structure for generating conscious perception or if it primarily contributes to transmitting visual information to other structures that subsequently select the visual representations for conscious processing. The latter scenario relates to the impact of a V1-lesion on neural responsiveness throughout the visual cortex given it holds a central role within the visual hierarchy as the principal source of extrastriate input and participates in recurrent loops with various visual areas (Azzopardi et al., 2003; Rodman et al., 1989; M. C. Schmid et al., 2009; M. C. Schmid et al., 2013). This could lead to alterations on whether or how visual information reaches perceptual awareness. There have been demonstrations, albeit limited in number, of awareness without V1, suggesting this region may not be the gatekeeper of awareness (Mazzi et al., 2019, for review see). Some studies also showed the induction of visual qualia through non-invasive stimulation (e.g., TMS), even in cases of V1 lesions, which would suggest it isn't essential for awareness (Mazzi et al., 2014; Silvanto et al., 2007). Nonetheless, in most circumstances, V1's involvement is thought to create conditions for awareness to arise (Silvanto, 2015).

1.6.2. Theories of consciousness in cognitive neuroscience

Various theoretical approaches in cognitive neuroscience and neurobiology aim to define consciousness by proposing different neuroarchitectural elements and processing stages. To gain a better understanding of the neural processes involved in conscious and unconscious visual processing, cognitive neuroscientific theories have offered various hypotheses, exploring how the brain renders visual percepts conscious, unconscious, or preconscious. These theories investigate the role of sensory areas in encoding stimulus content as a prerequisite (Levinson et al., 2021) and whether stimulus content is broadcast beyond these areas to

elicit a conscious percept (for a detailed comparison of theories, see Mashour et al., 2020). Prominent theories in the field include the global neuronal workspace theory, recurrent (or re-entry) and predictive processing theories, higher-order thought theory, and integrated information theory (for review see Seth & Bayne, 2022).

The global neuronal workspace theory is perhaps the most influential theoretical framework of consciousness and suggests that multiple cerebral networks process information in parallel, through long-distance connections and a closed loop system (Dehaene & Naccache, 2001). The information first travels bottom-up unconsciously to specialized brain areas, such as V5/MT, for processing specific visual features like motion. Then, through top-down attention, the signal is amplified and boosts the activity of the current active neurons which allow the specialized processes to become available to the global workspace. This enables access to the global workspace via a nonlinear network "ignition," which rapidly amplifies and sustains neuronal representations. Local processors are mobilized into the workspace by ignition. The content of consciousness is thought to be the global available information in the workspace, associated with several brain regions, with prefrontal and parietal cortices playing a crucial but not exclusive role in conscious access (Mashour et al., 2020). This framework is based on the three empirical properties of consciousness: 1) cognitive processing can occur without consciousness; 2) attention is necessary for information to reach consciousness and 3) specific cognitive tasks require consciousness, such as novel combinations of mental operations. In the case of blindsight, the inability of individuals to describe stimuli in their impaired visual field may be due to insufficient availability of the global workspace, resulting from modified attention and perception processes, a lack of long-distance connections in the brain, and altered interactions with the conscious network, leading to reduced or no visual qualia (Hadid & Lepore, 2017).

Recurrent or predictive processing theories emphasize the importance of top-down signalling. These theories propose that the content of consciousness depends on what recurrent neurocognitive circuits are activated, with a critical role for feedback from higher-order to lower-order areas, such as early sensory areas (V. A. Lamme, 2010, 2006a; V. A. F. Lamme, 2018). Predictive processing theories suggest that the brain generates predictions about

the causes of sensory signals, and prediction errors are minimized through continuous feedback loops. These processes can be seen as an approximation to Bayesian inference, where the brain updates its predictions based on incoming sensory information (de Lange et al., 2018; Melloni et al., 2011). Conscious experience would be shaped by the expectations and predictions generated by the brain. Higher-order thought theory posits that mental content becomes conscious when a lower-order representation of visual signals, generated by the primary sensory cortex, enters a higher-order meta-cognitive representation, mainly associated with the prefrontal and parietal cortex (Brown et al., 2019; Lau & Rosenthal, 2011). Lastly, integrated information theory provides a mathematical framework to characterize phenomenology, related to one's conscious subjective experience (Tononi, 2008, 2012; Tononi et al., 2016), suggesting that content-specific neural correlates of conscious perception to be differentiated, yet integrated with one another (Tononi et al., 2016). The integration can be measured with the phi metric (φ), which broadly refers to the amount of information generated by a physical system as a whole, compared with its parts considered independently. Additionally, integrated information theory proposes that the level of consciousness experienced is directly proportional to the amount of integrated information generated by the brain and suggests a posterior cortical hot zone.

The neural activity underlying conscious pereption likely covaries with selective attention and unconscious processing (de Graaf et al., 2012; V. A. Lamme, 2003). Additionally, cognitive processes such as working memory, decision making, task planning, and executive control likely shape conscious perception (Antonietti, 2011; Koch et al., 2016; Koivisto & Revonsuo, 2010; V. A. Lamme, 2006a; Miller, 2014; Soto & Silvanto, 2014). The state of the brain before experiencing a stimulus, as well as the level of processing required for specific task demands, also impact conscious visual perception (Binder et al., 2017). Gaining a better understanding of how these cognitive processes are interrelated could shed light on the neural correlates of conscious awareness. In the first study of this thesis, two quantitative meta-analyses were conducted to first reveal consistently activated regions across 54 independent studies, which employed various experimental methods and task designs, associated with

conscious visual awareness and unconscious perception. Then, cognitive decoding was also implemented to characterize the functional activation in relation to these cognitive processes.

1.7. Considerations for functional neuroimaging

Since its emergence in the early 1990s (Ogawa et al., 1990; Ogawa et al., 1992), fMRI has revolutionized our ability to image brain activity, offering higher spatial and relatively good temporal resolution compared to previous methods such as positron emission tomography (PET), with the advantage of being safe and non-invasive. fMRI capitalizes on the assumption that activated neurons trigger increased local blood flow and oxygenation (Poldrack et al., 2011). The measured signal is contingent upon this change in oxygenation and is known as the blood oxygenation level dependent (BOLD) signal. When building experimental designs using fMRI, it is crucial to find the right balance between the best spatial and temporal resolution, as the acquisition of one comes at the expense of the other (Lazar, 2008; Lindquist, 2008). The neuroimaging protocols included in chapter 4 and the third study of this thesis were developed in collaboration with an MRI physicist, with a focus on optimizing the trade-off between temporal and spatial resolution, to produce high resolution data (i.e., smaller voxels) and improve the ability to make inferences about neural anatomy, especially for smaller subcortical structures. Moreover, the haemodynamic response function (HRF) corresponds to the increase in blood flow following neural activity and exhibits distinct features, including peak height, up to 5% for primary sensory stimulation and 0.1 - 0.5% for general cognitive processes, in addition to time to peak, width, initial dip, and post-stimulus undershoot (see Fig. 5.2, (Poldrack et al., 2011)). The third article in this thesis assesses this percent of signal change in pre-defined regions of interest (ROI). In modeling neural activity, the BOLD HRF is a linear transform of neural signals, scaling according to the presented stimulus, demonstrating additivity when events occur close in time, and remaining time invariant. Given that HRF characteristics vary based on the experimental design, this emphasizes the importance of careful planning of task design throughout the studies included in this thesis, to optimize fMRI signal quality.

For analyzing fMRI data, the general linear model (GLM) is a common approach, accommodating both within-subject (1st level) and between-subject (2nd level) variability, and is used in the included studies. The GLM enables the observation of brain activity changes related to behavioral factors, facilitating various analyses such as one-sample t-tests, two-sample t-tests, paired t-tests, ANOVA, and ultimately reveals differences across conditions. Inferences can be made at different levels, including the voxel-level, cluster-level, or set-level, with necessary corrections for multiple comparisons. To enhance efficiency, ROIs can be defined based on voxel-level or cluster-level inference (Lindquist, 2008; Poldrack et al., 2011). For the statistical modeling and analysis phase, neuroimaging workflows typically result in non-reproducible, heterogeneous scripts. The third study used our recently developed BIDS statistical model analysis app (bidSPM), openly available **here**. Recent initiatives in the field have led to standardizing the format of neuroimgaging data, such as the Brain imaging data structure (BIDS, (Gorgolewski et al., 2016), and preprocessing pipelines such as fmriprep (Esteban et al., 2019). bidSPM (Gau, Barilari, Battal, Rezk, Gurtubay, Falagiarda, MacLean, et al., 2023) represents the next step to integrate the BIDS statistical model with SPM12. This new app was developed to facilitate automated model fitting via standardized pipelines, while still allowing necessary user flexibility, aiming to enhance the community's ability to adopt practices that promote reproducible results. The third study leads by example and supports the usage of bidSPM for further research, including univariate and ROIs analyses.

Another key consideration is that the studies in this thesis adopt a systematic, empirical and positive approach, using both behavioural and neuroimaging techniques, drawing inspiration from the pioneering neuroscientist Prof Brenda Milner's approach to addressing research objectives (Zatorre, 2018). Rather than emphasizing the deficits or lost abilities in brain-injured participants, as many studies tend to, the CVI studies included in this thesis investigate the visual pathways that are retained or dynamically modulated post brain injury and their association with residual visual abilities in the second and third article. This comprehensive perspective - in addition to the two systematic empirical meta-analyses

derived from neurotypical population data presented in the first article - further allows to better infer the roles of identified brain regions in specific cognitive and visual functions.

1.8. Thesis objectives and hypotheses

Cortical visual impairment (CVI) provides a unique, clinical model to study the neuronal architecture of the visual system and its modulation following occipital cortex lesions. Investigating the neuronal mechanisms of visual processing post-CVI can shed light on essential structures and visual pathways that contribute to conscious visual perception in addition to those potentially associated with unconscious perception. This can also reveal functionally activated structures that are less prominent in the neurotypical state but likely contribute to conscious visual processing. However, comprehensively understanding the core brain regions involved in generating a conscious perception and their modulation through experience or brain damage remains a challenge. This is amplified by the general limited spatial resolution in neuroimaging studies and the rarity and diversity of CVI participants.

General objective: The overall goal of this thesis was to investigate conscious and unconscious processing of visual information through a series of visual tasks using behavioural and neuroimaging techniques. The aim was to understand how these processes are reflected in the neurotypical brain and how they can be modulated by damage to the visual cortex, using fMRI. This thesis comprises three empirical articles, in addition to a chapter presenting a novel scientific dataset before the last empirical study, and aims to address the following briefly presented respective objectives, in addition to specific aims.

Objective 1. **Article 1** aimed to empirically identify convergence in functional brain activity engaged during conscious and unconscious visual processing across independent neuroimgaging studies. A comprehensive systematic search of the literature was first performed to collect whole-brain data of the corresponding neural correlates.

Aim 1.1. (meta-analysis 1): Conduct a first meta-analysis using activation likelihood estimation (ALE) to identify reliable patterns of functional activation associated with conscious visual awareness.

Aim 1.2. (meta-analysis 2): Carry out a second novel independent meta-analysis using ALE, focusing on unconscious visual perception. Aims 1.1. and 1.2. were structured as individual objectives that independently guided the course towards Aim 1.3.

Aim 1.3. (cognitive decoding): Employ meta-analytical cognitive decoding to characterize the functional activation associated with conscious and unconscious visual perception respectively, through comparison with over 14,300 studies using Neurosynth.

Aim 1.4. (contrast-specific meta-analyses): Conduct three novel meta-analytical contrasts to account for the different standard experimental task designs and precisely distinguish the regions associated with conscious visual awareness when contrasted with either an unconscious, competing (not currently conscious), or preconscious visual percept.

Hypothesis. For conscious visual awareness, we expected reliable activation across a distribution of regions involved in high-level cognitive processes such as visual attention and working memory, notably prefrontal regions including the inferior frontal junction (Bedini & Baldauf, 2021) in addition to parietal regions such as the intraparietal sulcus (Power et al., 2011). We predicted weaker activation of attentional regions during unconscious perception and a greater involvement of posterior regions.

Objective 2. **Article 2** sought to explore both cortical and subcortical responses in a patient with homonymous hemianopia and type II blindsight, leveraging a motion detection paradigm in conjunction with fMRI.

Aim 2.1. (behavioural accuracy): Evaluate blindfield performance and residual visual capabilities when presented with stimuli at varying eccentricities, prior to MRI testing.

Aim 2.2. (neural mechanisms): Assess cortical and subcortical activations external to the lesion during a blindsight performance using an event-related fMRI design. Provide new evidence of the neuronal fingerprint of blindsight, specifically by identifying V1-independent neural correlates during a motion detection blindsight performance.

Hypotheses: We hypothesized to identify activation in motion processing areas, such as the middle temporal regions, thereby indicating that motion stimuli in the participant's blind field were represented in the brain, despite a primary visual area lesion. Further, we predicted the observation of superior colliculi activation, which would suggest subcortical

engagement in the foundational mechanisms of motion blindsight and its role within a potential alternative visual pathway.

Objective 3. The next aim was to conceptualize and generate a comprehensive MRI and behavioural dataset examining motion perception in both individuals with CVI and neurotypical controls. Given ethical considerations, this dataset is documented as **Chapter 4** of this thesis, preceding the third study, which uses a section of the data. As this chapter presents a dataset no *a priori* hypotheses were formulated.

Aim 3.1. (neuroimaging data & meta-data): Acquire a wide range of neuroimaging measures including structural, functional task-based MRI, resting-state MRI, as well as diffusion MRI, and provide in a BIDS-standardized format. Include preprocessed fMRI data and quality control metrics, supplemented with descriptive metadata to support secondary data usage. In addition, electrophysiological and eye-tracking evaluations performed during MRI scans are incorporated.

Aim 3.2. (behavioural data): Develop custum experimental motion pereption tasks, provide data for behavioural experiments and neuropsychological and demographic profiles of participants.

Objective 4. **Article 3** aimed to characterize the neurological consequences of brain damage as well as the adaptive ability of the brain in the context of various individuals with CVI, encompassing those with residual vision. This study sought to comprehensively investigate functional modulation of visual pathways following occipital cortex damage- contingent upon the lesion's size and extent, and the resulting impact on visual perception, by using robust behavioural paradigms, functional magnetic resonance imaging (fMRI), with a comparative analysis alongside a group of matched neurotypical controls.

Aim 4.1. (automated structural lesion mapping): Evaluate the anatomical alterations to characterize the CVI cohort, specifically quantifying the extent of brain damage via a voxel-based approach and identifying lesioned structures. Optimize and customize the algorithm from SPM's automated lesion identification (ALI) toolbox and implement in the bidSPM app. Ensure the controls exhibit neurotypical brain structures.

Aim 4.2. (behavioural assessments): Assess the impact of occipital cortex lesions on CVI participants' residual visual abilities by comparing with their intact visual field and neurotypical controls, using a comprehensive behavioural assessment, including global motion discrimination thresholds, the presentation of diverse motion stimuli and a general data assessment (demographic, medical history). Characterize CVI participants based on behavioural outcomes.

Aim 4.3. (cortical neural correlates): Identify neuroplastic alterations in the functional activation of cortical structures in CVI participants compared to neurotypical controls, using exploratory whole brain coverage as well as targeted cortical regions of interest analyses.

Aim 4.4. (high resolution fMRI): Identify the neuroplastic alterations in the functional activation of subcortical strucutres, with a particular focus on thalamic regions, in CVI participants compared to neurotypical controls using high-resolution fMRI with a sub-1mm voxel size and targeted subcortical regions of interest analyses.

For both aims 4.3 and 4.4: Investigate the neural responses associated with stimulus presentation of diverse types of motion stimuli - including looming and biological motion stimuli, in both the impaired and sighted fields of CVI participants, compared to a neurotypical control group. Characterize the functional response to visual motion presentation with residual visual abilities and extent of brain damage.

Hypotheses: We anticipate that functional activation patterns will reflect the extent and location of the lesion and resulting visual impairment, yielding significant variations between stimulus presentation sides compared to neurotypical controls. We anticipate to categorize residual visual abilities based on the the behavioural assessment. We hypothesize to observe activation within middle temporal areas, in response to salient looming and biomotion stimuli, demonstrating that even after occipital cortex injury, the brain can represent visual motion in members of our CVI participant cohort. Considering the association of the lateral occipital complex with unconscious visual perception in the first article, we postulate that this region may facilitate low-level visual information processing. Building on the previous findings from the second article, we further postulate that the thalamus and pulvinar may facilitate residual motion perception.

Chapter 2

Article 1

Revealing robust neural correlates of conscious and unconscious visual processing: activation likelihood estimation meta-analyses.

Michèle W. MacLean[1], Vanessa Hadid[2], R. Nathan Spreng[3,4,5] and Franco Lepore[1]

(1) Département de Psychologie, Université de Montréal, Montréal, Québec, Canada

(2) Département de Sciences Biomédicales, Université de Montréal, Montréal, Québec, Canada

(3) Laboratory of Brain and Cognition, Department of Neurology and Neurosurgery, Montreal Neurological Institute, McGill University, Montréal, Québec, Canada

(4) Departments of Psychiatry and Psychology, McGill University, Montréal, Québec, Canada

(5) McConnell Brain Imaging Centre, McGill University, Montréal, Québec, Canada

Published: **MacLean, M.W.**, Hadid, V., Spreng, R.N., Lepore, F.(2023) Revealing robust neural correlates of conscious and unconscious visual processing: Activation likelihood estimation meta-analyses. *Neuroimage.* doi.org/10.1016/j.neuroimage.2023.120088

Abstract

Our ability to consciously perceive information from the visual scene relies on a myriad of intrinsic neural mechanisms. Functional neuroimaging studies have sought to identify the neural correlates of conscious visual processing and to further dissociate from those pertaining to preconscious and unconscious visual processing. However, delineating what core brain regions are involved in eliciting a conscious percept remains a challenge, particularly regarding the role of prefrontal-parietal regions. We performed a systematic search of the literature that yielded a total of 54 functional neuroimaging studies. We conducted two quantitative meta-analyses using activation likelihood estimation to identify reliable patterns of activation engaged by i. conscious (n = 45 studies, comprising 704 participants) and ii. unconscious (n = 16 studies, comprising 262 participants) visual processing during various task performances. Results of the meta-analysis specific to conscious percepts quantitatively revealed reliable activations across a constellation of regions comprising the bilateral inferior frontal junction, intraparietal sulcus, dorsal anterior cingulate, angular gyrus, temporo-occipital cortex and anterior insula. Neurosynth reverse inference revealed conscious visual processing to be intertwined with cognitive terms related to attention, cognitive control and working memory. Results of the meta-analysis on unconscious percepts revealed consistent activations in the lateral occipital complex, intraparietal sulcus and precuneus. These findings highlight the notion that conscious visual processing readily engages higher-level regions including the inferior frontal junction and unconscious processing reliably recruits posterior regions, mainly the lateral occipital complex.

Highlights

(1) Joint fMRI meta-analyses of conscious visual awareness & unconscious perception

(2) Conscious awareness recruits IFJ, IPS, dACC, AG, temporo-occipital cortex & aINS

(3) Unconscious perception elicits reliable activation in the LOC, IPS & precuneus

(4) Conscious awareness associated with attention, cognitive control & working memory

Keywords: Conscious visual awareness, Unconscious perception, fMRI, Inferior frontal junction, Intraparietal sulcus, Lateral occipital complex

1. Introduction

The functional complexity of the human brain enables visual information represented on the retina to transcend into a meaningful coherent conscious experience. Only a fraction of information from the visual scene reaches conscious awareness, yet the remaining information can still be processed preconsciously or unconsciously. A series of fundamental and intrinsic neural mechanisms seemingly give rise to different degrees of conscious, preconscious, or unconscious perception. Functional magnetic resonance imaging (fMRI) studies have largely been used to understand the neural correlates of conscious perception and disambiguate the neural signals contributing to each type of perceptual processing. It is however still debated how brain activation patterns are modulated by the level of perceptual processing required to accomplish specific tasks.

Consciousness, though multifaceted and intrinsically complex, can be defined by two main components: the content of consciousness (i.e., awareness of self or the environment or experience) and level of consciousness (i.e., wakefulness) (Baars, 1993; Laureys, 2005). This study focuses on neural correlates that give rise to different degrees of awareness of environmental content or external visual stimuli in the full wakefulness state. Several standard report-based paradigms enable to dissociate the neural correlates pertaining to the content of conscious visual perception from those pertaining to unconscious or preconscious visual perception by manipulating the experimental visual input to induce and observe changes in the experienced phenomenal percept and associated neural signal. Standard designs contrasting unconscious perception include visual masking or interocular suppression (Breitmeyer & Ogmen, 2000; Francis, 2000; Tsuchiya & Koch, 2005), whereas those contrasting preconscious perception include attentional blink or inattentional blindness techniques (Hutchinson, 2019; Kranczioch et al., 2005; Thakral, 2011). Other designs rather induce a shift in visual awareness despite invariant physical visual input (for a review see C. Y. Kim & Blake, 2005), where a first conscious percept is contrasted with a second competing percept induced by the same stimulus but not currently consciously seen. These designs include bistable perception, binocular rivalry and pop-out stimuli techniques (Blake & Logothetis, 2002; Kleinschmidt et al., 1998; Mamassian & Goutcher, 2005; Portas et al., 2000).

A variety of cognitive neuroscience and neurobiological approaches have sought to define conscious awareness and suggest different specific neuroarchitectural elements and stages of visual processing. Given the immense amount of visual information processed by the human brain, to remain efficient, it would not be possible for each visual input to evoke a conscious percept (Ajina & Bridge, 2017). Many approaches highlight how conscious awareness is preceded by unconscious processing, where underlying unconscious processes must first converge onto one interpretation of a visual input (Baars, 1993) and where most of visual processing occurs without awareness (for a review see Kouider et al., 2010). Moreover, within unconscious processing, preconscious processing refers to a transient state of activity where information is potentially accessible, yet not accessed (Dehaene et al., 2006), seemingly by a lack of top-down attentional activity (Hutchinson, 2019). One of the most influential theoretical frameworks of conscious processing, known as the Global Neuronal Workspace (GNW), suggests that information first travels unconsciously bottom-up to specialized brain areas, then top-down attention amplifies the signal and boosts the activity of the current active neurons to allow the processes to become available to the global workspace thought to be the content of conscious processing (Dehaene & Naccache, 2001). Understanding how information succeeds in reaching conscious awareness or rather remains at a preconscious or unconscious state of perceptual processing requires further research.

Neuroimaging studies have yielded different results as to what brain regions are necessary and sufficient to sustain a conscious visual percept. Establishing whether visual awareness emerges at the early stages of processing within the sensory cortices (V. A. Lamme, 2010), or later once prefrontal and parietal regions are involved (Aru et al., 2012; Bor & Seth, 2012; Lau & Rosenthal, 2011), in other words whether anterior vs. posterior regions of the cortex are engaged (Boly et al., 2017)) remains a challenge in the field. An earlier meta-analysis on the neural correlates of conscious visual processing suggested reliable activations in subcortical-extrastriate-frontal-parietal regions (Bisenius et al., 2015). The extent to which the sensory cortices vs. the prefrontal parietal regions are engaged at each stage of perceptual processing and whether – or how – broadcasting of content takes place for conscious as opposed to unconscious visual processing needs further investigation. Moreover, conscious awareness is

seemingly shaped by attention and working memory to accomplish complex goals (Bor & Seth, 2012; Soto & Silvanto, 2014) and, as many brain regions are recruited for a diverse range of cognitive demands (Duncan & Owen, 2000), understanding how these cognitive processes relate may give insight on the neural correlates of conscious awareness.

Here, we aim to identify areas of convergence in the functional activity of brain regions engaged during conscious and unconscious visual perception using quantitative meta-analyses. We extend beyond the work of a previous meta-analysis (Bisenius et al., 2015) to account for recent advances as well as disentangle and unmask core structures reliably associated with conscious and unconscious visual processing respectively, and provide an empirical foundation for theories of conscious awareness. We performed a comprehensive systematic search of the literature and categorized neuroimaging studies based on the state of perceptual processing involved (i.e., conscious, preconscious, unconscious). We then performed two distinct meta-analyses to identify reliable whole-brain activation patterns associated with conscious visual awareness and unconscious visual perception. Moreover, we carried out meta-analytical functional decoding of the cognitive processes associated with the significant activations from these two meta-analyses using Neurosynth (Yarkoni et al., 2011). We further performed three meta-analytical contrasts to account for the different standard experimental task designs and disambiguate which reliable regions are precisely identified when conscious visual awareness is contrasted with either i) unconscious visual perception, ii) a second competing percept (not currently conscious) induced by the same stimulus or iii) preconscious visual perception. For conscious awareness, we hypothesized to find reliable activations across a distribution of areas involved in high-level cognitive processes such as visual attention and working memory, notably prefrontal regions including the inferior frontal junction (Bedini & Baldauf, 2021) in addition to parietal regions such as the intraparietal sulcus (Power et al., 2011). We expected less robust activations of attentional regions during unconscious perception and a stronger role of posterior brain regions.

2. Methods

2.1. Literature search and study selection

We performed a comprehensive systematic search of functional magnetic resonance imaging studies investigating the neural correlates associated with conscious, unconscious and preconscious visual perception and further subdivided them according to task design. All articles in the literature published before April 20th, 2022 were considered for this meta-analysis. We used PubMed/MEDLINE, Embase, APA PsychINFO, Web of Science, and EBM Reviews online databases to search for articles with the following search string composed of MESH terms and keywords:

(1) (Magnetic Resonance Imaging/ OR (fMRI or functional MRI or functional magnetic resonance imaging). ab,kw,ti.)

(2) AND Awareness/ or Consciousness/ OR (aware* or conscious* or implicit or sentience or subliminal). ab,kw,ti.)

(3) AND exp Visual Perception/ or Optical Illusions/ or Subliminal Stimulation/ OR ((vis* adj3 (attention or perception* or process*)) or ((motion or movement) adj3 (detection* or perception*)) or ambiguous figures or attentional blink* or binocular rivalry or bistable perception* or ((change or inattentional or motion-induced) adj2 blindness*) or colo?r perception* or contrast sensitivit* or flash suppression* or flicker fusion* or ((optic* or visual) adj3 illusion*) or masking* or optic* flow* or ((subliminal or subtrheshold) adj2 (stim* or perception* or threshold*)) or pop-out*). ab,kw,ti.

The search string and filters were adapted and refined for each specific database, reviewed and validated by a librarian from the Université de Montréal. The search yielded 1,746 non-duplicate articles. Five additional articles were identified through reference lists of relevant articles yielding a total of 1,751 articles to screen. The studies were systematically reviewed and considered eligible if they met the following criteria: (i) employed behavioral paradigms to study conscious, unconscious, or preconscious processing of visual stimuli; (ii)

were empirical investigations (i.e., not review articles or opinion pieces); (iii) used fMRI; (iv) used whole-brain analyses and reported the contrasts: (a) conscious visual awareness > unconscious visual perception, (b) competing conscious percepts, (c) conscious visual awareness > preconscious visual perception, and/or (d) unconscious visual perception contrasts; (v) reported foci in Montreal Neurologic Institute (MNI) or Talairach coordinates and (vi) studied neurotypical subjects in at least one of the contrasts. For articles including both clinical and neurotypical control groups, only contrasts in the neurotypical control group were included in the meta-analyses. Only results published in peer-reviewed journals, with whole brain data readily accessible, were included. In accordance with ALE standards, 31 studies were excluded for not reporting a whole brain analysis and using exclusively region of interest (ROI) analyses based on a priori hypotheses. Also, 8 studies were excluded for not covering the whole brain as determined through the fMRI acquisition parameters. A PRISMA flowchart illustration of the literature review and study selection process can be viewed in Fig. 1. Following the criteria defined above, 54 studies were included in the present study and organized into two main categories according to the nature of the study and the contrasts included: (1) conscious visual processing (n = 45 studies, comprising 704 participants) and (2) unconscious visual processing (n = 16 studies, comprising 262 participants). The first main category was further subdivided into three contrasts: (1) conscious contrasted with unconscious, (2) a first conscious percept contrasted with a second competing percept (not currently seen), (3) conscious contrasted with preconscious. A separate contrast category containing each type of visual processing versus baseline was not extracted from the literature due to the low amount of this type of reported contrast with data readily accessible. Studies in both main categories are organized based on the paradigm or visual task used (i.e., conscious visual processing: contrast (1): masking, threshold, subliminal, flash suppression, priming, other; contrast (2): bistable perception, pop-out; contrast (3): attentional blink, change detection, inattentionnal blindness; unconscious visual processing: masking or priming, threshold, other). The list of all relevant categorized studies is presented in Table 1.

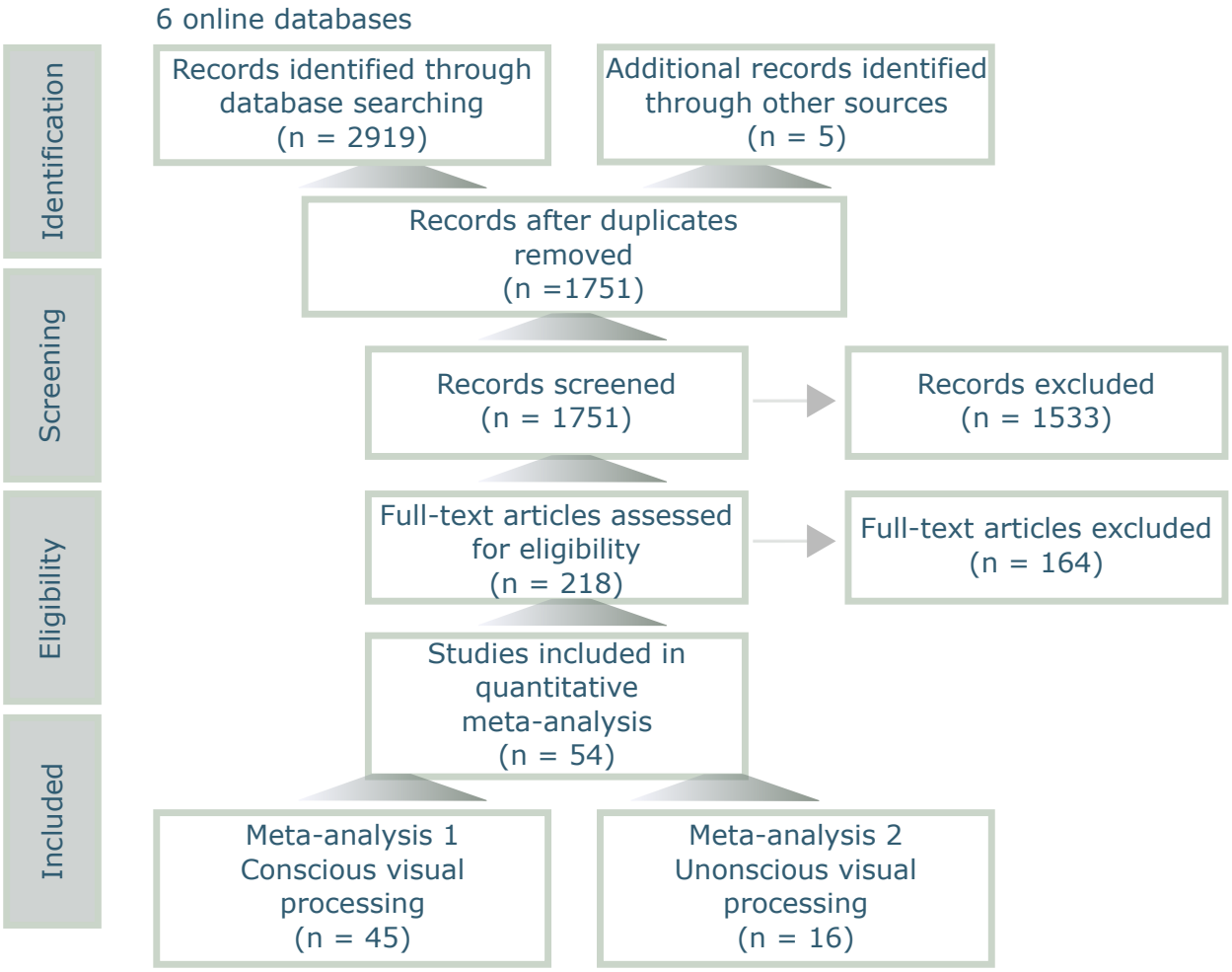

Figure 1 – Flowchart of systematic literature search and article selection, following PRISMA guidelines. Adapted from (Moher et al., 2009).

Table 1 – Studies meeting the inclusion criteria for the meta-analysis.

First author	Year	N	Gender ratio (F/M)	Age M (sd or range)	Included Contrast	N (foci)	Correction for whole brain volume
Meta-analysis 1 - Conscious visual processing							
Contrast 1: Studies showing differences between a conscious and unconscious percept (conscious > unconscious)							
Masking							
Binder	2017	27	(20/10)	21.94(2.96)	Linear contrast for visibility: High Level	4	$p < 0.05$ corrected
Christensen	2006	13	(5/8)	29.4 (24-39)	Clear perceptual experience of the stimulus> no perceptual experience of the stimulus	47	$p = 0.007$ uncorrected
Dehaene*	2001	15	(12/3)	23.3 (19-34)	Visible words > masked words	15	$p < 0.05$ corrected
Dutta*	2014	17a	(14/10)	22 (20-24)	Linear contrast increased awareness	5	p=0.05 corrected
Haynes	2005	8	.	22-33 (no sd)	Correlation between psychometric visibility function and brain responses	10	$p < 0.05$ corrected
Huang	2020	18a	(18/9)	18-27 (no sd)	Visible > invisible	6	$p< 0.001$, p=0.001 corrected
Imamoglu	2014	14	(6/8)	21-36 (no sd)	Correlation between psychometric visibility function and brain responses	4	$p < 0.05$ corrected
Lau	2006	13a	(9/5)	24.2(2.4)	Subjective awareness > subjective unawareness	1	$p < 0.001$ uncorrected
Rodriguez*	2012	18	(8/10)	42-63 (no sd)	Correctly detected faces > correctly rejected nonfaces (scrambled stimuli)	30	$p < 0.001$ corrected
Sato*	2016	27	(3/24)	25.0(4.6)	Interaction of supraliminal > subliminal and attended > unattended	2	p=0.002, p=0.001 uncorrected

Table 1 *(continued)* _

First author	Year	N	Gender ratio (F/M)	Age M (sd or range)	Included Contrast	N (foci)	Correction for whole brain volume
Tacikowski	2017	26	(11/15)	25(4)	Perceptual awareness (self-aware + other-aware) - (self-unaware + other-unaware)	7	p<0.05 corrected FWE
Tsubomi	2012	10	(3/7)	22-27 (no sd)	Attend flankers > attend masks	1	p < 0.001 uncorrected
VanDoren	2010	28	(15/13)	19-29 (no sd)	Positive consciousness report > negative consciousness report	4	p < 0.01 corrected, p < 0.05 corrected
Webb	2016	25	(14/11)	18-48 (no sd)	Aware > unaware	12	p < 0.01 corrected
Threshold							
Chica	2016	19	(10/9)	26 (4)	Seen > unseen	11	p < 0.05, corrected
Lefebvre*	2021	19	(17/2)	31.2 (6.5)	Conscious access: Conscious > unconscious	5	p = 0.01 corrected
Levinson	2021	25a	(26/12)	27.18 (20-38)	Conscious recognition > unrecognized when above chance level (unconscious)	25	p < 0.05, FWE-corrected
Flash suppression							
Madipakkam	2015	16	(3/13)	25 (0.74)	Aware > unaware	7	p < 0.001, corrected; p=0.006 corrected; p=0.003 corrected
Priming							
Yomogida*	2014	20	(9/11)	20.65 (2.13)	Explicit > implicit	17	p<0.05; p<0.001 uncorrected
Other							
Heinzel*	2008	12	(0/12)	28.6 (19-41)	Supraliminal > subliminal letter processing	2	p = 0.021 corrected, p < 0.001 corrected

Table 1 *(continued)* _

First author	Year	N	Gender ratio (F/M)	Age M (sd or range)	Included Contrast	N (foci)	Correction for whole brain volume
Malekshahi*	2016	12	(5/7)	28.41 (3.98)	Explicit detection > express saccades for detected > undetected	4	$p < 0.005$ corrected
Contrast 2: Studies showing differences between a conscious percept and a competing percept (conscious > competing percept)							
Bistable perception							
Brouwer	2005	7	.	.	Alternations > random button presses	7	$p < 0.005$ corrected
Carmel	2006	13	(11/2)	26.4 (22-34)	Flicker percepts > fused percepts	11	$p < 0.001$ uncorrected
Frassle	2014	20	(11/9)	19-30 (no sd)	Rivalry > replay	11	$p < 0.001$ uncorrected
Kleinschmidt	1998	6	.	23-33 (no sd)	Perceptual reversal > stable percept	9	$p < 0.001$ uncorrected, $p < 0.05$ corrected
Knappen	2011	5	.	.	Rivalry transition > instantaneous replay	9	$p < 0.001$ uncorrected
Kovacs	2008	12	(6/6)	22 (2)	Self motion > object motion	5	$p < 0.05$, $p = 0.05$
Lumer	1998	6	.	.	Rivalry > replay	4	$p < 0.05$ corrected
Ozaki	2012	20	(4/16)	21-44 (no sd)	Necker cube > alternating unambiguous cubes	8	$p < 0.005$ uncorrected
Roy	2017	20	.	.	Rivalry > replay	10	$p < 0.001$ FDR corrected
Sterzer	2005	12	(4/8)	23-27 (no sd)	Colour and luminance consistent > inconsistent apparent motion contrasts	4	$p < 0.001$, uncorrected; $p < 0.005$, uncorrected.
Stottinger	2015	17	(11/6)	27.65 (8.01)	Stable > change	6	$p = 0.05$ FDR corrected
Weilnhammer	2021	33	(21/10)	27.3 (1.42)	Change > baseline	11	$p < 0.05$ FWE
Wilcke	2009	6	(2/4)	27 (20-32)	Binocular rivalry > binocular fusion	7	$p < 0.001$ uncorrected
Zaretskaya	2013	18	(9/9)	21-33 (no sd)	Global > local	5	$p < 0.0001$ (uncorrected) and surviving $p<0.05$
Pop-out							

Table 1 *(continued)* _

First author	Year	N	Gender ratio (F/M)	Age M (sd or range)	Included Contrast	N (foci)	Correction for whole brain volume
Eriksson	2004	6a	(3/5)	23-35(no sd)	Pop-out > (sustained perception + sensorimotor integration)	12	$p < 0.01$ corrected
Eriksson	2007	11a	(6/6)	20-42(no sd)	Pop-out > (sustained perception + sensorimotor integration) (experiment 2)	15	$p < 0.001$ uncorrected, $p < 0.05$ corrected
Portas	2000	9	(1/9)	29(24-34)	Pop-out > (sustained perception + sensorimotor integration)	10	$p < 0.001$ uncorrected, $p < 0.05$ corrected
Reinders	2005	15	(8/7)	25.8(18-36)	Pop-out house > face	2	$p<0.01$ corrected

Table 1 *(continued)* _

First author	Year	N	Gender ratio (F/M)	Age M (sd or range)	Included Contrast	N (foci)	Correction for whole brain volume
Contrast 3: Studies showing differences between a conscious and preconscious percept (conscious > preconscious)							
Attentional blink							
Bergstrom	2014	21	(13/8)	24 (18-39)	Target > low level baseline (exp. 2)	3	p 0.001 uncorrected
Johnston	2011	16	(9/7)	22.5 (1.4)	AB > no AB	9	p<0.05
Kranczioch	2005	5	(4/1)	19-34 (no sd)	Target detected > target missed	12	p 0.0004
Slagter	2010	24	(19/5)	21.3 (2.4)	No blink > blink	16	p<0.05 FDR corrected
Change detection / Inattentional blindness							
Beck	2001	6	(5/1)	25-33	Conscious change detection > change blindness (experiment 1)	3	p<0.05 corrected
Thakral	2011	9	.	.	Aware > unaware	1	p <0.05

Table 1 *(continued)* _

First author	Year	N	Gender ratio (F/M)	Age M (sd or range)	Included Contrast	N (foci)	Correction for whole brain volume
Meta-analysis 2. Unconscious visual processing							
Studies showing unconscious visual processing							
Masking/Priming							
Badgaiyan	2000	10	(6/4)	19.9 (no sd)	Priming > baseline (decrease)	1	$p < .001$
Dehaene*	2001	15	(12/3)	23.3 (19-34)	Activation to masked words	6	$p < 0.05$ corrected
Diaz	2007	12	(9/3)	22.3 (3)	Masked words > masked nonwords	3	$p < .001$
D'Ostilio	2012	24	(18/6)	21 (2)	Incompatible (subliminal conflict processing) > neutral	9	$p < 0.001$ uncorrected
Dutta*	2014	17	(14/10)	22 (20-24)	Correct > incorrect discrimination on unaware trials	5	$p = 0.05$ corrected
Emmanouil	2013	7	(4/3)	24-29 (no sd)	ScCc > ScCi, SiCc + SiCi (congruent>incongruent)	1	$p < .01$
Gomes	2017	21	.	23.33 (4.86)	Masked primed > unprimed (random)	6	$p < 0.05$ corrected
Heinzel*	2008	12	(0/12)	28.6 (19-41)	Subliminal > supraliminal letter processing	2	$p = 0.021$ corrected, $p < 0.001$ corrected
Ito	2015	28	(14/14)	21.6 (20-23)	Subliminal > supraliminal	1	$p = 0.021$ corrected, $p < 0.001$ corrected
Kouider	2009	16	(8/8)	23 (0.2)	Subliminal masked priming	9	$p < 0.001$
Lefebvre*	2021	19	(17/2)	31.2 (6.5)	Unconscious vision	8	$p < 0.001$ corrected
Malekshahi*	2016	12	(5/7)	28.4 (3.98)	Express saccades (implicit detection)	4	$p < 0.05$ FDR corrected
Reber	2014	12	(0/12)	24.6 (4.6)	Subliminal word pairs > subliminal consonant	7	$p = 0.005$
Sato*	2016	27	(3/24)	25 (4.6)	Subliminal masking	2	$p = 0.002$ corrected, $p = 0.01$ corrected

Table 1 *(continued)* _

First author	Year	N	Gender ratio (F/M)	Age M (sd or range)	Included Contrast	N (foci)	Correction for whole brain volume
Ursu	2009	10	(3/7)	24.4 (20-32)	Implicit conflict > no conflict	10	$p < 0.05$ corrected
Yomogida*	2014	20	(9/11)	20.65 (2.13)	Implicit event simulation processing (implicit > control)	16	$p < 0.001$ corrected $p < 0.001$ uncorrected
Threshold							
Lefebvre*	2021	19	(17/2)	31.2(6.5)	Unconscious vision	8	$p < 0.001$ corrected
Other							
Heinzel*	2008	12	(0/12)	28.6 (19-41)	Subliminal > supraliminal letter processing	2	$p = 0.021$ corrected, $p < 0.001$ corrected
Malekshahi*	2016	12	(5/7)	28.4 (3.98)	Express saccades (implicit detection)	4	$p < 0.05$ FDR corrected

Note: aThere is a discrepancy between the total number of subjects listed and the gender ratio listed in this reference. - Data unavailable. *Studies with distinct contrasts included in both Meta-analysis 1 Conscious visual processing and Meta-analysis 2 Unconscious visual processing (separate meta-analyses).

2.2. Coordinate based meta-analysis

2.2.1. Activation likelihood estimation (ALE) analysis. Coordinate-based meta-analyses were conducted with the revised version of the activation likelihood estimation (ALE) algorithm (Eickhoff et al., 2012; Eickhoff et al., 2009) using the GingerALE version 3.0.2 software package (available at www.brainmap.org/ale). To investigate conscious visual awareness, unconscious perception and preconscious perception, we conducted two separate meta-analyses, in addition to 3 distinct meta-analytical contrasts in the first, on coordinates pooled from the fMRI studies identified by the literature search (Eickhoff et al., 2012; Laird et al., 2009). Prior to conducting the ALE meta-analyses, we transformed the foci coordinates reported in Talairach into MNI through Lancaster transformation (Lancaster et al., 2007) using the GingerALE software (Eickhoff et al., 2012).

The ALE approach computes the statistical spatial convergence of activation coordinates (foci) across independent studies, thus identifying reliable patterns of significant activation in brain regions. In a probabilistic fashion, a 3-dimensional Gaussian distribution is modeled for each significant activation location accounting for the spatial uncertainty around each coordinate, using a full-width half-maximum (FWHM) calculated based on the number of participants in each study. Thus, the width of the distribution is weighted by the number of participants for each study (i.e., larger sample sizes have smaller Gaussian distributions). A brain activation map is first computed for each study and then the maps are combined to estimate regions of spatial conver- gence between activation foci and calculate voxel-wise ALE scores. A permutation procedure, accounting for the number of experiments, foci per experiment and number of subjects, is used to test the differentiation between the estimate of true convergence of foci and the null hypothesis of random spatial distribution of foci between experiments, (i.e., noise) (Eickhoff et al., 2016). To control for false-positive rates, a first conservative threshold was applied to the ALE images and the meta-analyses were corrected for multiple comparisons ($p < 0.05$ family-wise error-corrected FWE corrected; 1000 permutations, $p < 0.001$ cluster forming threshold). A second more liberal threshold was applied to the ALE meta-analyses ($p < 0.05$ FWE corrected; 1000 permutations, p

< 0.05 cluster forming threshold) comprising a fewer number of studies, i.e., conscious > preconscious (n = 6 studies); unconscious contrast (n = 16 studies). For data visualization of the meta-analysis results, the ALE results images were imported into MRIcroGL and BrainNet Viewer and overlayed onto an anatomical image (i.e., MNI152 template).

2.3. Neurosynth cognitive decoder

We used Neurosynth, an online large-scale automated meta-analytical platform, containing over 14,300 functional neuroimaging studies, to decode the cognitive terms associated with the ALE analyses ((Yarkoni et al., 2011) ; available at https://neurosynth.org). Neurosynth associates cognitive terms with brain activation patterns and peak coordinates from all neuroimaging studies in its vast database. Through a reverse inference approach, the unthresholded ALE map from the first meta-analysis (i.e., conscious visual processing, 45 studies, comprising 704 participants, 409 foci), allowing to find consistent sub-threshold effects (Gorgolewski et al., 2015), was uploaded to the NeuroVault repository to compare to all studies in the database. Using the Neurosynth decoder, a voxel-wise product-moment correlation coefficient was computed between the ALE map and all the term-based z-statistics maps from Neurosynth. This generated a list of 1,307 entry terms with a corresponding correlation score for each representing the strength of the association with the ALE map. After manually excluding all brain regions and methodological terms, the remaining terms were ranked by strength of correlation. These terms represent the association of the brain regions reliably activated during conscious contrasted with unconscious, a competing (not currently seen) percept or preconscious visual processing with the Neurosynth maps of all neuroimaging studies. We displayed the terms using a word cloud for data visualization purposes. We repeated the reverse inference approach with the unthresholded ALE map from the second meta-analysis (i.e., unconscious visual processing, 16 studies, comprising 262 participants, 90 foci).

3. Results

3.1. Meta-analysis on the full sample of conscious visual processing studies

To examine reliable patterns of activity during conscious visual processing, we used gingerALE to perform an ALE analysis using activation foci obtained from the full sample of conscious visual processing studies assessed either versus unconscious, a second competing percept (not currently conscious), or a preconscious visual processing condition. This corresponds to combining contrasts 1, 2 and 3 in Table 1. Brain regions showing consistent activation across the full sample of conscious visual processing studies assessed versus a matched control condition were the bilateral inferior frontal junction (IFJ) in addition to the right intraparietal sulcus (IPS), left dorsal anterior cingulate cortex (dACC), the left angular gyrus (AG), the left temporo-occipital cortex and the right anterior insula (aINS). Coordinates of the activation maxima and cluster size as well as the number of studies and foci contributing to the activated brain regions are given in Table 2. See the corresponding fig2 for visualization of the activated brain areas projected onto a surface map and corresponding axial slices.

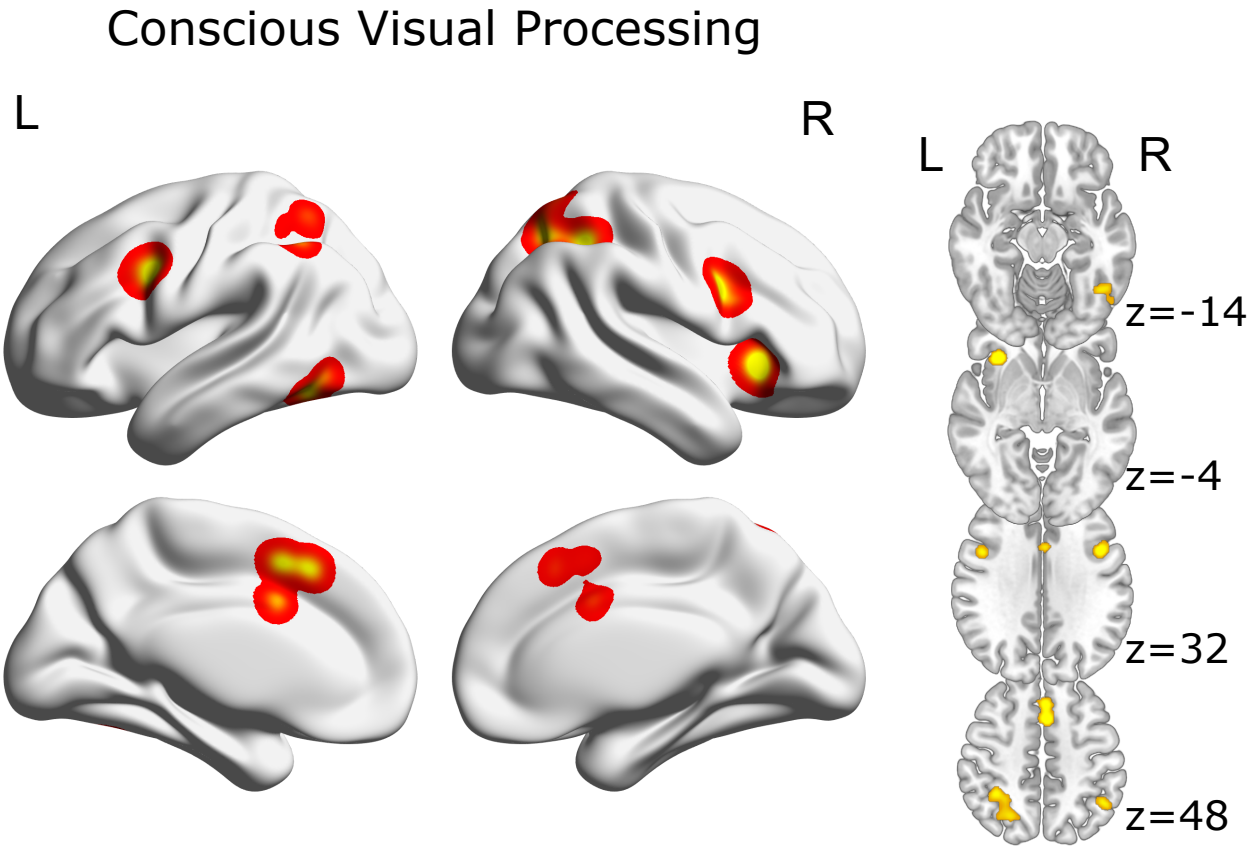

Figure 2 – Activation likelihood estimation map showing significant convergent activity for the full sample of studies on conscious visual processing assessed versus a matched control condition. Results of the ALE clusters (thresholded at $p<0.001$, FWE cluster-level corrected at $p<0.05$) across the sample of conscious visual processing studies (45 studies, 704 subjects, 409 foci) included in the first meta-analysis, are shown on an inflated surface map in BrainNet Viewer, projected over the MNI152 atlas. Four axial slices corresponding to the same activated clusters are shown using MRIcroGL for visualization purposes. See Table 2 for coordinates.

Table 2 – Brain regions showing consistent activation during conscious visual processing tasks ($p < 0.001$). For each cluster, brain region label, hemisphere, MNI coordinates, ALE maxima, cluster number and size (mm3), and number of studies and foci are provided.

Brain regions	**Hemi**	**x**	**y**	**z**	**ALE max.**	**Cluster Number**	**Volume (mm3)**	**N studies (foci)**
Meta-analysis 1 - Conscious visual processing p<0.001								
Intraparietal Sulcus	R	36	-46	46	0.023016	1	2816	14(14)
Dorsal anterior cingulate	L	-4	10	48	0.026296	2	2744	12(14)
Inferior frontal junction	L	-46	8	34	0.028524	3	1392	7(7)
Angular Gyrus	L	-44	-52	52	0.02512	4	1392	6(8)
Temporal occipital cortex	L	-50	-56	-16	0.019037	5	1280	7(9)
Inferior frontal junction	R	46	8	28	0.024727	6	1280	5(5)
Anterior insula	R	34	22	-4	0.032269	7	1264	7(8)

3.2. Meta-analysis on the full sample of unconscious visual processing studies

To examine reliable patterns of activity during unconscious visual processing, we used gingerALE to perform an ALE analysis using activation foci obtained from studies with unconscious visual processing contrasts. The left superior lateral occipital cortex (LOC) showed consistent activation during unconscious visual processing. This reliably activated cluster extended from this peak region up to the left intraparietal sulcus (IPS) and left precuneus, two reliable distinct subpeaks within the cluster. Brain regions in the right hemisphere did not show consistent activation during unconscious visual processing for the studies included in this meta-analysis. Coordinates of the activation maxima and cluster size as well as the number of studies and foci contributing to the activated brain regions are given in Table 3. See the corresponding fig3 for visualization of the activated brain areas projected onto a surface map and corresponding axial slices.

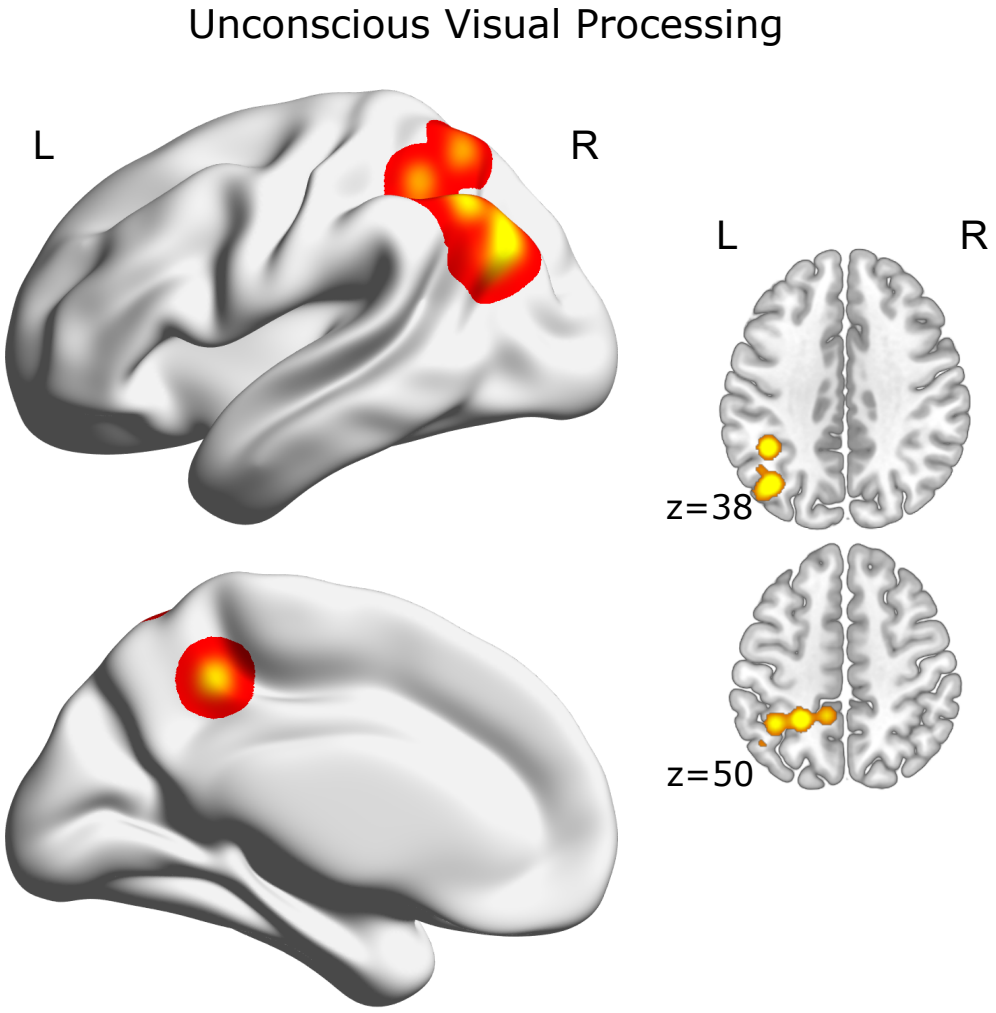

Figure 3 – Activation likelihood estimation map showing significant convergent activity for studies on unconscious visual processing. Surface maps of the ALE clusters (thresholded at $p < 0.05$, FWE cluster-level corrected at $p < 0.05$) across the sample of unconscious visual processing studies (16 studies, 262 subjects, 90 foci) included in the second main meta-analysis, are shown on an inflated surface map in BrainNet Viewer, projected over the MNI152 atlas. Two axial slices corresponding to the same activated cluster are shown using MRIcroGL for visualization purposes. See Table 3 for coordinates.

Table 3 – Brain regions showing consistent activation during unconscious visual processing tasks. For each cluster, brain region label, hemisphere, MNI coordinates, ALE maxima, cluster number and size (mm3), and number of studies and foci are provided.

Brain regions	**Hemi**	**x**	**y**	**z**	**ALE max.**	**Cluster Number**	**Volume (mm3)**	**N studies (foci)**
Meta-analysis 2 - Unconscious visual processing (p<0.05)								
Superior Lateral Occipital Cortex	L	-40	-68	38	0.00919	1	1057	7(9)
Sub-peaks include:								
Intraparietal sulcus	L	-24	-46	50	0.0083	1	/	
Precuneus	L	-38	-48	50	0.00559	1	/	

3.3. Meta-analysis of contrast-specific neural correlates of conscious visual processing

To examine reliable contrast-specific neural correlates associated with conscious visual processing, we performed the following three contrasts: (i) conscious > unconscious, (ii) conscious percept > competing percept (not currently consciously seen) and (iii) conscious > preconscious. Brain regions that showed consistent activation during conscious visual processing when contrasted with unconscious visual processing were the bilateral inferior frontal junction (IFJ), left intraparietal sulcus (IPS), left dorsal anterior cingulate cortex (dACC) and bilateral anterior insula (aINS). On the other hand, a conscious visual percept contrasted with a competing visual percept (not currently seen) induced activation in the right intraparietal sulcus. Finally, the left inferior lateral occipital cortex showed consistent activation during conscious visual processing contrasted with preconscious visual processing.

Coordinates of the activation maxima and cluster size as well as the number of studies and foci contributing to the activated brain regions of all three contrasts respectively are given in Table 4. See the corresponding Fig. 4 for visualization of the activated brain areas projected onto a surface map and corresponding axial slices.

Table 4 – Brain regions showing consistent activation during conscious visual processing tasks for conscious contrasted with unconscious, a competing percept and preconscious visual processing, respectively. For each cluster, brain region label, hemisphere, MNI coordinates, ALE maxima, cluster number and size (mm3), and number of studies and foci are provided.

Brain regions	**Hemi**	**x**	**y**	**z**	**ALE max.**	**Cluster Number**	**Volume (mm3)**	**N studies (foci)**
Contrast 1 - Conscious contrasted with unconscious p<0.001								
Dorsal anterior cingulate	L	-4	10	48	0.022332	1	2368	8(10)
Intraparietal Sulcus	L	-44	-52	52	0.023751	2	1608	5(7)
Anterior Insula	R	34	22	-4	0.029784	3	1448	6(7)
Inferior Frontal Junction	R	48	10	28	0.017296	4	984	5(5)
Inferior Frontal junction	L	-46	8	34	0.022136	5	976	4(4)
Anterior Insula	L	-30	24	-4	0.01911	6	896	4(4)
Contrast 2 - Conscious contrasted with a competing percept (not currently conscious) p<0.001								
Intraparietal Sulcus	R	28	-50	46	0.01532	1	2656	10(10)
Contrast 3 - Conscious contrasted with preconscious p<0.05								
Inferior lateral occipital cortex	L	-40	-86	-4	0.008233	1	24872	4(10)

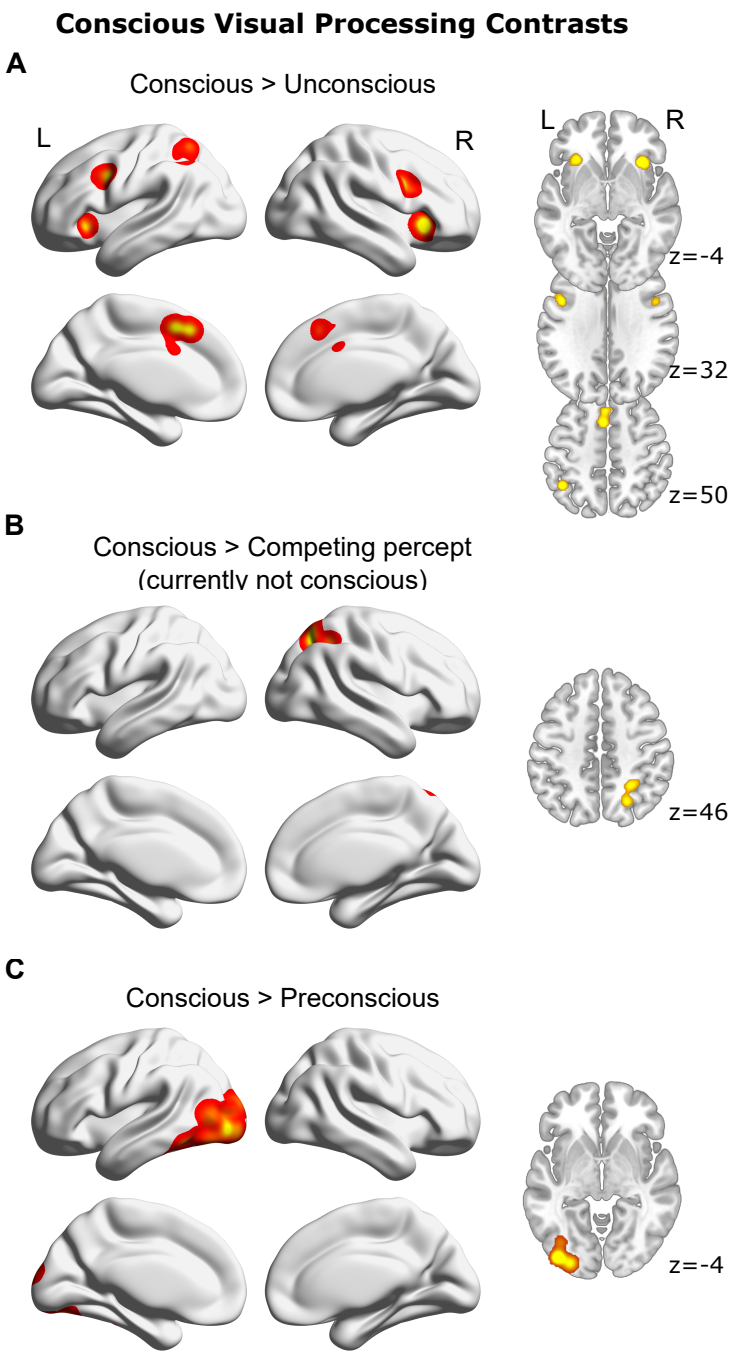

Figure 4 – Activation likelihood estimation maps showing significant convergent activity during conscious visual processing for conscious contrasted with unconscious, a competing percept and preconscious visual processing, respectively.

Fig. 4 (continued). Surface maps of the ALE clusters are shown for A. Conscious contrasted with unconscious visual processing (21 studies, 375 subjects, 219 foci), B. Conscious percept contrasted with a second competing percept (not currently conscious) (18 studies, 236 subjects, 161 foci) and C. Conscious contrasted with preconscious visual processing (6 studies, 81 subjects, 44 foci). Results (thresholded at $p < 0.001$ for A and B; $p < 0.05$ for C, FWE cluster-level corrected at $p < 0.05$) are shown on inflated surface maps in BrainNetViewer, projected over the MNI152 atlas. Five axial slices corresponding to the same activated clusters are shown using MRIcroGL for visualization purposes. See Table 4 for coordinates.

3.4. Neurosynth decoder- Cognitive terms associated with the patterns of functional activation

Using the Neurosyth decoder function, we provide reverse inference into the cognitive processes associated with the results of the two meta- analyses for conscious and unconscious visual processing. We performed functional decoding of the results by comparing the unthresholded ALE map with the term-based statistical maps of all neuroimaging studies included in the Neurosynth database. A list of neurocognitive terms and their corresponding correlation values was generated. The significant activated clusters from the first meta-analysis on conscious visual processing were associated with terms including working memory (i.e., the strongest correlation: r = 0.34), visual, attention and cognitive control. See Fig. 5 for data visualization of the word cloud including 30 terms. The significant activated clusters from the second meta-analysis on un- conscious visual processing were associated with terms including visu- ally presented, retrieval and rest. See Fig. 6 for data visualization of the word cloud including 14 terms.

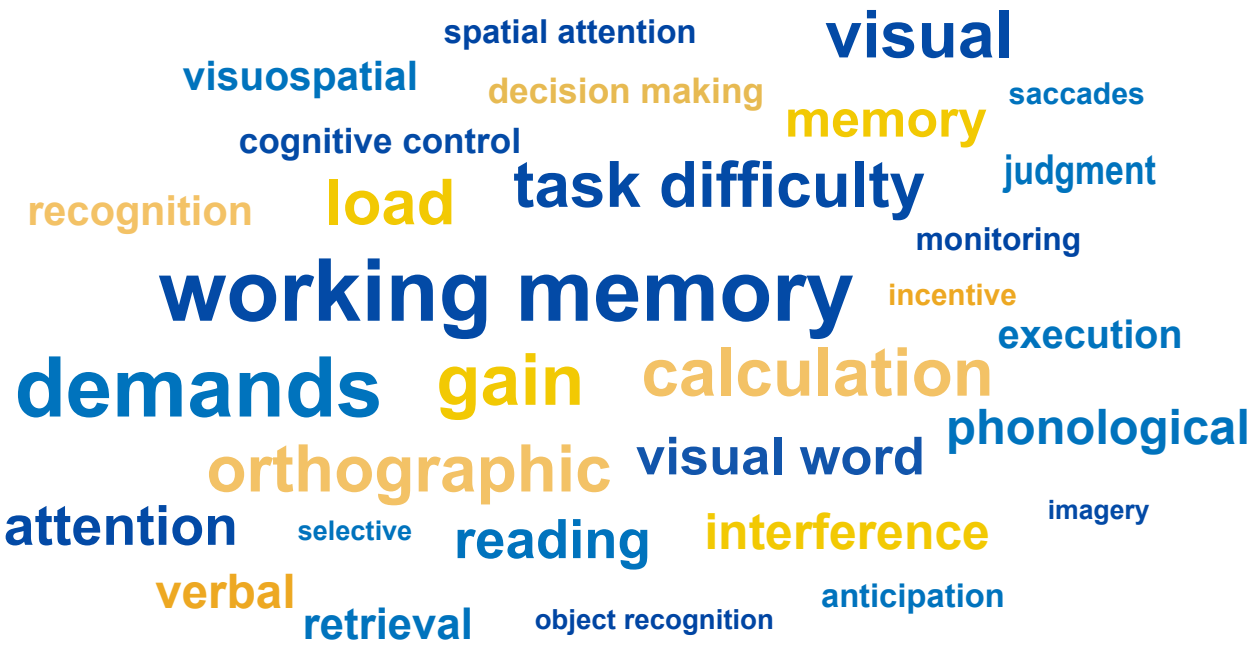

Figure 5 – Decoding of the ALE map for conscious visual processing using Neurosynth decoder displayed on a word cloud. Neurosynth decoder was used to compare the unthresholded ALE map (Meta-analysis 1) with statistical maps in the Neurosynth database (1,307 terms generated). The terms that were the most correlated with the patterns of functional activations corresponding to the meta-analysis on conscious visual awareness are shown above. Relative correlation strength is represented by font size.

Figure 6 – Decoding of the ALE map for unconscious visual processing using Neurosynth decoder displayed on a word cloud. Neurosynth decoder was used to compare the unthresholded ALE map (Meta-analysis 2) with statistical maps in the Neurosynth database (1,307 terms generated). The terms that were the most correlated with the patterns of functional activations corresponding to the meta-analysis for unconscious visual processing are shown above. Relative correlation strength is represented by font size.

4. Discussion

We conducted two main coordinate-based meta-analyses of conscious and unconscious visual perception neuroimaging studies featuring a variety of task designs. The first meta-analysis of conscious visual awareness revealed reliable activation in a constellation of regions including the inferior frontal junction in addition to the intraparietal sulcus, dorsal anterior cingulate, angular gyrus, temporo-occipital cortex and anterior insula. Conscious visual awareness was associated with high-level cognitive processes such as attention, cognitive control and working memory. The second meta-analysis of unconscious perception rather reliably involved the superior lateral occipital complex in addition to the precuneus and intraparietal sulcus.

4.1. Neural bases of conscious visual processing

The first neuroimaging meta-analysis focused on conscious awareness. We demonstrate a distribution of regions commonly engaged across numerous standard task designs, thus bringing forth convergent reliable activation associated with the neural correlates of conscious awareness. As common brain regions are known to be recruited by a broad range of cognitive demands (Duncan & Owen, 2000), we will discuss how the identified regions can be further mapped onto high-level cognitive processes, as revealed through functional decoding using Neurosynth.

First, the inferior frontal junction, a region within the prefrontal cortex and a main cluster in the meta-analysis, is a central component associated with top-down modulation of attention to visual features in addition to being engaged during cognitive control and working memory (Baldauf & Desimone, 2014; Bedini & Baldauf, 2021; Sundermann & Pfleiderer, 2012; Zanto et al., 2011). Moreover, neuroimaging studies have demonstrated an increase in the functional activity of the inferior frontal junction for a diverse range of complex behaviours and cognitive demands, positioning it in the multiple-demand system of the brain, thus capable of integrating a myriad of cognitive operations (Assem et al., 2020; Duncan, 2010; Fedorenko et al., 2013), with a clear reliable activation for conscious visual awareness

as demonstrated by the results. Moreover, the intraparietal sulcus, involved in higher visual functions such as perceptual grouping responses (Dehaene et al., 2003; Yokoi & Komatsu, 2009), is also recruited via the dorsal attention system and associated with spatial attention, attentional shifting, context-dependent working memory and a core contributor to numerical cognition (Dehaene et al., 2003; Gillebert et al., 2011; Power et al., 2011; Velenosi et al., 2020; Yantis et al., 2002). The angular gyrus, located in the posterior part of the inferior parietal lobule, is associated with multiple cognitive concepts including consciousness as well as attention, memory retrieval, and semantic cognition (Humphreys et al., 2021; Seghier, 2013). The dorsal anterior cingulate cortex is a key region implicated in domain-general executive control functions, such as cognitive control in addition to reward-based decision making (Rushworth et al., 2012; Shenhav et al., 2013; Shenhav et al., 2016). The insula, known for processing visually salient or novel stimuli, also contributes to high-level cognition with the anterior portion associated with cognitive control in addition to perceptually difficult tasks involving content uncertainty, decision making, conscious perception of error and performance monitoring(Engstrom et al., 2014; Uddin et al., 2017; Ullsperger et al., 2010). Collectively, as expected, the reverse inference results corroborate with studies suggesting a covariance between the underlying neural activity of perceiving conscious content with visual attention in addition to cognitive control (for for reviews see Martin-Signes et al., 2019; Persuh et al., 2018; Pitts et al., 2018) and updating visual representations in working memory (Soto & Silvanto, 2014). Though the nature of the reliable activations can be partially understood by the interplay of these cognitive demands, the results demonstrate emerging neural activity consistently associated with conscious awareness and underline a potential common ground with higher-level cognitive processes.

We further characterized the identified regions according to experimental design and the state of perceptual processing required to complete standard tasks by performing three meta-analytical contrasts to compare conscious visual processing with (1) unconscious processing, (2) a competing percept (not currently seen), and (3) preconscious visual processing. Compared to the full sample, the first contrast highlights similar activity in the bilateral inferior

frontal junction in addition to the intraparietal sulcus, dorsal anterior cingulate and bilateral anterior insula. The inferior frontal junction is solely recruited in this first of three contrasts, implying frontal regions don't reliably surface during unconscious processing and may have a crucial role in enabling conscious awareness to arise (for a review see Mashour et al., 2020) and be interlinked with the multiple higher-level cognitive demands at play (see a review by Tsuchiya et al., 2015). Next, contrasting a first conscious percept to a second competing percept (not currently seen) led to reliable activation in the intraparietal sulcus, as expected given its association with attentional shifts (Yantis et al., 2002) and the cognitive requirements for performing bistable perception tasks where participants typically alternate between two percepts. Finally, isolating conscious from preconscious perception elicited reliable activations in the inferior lateral occipital complex, a sub-peak of the full sample and a region involved in visual perception of simple visual features, object recognition, visual awareness of objects and perceptual processing during inattentional blindness (Amedi et al., 2001; Grill-Spector et al., 2001; Hutchinson, 2019; Lindh et al., 2019; Pitts et al., 2012). Conscious contrasted with preconscious perception reveals a tendency for greater occipital cortex activation, as opposed to when contrasted with unconscious perception. The absence of strongly activated clusters in occipital areas is expected when contrasting conscious to unconscious perception as these regions are recruited during both states (de Graaf et al., 2012) and thus isolated during the contrast. While sustaining visual representations requires recurrent processing of neural signals, it has mainly been associated with conscious visual awareness (V. A. Lamme, 2006a). Preconscious perception is rather thought to be driven by a relatively early feedforward sweep (V. A. F. Lamme, 2006b), yet the neural signal may not reach higher-order association areas, resulting in a lack of feedback and limited enhancement of activation in occipital areas. Thus, the difference of activation within these regions would reliably surface when contrasting conscious with preconscious perception. Moreover, the results suggest that unconscious perception may rely more on occipital regions during visual processing compared to preconscious perception. This could be associated with unconscious perception processing a constant flow of visual information (Kouider et al., 2010) and perceptual representations perhaps enhanced by recurrent processing, whereas preconscious

perception is rather associated with a transitory state of activity preceding visual awareness (Dehaene et al., 2006). Given that a more conservative threshold was applied when contrasting conscious to unconscious perception compared to when contrasting preconscious perception, and that the experiments associated with the conscious state are independent, the speculations provided directly comparing the two contrasts as well as the unconscious and preconscious states should be nuanced and would require further investigation. The experimental design manipulations for each specific meta-analytical contrast highlight distinct contributing perceptual and cognitive processes potentially associated with different representations of the conscious state. Nevertheless, the identified regions are spatially coherent with the reliable patterns of activation of the full sample of studies for conscious visual processing, as expected as each contrast includes a subset of the experiments, and can account for a more comprehensive framework of conscious visual awareness.

4.2. Neural bases of unconscious visual processing

The second neuroimaging meta-analysis focused on unconscious visual processing and revealed consistent functional activity. First, the lateral occipital cortex has been observed under conditions of inattentional blindness without awareness (Hutchinson, 2019) and recruited during implicit processes, such as implicit memory encoding (H. Kim, 2019). This region is thought to receive feedforward visual input from the early visual cortex, linked to unconscious processing, and feedback from higher-level areas, linked to conscious processing. Feedback processes are known to modify visual representations, resulting in less overlap between the two associated perceptual states (Dijkstra et al., 2021). Although the results of the current study show the lateral occipital cortex activating for both, the inferior division seems preferably recruited in association with conscious processing and the superior division with unconscious processing. Cytoarchitectural differences have been reported in the lateral occipital cortex (Malikovic et al., 2016); however, the link between the anatomy and function of these subdivisions has yet to be fully understood. Future studies exploring how feedback processes modify visual representations could further investigate the anatomic dissociation

between the superior and inferior division of the lateral occipital complex. Both the precuneus and intraparietal sulcus were identified as activated clusters in a meta-analysis of unconscious visual perception in blindsight patients (Celeghin et al., 2018). The precuneus is more specifically implicated in visual processing and object priming as well as unconsciously storing an abstract intention until it reaches awareness (Koutstaal et al., 2001; Soon et al., 2008; Soon et al., 2013). Despite the involvement of the precuneus in multiple cognitive functions, including visuo-spatial imagery, episodic memory retrieval and attention, it has been shown to be prominently active during rest and is prone to task-induced deactivation, presumably reflecting the brain's ability to dynamically reallocate resources as required (Cavanna & Trimble, 2006; Gusnard & Raichle, 2001). Moreover, damage to the regions associated with unconscious visual processing in the current work is thought to result in symptoms apparent to the Balint syndrome, notably characterized by disruptions in orienting attention and the inability to perceive more than one object at a time, known as simultanagnosia (Balint, 1909; Cavanna & Trimble, 2006). While the precise link between these regions and the role of unconscious visual processing in the Balint syndrome is yet to be fully understood, this could be considered for future cognitive investigation. Although an active research area, the understanding of unconscious processing is limited, and this is effectively conveyed through the weaker correlation scores between the Neurosynth terms and the ALE map. This highlights the need for additional cognitive experiments to investigate the association of the functional activations related to unconscious processing with cognitive states such as rest, memory retrieval as well as relevant modulations in cognitive and perceptual abilities. Although the left hemisphere activation and decoder also presumably reflect the nature of the subliminal language tasks (e.g., implicit letter or word processing) used by five contributing studies, the results attest to the neural activity consistently associated with unconscious processing as the cluster is not unique to language areas. As aforementioned, the intraparietal sulcus is a key contributor to the dorsal attention system (Power et al., 2011) and attention presumably serves as a 'gateway' to regulate which information reaches conscious awareness (Dehaene & Changeux, 2011; Nani et al., 2019). The results show the intraparietal sulcus as a subpeak for unconscious perception and at the forefront of conscious

perception, further demonstrating that regions associated with conscious vs. unconscious perception (or vice versa) are not mutually exclusively engaged, rather they are differentially activated. Common regions differentially activated across the distinct meta-analyses may also suggest the modulation of functional activity along with the extent of conscious or unconscious processing. Further research is required to investigate whether these modulated regions hold a pivotal role in enabling visual information to reach conscious awareness.

Moreover, the lack of activated clusters in primary visual areas was expected, as recruitment of these regions is thought to be a prerequisite for conscious visual processing (de Graaf et al., 2012) and this meta-analysis includes studies isolating it out. Conversely, the absence of primary visual areas in the resulting statistical map from the full sample of studies associated with conscious visual processing is also coherent as this meta-analysis isolated out matched nonconscious control conditions, in particular when considering the contrast conscious versus unconscious visual processing. This coheres with a study demonstrating both perceived and not perceived stimuli eliciting activation in V1 and V4 in monkeys, with only perceived stimuli leading to frontal activity suggesting that the visual signal associated with unconsciously perceived stimuli weakens in the successive visual stages en route from the visual to the frontal cortex (van Vugt et al., 2018). Albeit, primary visual areas are not necessary for unconscious perception as shown through V1 lesion studies, where blindsight patients have reduced or absence of visual qualia in the blind field which is thought to be a form of unconscious perception(Celeghin et al., 2018; Weiskrantz, 1996). This type of unconscious processing has also shown to engage an alternative pathway including subcortical structures such as the superior colliculi and pulvinar (Tran et al., 2019). In this current study, the absence of midbrain structures was expected given the spatial resolution of the whole brain data extracted from the included studies. However, the involvement of these regions during unconscious visual processing can not be excluded and would require future studies to adapt fMRI acquisition parameters to increase spatial resolution. All told, the findings essentially underscore that unconscious perception also elicits regions beyond the

primary visual areas, incidentally further in the visual hierarchy. The results combine functional characterization and robust activation analyses, seeking to contribute to consolidating the knowledge of the neural and cognitive building blocks of unconscious perception.

In brief, the current work validates a previous meta-analysis consisting of 19 studies (Bisenius et al., 2015), and extends beyond by systematically searching five online data bases, accounting for recent advances, new studies encompassing a total of 54 independent studies, various experimental methods and task designs, a first main meta-analysis of 45 studies (comprising 409 foci, 704 subjects) associated with conscious visual awareness and further distilling the implications of conscious awareness in relation with either an unconscious, competing or preconscious percept with 3 novel meta-analytical contrasts. In addition, a novel second main meta-analysis was performed to quantitatively reveal reliable activation associated with unconscious perception (16 studies, 262 subjects, 90 foci). Finally, this was conducted along with implementing cognitive decoding to characterize the functional activation associated with conscious and unconscious visual perception respectively in comparison with over 14,300 studies and providing insight on the prominent theories of consciousness which we will discuss next.

4.3. Contributions to theories of conscious awareness

Leading theories of conscious awareness dive into the behavioural and functional mechanisms by which the brain renders a visual percept conscious. In doing so, they formulate hypotheses with regards to sensory areas encoding stimulus content as a prerequisite (Levinson et al., 2021) and whether information is broadcast past these areas to elicit a conscious percept (Mashour et al., 2020). A meta-analysis is particularly well positioned to address these main hypotheses and identify convergent activation across the bulk of various evidence coming from experimental cognitive neuroscience. The field currently brings forth the global neuronal workspace theory (GWT), recurrent processing theory (RP), higher-order thought theory (HOT) and integrated information theory (IIT). The GWT (Dehaene & Naccache, 2001) is empirically consistent with the results for conscious visual processing. The model

describes a large-scale network comprising many brain regions, in which prefrontal and parietal cortices hold a key, yet not exclusive, role to conscious access. A nonlinear network 'ignition', in which neuronal representations are rapidly amplified and sustained, enables access to the global workspace. Consistent with the results from the current study, conscious perception seems linked with visual information broadcast past sensory cortices and involving higher-level cortical association areas. For unconscious processing, we demonstrate the involvement of the superior lateral occipital complex in addition to the intraparietal sulcus and precuneus, thus driving the activation outside the primary sensory cortices. Visual stimuli are thought to remain unconscious due to a lack of long-range synchrony within the global workspace combined with a quickly decaying neural signal (Dehaene et al., 2006; Melloni et al., 2007). The results in this study suggest that the visual signal may decay during its transmission beyond the visual cortex as reliable activations of the visual cortex associated with the unconscious state were found. In contrast, during the conscious state, a more robust signal would presumably be transmitted to higher-order association areas. While the results suggest a divergence in the neural signatures associated with both states, the exact mechanism responsible for the visual cortex signal's decay, including the neural signal's strength and duration during the unconscious state still requires investigation. Unconscious and conscious visual processing are also thought to be modulated by the content of the visual input and the attentional load (Fang & He, 2005; Y. Jiang & He, 2006; Levinson et al., 2021; Mashour et al., 2020; Song & Yao, 2016). Both the recurrent processing theory, where the content of consciousness depends on what recurrent neurocognitive circuits are activated (V. A. Lamme, 2010; V. A. F. Lamme, 2006b), and global workspace theory postulate that feedforward and feedback from higher to lower-order areas are necessary for conscious processing to occur, the latter proposing a more extensive map of recurrent loops comprising frontal-parietal regions (Mashour et al., 2020). The meta-analytical results from the current study show certain regions to be differentially activated along with conscious and unconscious visual processing, such as the intraparietal sulcus, which suggests that recurrent neurocognitive circuits amplify the strength of neuronal representations within this

region for conscious access. Higher-order thought theory proposes mental content to be conscious when a lower-order representation of visual signals (in early visual areas) enters a higher-order meta-representation, mainly associated with the prefrontal and parietal cortex (Brown et al., 2019; Lau & Rosenthal, 2011). Integrated information theory (IIT) proposes a mathematical framework to characterize phenomenology, related to one's conscious subjective experience (Tononi, 2008, 2012; Tononi et al., 2016). The task designs included in the current study such as masking, bistable perception and attentional blink do not provide insight on phenomenology, which proves challenging to measure empirically (Mashour et al., 2020). Attempting to adjudicate experimentally across these prominent theories is intricately complex as they share important features, enabling interpretation of results to bend towards more than one, differ in terms of abstract conceptualization and thus testability, leading to respective or unbalanced amounts of empirical support. Although they hold some inconsistencies (for main similarities and differences, see Mashour et al., 2020; Seth & Bayne, 2022), given that these neuroscientific hypotheses are not mutually exclusive, relevance for practical scientific progress perhaps lies in incorporating pieces of these theories into a viable more comprehensive account of the neural basis of consciousness. For instance, prefrontal and parietal cortices might be activated –though not exclusively- and rely in part on attentional processes when content is conscious (GWT), while recurrent neurocognitive circuits might amplify the strength of neuronal representations within these regions for conscious access (RP), and this state may be accompanied by appropriate higher-order meta-representational states (HOT), whilst the content is conscious when incorporated into information complexes (IIT). Further combining elements of these theories and viewing them as describing different states of the same underlying process may ultimately outline a blueprint for characterizing the emergence of consciousness.

4.4. Limitations

The meta-analyses revealed reliable activation in regions pertaining to conscious and unconscious visual processing across previously published functional neuroimaging studies, yet important limitations need to be considered. First, the inclusion in the analyses of

heterogeneous designs, stimuli, fMRI acquisition parameters and analysis pipelines should be considered when interpreting results. Nevertheless, neuroimaging meta-analyses commonly compare studies across different control conditions or baselines (Salimi-Khorshidi et al., 2009; Wager et al., 2009). Second, we did not include studies using affective paradigms, such as fear processing, as they are known to elicit activations of different structures (e.g., amygdala) (for a meta-analysis see Tao et al., 2021). Therefore, inferences can not be generalized to emotional conscious or unconscious processing paradigms. Third, as we pooled coordinates across published studies, this study is subject to publication bias (i.e., the tendency to publish significant positive results) as well as the potential small sample size and low statistical power of the individual fMRI studies that can lead to inflated effects and false interpretations of the results (Button et al., 2013). However, in the ALE meta-analyses of this study, results from small sample size studies are represented with wider Gaussian distribution properties as opposed to results from larger sample size studies (Eickhoff et al., 2009). Moreover, performing a meta-analysis is the most efficient approach to aggregate significant activated regions across studies and provide a better estimate of the true effect. Although fMRI data from this study doesn't provide temporal unfolding of information processing across networks of neurons, which would require different acquisition and analysis techniques, the results offer insight as to what brain regions reliably surface from the underlying neural computation. Despite these limitations, the current study provides an empirical foundation for further studies to investigate visual information processing pertaining to conscious and unconscious visual processing.

5. Conclusion

The meta-analysis on neuroimaging studies of conscious visual processing reveals reliable patterns of functional brain activity distributed across structures located higher up in the visual hierarchy, including the inferior frontal junction in addition to the intraparietal sulcus, dorsal anterior cingulate, angular gyrus, temporo-occipital cortex and anterior insula. Neurosynth revealed an overlap of the identified functional patterns of conscious awareness with those related to attention, cognitive control and working memory, suggesting a common ground between higher-level cognitive processes. The meta-analysis of unconscious visual processing reveals reliable activations in the superior lateral occipital cortex, in addition to the intraparietal sulcus and precuneus. The results provide evidence to empirically support and incorporate certain features of prominent theories of the neural basis of consciousness, whilst ultimately yielding space for how we define conscious awareness and unconscious perception to emerge over time.

Data and code availability statement

All data are accessible within the studies cited in Table 1. Extracted coordinates and foci are available from the corresponding author upon request. All unthresholded ALE images of this current study have been uploaded to Neurovault and can be found here: https://neurovault.org/collections/ZWFXMQJB/ All data were analyzed with software publicly available from http://www.brainmap.org/ and https://neurosynth.org/

Author Contributions

Michèle W. MacLean (Conceptualization, Project administration, Methodology, Investigation, Formal analysis, Data curation, Visualization, Writing – Original Draft, Contrast selection - Review & Editing, Writing – Review & Editing); Vanessa Hadid (Conceptualization, Data curation (Review & Editing of Contrast selection), Writing – Review & Editing); R. Nathan Spreng (Methodology, Writing – Review & Editing, Supervision); Franco Lepore (Supervision).

Funding

Project administration was supported by the Canada Research Chair Program RGPIN-8245-2014 [FL]; and the Natural Sciences and Engineering Research Council of Canada RGPIN/05053-2014 [FL]; and the Canadian Institutes of Health Research 166197 [FL] grants. MWM was supported by a salary award from Fonds de Recherche Nature et Technologies (FRQNT).

Declarations of interest:

none.

Ackowledgements

We would like to thank Nathalie Clairoux, librarian from l'Université de Montréal, for reviewing and validating the search string for the systematic literature search.

Chapter 3

Article 2

Neuronal mechanisms of motion detection underlying blindsight assessed by functional magnetic resonance imaging

(Co-first author) Antonin Tran[1,3,*], **Michèle W. MacLean**[1,2,*], Vanessa Hadid[1,3,*], Latifa Lazzouni[1,2], Dang Khoa Nguyen[3,6], Julie Tremblay[5], Mathieu Dehaes[4] and Franco Lepore[1,2]

(1) Centre de recherche en neuropsychologie et cognition (CERNEC), Université de Montréal, Québec, Canada

(2) Département de Psychologie, Université de Montréal, Montréal, Québec, Canada

(3) Département de Sciences Biomédicales, Université de Montréal, Montréal, Québec, Canada

(4) Département de Radiologie, Radio-Oncologie et Médecine Nucléaire, Université de Montréal, Montréal, Québec, Canada

(5) Centre Hospitalier Universitaire Sainte-Justine, Montréal, Québec, Canada.

(6) Centre Hospitalier de l'Université de Montréal, Montréal, Québec, Canada

Published: **(Co-first author)** Tran, A.*, **MacLean, M.W.***, Hadid, V.*, Nguyen, D.K., Lazzouni, L., Tremblay, J., Dehaes, M.**, Lepore, F**. (2019). Neuronal mechanisms of motion detection underlying blindsight assessed by functional magnetic resonance imaging. *Neuropsychologia.* doi.org/10.1016/j.neuropsychologia.2019.02.012

*Selected as part of the special issue: Neural Routes to Awareness in Vision, Emotion and Action: A tribute to Larry Weiskrantz.

Abstract

Brain imaging offers a valuable tool to observe functional brain plasticity by showing how sensory inputs reshape cortical activations after a visual impairment. Following a unilateral post-chiasmatic lesion affecting the visual cortex, patients may suffer a contralateral visual loss referred to homonymous hemianopia. Nevertheless, these patients preserve the ability to unconsciously detect, localize and discriminate visual stimuli presented in their impaired visual field. To investigate this paradox, known as blindsight, we conducted a study using functional magnetic resonance imaging (fMRI) to evaluate the structural and functional impact of such lesion in a 33-year old patient (ML), who suffers a complete right hemianopia without macular sparing and showing strong evidences of blindsight. We thus performed whole brain and sliced thalamic fMRI scan sequences during an event-related motion detection task. We provided evidence of the neuronal fingerprint of blindsight by acquiring and associating neural correlates, specific structures and functional networks of the midbrain during blindsight performances which may help to better understand this condition. Accurate performance demonstrated the presence of residual vision and the ability to unconsciously perceive motion presented in the blind hemifield, although her reaction time was significantly higher in her blind-field. When the normal hemifield was stimulated, we observed significant contralateral activations in primary and secondary visual areas as well as motion specific areas, such as the supramarginal gyrus and middle temporal area. We also demonstrated sub-thalamic activations within the superior colliculi (SC) and the pulvinar. These results suggest a role of secondary subcortical structures in normal spontaneous motion detection. In a similar way, when the lesioned hemifield was stimulated, we observed contralateral activity in extrastriate areas with no activation of the primary lesioned visual cortex. Moreover, we observed activations within the SC when the blind hemifield was stimulated. However, we observed unexpected ipsilateral activations within the same motion specific areas, as well as bilateral frontal activations. These results highlight the importance of abnormal secondary pathways bypassing the primary visual area (V1) in residual vision. This reorganization in the structure and function of the visual pathways correlates with behavioral changes, thus offering a plausible explanation for the blindsight phenomenon. Our results may potentially

impact the development of rehabilitation strategies to target subcortical pathways. Keywords: Functional magnetic resonance imaging (fMRI), Blood oxygenation level dependent (BOLD), Event-related motion detection paradigm, Homonymous hemianopia, Blindsight, Neuroplasticity

Highlights

(1) Unconscious, yet accurate motion detection in a cortically blind individual.;

(2) Midbrain fMRI data acquisition during blindsight performances.;

(3) Cortical blindness alters BOLD activations of motion specific areas.

(4) Blindsight elicits sub-thalamic BOLD activations within the superior colliculi and pulvinar.

(5) Specific subcortical pathways process visual information in the blindfield.

1. Introduction

Blindsight is the ability to detect, localize, and discriminate objects presented in the blind hemifield without having consciousness of seeing the objects (Weiskrantz, 1996). The term was first coined in the 1970's (Sanders et al., 1974; Weiskrantz et al., 1974) and the phenomenon has since raised strong interests in cognitive neuroscience as it notably portrays a rare case of dissociation between conscious awareness and performance (Berlucchi, 2017; Hadid & Lepore, 2017; Heeks & Azzopardi, 2015). Blindsight also offers a natural and unique experimental platform to understand the neuronal architecture of the visual system while integrating anatomical, functional and behavioral evidence (Tamietto & Morrone, 2016). Investigating residual vision in blindsight is key to gain a better understanding of the human visual system as it reveals neuronal mechanisms that likely contribute to normal vision (Ajina & Bridge, 2017). Damage to the primary visual cortex (V1) may result in clinical blindness, yet sheds light on parallel subcortical pathways that bypass V1 and harness residual vision abilities (Tamietto & Morrone, 2016). Previous studies showed a wide variety of abilities and residual functions including shape discrimination or object recognition

(Trevethan et al., 2007; Van den Stock et al., 2015; Van den Stock et al., 2014; Weiskrantz, 1987), color perception (Kentridge et al., 2007; Morland et al., 1999), emotional content or face recognition (Bertini et al., 2013; Celeghin et al., 2015; Gerbella et al., 2017; Pegna et al., 2005; Van den Stock et al., 2011), actions towards, manual localization or spontaneous anti-pointing of unseen targets (de Gelder et al., 2008; Smits et al., 2018), processing gaze direction Burra2013, accurately performing a mental imagery task (de Gelder et al., 2015) and motion processing or discrimination (Grasso et al., 2018; Hervais-Adelman et al., 2015). Distinct residual behaviours, or patients' abilities regarding the blind-field, have led to various taxonomies such as: action-blindsight, known as the ability to correctly act upon blind-field stimuli (i.e. visuo-motor abilities, such as saccades or pointing); attention-blindsight, when abilities rely upon allocating sufficient attention to the blind-field and affective-blindsight, referring to the ability to respond accurately to emotionally salient visual stimuli (Celeghin et al., 2015; Cowey, 2010; Danckert & Rossetti, 2005; de Gelder et al., 1999). Finally, previous works provided a classification of two types of blindsight: Type 1, where the subject has no awareness or conscious perception, and Type 2 blindsight, where the subject has awareness of visual presentation in the blindfield without visual qualia (see review in Leopold, 2012; Weiskrantz, 1990).

Representing over half of a million Americans, homonymous hemianopia (HH) patients frequently demonstrate blindsight abilities. HH refers to a post-chiasmatic lesion of the primary visual cortex (V1), in the right or left hemisphere, leading to contralateral cortical blindness (Barleben et al., 2015; Leh et al., 2008). Most commonly caused by a stroke, HH represents the leading cause of cortical deficits causing visual field loss and resulting in a significantly reduced quality of life (see reviews in Goodwin, 2014; C. Perez & Chokron, 2014; Urbanski et al., 2014). Following this post-chiasmatic lesion, neuronal plasticity with various degrees of structural and physiological adaptation, and major changes in brain circuitry were previously observed: 1) loss of function in the impacted region (Binda et al., 2013), 2) reinforcement of spared pathways or formation of new pathways to strengthen the original connections (Bridge et al., 2008), and 3) emergence of new or modified functions (de Gelder et al., 2008). While occipital cortical connectivity may change following a lesion, this plasticity

is seldom associated with regaining of visual function. However, when subcortical – thus unconscious – visual processing emerges, restoration therapies might be calibrated to exploit these alternative pathways (see meta-analysis in G. A. de Haan et al., 2014). In particular, neuroimaging studies on patients with visual field defects demonstrated a reorganization of the cerebral neuronal networks following visual training (see review in C. Perez & Chokron, 2014).

Specific to the performance of blindsight in the absence of V1, on the one hand there is evidence of a connection between the lateral geniculate nucleus (LGN) and visual area 5 as well as the middle temporal areas (V5/MT+) involved in motion processing (Ajina et al., 2015b; Hervais-Adelman et al., 2015). On the other hand, experiments have suggested the implication of the superior colliculus (SC) in the midbrain with indirect projections to cortical extrastriate visual areas in the occipital and temporal lobes (de Gelder et al., 2008; Tamietto et al., 2010). Moreover, research models on hemispherectomized patients, (i.e. removal or disconnection of an entire hemisphere, including the occipital lobe) are relevant for eliminating the notion that blindsight is attributed to spared islands in the visual cortex and also showed the pivotal role of the superior colliculus (SC) (Georgy et al., 2016; Leh et al., 2010; Wessinger et al., 1996). Specifically, these studies demonstrate that the SC is sensitive to perceptual organization, stimulus configuration and type (e.g. achromatic) and suggest that blindsight is mediated by a collicular pathway. Results from Leh et al. (2010) suggest that hemispherectomized individuals only demonstrate blindsight abilities when the stimuli presented is visible to the SC and show that it is color blind to S-cone-isolating stimuli. This could also explain the dissociation between discriminating color and motion in blindsight Chabanat2018. Further research supports the role of the superior colliculi involved in a subcortical pathway processing information in low spatial frequency regarding emotional stimuli (Burra et al., 2017). A recent meta-analysis that considered the entire fMRI literature on blindsight reported that neural correlates and blindsight abilities are selectively linked to experimental features such as the behavioral task and specific type of stimuli used (Celeghin et al., 2018). This meta-analysis showed the relevance of moving or biologically salient stimuli to elicit subcortical activations, namely of the SC (Van den Stock et al., 2011) as

well as bilateral activations of motion sensitive area V5/MT+ (de Gelder & Hadjikhani, 2006; Van den Stock et al., 2014). In addition, research on animal models elucidated our current understanding of blindsight and provided a strong foundation for plausible new insights associating the structure and function responsible for this residual vision in humans. Studies in cats also showed implications of extrastriate areas such as (V5/MT+), the area around the Sylvian sulcus and subcortical structures (Ciaramitaro et al., 1997), as well as the pulvinar and colliculi (H. Jiang et al., 2015; Piche et al., 2015). Results on non-human primates provided evidence of a pathway connecting LGN neurons to the extrastriate cortex (Yu et al., 2018) and a direct pathway from the SC to the ventrolateral pulvinar during visually guided saccades contributing to residual vision in blindsight (Kinoshita et al., 2019). Furthermore, the SC and pulvinar in the monkey were shown to rapidly send facial information to cortical structures in a bottom-up process (Nguyen et al., 2016). Thus, subcortical pathways are thought to mediate blindsight, notably projecting from the retina to the SC and contributing to nonconscious vision (de Gelder et al., 2008; Leh et al., 2006; Morland et al., 1999; Tamietto et al., 2010). Given this body of research, we hypothesized the superior colliculi (SC) to be highly connected to motion specific areas (V5/MT+), thus acting as the second visual relay after the LGN.

Previous functional magnetic resonance imaging (fMRI) studies have suggested associations between blindsight performance, specific structures and functional networks (see meta-analysis Celeghin et al., 2018). However, the implication of subcortical structures in the functioning of residual vision in humans is yet to be fully understood. To our knowledge, this blindsight study is the first to propose the use of an event-related motion detection paradigm to measure blood oxygenation level dependent (BOLD) activations in the subcortical structures during a blindsight performance of an HH individual. Our approach included behavioral testing and imaging techniques to evaluate the structural and functional impact of the striate cortex lesion. Our goals were 1) to assess the anatomical state of the brain by imaging structures that are likely damaged by the lesion, 2) to represent cortical activations external to the lesion with fMRI whole brain analysis scan and 3) to determine the implication of subcortical structures in blindsight using an event-related fMRI design that

focused around the thalamus and the superior colliculi. Hence, we anticipated to observe an increase in the projections from the superior colliculi to the middle temporal areas acting as the second visual relay after the LGN. As the main visual pathways are lesioned, these alternative pathways could represent the underlying mechanisms of blindsight.

2. Materials and methods

This study was approved by the Comité d'Ethique de l'Unité de Neuroimagerie Fonctionnelle (UNF) of the Centre de recherche de l'Institut universitaire de gériatrie de Montréal (IUGM), Montréal, Canada.

2.1. Patient history

While being investigated for MRI signal abnormalities in the left occipital cortex and right lenticular nucleus, a 17 year-old woman developed right hemianopia following a stereotactic biopsy which was complicated by a left occipital hemorrhage (3.7cm by 3cm). Since this event, the patient (now 33 years old) has remained in good health with no cognitive and neurological deficits other than the right homonymous hemianopia without macular sparing. Notably, she reports sometimes "forgetting her things in her right field of view and bumping into objects". Vision in the left hemifield was clinically assessed and did not require any correction with surgery or lenses.

2.2. Blindsight evaluation

The patient's hemianopia and visual field evaluation Fig. 2B was provided by neurologist Dr. Dang Khoa Nguyen and a team of therapists from the Centre Hospitalier de l'Université de Montréal (CHUM). The patient underwent a first behavioral testing prior to MRI examination with stimuli presented at various eccentricities which evaluated her visual residual abilities and confirmed her visual field. The behavioral tests showed performances at chance level for static stimuli suggesting no sign of blindsight. However, when the blindfield was stimulated with moving stimuli, the patient was able to spontaneously detect the stimuli. The patient reported that she "was unable to see the moving stimulus, but she only had a

vague feeling that something just happened in her blind-field, without being able to describe it". This ability refers to Type II blindsight (see review in Leopold, 2012; Weiskrantz, 1990).

2.3. Stimuli – peripheral motion detection paradigm

Visual stimuli were presented using Presentation® software (Version 18.0, Neurobehavioral Systems, Inc., Berkeley, CA) on a screen located behind the MRI magnet and reflected through the mirror of the head coil. Prior to data acquisition, the position of the mirror was adjusted and located such that the field of view (150×110mm2) was sufficiently large to display all stimuli. Visual stimuli consisted of static dots presented bilaterally, or moving dots which moved either in the right or left hemifield with static dots presented on the other side. Three conditions were analyzed: 1) left visual motion, i.e. dots in motion on the left side of the screen, 2) static condition, i.e. static dots presented with no motion, and 3) right visual motion, i.e. dots in motion on the right side of the screen (Fig. 1).

Moving stimuli were generated using the random-dot kinematogram (RDK) model (Morrone et al., 2000). Black dots patches (8°×8°) were presented on a white background either at the left or the right of the fixation cross at 8° of eccentricity (Fig. 3). The diameter of each dot was 0.75° and the number of dots was 150. The speed of each dot was 12°/s with a limited lifetime of 150ms. The dots moved with 100% coherency. An event-related design was selected to present the three conditions. Thirty-three (33) events were distributed randomly per trial. Inter-stimulus interval (ISI) duration was 6s on average, varying following a Poisson distribution (Hagberg et al., 2001) while the duration of each stimulus was 3s. The patient was instructed to detect as fast as possible the moving dots in the left or right hemifield and report this motion using a response box. She was asked to answer using the response key on the left (represented by 1 in Fig. 1) for motion occurring in the left hemifield or using the response key on the right (represented by 2 in Fig. 1) for motion occurring in the right hemifield. The response keys were side by side on the response box. The subject's responses were always registered using the right hand on the response box. The accuracy rate and the reaction time (RT) were collected for behavioral analyses. Through the entire scanning session, none of the details about the nature of the stimuli, their duration or location

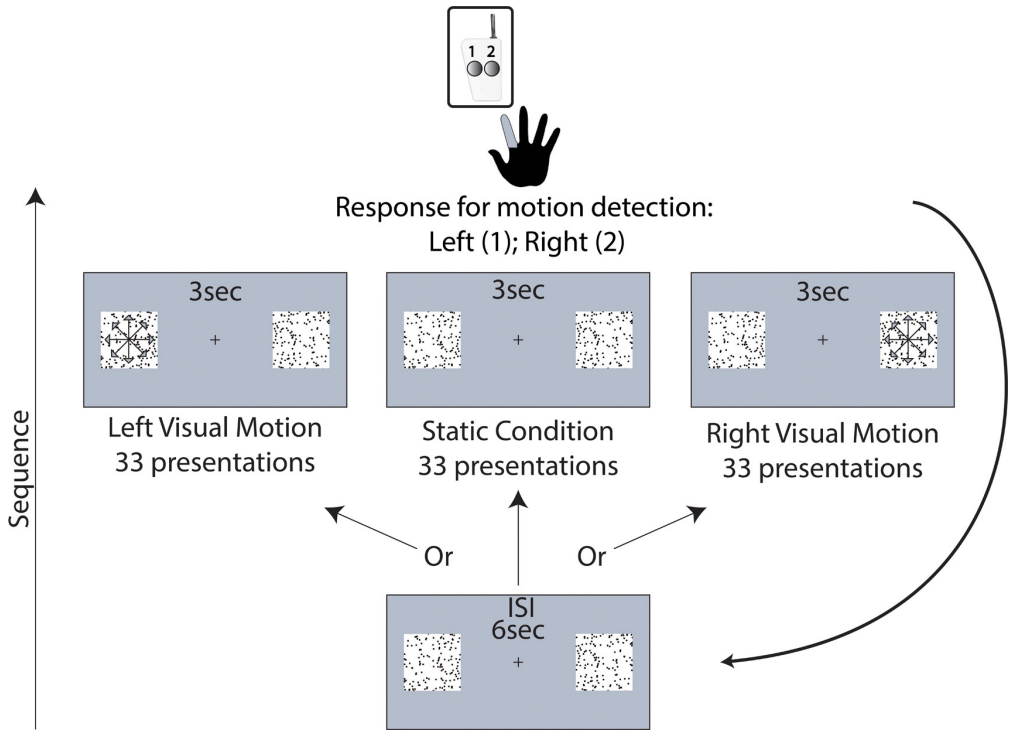

Figure 1 – Peripheral motion detection task with an event-related stimulation design. The patient was instructed to detect motion as fast as possible and respond using the response key on the left (represented by 1) for motion presented on the left (intact hemifield) or using the response key on the right (represented by 2) for motion presented on the right (blind hemifield). The task displayed three conditions (left visual motion, right visual motion and static condition). The task began by displaying the static dots at 8° of eccentricity on either side of the fixation cross. Each condition was then presented at the same eccentricity for a duration of 3s with 33 events per condition distributed randomly per trial and an interstimulus interval (ISI) average duration of 6s. The expansion motion was presented with 100% coherency and separately in each hemifield for right and left visual motion. The dots moved at 12°/s with a limited lifetime of 150ms. The arrows on the dots are there to describe the motion. Click to view the video and see the three conditions (only in Supplementary material).

were provided to the subject. After completing the scanning session, the patient's subjective feeling about the nature of the stimuli and her ability to detect them was assessed through

a semi-structured interview. She was asked about the nature of the stimuli and rated her motion detection performance on a 5-level Likert-type scale from 1 (not very confident) to 5 (very confident).

2.4. Data acquisition

Prior to data acquisition, stimuli were presented in the patient's blindfield (right hemifield) to ensure she was unable to see the visual stimuli. During fMRI scans, eye movements were recorded with a MRI-compatible optical eye-tracker device (IScan RK-464B, ISCAN Inc., Woburn, MA, USA). We ensured that the visual gaze was kept focused on the centre of the screen to consider all time-series data for analysis. MRI data were acquired with a Siemens 3T Trio system (TrioTim, version Syngo MR B17) using a 12-channel array head coil. The total scanning time was 39min which included a high-resolution T1-weighted anatomical scan of 5min as well as two fMRI sequences of 17min each, one with a field of view (FOV) of the whole brain and another one with a FOV focused on subcortical structures. The fMRI parameters of the whole brain sequence were the following: repetition time (TR) 2750ms, echo time (TE) 30ms, no delay time in TR, FOV 192×192mm2, slice thickness 3mm, spacing between slices 0mm, flip angle 90°, acquisition matrix 64×64. The fMRI scan that focused on subcortical structures was designed with 17 continuous axial interleaved slices centered on the thalamus. The position of the slices was selected manually to ensure inclusion of all subcortical structures in the FOV. The fMRI parameters for the subcortical structures sequence were the following: repetition time (TR) 1500ms, echo time (TE) 36ms, no delay time in TR, FOV 192×192mm2, slice thickness 3mm, spacing between slices 0mm, flip angle 80°, acquisition matrix 64×64. The structural T1-weighted 3D magnetization prepared rapid gradient echo sequence (MPRAGE) was acquired with the following parameters: voxel size of 1×1×1.2mm3, acquisition matrix size 240×256, flip angle 9°, TR 2300ms, TE 2.91ms, inversion time (TI) 900ms, FOV 256×256mm2, 160 slices.

2.5. Data analysis

2.5.1. Behavioral data analysis. Behavioral tests were first analyzed using IBM SPSS Statistics (IBM Corp., New York, USA, 2012). The number of correct answers for both conditions was acquired by recording each response associated with the presentation of global motion on either side. Reaction times were compared between the left and right visual motion and analyzed with t-tests. Significance level was set to $p<0.05$. We then used the signal detection theory (SDT) (Green and Swets, 1966, Macmillan and Creelman, 1991) that considers decisions as depending on subject's perceptual sensitivity to differences between stimuli (d'), as well as on subject's response criterion (or bias), which is the tendency to favor a response independently of sensitivity. Hits corresponded to the correct button press (left or right) when motion occurred; misses corresponded to an incorrect response when motion occurred (no response); correct rejections corresponded to the correct response when the static condition was presented (no response); false alarms corresponded to a button press during the static condition. We extracted the rates for each of these four parameters and calculated the subject's perceptual sensitivity (d') and response bias (C). For the response bias, C =0 would be an ideal observer. For positive C values, the participant was considered to be conservative with regards to her decisions and does not respond more often than the ideal observer. However, for negative C values, the participant was considered to make liberal decisions.

2.5.2. Whole brain fMRI data analysis. A first analysis was performed to assess cortical activations of the whole brain. Functional MRI data of the whole brain were preprocessed and analyzed with SPM12 (Statistical Parametric Mapping, Wellcome Trust Centre for Neuroimaging, London, UK) using MATLAB (MathWorks, Natick, MA, USA). Preprocessing of functional images for the three conditions included: discard of the four initial volumes (Wall et al., 2009), realignment of functional time series with the first image as a reference to correct for head motion, coregistration of functional and anatomical data with the subject's anatomy, spatial normalization in the Montreal Neurological Institute (MNI) space, and spatial smoothing with a three-dimensional isotropic Gaussian kernel (8mm full-width

at half-maximum, FWHM). Subsequent to preprocessing steps, fMRI model specification was performed. Changes in brain regional responses were modeled using the convolution of a boxcar function (onsets and duration of stimulation) and the canonical hemodynamic response function (HRF). The general linear model was used to account for changes in brain response explained by changes in the experimental conditions. Movement parameters derived from realignment of the functional volumes (translations and rotations around the three directions) were also included. Removing artefactual low-frequency trends was performed using high-pass filtering with a discrete cosine basis function and a cut-off period of 128s. Statistical parametric maps were generated for the main effects of the visual stimulation, i.e. the left and right visual motion conditions. Next, both the left and right visual motion conditions were respectively contrasted by the static condition. In addition, analysis was performed for movement presented on one side (left or right) contrasted by movement on the opposite side combined with static images (defined by the left and right contrast, respectively). Further analysis was performed to describe common regions activated by the combination of the main left and right visual motion conditions. Statistical inferences were adjusted for multiple comparisons with the family-wise error (FWE) correction for the entire brain volume, a standard correction within the SPM12 software accounting for false positives. As FWE thresholds use corrected p-values, the probability of a false positive at each voxel corresponds to the p-value, i.e. $p<0.05$. One sample t-tests were performed for the left and right visual motion conditions separately. Paired sample t-tests were performed for each contrast: 1. [left-static] stimuli; 2. [right-static] stimuli; 3. left contrast; 4. right contrast; 5. common regions. We labeled significant clusters with structural neuroanatomy information using an available brain atlas (Tzourio-Mazoyer et al., 2002) to ease the location and identification of activated regions. The results of the analyses were also presented through a list of regions showing significant activations for each condition and contrast. However, to enhance spatial accuracy and visualization of activated regions in the midbrain, a specific pipeline implemented through FSL (FMRIB Software Library, Oxford, UK) (Jenkinson et al., 2012; Woolrich et al., 2009) was performed.

2.5.3. Midbrain fMRI data analysis. A second analysis was performed to assess activations in the midbrain. Functional MRI volumes of the midbrain were preprocessed and analyzed with FSL. Preprocessing included discard of the four initial volumes, realignment of functional time-series using FSL linear motion correction and noise correction. Functional data were not registered in a stereotaxic template and were kept in the native space. This strategy allowed to preserve fMRI data, as a non-linear transformation used to coregister data may induce signal loss. Anatomical data were then registered in the functional space using FSL FLIRT routine with 6 parameters rigid body fitting technique. Three iterations of brain tissue extraction were performed using FSL BET (Smits et al., 2018) and applied to anatomical data using a measure of fractional intensity threshold. This strategy was used to preserve accurate tissue segmentation, which can be affected by T1 signal inhomogeneity due to the presence of the lesion. The skull was first removed with an initial fractional intensity threshold of 3.0. Eye removal was then performed with a fractional intensity threshold of 2.0. To complete brain extraction, the neck was removed with a fractional intensity threshold of 1.0. Brain tissue surrounding the lesion was then preserved at the proximity of the skull. The resulting BET mask was applied to functional data. Our technique was compared against an automated script (OptiBET) (Lutkenhoff et al., 2014) that failed to segment correctly brain structures around the lesion in Fig. 2. Statistical analyses were then performed in masked functional volumes. Functional data were analyzed using FSL FEAT pipeline (Woolrich et al., 2009). Changes in BOLD regional responses were estimated using a general linear model that included three regressors, i.e. one regressor for each condition (left and right visual motion, and static images). High-pass filter of 0.11Hz was applied to functional data, spatial smoothing was performed at FWHM =5mm as the size of the sub-structures of interest was between 3 and 9mm3. Two explanatory variables were included in the model, i.e. one for each moving stimuli (left and right visual motion). A double gamma HRF was used to model the stimuli and to further fit fMRI data (Glover, 1999). This selection allowed a higher number of degrees of freedom to define the HRF which is particularly relevant as the BOLD signal arising from the colliculi is thought to differ from the cortical signal (Wall et al., 2009). This technique allowed reducing the risk of removing signals from sub-cortical structures and

their neighboring voxels that fit highly constrained HRF models. A cluster-based inference method was used to correct for multiple comparisons with an initial arbitrary cluster z-threshold of 2.3 (corresponding to $p<0.01$) and a corrected cluster significance threshold of $p=0.05$ (Worsley, 2001). Results included BOLD activation maps estimated for left and right contrasts defined above. As for whole brain analysis, activation maps were corrected for multiple comparisons.

3. Results

3.1. Anatomical MRI description of the lesion

Anatomical MRI scan reveals complete damage of the primary visual cortex in the left hemisphere leading to destruction of the primary visual areas (V1). Damaged areas are visible in the T1-weighted images shown in Fig. 2A, with no preserved region of V1 in the left hemisphere.

3.2. Behavioral results: reaction time and accuracy

Fig. 3 shows reaction time (s) for spontaneous detection of visual motion in both hemifields. For stimuli presented in the left hemifield (intact vision), the performance was optimal, i.e. 100% detection rate accuracy with a mean RT of 665.09ms (standard deviation 131.35ms). In the right hemifield (blind), detection rate was 93% with a mean RT of 1590.42ms (standard deviation 587.49ms). Reaction time of detection of stimuli presented in the right hemifield (left hemisphere motion processing/lesion side) was significantly slower than RT in the left hemifield (right hemisphere motion processing/intact side, $p<0.0001$).

The signal detection analysis revealed a distance between the signal and noise distributions known as perceptual sensitivity (d' = 4.21). As indicated by d', the patient clearly discriminates between left and right visual motion conditions. Also, the subject's response criterion provides an index of the subject's response bias and reveals that the participant's strategy is conservative (C = 0.325). This parameter is positive and suggests that in case of

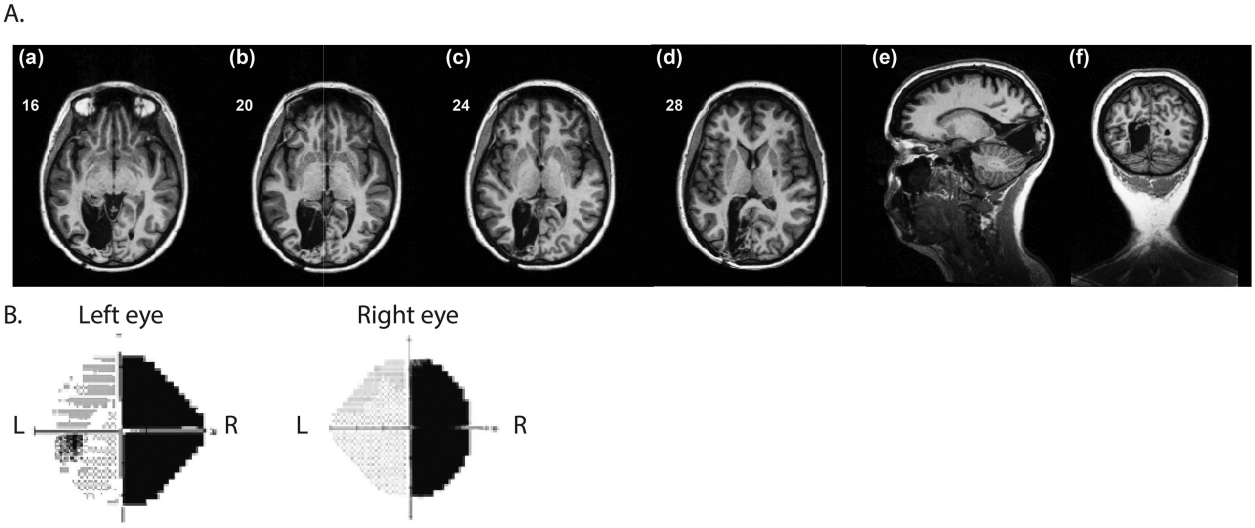

Figure 2 – Patient's T1 weighted anatomical scan and field of view. A. T1-weighted anatomical scan with three different slice views of the lesion: (a)-(d) transverse, (e) sagittal and (f) coronal slice view showing the primary visual cortex removal in the left hemisphere and the destruction of the primary visual areas (V1). B. The patient's visual field shows a symmetric loss across both eyes leading to a complete contralateral visual loss in the right visual field.

doubt, the patient will report no movement (in this case no response) rather than responding that there was movement.

During the semi-structured interview, the patient reported no awareness of the nature of the stimuli presented in her blind (right) hemifield with a clear perception of the stimuli presented in her left hemifield. However, the patient deduced stimuli of both hemifields to be of the same nature. The patient also reported a total lack of confidence in her accuracy with respect to the right stimuli presentation, reporting 1 (not very confident) on the Likert-type scale. The patient reported randomly pressing the right button arguing that even if she felt something happened in her blindfield, it was very faint. The patient described this feeling such as Eigengrau patches in the middle of the scotoma (Ladd, 1894).

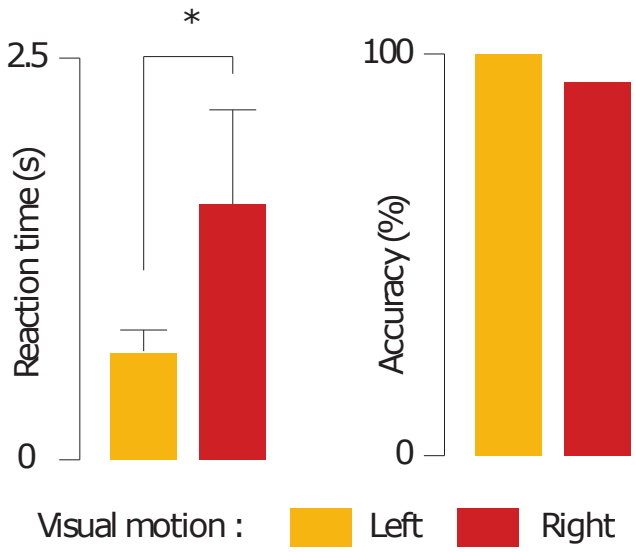

Figure 3 – Patient reaction time (s) on the left image and accuracy (%) on the right image to spontaneous detection of moving targets for left visual motion (dark grey) and right visual motion (light grey) (*p<0.01). ML was significantly faster when stimuli were presented on the left side (normal hemifield) of the screen compared to the right side (blind hemifield). However, ML's response accuracy was comparable between conditions.

.

3.3. Functional Results - whole brain fMRI analysis

Fig. 4 shows cortical BOLD activation maps analyzed with the whole brain approach across specific conditions and contrasts. Fig. 4 ((a-c), (f-h), (k-m)) shows axial view slices, separated by 12mm3, for the left and right visual motion conditions, and for both conditions together, respectively. Fig. 4((d, e), (i, j), (n, o)) shows specific sagittal and coronal views of axial slice z=4 and z=8, for left and right visual motion condition, and for both conditions together, respectively. Table 1 shows the list of significant cortical regions (as clusters) corresponding to the BOLD activations depicted in Fig. 4(a-j). Clusters are described with their name, size (in voxels), MNI peak coordinates, significant t-value and corresponding z-score, and specific brain areas that are included in the cluster. Only cluster sizes >10 voxels are presented in the table. Brain regions in bold font are further described below.

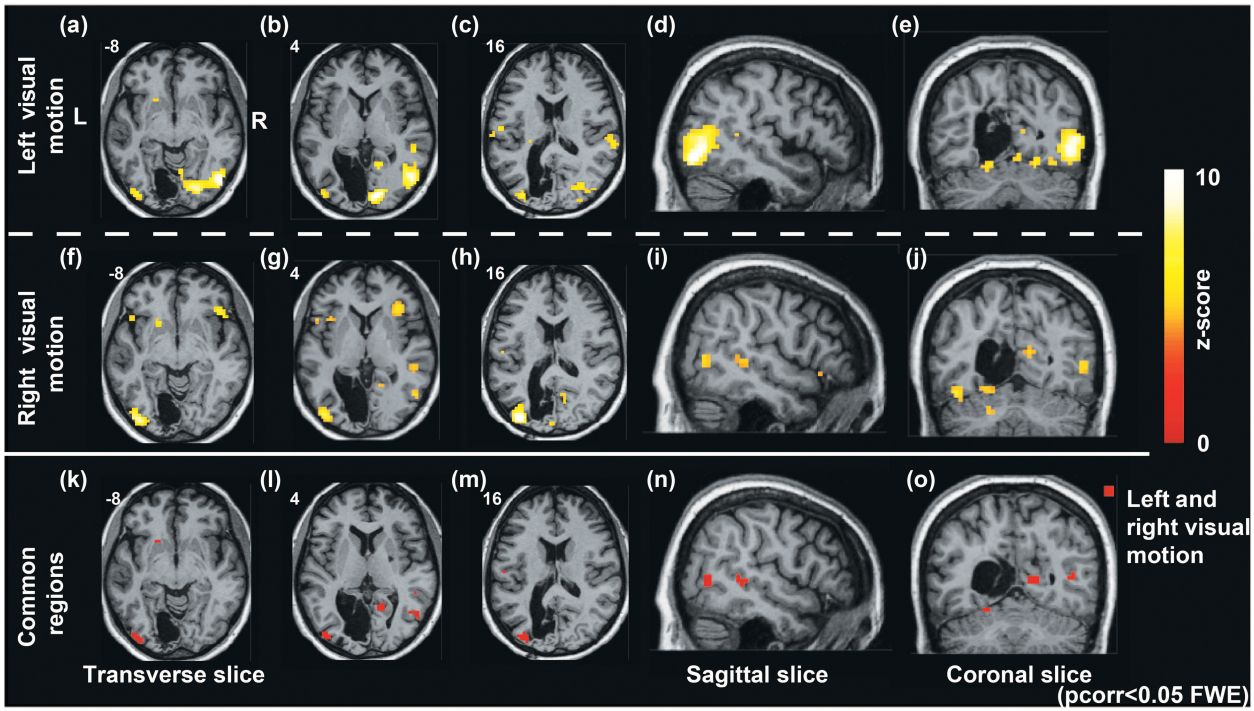

Figure 4 – Patient cortical blood oxygen level dependent (BOLD) activations for the whole brain data analysis. BOLD activations are reported for each condition: (a-e) left visual motion, (f-j) right visual motion, and (k-o) common left and right motion. For each condition, three transverse slices separated by 12mm3, one sagittal slice (at axial z=4) and one coronal slice (at axial z=8) are provided. Additional details on BOLD maps are presented in Table 1, Table 2, Table 3. Activations were corrected for multiple comparisons with family wise error (FWE) method (pcorr < 0.05).

.

For the main effects of the visual motion stimulation for the whole brain, the left visual motion condition (i.e. conscious perception) elicited sizeable activations (Table 1 and Fig. 4(a-e)). The largest cluster was found in the right inferior temporal region including around the right calcarine region and right middle temporal cortex (MT). Further clusters were apparent in the left inferior occipital, right lingual including around the right calcarine and right supramarginal areas. When controlling for the static condition, the [left - static] stimuli (subtracting the static condition from left visual motion condition) yielded considerable

activation clusters with the largest located next to the right calcarine (see Table 2 for a description of these specific regions). A second cluster was located in the right postcentral region including activations in the right inferior and superior parietal areas. Further clusters were located in the left rolandic operculum and right supramarginal areas. In addition, activation clusters resulting from the left contrast [left - (right + static)] were located in the right superior occipital, right MT and right lingual regions, including clusters in the calcarine and fusiform areas (see Table 3 for a description of these specific regions).

For the main effects of the right visual motion condition (i.e. unconscious perception), the largest cluster was located in the left middle and inferior occipital areas, followed by regions around the left calcarine, left and right frontal inferior orbital as well as in the left and right MT, right lingual, and right middle frontal regions (Table 1 and Fig. 4(f-j)). When controlling for the static condition, the [right-static] stimuli (subtracting the static condition from right visual motion condition) resulted in a large activation cluster located in the left middle occipital region Table 2. Further clusters were activated in the right and left insula, right superior frontal, middle superior frontal, right supramarginal and notably the right MT areas. The activation clusters resulting from the right contrast [right - (left + static)], included the left frontal inferior orbital and right insula regions Table 3. Finally, for the whole brain results, when combining both left and right visual motion conditions (i.e. conscious and unconscious perception), common activated regions included left inferior occipital, right MT and right lingual areas (Table 3 and Fig. 4(k-o)).

3.4. Functional results - midbrain fMRI analysis

Fig. 5 shows BOLD activation maps resulting from the midbrain analysis and estimated for left and right visual motion conditions contrasted with static stimuli. For left visual motion (i.e. conscious perception), Fig. 5(a) and (b) show significant activated regions in the bilateral medial temporal gyri (MT+/V5) and V1 areas, respectively. In addition, Fig. 5(c) and (d) show significant activations in the bilateral pulvinar and SC areas, respectively. For right visual motion (i.e. unconscious perception), Fig. 5(e) and (f) show significant activations in the right MT+/V5 regions and the right calcarine sulcus areas, respectively. In addition, Fig. 5(g) and (h) show significant activations in the left pulvinar and the left SC.

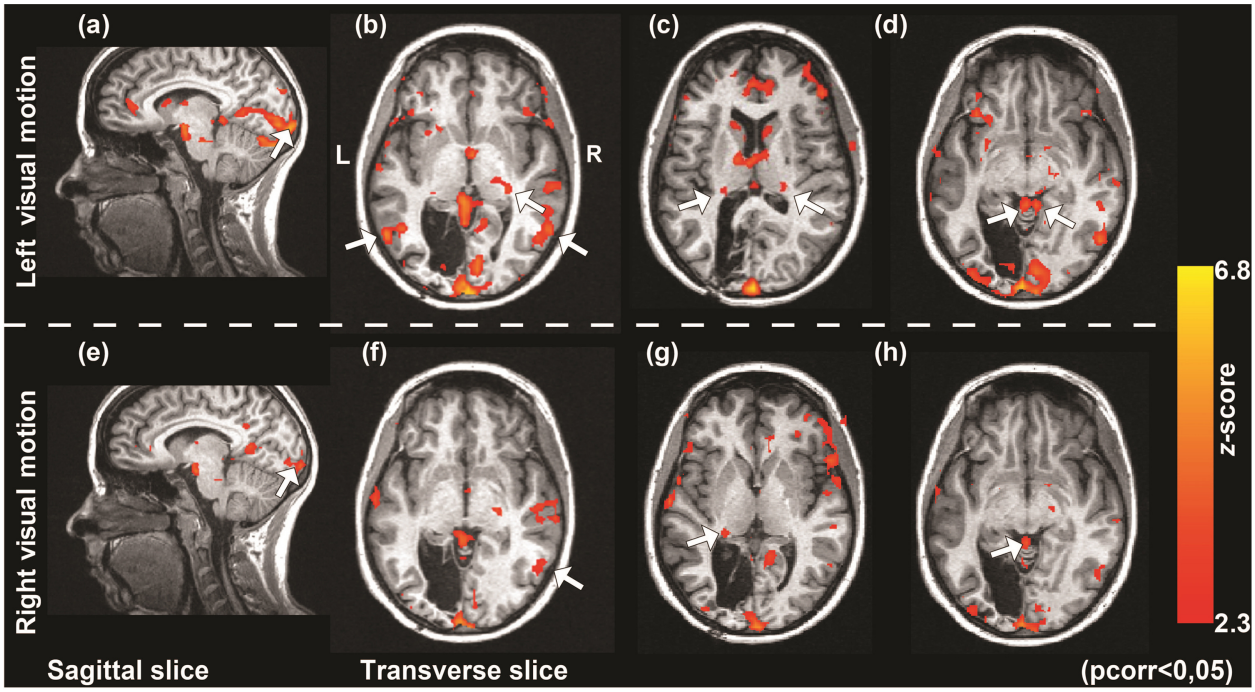

Figure 5 – Patient cortical and subcortical blood oxygen level dependent (BOLD) activations in the midbrain sequence scan for the left (a)-(d) and right (e)-(h) stimulations. For the left stimulation, BOLD activations are observed in the (a) right calcarine sulcus, (b) bilateral medial temporal gyri (MT+/V5) and right pulvinar, (c) right and left pulvinar and (d) bilateral superior colliculi. For the right stimulation, BOLD activations are observed in the (e) right calcarine sulcus, (f) right MT+/V5, (g) left pulvinar and (h) left superior colliculus. Activations were corrected for multiple comparisons with cluster-based inference method (pcorr < 0.05).

4. Discussion

Behavioral and fMRI results suggest that visual information presented in the blindfield is processed through different pathways and/or structures, notably through the geniculo-extrastriate pathway and the colliculo-pulvinar-extrastriate pathway depending on the visual residual abilities found in the blind hemifield (Cowey, 2010; Danckert & Rossetti, 2005; Hadid & Lepore, 2017). However, while previous blindsight studies have employed block design methods and/or whole brain fMRI analysis (Ajina & Bridge, 2018; Ajina et al., 2015a; Leh et al., 2010; Morland et al., 2004; Persaud et al., 2011; Urbanski et al., 2014), to our knowledge, our study was the first to provide a functional description of a single V1-lesioned patient with blindsight abilities using an event-related motion detection fMRI design focused on cortical and subcortical areas. In addition, this design allowed us to associate the sense of awareness that the patient presented in the blindfield with BOLD activations, providing unique new insights on Type II blindsight. In fact, the patient triggered a response every time she had a sense that something was happening in her blind hemifield inducing highly accurate performances for detecting moving stimuli. Subsequently, the responsiveness to stimuli in the sighted hemifield was not significantly different than the one in the blind-field. However, there was a downside to this accuracy: the reaction time to stimuli in the blind-field was significantly longer than in the normal field. We postulate that due to the fact that her decision making was based on subjective criteria, it is less robust than decision making based on perceptual evidences, thus potentially inducing longer reaction times (Kang et al., 2017) which could account for behavioral differences in blindsight.

Motion detection in the normal left hemifield (i.e. conscious perception) induced significant BOLD activity in the right calcarine (primary visual areas) (Tootell et al., 1995b; J. D. Watson et al., 1993), as well as activations in the contralateral right MT visual area, thought to be specific to motion (Ajina et al., 2015a; Dukelow et al., 2001). Activations of the visual cortex were only contralateral when the static condition was subtracted from the left visual motion condition, cancelling out ipsilateral activity observed in visual areas. Bilateral activations were found in parietal regions possibly reflecting shift of attention between the left and the right hemifield (Saygin & Sereno, 2008) and in the supramarginal gyrus known to

be responsive to visual motion (Dupont et al., 1994). Therefore, in agreement with previous literature on motion detection and perception, activations following stimulation of the normal hemifield were consistent.

However, when we compared activations of the [left - static] condition (i.e. conscious perception) to the [right - static] condition (i.e. unconscious perception), we observed that stimulating the blind hemifield did not induce activity in the left calcarine, which was expected due to the lesion in the left primary visual area. This result led us to reject the hypothesis that surviving residual V1 islands are responsible for blindsight, as left calcarine activity was observed in the right visual motion condition because it implies bilateral stimulation of static dots. Nonetheless, motion in the right hemifield [right - static] induced significant BOLD activity in the left striate, i.e. calcarine, and extrastriate visual areas including the inferior and middle occipital gyri, which showed that visual information was received by the typical contralateral visual areas. However, these activations were not strong enough to trigger a response in MT within the same hemisphere. Nonetheless, activations were observed in the ipsilateral MT instead of the contralateral counterpart which could explain implicit motion detection in the blind hemifield. Moreover, when either hemifield was stimulated [left - static] or [right - static], activations were found in the right inferior parietal lobe, notably the right supramarginal gyrus, which is likely responsible for attentional capture even in the absence of awareness (Hervais-Adelman et al., 2015) specific to visual motion processing (Dupont et al., 1994).

Common regions observed when combining left and right visual motion conditions were found in the right calcarine, left inferior occipital and right MT, indicating that mechanisms of compensation driven by visual areas were used, and allowed for some processing of information when the blind hemifield was stimulated. Therefore, we hypothesize that a secondary residual pathway that prioritizes the use of the "healthy" hemisphere may be used to allow performances above chance level in the absence of consciousness. Evidence of the contribution, or compensatory changes in functional brain activity, of the intact hemisphere to blindsight has been previously provided (Celeghin et al., 2017). When compared with the blind hemifield [left contrast], the normal hemifield exhibited significantly higher responses

within the right striate and extrastriate visual areas and MT, which was expected. Interestingly, in the [right - static] condition, the presence of activity in the frontal areas and in the insula (contralateral left frontal operculum and frontal inferior orbital) could explain why the patient preserved the sense that something happened within the blind regions and the high performances she exhibited (Persaud et al., 2011). Previous studies have suggested a role of the anterior insula in awareness as well as interoception, with activations also located in the adjoining frontal operculum and the inferior frontal gyrus (Craig, 2009; Van den Stock et al., 2014). The anterior insula may respond more to unconscious than conscious motion perception and could be considered when further investigating the neural correlates of awareness in blindsight.

Taken together, these results could indicate that abnormal activations of ipsilateral MT areas are able to drive some insular and frontal activity which could explain the lack of real visual percept. Therefore, we speculate that frontal activations would not have been generated without MT responses which could have been driven by subcortical structures as the superior colliculus.

In fact, stimulation of the normal field was accompanied by a bilateral activation of the colliculi, as well as activations in the left pulvinar region and stimulation of the blind-field elicited responses in the contralateral colliculus and pulvinar. Why the pattern differs when one hemifield is stimulated compared to the other is yet to be understood. The activation pattern following stimulation of the normal hemifield observed in the ipsilateral superior colliculus and pulvinar appears to be abnormal, because collicular activations should be essentially contralateral (Wall et al., 2009). Therefore, if we admit that in normal behavior a subcortical pathway from the contralateral SC to the contralateral MT could induce perception of motion, it leads us to postulate that the activity found in the ipsilateral colliculus and pulvinar is not typical. One hypothesis would be that stimulation of the normal hemifield induces ipsilateral activations. These activations act as a system destined to stimulate the colliculus so that it does not degenerate and contribute to processing motion stimuli even in the absence of visual awareness. Therefore, the SC is thought to project to the ipsilateral MT, which is consistent with the activity we observed after stimulating the right

hemifield. In other words, when the blind-field (right) is stimulated, the contralateral SC (left) is activated in association with the ipsilateral MT (right) which is likely to respond to stimulation of the normal hemifield (left). These observations may contribute to the understanding of the human blindsight literature and suggest that the lesion disturbs not only the ipsilesional brain circuitry but also impacts the functional contralateral network. Therefore, understanding and guiding cortical plasticity could allow the rehabilitation and restoration of visual functions following a lesion in the occipital areas. Research groups have demonstrated that it's possible to potentiate visual recovery and improve motion perception of cortically blind patients through perceptual visual training of complex motion stimuli in the blind-field (Cavanaugh et al., 2017; Chokron et al., 2008; Das et al., 2014; Huxlin, 2008). These studies also showed transferable training effects to numerous types of stimuli and tasks. Tailoring these training approaches to our patient could potentially foster the recovery of her impaired visual functions. Thus, investigating the neural and vascular basis of blindsight is of importance to enable personalized clinical treatments, such as these specific visual trainings to improve exploration and visual-orientation abilities, with long-term effects.

fMRI is a relevant tool to study subcortical functional activations evoked by external stimulation in a non-invasive setting. However, SNR in small deep brain structures remain a limitation due to MRI physics (Amaro & Barker, 2006; Wall et al., 2009). For the midbrain data analysis, we were constrained to use the cluster method (Worsley, 2001) with low smoothing (5mm) to avoid that focal signals originated from sub-cortical structures being blurred. An influential article by Eklund and collaborators has recently raised awareness on the risk of inflated false-positive rates in exploratory fMRI studies (Eklund et al., 2016), in particular when group-analysis is performed. We acknowledge this important caveat, and we also reckon that single case studies of individuals with brain lesions present advantages over group analysis or large study approaches and have historically been the foundation providing a detailed understanding of cognitive constructs (Medina & Fischer-Baum, 2017). In contrast to the class of studies assessed by Eklund and colleagues, in our study the analyses were not exploratory in nature, rather theory and hypotheses driven, making our results less

susceptible to high false-positive rates. We present new findings of the neural correlates of blindsight that are consistent with previous theoretical and experimental literature and map onto defined cognitive processes. As mentioned by Cox et al. (2017) conclusions from neuroimaging studies are based on previous knowledge and should not only depend on the statistical arguments from the data (Cox et al., 2017). We also designed an experimental paradigm with stimuli known to elicit activations of the structures related to our hypotheses. Thus, despite concerns in statistical approaches in neuroimaging research, we are confident that our results are not simply noise in the data that would average out to zero when comparing with multiple studies.

In addition, from an experimental perspective, event-related designs are also challenging as they require a higher number of stimulation events and longer acquisition time than block-averaged designs for equivalent performance. Also, the presence of blood vessels in close proximity to the subcortical structures may affect the quality of images with additional physiological noise and distortions. Nevertheless, these limitations can be mitigated by using precise analysis and experimental designs (Amaro & Barker, 2006; Celeghin et al., 2018; Wall et al., 2009).

Finally, our results are likely limited with regards to explaining different types of blindsight, performances and phenomenology due to the unique nature of the patient's lesion (Hadid & Lepore, 2017; Swienton & Thomas, 2014). As an example, contralateral activation of MT could occur in blindsight, but would be associated with a different form of blindsight (i.e., Type I) due to the fact that the signal would be too weak to propagate through the dorsal pathway and create a sense of awareness. Nonetheless, these results address perceptual awareness and contribute to how conscious vs. unconscious visual perception is mediated in the absence of V1. Previous studies have reported that V1, though important in normal conscious vision, may not be necessary for awareness and conscious visual perception to arise following damage to V1 (see the review by Mazzi et al., 2017). In fact, the implication of a pathway from the retina through the pulvinar to area MT was suggested in a recent case study of a child with bilateral damage to V1 who strikingly preserved intact and conscious

visual perception (Mundinano et al., 2017). Further work is needed to compare different lesions, behavioral accuracy and subjective awareness in a cohort of hemianopic patients with a delimited lesion of V1 using event-related fMRI design to assess the role of subcortical structures and increase the effectiveness of a rehabilitation approach based on subcortical pathways.

5. Conclusion

In conclusion, a subcortical dorsal pathway implicating the contralateral SC, ipsilateral MT and contralateral frontal areas may mediate Type II blindsight for motion detection. The SC could have an essential role in allocating attention, enhancing perceptual sensitivity in the blind-field and sending visual information directly to MT of the non-lesioned hemisphere (right) or indirectly to MT (right) circulating in priority through the extrastriate visual areas of the lesioned hemisphere (left). As this pathway is not commonly used in conscious vision in humans, the visual signal sent could be less rich in information or not appropriate to be processed by cortical areas to generate explicit vision. Nonetheless, we hypothesized that MT was able to process visual properties linked to motion explaining performance above chance level, but then again with less accuracy and precision keeping the level under the threshold of consciousness. Propagation of the signal through the dorsal pathway and to frontal areas could induce a sense of awareness without reaching the threshold of visual awareness allowing for the phenomenon of Type II blindsight. Thus, the role of plasticity in our case study shows that stimulation of the normal hemifield leads to activation of the ipsilateral SC and enhances perception in the blind-field. This notion may potentially help develop rehabilitation strategies focused on subcortical pathways.

Acknowledgements

We sincerely thank ML for participating in this study.

Funding

This research was supported by the Canada Research Chair Program [FL] and the Natural Sciences and Engineering Research Council of Canada grants RGPIN-8245-2014 [FL] and RGPIN-04672-2015 [MD].

Credit author statement

Michèle W. MacLean (Formal analysis, Data curation, Visualization, Writing – Original Draft, Writing – Review & Editing); Antonin Tran (Conceptualization, Investigation, Data curation, Formal analysis, Writing - Original draft); Vanessa Hadid (Conceptualization, Investigation, Writing - Original draft, Writing – Review & Editing); Latifa Lazzouni (Software, Formal analysis, Writing – Review & Editing); Julie Tremblay (Software); Dang K. Nguyen (Resources, Writing - Review & editing); Mathieu Dehaes (Funding acquisition, Resources, Writing - Review & editing, Supervision); Franco Lepore (Conceptualization, Funding acquisition, Resources, Writing - Review & editing, Supervision). M.W.M, A.T. and V.H. are co-first authors on this work. M.D. and F.L. contributed equally as co-senior authors on this work. All authors approved this work.

Table 1 – Brain regions showing significant activations for the left and right visual motion conditions.

Brain regions (label at peak)	**Cluster Size (voxels)**	**x**	**y**	**z**	**T -values**	**Z score**	**Regions included in the cluster**
Left visual motion							
Left Hemisphere							
Inferior Occipital	94	-42	-85	-11	7.3	7.02	Middle Occipital
Precuneus	77	-12	-43	70	7.13	6.87	Superior Parietal, Postcentral
Postcentral	14	-57	-13	13	6.23	6.05	
Precuneus	13	-3	-40	58	6.06	5.89	
Superior Temporal	62	-60	-37	22	5.77	5.63	
Right Hemisphere							
Inferior Temporal	858	48	-73	-11	10.03	Inf	Calcarine, Middle Temporal
PostCentral	89	30	-49	64	6.82	6.59	Postcentral, Superior Parietal
Lingual	44	15	-55	1	6.38	6.19	Calcarine
SupraMarginal	47	60	-25	19	6.26	6.08	Superior Temporal
Middle Temporal	13	54	-40	1	5.8	5.66	
Right visual motion							
Left Hemisphere							
Middle Occipital	376	-39	-85	13	11.11	Inf	Inferior Occipital
Calcarine	57	-6	-97	7	7.52	7.22	
Frontal Inferior Orb	21	-48	17	-5	5.95	5.79	
Putamen	11	-18	14	-8	5.94	5.78	
Middle Temporal	14	-42	-52	10	5.52	5.39	
Right Hemisphere							
Frontal Inferior Orb	61	45	26	-5	6.91	6.67	
Middle Temporal	22	54	-64	1	5.91	5.76	
Lingual	34	15	-55	4	5.9	5.75	Calcarine
Middle Frontal	12	45	8	52	5.77	5.63	
Middle Temporal	11	51	-37	1	5.36	5.24	

Note. Significant cortical activations (FWE correction, $p < 0.05$) for left and right visual motion when controlling for the static condition. Brain regions are labeled according to cluster peak and cluster size represents the number of voxels in specific clusters. Each cluster is listed with MNI peak coordinates across x, y and z, significant t-value and corresponding z-score as well as specific brain areas that are included in the cluster. Only cluster sizes >10 voxels are presented. L: Left, R: Right.

Table 2 – Brain regions showing significant activations when subtracting the static condition from left and right visual motion conditions separately.

Brain regions (label at peak)	**Cluster Size (voxels)**	**x**	**y**	**z**	**T -values**	**Z score**	**Regions included in the cluster**
[Left-static] Stimuli							
Left Hemisphere							
Rolandic Operculum	166	-57	2	4	6.5	6.3	Supermarginal, Postcentral
Superior Motor Area	10	-3	2	46	5.56	5.43	
Right Hemisphere							
Calcarine	1202	18	-85	1	10.52	Inf	Lingual, Superior Occipital
Postcentral	149	27	-49	64	7.4	7.11	Superior and Inferior Parietal
Precuneus	171	3	-52	61	6.47	6.27	Superior Parietal, Precuneus
Supramarginal	36	60	-22	19	6.13	5.96	
[Right-static] Stimuli							
Left Hemisphere							
Middle Occipital	325	-36	-88	10	8.5	Inf	Inferior Occipital
Insula	128	-39	17	4	6.8	6.57	Frontal Inferior Orbital, Rolandic Operculum
Cingulum Middle	28	-6	23	31	6.05	5.88	
Insula	12	-27	23	-5	5.63	5.5	
Right Hemisphere							
Insula	93	39	26	-5	7.32	7.03	Insula
Superior Frontal	34	21	53	22	6.87	6.63	
Middle Frontal	63	39	8	40	6.5	6.3	
Middle Frontal	41	42	41	28	6.22	6.04	
Supramarginal	48	51	-34	43	5.93	5.78	Inferior Parietal
Middle Temporal	10	48	-22	-8	5.63	5.5	

Note. Significant cortical activations after family wise error correction (pcorr < 0.05) for left and right visual motion when controlling for the static condition. Brain regions are labeled according to cluster peak and cluster size represents the number of voxels in specific clusters. Each cluster is listed with MNI peak coordinates across x, y and z, significant t-value and corresponding z-score as well as specific brain areas that are included in the cluster. Only cluster sizes >10 voxels are presented in the table. L: Left, R: Right.

Table 3 – List of regions showing significant activations when combining left and right visual motion conditions as well as for left and right contrasts.

Brain regions (label at peak)	**Cluster Size (voxels)**	**x**	**y**	**z**	**T -values**	**Z score**	**Regions included in the cluster**
Common Regions							
Left Hemisphere							
Inferior Occipital	94	-42	-85	-11	7.3	7.02	Middle Occipital
Right Hemisphere							
Middle Temporal	22	54	-64	1	5.91	5.76	Middle Temporal
Lingual	24	15	-55	4	5.9	5.75	Calcarine
Left Contrast							
Right Hemisphere							
Superior Occipital	280	27	-91	22	7.67	7.34	Cuneus, Middle Occipital
Middle Temporal	53	48	-76	7	6.92	6.68	
Lingual	114	18	-82	-8	6.83	6.6	Calcarine, Fusiforme
Right Contrast							
Left Hemisphere							
Frontal Inferior Orb	63	-33	17	-14	4.67	4.59	Insula
Right Hemisphere							
Insula	96	33	17	-14	3.87	3.82	Insula
Cingulum Middle	17	12	14	37	3.65	3.61	

Note. Significant cortical activations after family wise error correction (pcorr < 0.05) for common activated regions between left and right visual motion conditions, as well as the left contrast [left visual motion- right visual motion- static condition) and right contrast [right visual motion - left visual motion - static condition]. Common regions activated correspond to Fig. 4(k-o). Brain regions are labeled according to cluster peak and cluster size represents the number of voxels in specific clusters. Each cluster is listed with MNI peak coordinates across x, y and z, significant t-value and corresponding z-score as well as specific brain areas that are included in the cluster. Only cluster sizes >10 voxels are presented in the table.

Chapter 4

A comprehensive visual motion perception MRI dataset

4.1. Chapter Overview

This chapter presents a novel neuroimaging dataset featuring task-based and resting state fMRI, structural and diffusion MRI, in addition to eye-tracking data, electrophysiological measures and behavioural records from both neurotypical and cortical visually impaired adults. This dataset provides whole brain coverage and high-resolution fMRI for detailed subcortical imaging. This chapter covers specifications (Sec 4.2), dataset description (Sec 4.3), materials and methods (Sec 4.4), including participant details, experimental procedures, data analysis protocols, technical validation and usage notes. The complete dataset was acquired during my doctoral studies and a section of the data presented in this chapter is further used in the third study of this thesis.

Keywords: functional MRI, structural MRI, diffusion MRI, visual motion perception, cortical visual impairment

4.2. Specifications

Subject	Cognitive neuroscience, neuroimaging
Available Modalities	Structural, functional and diffusion MRI
Available tasks	Rest, motion
Included measurements	Behavioural, eye tracking, electrophysiological, neuropsychological & neurological evaluations
Sample characteristic	Neurotypical and individuals with cortical visual impairment
Sample Location	Montréal, Québec, Canada

Table 1 – Specifications of the dataset

Value of the data

(1) The data are organized according to the Brain-Imaging-Data-Structure (BIDS) and can be readily used for analysis pipelines following these standardized specifications. Preprocessed data is readily available.

(2) The data allows for further analyse, in addition to our planned publication entitled: "Residual visual function in cortical visual impairment: a high resolution fMRI study", on the functional response to visual motion, including looming and biomotion stimuli with tasked-based fMRI.

(3) The data allows for effective connectivity analyses related to tasked-based fMRI.

(4) The data allows for assessing resting state functional connectivity of individuals with occipital cortex lesions, resulting in cortical visual impairment, compared to neurotypical controls.

(5) The anatomical data can be used for voxel-based morphometry analyses.

(6) The diffusion MRI data can be used for analyzing alterations in white matter tracts, investigating individual differences amongst CVI indiviuals and comparing to neurotypical controls.

(7) The data can be used to investigate the relationship between eye movements and neural signals.

4.3. Dataset Description

The dataset documented in this chapter presents unique high resolution MRI images, including functional, structural and diffusion MRI in neurotypial adults (N=25) and cortically visually impaired participants (N=8). Behavioural, electrophysiological and eyetracker measurements are also included. One additional patient did not undergo the MRI portion of the study due to MRI incompatibility but completed the accompanying behavioral experiment. Data were converted from DICOM to nifti format and are available in the standardized the Brain Imaging Data Structure (BIDS). In addition to raw data, the dataset also includes preprocessed data, code for the behavioural motion task, quality control metrics and technical validation. Code used to perform technical validation are openly available via our bidspm pipeline available here, DOI. Providing this chapter facilitates scientific reproducibility of results and the secondary usage of robust data. This dataset provides an opportunity to study and advance our understanding of motion processing and the structural, functional and behavioural consequences of cortical visual impairment.

4.4. Materials and methods

Participants

This study was approved by the Comité d'Ethique de l'Unité de Neuroimagerie Fonctionnelle (UNF) of the Centre de recherche de l'Institut universitaire de gériatrie de Montréal (IUGM), Montréal, Canada and the Comité d'éthique de l'Université de Montréal, Montréal, Canada. This data set includes eight CVI participants (5 females) with V1 damage and visual field loss, with an average age of 56.75 years (SD = 15.97; max:80, min:32) and an average educational level of 15.25 years (SD = 3.196). Twenty-five neurotypical participants (13 females) with an average age of 39.22 years (SD = 15.42, max:71; min: 22) and an average educational level of 16.9630 years (SD = 3.4915) were also included. CVI participants

were recruited from the Centre Hospitalier de l'Université de Montréal, refered by Dr. Dang K. Nguyen, neurologist, and had received a clinical diagnosis of hemianopia or quadranopia following occipital cortex damage. Participants from the neurotypical control group were recruited via public online flyers.

All participants had normal or corrected-to-normal vision, verified by the Freiburg Visual Acuity Test (FRACT) (Bach, 1996), including CVI participants in their intact visual field and central visual field, and reported no history of psychiatric disorders or neurological condition other than the one causing the visual impairment. CVI participants showed no noticeable signs of unilateral neglect, i.e. failure to attend to the contralesional side of space, an exclusion criterion for this study. The participants were predominantly right-handed as determined by the Edinburgh Handedness Inventory (Oldfield, 1971). One CVI participant was excluded for MRI incompatibility on the day of testing. All participants provided written informed consent before participating in the study, and consented to share anonymized data and allow usage for future research projects. Participants received financial compensation for their time.

Experimental procedure

All data was acquired at l'Unité de neuroimagerie fonctionnelle de l'Institut de gériatrie de Montréal. Participants were asked to respond to a general data assessment, unilateral neglect tests, visual acuity, contrast sensitivity and visual field test (FRACT). Subsequently, participants were asked to perform visual motion detection or discrimination tasks for a set of presented stimuli both inside and outside the MRI scanner.

Task Paradigms

Unilateral neglect assessment. Unilateral neglect, i.e. failure to attend to the controlesional side of space, is an exclusion criterion for this study as participants must be able to attend to their blind hemifield and process the presented motion consciously or non-consciously. Two tests were selected from «A battery of tests for the quantitative assessment

of unilateral neglect» (Azouvi et al., 2006). Line bisection: participants were asked to indicate the middle point of horizontal lines with different lengths. Deviation from the true middle was measured to ensure no tendency to deviate towards a certain direction. Clock drawing: the participants must place the 12 hours in a circle and indicate a given time. A three level scale is used: 0 (optimal performance), 1 (omission on part of the left side), 2 (omission on part of the right side or rightward displacement). Participants who completed these two tests with no noticeable signs of UN, continued with the rest of the experimental procedure.

Visual acuity and contrast sensitivity evaluation. Visual acuity and contrast sensitivity was measured using the validated and free software program «Freiburg Vision Test FrACT», Version 3.10.0g Bach, 1996, 2007. The general settings were calibrated: observer distance of 285mm, luminance of 105 cd/m2 , the Landolt C optotype (letter "C") positioned in the center of the screen, background luminance of 60 lux. For both the visual acuity and contrast tests, participants were asked to identify the orientation of a Landolt C, in a 4 forced choice test with a chance level set at 12.5%. The program uses the best parameter estimation by sequential testing (PEST) algorithm for threshold determination. This measures the minimal visible Landolt C by determining the most likely position of the threshold given past optotype sizes as well as responses and presents the next optotype at this estimated threshold. Both tests will have 24 trials/run. Auditory feedback was given for correct and incorrect responses. For the visual acuity test, the contrast is set at 100% with the optotype size getting typically increasingly smaller. Visual acuity is defined by the Snellen ratio (in decimals) that accounts for the distance where the optotype was recognized and the distance where a normal observer would have recognized it. For the contrast test, one large Landolt C optotype is composed of a mixture of low to medium spatial frequencies, with the contrast getting typically lower. The threshold is defined by the Weber contrast which measures the difference between the maximum and minimum luminance divided by the maximum luminance (Pelli & Bex, 2013).

Visual motion tasks. See the third study for a detailed description of the visual motion tasks that the participants were asked to perform inside and outside the MRI scanner, which includes figures of experimental procedures. This consisted of a peripheral motion perception task during a functional MRI scan, including looming motion, static, biomotion and bioscramble stimuli, in addition to a global motion direction discrimination task conducted outside the scanner. Visual tasks were generated using custom scripts in MATLAB (MathWorks, Inc.) and the Psychophysics Toolbox (Brainard, 1997; Pelli, 1997).

Magnetic resonance imaging acquisition

MRI data was acquired with a high resolution 3 Tesla scanner (Siemens Trio system) using a 64-channel phased-array head coil at l'Unité de neuroimagerie fonctionnelle of l'Institut de gériatrie de Montréal. We collected structural MRI, resting state fMRI, task-based fMRI, field maps, and diffusion MRI in one scan session approximately 90min duration. Physiological data including heartbeat, breathing and pulse rates were recorded. Eyetracker data were recorded during the functional MRI scans. Earplugs were used to reduce the scanner noise for the participants.

Structural MRI. A 5 minutes structural T1-weighted scan (MPRAGE) was acquired with the following parameters: voxel size of 0.9mm^3, acquisition matrix size 256x256, flip angle 8°, Repetition time (TR) = 2400ms, Echo time(TE) = 2.25ms, Field of view (FOV) 230x230mm^2, 192 slices. The resulting anatomical images were aligned to the Montreal Neurological Institute (MNI) template.

Resting state and tasked-based functional MRI. Blood-oxygenation-level-dependent (BOLD) task-based fMRI data were collected for 1) resting state fMRI and 2) task-based fMRI. First, a 10 minutes resting state fMRI scan was acquired using a T2-star echo planar image sequence with the following parameters: TR =853ms, TE=25ms, no delay time in TR, FOV= 100×100mm2, slice thickness 3mm, spacing between slices 3mm, flip angle 59°, acquisition matrix 74×74, multiband acceleration factor 3. Participants were

instructed to focus on a central white fixation cross presented on a black screen and to remain still during the sequence.

The task-based fMRI was run 4 times (10minutes per run) for a total duration of 40 minutes and included two different types of scan sequences, two scans for the whole brain and two for a high resolution scan focused on thalamic regions. For the initial whole brain scans, alterations in the BOLD signal were assessed using an echo-planar T2 imaging sequence with the following parameters: Repetition time TR = 853ms, TE = 25ms, no delay time in TR, FOV of 222×222mm^2, voxel size of 3mm^3, flip angle of 59°, acquisition matrix of 74×74, and a multiband acceleration factor of 3, 42 slices, 750 volumes, interleaved slices. For the second high resolution scan, focused on subcortical structures, the parameters for the T2 sequence are: TR = 826ms, TE = 26ms, no delay time in TR, FOV = 220×220mm^2 (placement was adapted for each participant), voxel size of 2mm^3, flip angle 56°, acquisition matrix 110×110, multiband acceleration factor 3, 30 slices, 820 volumes, interleaved slices. Field maps obtained for the whole brain and high resolution scans had the same respective acquisition parameters, except for a reversed phase encoding direction denoted as *j*.

Diffusion MRI. Diffusion MRI acquired using the following parameters: 60 slices, slice thickness 2mm, voxel size of 2mm, FOV = 100×100mm, TR = 2400ms, TE = 71ms, and flip angle 90°. Field maps are also available for diffusion MRI.

Electrophysiological acquisition

Electrophysiological measures were acquired using the MRI compatible BIOPAC MP160, Systems, i.e., peripheral finger pulse, respiratory belt, and electrocardiogram (ECG) measures during the entire experimental procedure.

Eyetracker acquisition

Eye tracking data were recorded during functional scans using the MRI compatible MRC eye tracker. Calibration was performed before the start of the first functional scan, i.e. resting state MRI, and repeated as needed in between the functional MRI scans. For calibration,

participants were asked to fixate a large black dot on a white background presented on the screen for 6 seconds intervals in the following order: center, top left, top right, bottom right and bottom left corner.

Data analysis

Data organization. DICOM images acquired from the Siemens scanner were converted into the Neuroimaging Informatics Technology Initiative (NIfTI) format and reorganized into the Brain Imaging Data Structure (BIDS) specification. Information and anatomical data that could be used to identify participants has been removed from the records. The raw data from each subject are saved in "sub-<ID>" directories and a derivatives directory contains the preprocessed and mriqc data. See corresponding Figure 1 for reference.

Automated lesion mapping. Patients with brain damage have lesions varying in shape, size and specific location making their precise identification challenging. These effects can complicate the accurate alignment of images, the identification of regions of interest, and the interpretation of data. Lesion-mapping is important to minimize tissue misclassification and give prior information to the segmentation and normalization procedure, thus improving data quality. Manual lesion tracing is a time-consuming, error-prone process that limits reproducibility. To increase reproducibility and minimize operator-dependant effects, we performed automated lesion identification on individual T1-weighted (T1w) images using a modified version of SPM's automated lesion identification (ALI) toolbox (Sanjuan et al., 2013). The algorithm, adapted with permission, is now implemented in the bidSPM app, available here. Thus, lesion masks were mapped out for each CVI participant and used in the following preprocessing steps. Lesion masks are also visible in the fmriprep output files.

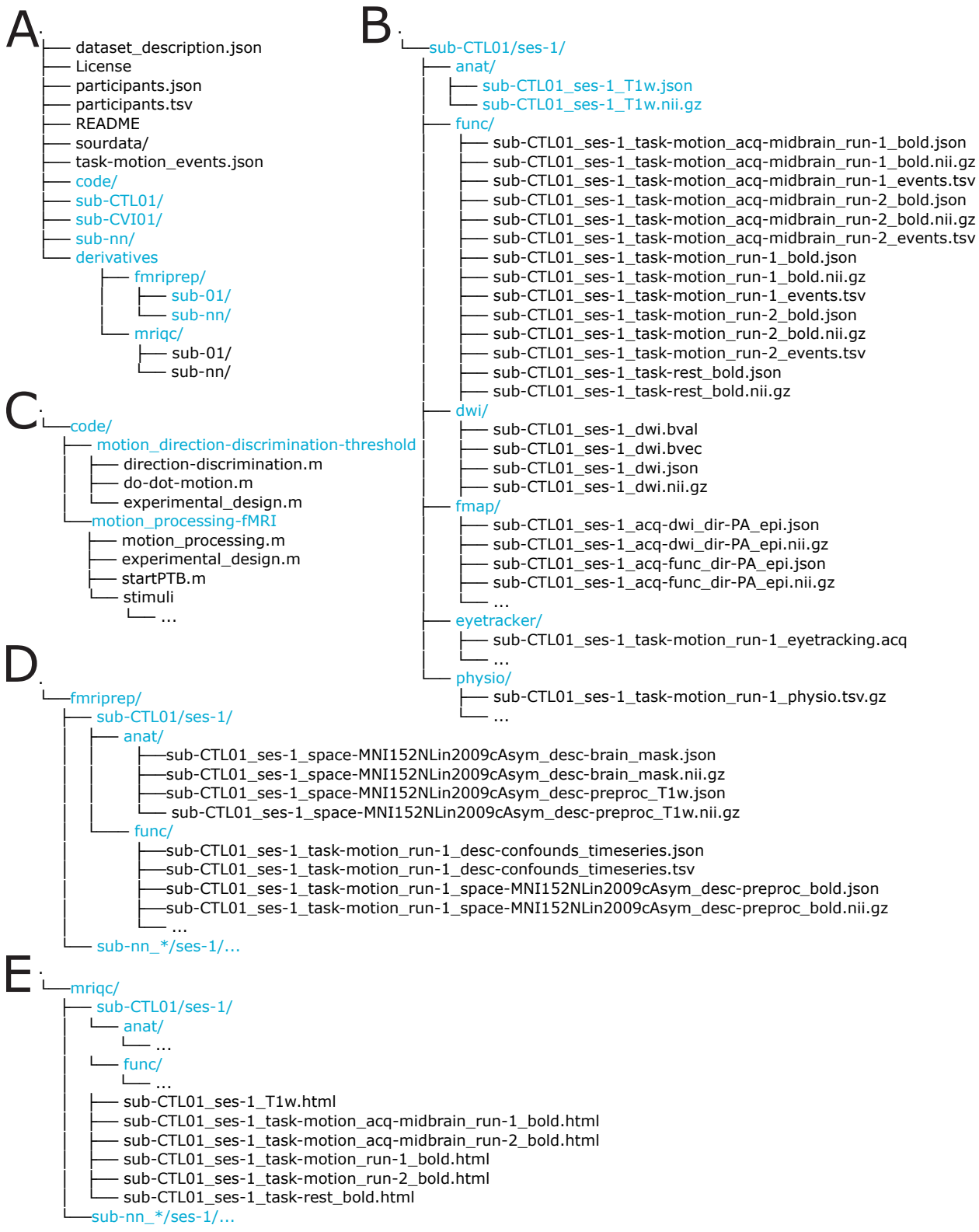

Figure 1 – File structure of the dataset.

Fig. 1 (continued). (A) The general file structure organized according to the Brain-Imaging-Data-Structure (BIDS) Specification. (B) The file structure of the raw data from a sample participant (i.e., CTL01), including anatomical, functional, diffusion MRI, field maps, in addtion to eyetracking measures and electrophysiological data. (C) The file structure of code for the visual motion processing tasks used both inside and outside the scanner. (D) The file structure of the derived fmriprep preprocessed data from a sample participant. (E) The file structure of the derived MRIQC (i.e., quality control for technical validation) data from a sample participant.

Data preprocessing. Preprocessing in this study was further performed using fMRIPrep 21.0.1 (fmriprep1; fmriprep2; RRID:SCR_016216), which is based on Nipype 1.6.1 (nipype1; nipype2; RRID:SCR_002502).

Anatomical data preprocessing

One T1-weighted (T1w) image was found within the input BIDS dataset. The image was corrected for intensity non-uniformity (INU) with N4BiasFieldCorrection (Tustison et al., 2010), distributed with ANTs 2.3.3 (Avants et al., 2008, RRID:SCR_004757). The T1w-reference was then skull-stripped with a Nipype implementation of the antsBrainExtraction.sh workflow (from ANTs), using OASIS30ANTs as target template. Brain tissue segmentation of cerebrospinal fluid (CSF), white-matter (WM) and gray-matter (GM) was performed on the brain-extracted T1w using fast FSL 6.0.5.1:57b01774, RRID:SCR_002823 (Zhang et al., 2001). A T1w-reference map was computed after registration of the T1w image (after INU-correction) using mri_robust_template FreeSurfer 6.0.1 (Reuter et al., 2010). Brain surfaces were reconstructed using recon-all FreeSurfer 6.0.1, RRID:SCR_001847 (Dale et al., 1999), and the brain mask estimated previously was refined with a custom variation of the method to reconcile ANTs-derived and FreeSurfer-derived segmentations of the cortical gray-matter of Mindboggle RRID:SCR_002438 (Klein et al., 2017). Volume-based spatial normalization to one standard space (MNI152NLin2009cAsym) was performed through nonlinear registration with antsRegistration (ANTs 2.3.3), using brain-extracted versions of both T1w reference and the T1w template. The following template was selected for spatial normalization: ICBM 152 Nonlinear Asymmetrical template version 2009c (Fonov et al., 2009), RRID:SCR_008796; TemplateFlow ID: MNI152NLin2009cAsym].

Functional data preprocessing

For each of the 5 BOLD runs found per subject (across all tasks and sessions, i.e., one resting state fMRI and 4 task-based fMRI), the following preprocessing was performed. First, a reference volume and its skull-stripped version were generated using a custom methodology of fMRIPrep. Head-motion parameters with respect to the BOLD reference (transformation matrices, and six corresponding rotation and translation parameters) are estimated before any spatiotemporal filtering using mcflirt (FSL 6.0.5.1:57b01774, Jenkinson et al.,

2002). BOLD runs were slice-time corrected to 0.362s (0.5 of slice acquisition range 0s-0.725s) or 0.388s (0.5 of slice acquisition range 0s-0.775s) or 0.386s (0.5 of slice acquisition range 0s-0.772s) using 3dTshift from AFNI (Cox & Hyde, 1997, RRID:SCR_005927). The BOLD time-series (including slice-timing correction when applied) were resampled onto their original, native space by applying the transforms to correct for head-motion. These resampled BOLD time-series will be referred to as preprocessed BOLD in original space, or just preprocessed BOLD. The BOLD reference was then co-registered to the T1w reference using bbregister (FreeSurfer) which implements boundary-based registration (Greve & Fischl, 2009). Co-registration was configured with six degrees of freedom. Several confounding time-series were calculated based on the preprocessed BOLD: framewise displacement (FD), DVARS and three region-wise global signals. FD was computed using two formulations following Power (absolute sum of relative motions, (Power et al., 2014)) and Jenkinson (relative root mean square displacement between affines, (Jenkinson et al., 2002)). FD and DVARS are calculated for each functional run, both using their implementations in Nipype following the definitions by (Power et al., 2014).The three global signals are extracted within the CSF, the WM, and the whole-brain masks. Additionally, a set of physiological regressors were extracted to allow for component-based noise correction CompCor (Behzadi et al., 2007). Principal components are estimated after high-pass filtering the preprocessed BOLD time-series (using a discrete cosine filter with 128s cut-off) for the two CompCor variants: temporal (tCompCor) and anatomical (aCompCor).tCompCor components are then calculated from the top 2% variable voxels within the brain mask. For aCompCor, three probabilistic masks (CSF, WM and combined CSF+WM) are generated in anatomical space. The implementation differs from that of Behzadi et al. in that instead of eroding the masks by 2 pixels on BOLD space, the aCompCor masks are subtracted a mask of pixels that likely contain a volume fraction of GM. This mask is obtained by dilating a GM mask extracted from the FreeSurfer's aseg segmentation, and it ensures components are not extracted from voxels containing a minimal fraction of GM. Finally, these masks are resampled into BOLD space and binarized by thresholding at 0.99 (as in the original implementation). Components are

also calculated separately within the WM and CSF masks. For each CompCor decomposition, the k components with the largest singular values are retained, such that the retained components' time series are sufficient to explain 50 percent of variance across the nuisance mask (CSF, WM, combined, or temporal). The remaining components are dropped from consideration. The head-motion estimates calculated in the correction step were also placed within the corresponding confounds file. The confound time series derived from head motion estimates and global signals were expanded with the inclusion of temporal derivatives and quadratic terms for each (Satterthwaite et al., 2013). Frames that exceeded a threshold of 0.5 mm FD or 1.5 standardised DVARS were annotated as motion outliers. The BOLD time-series were resampled into standard space, generating a preprocessed BOLD run in MNI152NLin2009cAsym space. First, a reference volume and its skull-stripped version were generated using a custom methodology of fMRIPrep. All resamplings can be performed with a single interpolation step by composing all the pertinent transformations (i.e. head-motion transform matrices, susceptibility distortion correction when available, and co-registrations to anatomical and output spaces). Gridded (volumetric) resamplings were performed using antsApplyTransforms (ANTs), configured with Lanczos interpolation to minimize the smoothing effects of other kernels (Lanczos, 1964). Non-gridded (surface) resamplings were performed using mri_vol2surf (FreeSurfer).

Many internal operations of fMRIPrep use Nilearn 0.8.1 (Abraham et al., 2014, RRID:SCR_001362), mostly within the functional processing workflow. For more details of the pipeline, see the section corresponding to workflows in fMRIPrep's documentation.

Data files nomenclature

The raw data file nomenclature as seen in the sample of Figure 1 sample consists of the following:

Structural MRI:

<Sub-ID>/ses-1/anat/<SUB-ID>_ses-1_run-01_T1w.nii.gz

Task-based Functional MRI:

<Sub-ID>/ses-1/func/<Sub-ID>_ses-1_task-motion_<Run-ID>_bold.nii.gz

<Sub-ID>/ses-1/func/<Sub-ID>_ses-1_task-motion_acq-mibrain_<Run-ID>_bold.nii.gz

Resting state Functional MRI:

<Sub-ID>/ses-1/func/<Sub-ID>_ses-1_task-rest_<Run-ID>_bold.nii.gz

Field mapping:

<Sub-ID>/ses-1/fmap/<Sub-ID>_ses-1_run-01_<magnitude/phasediff>.nii.gz

Diffusion MRI:

<Sub-ID>/ses-1/func/<Sub-ID>_ses-1_dwi.nii.gz

Task events:

<Sub-ID>/ses-1/func/<Sub-ID>_ses-1_task-motion_<Run-ID>_events.tsv

Electrophysiological:

<Sub-ID>/ses-1/func/<Sub-ID>_ses-1_task-motion_<Run-ID>_physio.tsv.gz

Eyetracker:

<Sub-ID>/ses-1/func/<Sub-ID>_ses-1_task-motion_<Run-ID>_eyetracking.acq

The event file describes onset, duration and trial type (i.e., condition) for each block during a run. Each file type has the equivalent meta-data file.

Technical validation

Motion visual task validation outside MRI scanner. Prior to the main study, participants were asked to perform a behavioral experiment outside the scanner to optimize the psycho-physical parameters of the peripheral motion processing task used in the third study. This additional experiment involved an independent neurotypical control group (n =15, 13 females) with an average age of 26.87years ±13.44SD(±3.4708SE). We optimized the visual motion task parameters by testing different combinations to aim for maximal performance, which would benefit the clinically blind individuals. Behavioral results of the peripheral motion processing task of neurotypical controls, combining both left and right visual field are shown in Supplementary Figure 1. Visual motion stimuli consisted of the same looming, static and biological motion stimuli. The task was run five times, each run had a different target duration, respectively, 1.5; 2s; 2.5s; 3s; or 3.5s. The overall performance for a target duration of 2.5, 3 and 3.5s is above a 95%, corresponding to the number of hits, indicating that neurotypical participants can successfully perform the task. Faster participant response times were significantly correlated with the number of correct responses ($R^2 = 0.549$, $p < 0.01$). Mean response times were significantly correlated with target durations ($R^2 = 0.95$, $p < 0.01$), where each augmented target duration of one second yields an increase ranging from 15 to 24% in response time. Moreover, the number of false alarms is below 3% across all motion conditions and target durations. Taking these factors into account, and given that the task would be conducted in the clinically blind field of individuals with cortical visual impairment, we selected a target duration of 3 seconds for the third study.

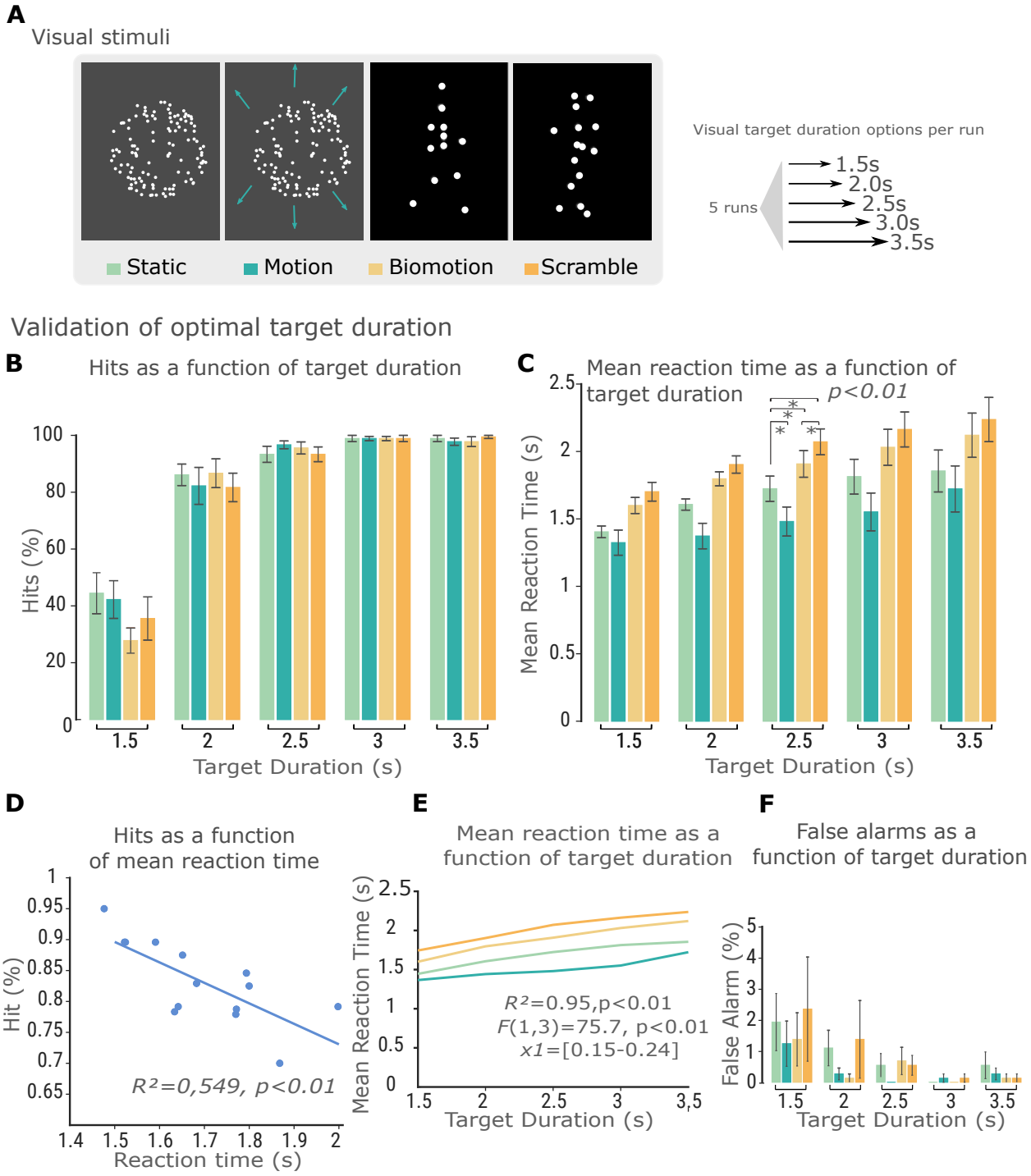

Figure 2 – Behavioral results of parameter optimization of the peripheral motion processing task of independent neurotypical controls combining both left and right visual field, performed outside the scanner.

Figure 1 (continued). (A) Visual Motion Stimuli with 5 different target durations per run, i.e., 1.5; 2s; 2.5s; 3s; or 3.5s. (B) Mean performance rates corresponding to the percentage of correct responses (hits) as a function of target duration (n =15). The overall performance for target durations [2.5-3.5]s is above a 95% success rate. (C) Mean Reaction time as a function of target duration. Significant differences for reaction times are shown, statistics were performed only on the 2.5s target duration, the first target duration category above 95% success rate. (D) Hit rates as a function of mean reaction time. Faster reaction times are also correlated with a correct number of responses. (E) Mean reaction time (s) for each motion condition as a function of target duration. Each augmented target duration (of 1s) yields an increase ranging from 15 tp 24% in reaction time. (F) False alarms (%), corresponding to the number of responses when no target was present, as a function of target duration is below 3% across all motion conditions.

Quality control of neuroimaging data with MRIQC. The dataset includes an objective data quality assessment of the neuroimaging data, i.e., the output of subject level and group level quality control from the MRI Quality Control tool (MRIQC) (Esteban et al., 2017). Performing a quality control check is an important step and can help identify any artifacts, noise, or inhomogeneity in the data, such as spiking and ghosting.

Data records / Usage notes

Description of the available content and all necessary specifications regarding individual files can be found in the README file on our repository.

Data Statement Availability

The data is accessible via a registered access, upon request to the corresponding author, in accordance with the limits established by the ethical committee.

Code availability

All codes for the experimental design, data organization, and technical validation are available on GitHub.

Acknowledgements

Data acquisition was supported by the Canada Research Chair Program [FL] and the Natural Sciences and Engineering Research Council of Canada grants RGPIN-8245-2014 [FL]. We thank the Functional Neuroimaging Unit (UNF) team at the Centre de recherche de l'Institut universitaire de gériatrie de Montréal (CRIUGM) for assistance in MRI data collection and experimental setup, in particular Carollyn Hurst, Basile Pinsard and Arnaud Boré as well as Prof Julien Cohen-Adad for advice on specifying MRI data acquisition parameters. We would like to thank all participants who took part in the experiment. Computational work was supported by resources provided by the High-performance Computing Platform Compute Canada and Calcul Québec.

List of current contributors to the dataset:

Michèle W. MacLean (Conceptualization, Project administration, Investigation, Data curation, Methodology, Software, Validation, Writing [Chapter] –Original Draft); Rémi Gau (Conceptualization, Data curation, Methodology, Software); Catherine Landry (Investigation); Mohamed Rezk (Software); Dang K. Nguyen (Resources); Olivier Collignon (Conceptualization, Supervision); and Franco Lepore (Funding acquisition, Supervision)

Chapter 5

Article 3
Reorganization of cortical and subcortical motion-selective brain regions in cortical visual impairment.

Michèle W. MacLean[1,2,3], Rémi Gau[3,4], Catherine Landry[1,2], Mohamed Rezk[3], Dang Khoa Nguyen[5,6] Olivier Collignon[3] and Franco Lepore[1,2]

(1) Centre de recherche en neuropsychologie et neuroscience cognitive et computationnelle, Université de Montréal, Québec, Canada;

(2) Département de Psychologie, Université de Montréal, Montréal, Québec, Canada;

(3) Crossmodal Perception and Plasticity Lab, Institute of Research in Psychology (IPSY) and Institute of Neuroscience (IoNS), Universite Catholique de Louvain, 1348 Louvain-la-Neuve, Belgium;

(4) Origami lab, McGill University, Montréal, Québec, Canada

(5) Département de neurosciences, Université de Montréal, Montréal, Québec, Canada

(6) Centre Hospitalier de l'Université de Montréal, Montréal, Québec, Canada.

To submit as: **Michèle W. MacLean**, Rémi Gau, Catherine Landry, Mohamed Rezk, Dang K. Nguyen, Olivier Collignon, Franco Lepore. Reorganization of cortical and subcortical motion-selective brain regions in cortical visual impairment.

Abstract

Cerebral Visual Impairment (CVI) refers to a loss of visual function resulting from damage to the brain's primary visual processing areas rather than to the eyes themselves. While functional magnetic resonance imaging (fMRI) studies have highlighted changes in neural activation patterns following CVI, the modulation of these patterns and their specific elicitation by tasks, particularly related to motion processing, remain subjects of ongoing debates. In this study, we investigate the neural correlates underlying residual vision for diverse motion stimuli, including looming and biological motion, following an occipital cortex injury, by collecting high-resolution and whole brain coverage fMRI data from CVI participants (n = 8) and a neurotypical control group (n = 25). Automatic lesion mapping allowed for reliable quantification of the extent of brain damage and participants were categorized based on residual visual ability from a motion direction discrimination task. Targeted regions of interest for cortical and subcortical regions were employed, in addition to exploratory whole brain analyses, and focused on neural responses following intact and impaired visual field presentation. The results show that, even without intact primary visual areas, visual information can still be processed and represented within the brain through a constellation of regions involving the middle temporal area and subcortical structures. In contrast to the contralateral dominance seen in neurotypical controls and the intact hemisphere of CVI participants, the ipsilesional middle temporal area and lateral occipital complex exhibit a more synergistic activation pattern in response to contralateral and ipsilateral visual motion. Additionally, the lateral occipital complex in the intact hemisphere can respond to motion presentation in the impaired visual field. High-resolution fMRI revealed the ipsilesional thalamus and pulvinar to display an ipsilateral dominance in response to looming motion, in contrast to the contralateral dominance in the intact hemisphere. However, the ipsilesional thalamus of high-performing CVI participants responds well to impaired visual field presentation. The findings contribute to our understanding of how occipital cortex lesions modulate visual processing pathways and shed light on potential neural mechanisms facilitating spared visual function and motion perception without the primary visual cortex.

Highlights

(1) Looming and biological motion stimuli can be represented within hMT without intact primary visual areas

(2) The lateral occipital complex within the intact hemisphere can respond to the impaired visual field

(3) Thalamus signal increase post occipital cortex injury

(4) Subcortical regions may facilitate residual visual abilities

Keywords: Functional magnetic resonance imaging (fMRI), Visual motion processing, V1 lesions, Cortical Visual Impairment (CVI), Residual vision, Neuroplasticity

1. Introduction

The human brain is capable of transforming raw visual information into a rich, conscious perceptual experience. However, damage to certain regions can disrupt cognitive and perceptual processes, leading to conditions such as cortical visual impairment (CVI). CVI is characterized by a loss of visual function associated with damage to the brain's primary visual processing areas rather than to the eyes themselves. Although individuals with CVI typically do not regain neurotypical vision, the brain can display a capacity to reorganize and adapt, sometimes facilitating residual processing of visual information. Functional magnetic resonance imaging (fMRI) studies have sought to reveal the post-injury neural activation patterns, yet the specific functional modulation of these patterns and their elicitation by specific tasks, particularly related to motion processing, remain a subject of ongoing debates.

Detecting motion holds a strong evolutionary significance, and even in CVI individuals, objects in motion presented in the blind visual field have been shown to activate the extrastriate cortex, specifically the human middle temporal complex (hMT) (Ajina et al., 2015a; Barbur et al., 1993; Bridge et al., 2010). This suggests the existence of alternative non-striate visual inputs to the hMT region, enabling the processing of visual motion information despite damage to the primary visual areas. Individuals with this type of visual loss have shown the ability to detect or discriminate motion in their impaired visual field, even without intact primary visual areas and without conscious visual awareness of the stimuli, a phenomenon often known as blindsight (Celeghin et al., 2018; Weiskrantz, 1996). Alternative pathways from the retina, which bypass V1 and involve intact cortical and subcortical structures like the thalamus and pulvinar, transmitting to hMT, have been suggested as potential mechanisms underlying this residual vision (Ajina & Bridge, 2018; Bourne & Morrone, 2017; Bridge et al., 2016; Tamietto & Morrone, 2016; Tran et al., 2019). Understanding the specific structures involved in enabling visual processing in the absence of V1 could provide valuable insights into alternative motion processing mechanisms after occipital cortex injury.

Motion stimuli elicit robust activation in the brain, as shown by combined neuroimaging and psychophysical experiments (Huk et al., 2002; Kolster et al., 2010; Tootell et al., 1995b). Looming stimuli have been shown to engage midbrain circuits across various animal models (D. Liu et al., 2022; Y. J. Liu et al., 2011; Salay et al., 2018; Shang et al., 2018). Avoidant head movements in non-human primates with unilateral visual cortex lesions (King & Cowey, 1992) and activation in the middle temporal area of a patient with bilateral CVI (Hervais-Adelman et al., 2015) both suggested the potential involvement of a subcortical pathway in transmitting the visual information to cortical regions. The thalamic nucleus and the superior colliculi, a structure located in the midbrain involved in receiving sensory visual input from the retina, generating eye movements, and orienting responses to visually salient stimuli, have also been shown to be responsive to looming objects in intact humans (Billington et al., 2011; May, 2006). Another informative aspect of visual processing is the recognition and understanding of others' actions through biological motion perception (Giese & Poggio, 2003). The visual system can extract meaningful information from sparse visual cues, such as point lights representing human movements (Blake & Shiffrar, 2007; Johansson, 1973; Troje, 2013), likely as a combination of visual motion (dorsal stream) and form information (ventral stream) analysis at various levels of processing (for a review see Mather et al., 2013). However, the processing mechanisms of these complex patterns, particularly in subcortical regions, remain largely unknown. While research has focused on cortical processing of biological motion, insights into the involvement of subcortical structures, such as the thalamus and pulvinar, in perceiving of human point-light walkers is still limited (for a review see Hirai & Senju, 2020).

fMRI studies have begun exploring the possible relationship between behavioral performance and neuronal correlates in CVI participants (Celeghin et al., 2018). However, precise identification of brain lesions can be complex due to variations in shape, size, and location. Brain lesions can distort structural anatomy and alter signal intensity patterns, posing challenges in MRI processing (Sanjuan et al., 2013). Additionally, the general spatial resolution achievable has made it challenging to disentangle activations in closely located regions, particularly at the subcortical level. Nonetheless, combining lesion studies with functional

measurements of brain activity can help provide causal evidence if the damaged region is necessary and / or contributes to visual information processes (Vaidya et al., 2019). Given the variability in the impact of CVI on visual experience among individuals, understanding how the specific location and extent of brain damage influence visual processing, as well as the modulation of functional activation, remains an area of scientific investigation.

Here, we investigate the neural mechanisms that underpin peripheral visual motion processing among individuals with cortical visual impairment (CVI), utilizing functional magnetic resonance imaging (fMRI) and robust behavioural paradigms. Ultimately, this study aims to comprehensively investigate how occipital cortex lesions modulate the organization of visual pathways, and the resulting impact on visual perception, thereby offering insights on structures mediating spared visual function. We sought to assess the ability of CVI individuals to process diverse types of motion stimuli - including looming and biological motion stimuli, with a comparative analysis alongside a group of matched neurotypical controls. Two distinct types of scanning techniques were conducted: exploratory whole brain coverage to assess cortical pathways and high-resolution fMRI to delve into the role of subcortical regions in visual motion processing. Automatic lesion mapping was conducted to further characterize the CVI cohort, based on the extent of their brain damage, as well as minimize tissue misclassification prior to the preprocessing procedure of neuroimaging data. Regions of interest were targeted based on a priori hypotheses and included the middle temporal area, lateral occipital complex, thalamus and pulvinar. The fMRI analyses focused on the neural responses associated with stimulus presentation in both the impaired and sighted fields of CVI participants, compared to neurotypical controls. We anticipated that functional activation patterns would reflect the extent and location of the lesion and resulting visual impairment, yielding significant variations between stimulus presentation sides compared to neurotypical controls. We hypothesized to first observe activation within hMT, in response to salient looming and biomotion stimuli, illustrating that even after occipital cortex injury, the brain can represent visual motion in certain members of our CVI participant cohort. Considering the role of the lateral occipital complex for processing of simple visual features, object recognition (Amedi et al., 2001; Grill-Spector et al., 2001; Margalit et al.,

2017), and its recent association with unconscious visual perception (for a meta-analysis see MacLean et al., 2023), we postulated that this region could facilitate low-level visual information processing. Building on our previous study (Tran et al., 2019) and other works previously mentioned, we further postulated that the thalamus and pulvinar would facilitate residual motion perception.

2. Materials and methods

2.1. Participants

This study includes eight CVI participants (5 females) with V1 damage and visual field loss, with an average age of 56.8 years (SD = 16.0; max = 80.0, min = 32.0) and an average educational level of 15.3 years (SD = 3.2). Twenty-five neurotypical participants (13 females) with an average age of 39.2 years (SD = 15.4, max:71; min: 22.0) and an average educational level of 16.9630 years (SD = 3.5) were also included. The CVI participants were recruited from the Centre Hospitalier de l'Université de Montréal (CHUM), referred by neurologist Dr. Dang K. Nguyen and had received a clinical diagnosis of hemianopia or quadranopia following occipital cortex damage. No patient was in treatment at the time of testing.

The demographic data of the CVI participants are available in Table 1. Structural T1 images of the CVI participants overlaid with lesion mapping of automatically detected abnormal brain tissue are depicted in Figure 1. Additionally, schematic representations of perimetry reports are presented. The percentage of brain damage in visual areas for each CVI participant is detailed in Table 2.

All participants had normal or corrected-to-normal vision, verified by the Freiburg Visual Acuity Test (FRACT) (Bach, 1996), including CVI participants in their intact visual field and central visual field, and reported no history of psychiatric disorders or neurological condition other than the one causing the visual impairment. CVI participants showed no noticeable signs of unilateral neglect, i.e. failure to attend to the contralesional side of space, an exclusion criterion for this study, and were predominantly right-handed as determined by the Edinburgh Handedness Inventory (Oldfield, 1971). One CVI participant was

excluded for MRI incompatibility on the day of testing. All participants provided written informed consent before participating in the study, and the study was approved by the Comité d'éthique de l'Université de Montréal and the Comité d'Ethique de l'Unité de Neuroimagerie Fonctionnelle (UNF) of the Centre de recherche de l'Institut universitaire de gériatrie de Montréal (CRIUGM) (ethics ID: CMER RNQ 13-14-016). Participants consented to share anonymized data and allow usage for future research projects and received financial compensation for their time.

Table 1 – CVI participants' demographics

CVI participant	Age	Time since lesion (Y)	Sex	Neurological description	Visual Field Deficit	Educational level (Y)	Augmented Laterality Index
CVI1	35	18	F	L occipital tumor	RHH	18	86.67 (R)
CVI2	45	45	F	R occipital stroke	LHH	13	86.67 (R)
CVI3	80	8	M	R occipital stroke	LSQ	21	100 (R)
CVI5	73	8	M	L occipital stroke	RIQ	16	100 (R)
CVI6	55	8	F	Cavernoma, L	RSQ	14	100 (R)
CVI7	65	3	F	R occipital stroke	LHH	16	100 (R)
CVI8	40	4	M	R occipital stroke	LHH	13	100 (R)
CVI9	61	0.4	F	R occipital stroke	LSQ	11	-23.33 (M)

Note. Neurological description includes pathology and anatomical location of lesion within the occipital lobe (see Table 2 for percentage of brain damage across visual brain regions), age at participation in the study, time since pathology onset, visual field deficit, level of education at time of participation in the study, augmented laterality index (handedness); L: Left; R: Right; HH: Homonymous Hemianopia; SQ: Superior Quadrantanopia; IQ: Inferior Quadrantanopia; Y: Years

Table 2 – Extent of brain damage in ROIS across CVI participants and categorized residual visual abilities.

CVI participants	V1	V2	V3	hV4	hMT	LOC	Residual visual abilities
Left hemisphere damage							
CVI1	39	29	24	15	0	2.4	High
CVI5	54	62	30	23	9.4	31	Mid
CVI6	-	-	-	-	-	-	High
Right hemisphere damage							
CVI2	7.2	9.5	15	35	0	1.7	Low
CVI3	4.3	17	10	2.4	0	0	Mid
CVI7	91	84	79	47	31	88	Low
CVI8	38	36	20	35	0	36	Low
CVI9	-	-	-	-	-	-	Mid

Note. Extent of brain damage in regions of interest (ROIs) in visual and motion defined areas for CVI participants and categorized residual visual abilities. Left hemispheric damage is presented first. The cavernome for CVI6 and the posterior cerebral artery damage for CVI9 were not automatically detected as lesioned tissue, as expected, and are not included in this table. %: indicates the percentage of damage present in the respective ROI. Lower values (<0.8%) are not shown. Residual visual lateralized abilities categorized as high (>.20; corresponds to neurotypical visual abilities), low (>.90) and mid (everything in between) performers from the motion direction discrimination task.

2.2. Behavioural Experimental Procedure

Participants were instructed to perform visual motion detection or discrimination tasks for a set of presented stimuli both inside and outside the MRI scanner, as described in detail below. Visual tasks were generated using custom scripts in MATLAB (MathWorks, Inc.) and the Psychophysics Toolbox (Brainard, 1997; Pelli, 1997).

Visual motion direction discrimination task performed outside the scanner. The behavioral experiment conducted outside the MRI scanner aimed to assess participants' threshold to discriminate global motion direction and categorize them based on their performance to facilitate interpretation of functional results. Participants were seated 57 cm

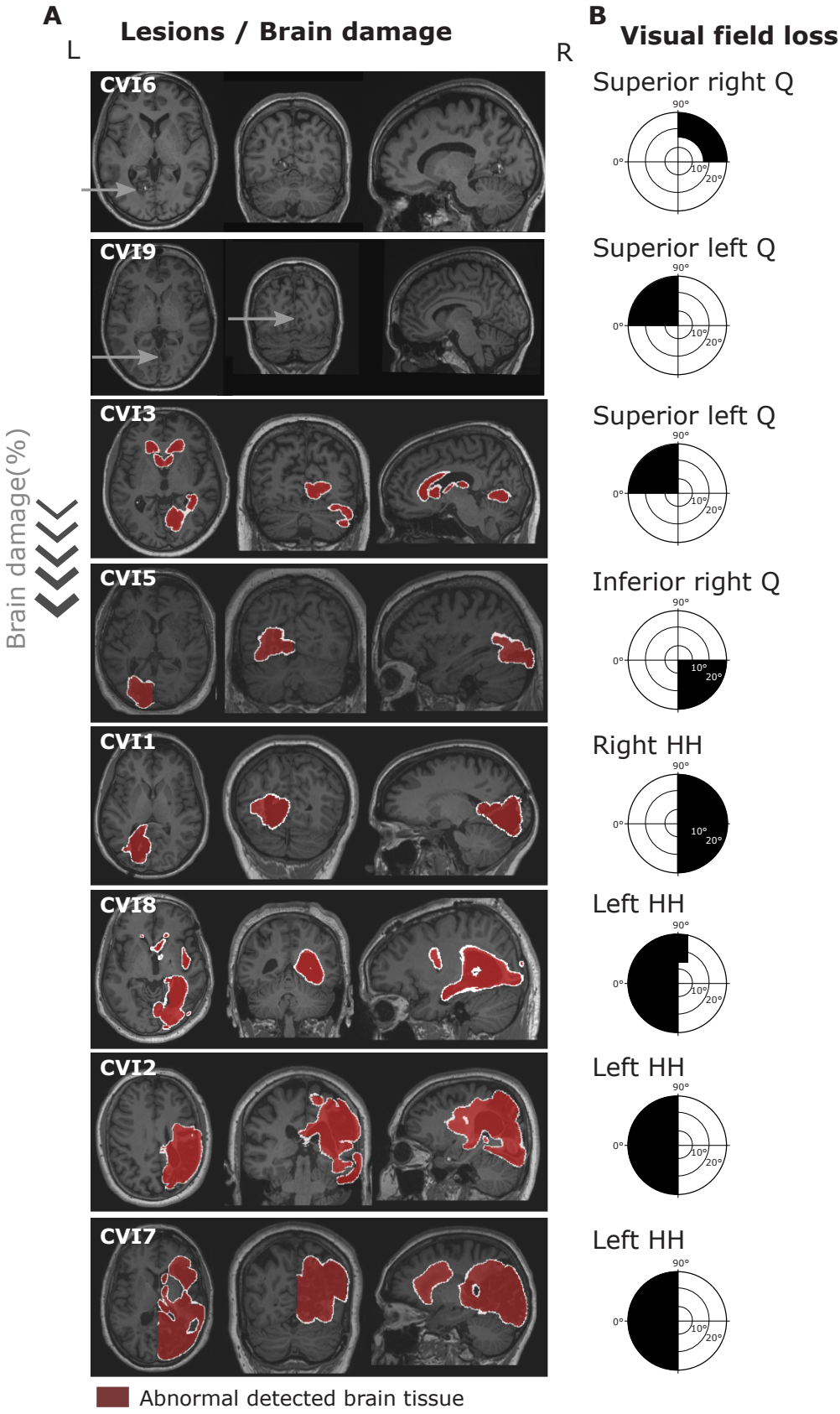

Figure 1 – Lesion mapping shown on structural T1 images for both left and right hemisphere lesions and corresponding visual field loss for each CVI participant.

Fig. 1 (continued). (A) Automatic mapping of abnormal detected brain tissue for left and right hemisphere lesions in CVI participants is shown via the red overlay on T1 structural axial, coronal, and sagittal slices, with increasing levels of brain damage from top to bottom. See corresponding Table 2 for percentage of brain damage in visual brain regions. Arrows indicate the cavernome for CVI6 and posterior cerebral artery damage for CVI9. (B) Perimetry reports are represented schematically. Visual field loss status is provided, HH: Homonymous Hemianopia, Q: Quadrantanopia (superior or inferior quandrant, left or right visual field). Motion visual stimuli presented in the impaired field were restricted to the corresponding visual field loss depicted for each participant with CVI.

away from a computer screen measuring 60 cm in width, with a refresh rate of 59Hz. The background luminance of the room was set at 60 lux. They were asked to discriminate between two motion directions (up vs. down) in a forced-choice manner. The visual motion stimuli consisted of a random dot kinematogram of a certain amount of dots moving coherently in one direction (signal) and the remaining dots moving in random directions (noise). Participants were asked to respond by pressing either "1" for upward motion or "2" for downward motion on a numerical keyboard. The task was presented a minimum of three times across three distinct runs, specifically in the central visual field, as well as the peripheral left and peripheral right visual fields, positioned on either side of the fixation cross. Participants were first asked to complete a practice run. The order of runs, corresponding to the peripheral visual field presentation side, was randomized across participants. The dots were white displayed on a black background, 8 pixels in size, with a speed of 8^{o}/s and a lifetime of 200 ms, and a maximum of 99 dots per frame was presented. Each of the 60 motion trials lasted 1.2 seconds, with a 5-second inter-trial interval, resulting in a total task duration of approximately 6 minutes. To determine the motion discrimination threshold, the QUEST procedure was employed. This Bayesian adaptive psychometric method (A. B. Watson & Pelli, 1983), implemented in Psychtoolbox (Brainard, 1997; Pelli, 1997) for Matlab, automatically adjusts the coherence of the signal dots individually for each participant. Starting with 50% coherence, the coherence level was adapted up or down (i.e., increasing

or decreasing in difficulty) in a staircase fashion based on the participant's performance. A threshold score was calculated indicating the percentage of coherence necessary to achieve a behavior accuracy of 75%. Event coherence was also calculated indicating the percentage of coherence across trials for each run of the task. When the task was performed within the peripheral visual field for all participants, the fixation cross doubled in size during the period when participants were expected to provide a response. This visual cue was designed to signal to participants with CVI the appropriate moment for their response. See Figure 2 for the experimental task procedure and the assessment of behavioural ability for neurotypical controls, in the left and right visual field respectively (20% average), and for three CVI participants to display how residual visual abilities in the impaired field were categorized as high performer (below 20% threshold) with residual visual abilities resembling neurotypical controls, as low performer (over 90% threshold) with no detected residual visual abilities on this task, or as mid performer with a minimal amount of residual abilities.

Visual motion processing tasks performed inside the scanner. On the same day of testing of the previous task, participants completed two peripheral motion perception tasks while inside the MRI scanner. The behavioral paradigm consisted of a **looming stimuli task** and a **biological motion task** presented in the same run, with participants instructed to respond as fast as possible when detecting the infrequent target stimulus lasting three seconds, while the frequent stimuli had a duration of one second. Participants were instructed to fixate a central fixation cross, while attending to the side of stimuli presentation located at 8° of eccentricity. An arrow pointing left or right preceded each block to indicate the side that should be attended. The looming motion task consisted of a random dot kinematogram, consisting of white dots displayed on a dark grey background, where dots alternated between moving radially outward or inward, and a static condition that served as control blocks. 120 dots were presented, with a dot speed of 8°/second, a width of 0.2°. In the static condition, dots were randomly allocated in each new trial and remained stationary throughout the entire trial. The second task included stimuli generated using a biomotion walker tool from the Biomotion Lab at York University (Ghorbani et al., 2021). This task included a human walker condition where white dots were displayed on a black background represented the

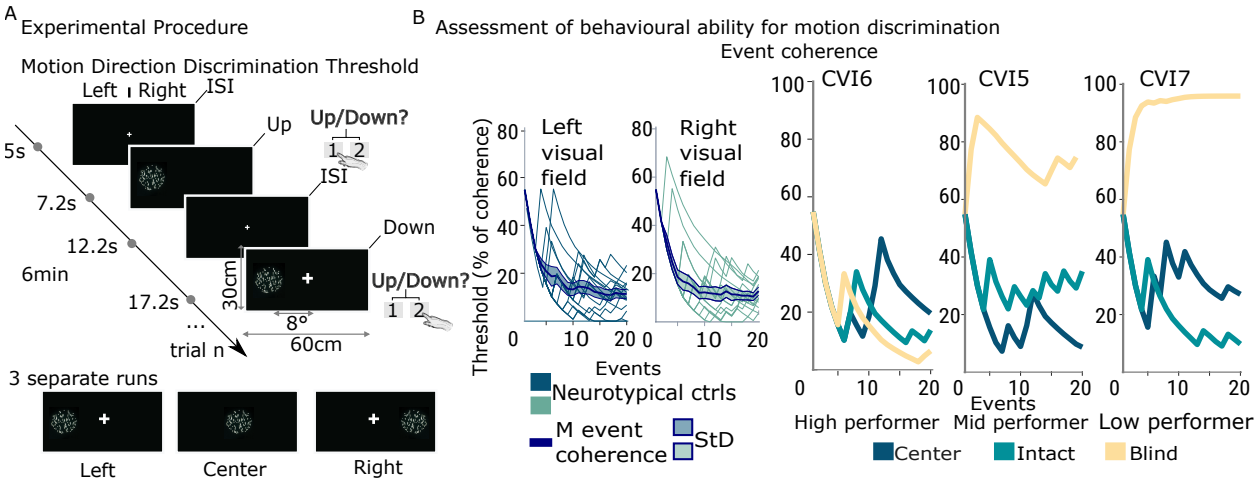

Figure 2 – Preliminary assessment of behavioral capacity of CVI participants and neurotypical controls using the global motion discrimination threshold task outside the scanner. (A) Experimental procedure showing the motion direction discrimination threshold two forced choice task (up vs down) as further described in the methods section. (B) Behavioural results showing the event coherence, i.e. threshold (%coherence) obtained across the events (each trial or occurrence of visual stimuli) during a run for neurotypical controls and three CVI participants corresponding to high (i.e., comparable to neurotypicals), mid and low performers are shown for visualization purposes.

biological motion of a human walking, as well as a control condition consisting of a scramble of the human walker stimuli. This condition was created by randomly modifying the phase and degree of each dot in the first image while keeping the same vector of movement for the duration of the video, with the dots scrambled horizontally, vertically and inverted locally. Each run of the block design paradigm lasted approximately ten minutes and included eight different types of blocks, with four blocks presenting one distinct type of motion condition repeated on the left or right of the screen (4 x 2 = 8). Each type of block lasted [18-24] seconds depending on the number of included targets [1-3] and was repeated three times (8 x 3 = 24 total presented blocks), with ten trials per block, a 200 ms inter-trial interval and four seconds inter-block interval, with an initial wait before starting the run of two seconds and an end wait of two seconds. Each block had one, two or three targets with a minimum of two

trials between targets, with the same number of targets for each type of block by the end of each run. The order of events within each block was randomized and the order of blocks was randomized across runs to balance the sequence of conditions across participants, though each motion or biomotion block was immediately followed by a block corresponding to the control condition, respectively static or scramble. The task was projected on a screen located behind the MRI magnet and reflected through the mirror of the head coil. Prior to data acquisition, the position of the mirror was adjusted for each participant such that the field of view was sufficiently large to display all stimuli. Participants were also asked to confirm the position of the center and four corners of the screen. When in the MRI, the viewing distance from the mirror was 10 cm and the distance from the mirror to the screen/projector was 170cm. Participants were asked to practice the task via a behavioural setup, prior to entering the MRI scanner, and feedback was provided to confirm their understanding of the task's requirements. Inside the scanner, response rates and reaction times were recorded via a response box, with participants using their right index finger for responding. The behavioural recordings were sufficient to verify if participants were performing the task as expected, see Supplementary Figure 1. Behavioral data were compiled and analyzed using MATLAB and IBM SPSS Statistics (MathWorks, Inc.; IBM Corp., New York, USA, 2012). See Figure 3 for visual motion stimuli and for the experimental task procedure.

Visually impaired field presentation. The tasks were designed to ensure that stimuli were only presented within the scotoma or "blind" field and its corresponding location in the sighted hemifield of CVI participants, making them not visible to them at that specific visual field location. The same stimulus location was used for age-matched neurotypical controls. The stimuli were presented within the limits of the fMRI display, which covered a visual angle of 18 degrees horizontally and 14 degrees vertically. For participants with quadrantanopia, the stimuli were adjusted horizontally and vertically on the screen to remain within the "blind" field, with a standard vertical displacement of 3° or -3° and a horizontal displacement of 6° or -6°. Prior to conducting the visual tasks, stimuli were presented in the blind visual field and participants were asked to describe the experience, confirming both the absence of visible stimuli in the impaired visual field and suggesting the absence of any related effects or

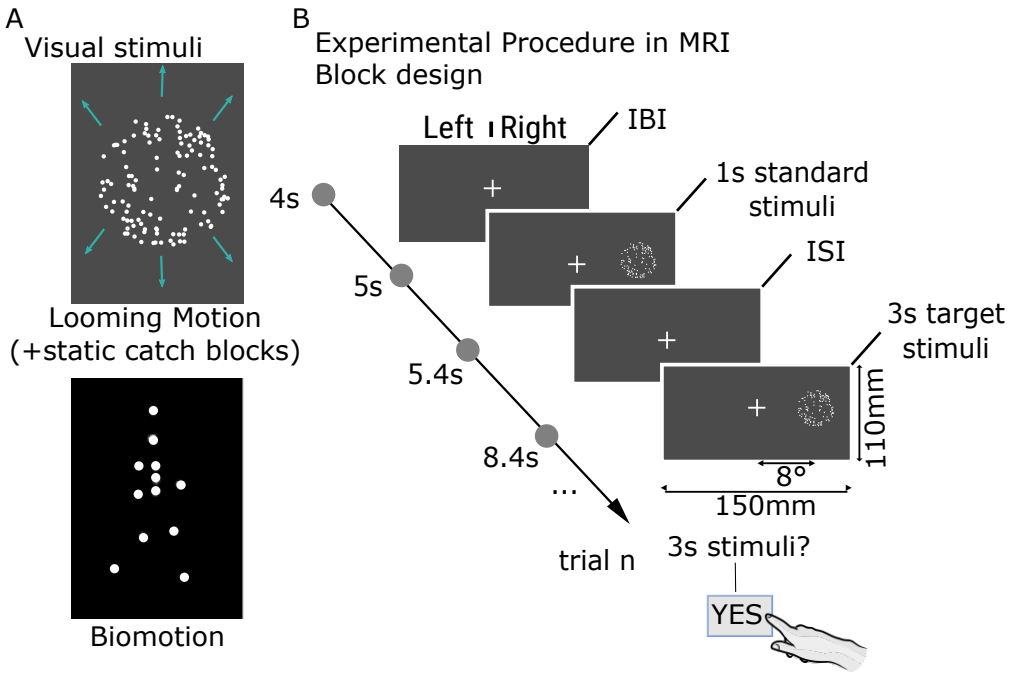

Figure 3 – Peripheral motion processing task performed within the MRI scanner environment. (A) Visual motion stimuli used for the analysis consisting of a random dot kinematogram presenting looming radial motion, interspersed with static catch blocks. Additionally, the task involves biological motion stimuli in the form of point light dots representing a human walker, with alternating sequences of walking in both leftward and rightward directions. (B) Depiction of the experimental procedure based on a block design paradigm, outlining the sequence of task and rest intervals.

descriptions in the intact visual field, such as those associated with light scatter. If necessary, further adjustments were made, yet the size of the stimuli remained consistent. Motion visual stimuli presented in the impaired field were restricted to the corresponding visual field loss, depicted for each participant with CVI in Figure 1.

2.3. MRI data acquisition

MRI data was acquired with a high resolution 3 Tesla scanner (Siemens Trio system) using a 64-channel phased-array head coil at l'Unité de neuroimagerie fonctionnelle of l'Institut de gériatrie de Montréal. The current study includes the structural MRI and task-based fMRI.

Structural MRI. A 5 minutes structural T1-weighted scan (MPRAGE) was acquired with the following parameters: voxel size of 0.9mm^3, acquisition matrix size 256x256, flip angle 8°, Repetition time (TR) 2400ms, Echo time(TE) 2.25ms, Field of view (FOV) 230x230mm^2, 192 slices. The resulting anatomical images were aligned to the Montreal Neurological Institute (MNI) template.

Functional MRI. Blood-oxygenation-level-dependent (BOLD) task-based fMRI data were collected. The task was run 4 times (10minutes per run) for a total duration of 40 minutes and included two different types of scan sequences, two scans for the whole brain and two for a high resolution scan focused on thalamic regions. For the initial whole brain scans, alterations in the BOLD signal were assessed using an echo-planar T2 imaging sequence with the following parameters: Repetition time TR: 853ms, TE: 25ms, no delay time in TR, FOV of 222×222mm^2, voxel size of 3mm^3, flip angle of 59°, acquisition matrix of 74×74, and a multiband acceleration factor of 3, 42 slices, 750 volumes, interleaved slices. For the second high resolution scan, focused on subcortical structures, the parameters for the T2 sequence are: TR 826ms, TE=26ms, no delay time in TR, FOV= 220×220mm^2 (placement was adapted for each participant), voxel size of 2mm^3, flip angle 56°, acquisition matrix 110×110, multiband acceleration factor 3, 30 slices, 820 volumes, interleaved slices. Field maps obtained for the whole brain and high resolution scans were acquired once for each type of scan, immediately following the completion of each respective scan type, and had the same respective acquisition parameters, except for a reversed phase encoding direction denoted as *j*.

2.4. Data analysis

MRI data preprocessing.

Automated lesion mapping. Lesion identification on individual T1-weighted (T1w) images was conducted using a modified version of SPM's automated lesion identification (ALI) toolbox (Sanjuan et al., 2013). The algorithm, adapted for this study with permission, is now implemented in the bidSPM app, available here. This method incorporates normalization and segmentation techniques, along with a lesion class to model the presence of abnormal tissue. The segmentation process identifies white and grey matter tissue with the addition of cerebrospinal fluid. Lesions were defined as sets of outlier voxels while considering anatomical variability observed in neurotypical individuals. To compare the CVI participants' tissue image with a group of neurotypical subjects, voxel-wise analysis was performed using 43 neurotypical controls, including the 25 controls from this current study and 18 controls from a prior project in our laboratory. Contralateral intact hemispheres were identified and excluded, cerebrospinal fluid was removed, a cluster threshold of 0.05 was applied and only lesion tissue was kept in the masks. Inverse normalization with nearest neighbor interpolation facilitated the transformation of lesion mask to T1w native space. Thus, lesion masks were mapped out for each CVI participant, initially used to quantitatively assess the percentage of brain damage across regions of interest (ROIs) associated with the visual system per CVI participant, using the Wang atlas (L. Wang et al., 2015), implemented in SPM12. The lesion masks were then incorporated into the fMRIprep preprocessing steps to mitigate the impact of the lesions by excluding the affected voxels from analysis and minimizing tissue misclassfication. The results of automatic detection of abnormal brain tissue, depicted as red overlays on axial, coronal, and sagittal T1 structural slices, are presented in Figure 1. The automated contours of lesions are also shown in white.

Anatomical data preprocessing. Preprocessing in this study was further performed using fMRIPrep 21.0.1 (fmriprep1; fmriprep2; RRID:SCR_016216), which is based on Nipype 1.6.1 (nipype1; nipype2; RRID:SCR_002502). One T1-weighted (T1w) image was found within the input BIDS dataset. The image was corrected for intensity non-uniformity

(INU) with N4BiasFieldCorrection (Tustison et al., 2010), distributed with ANTs 2.3.3 (Avants et al., 2008, RRID:SCR_004757). The T1w-reference was then skull-stripped with a Nipype implementation of the antsBrainExtraction.sh workflow (from ANTs), using OASIS30ANTs as target template. Brain tissue segmentation of cerebrospinal fluid (CSF), white-matter (WM) and gray-matter (GM) was performed on the brain-extracted T1w using fast FSL 6.0.5.1:57b01774, RRID:SCR_002823 (Zhang et al., 2001). A T1w-reference map was computed after registration of the T1w image (after INU-correction) using mri_robust_template FreeSurfer 6.0.1 (Reuter et al., 2010). Brain surfaces were reconstructed using recon-all FreeSurfer 6.0.1, RRID:SCR_001847 (Dale et al., 1999), and the brain mask estimated previously was refined with a custom variation of the method to reconcile ANTs-derived and FreeSurfer-derived segmentations of the cortical gray-matter of Mindboggle RRID:SCR_002438 (Klein et al., 2017). Volume-based spatial normalization to one standard space (MNI152NLin2009cAsym) was performed through nonlinear registration with antsRegistration (ANTs 2.3.3), using brain-extracted versions of both T1w reference and the T1w template. The following template was selected for spatial normalization: ICBM 152 Nonlinear Asymmetrical template version 2009c (Fonov et al., 2009), RRID:SCR_008796; TemplateFlow ID: MNI152NLin2009cAsym].

Functional data preprocessing. For each of the 4 BOLD runs found per subject (across all tasks and sessions), the following preprocessing was performed. First, a reference volume and its skull-stripped version were generated using a custom methodology of fMRIPrep. Head-motion parameters with respect to the BOLD reference (transformation matrices, and six corresponding rotation and translation parameters) are estimated before any spatiotemporal filtering using mcflirt (FSL 6.0.5.1:57b01774, Jenkinson et al., 2002). BOLD runs were slice-time corrected to 0.362s (0.5 of slice acquisition range 0s-0.725s) or 0.388s (0.5 of slice acquisition range 0s-0.775s) or 0.386s (0.5 of slice acquisition range 0s-0.772s) using 3dTshift from AFNI (Cox & Hyde, 1997, RRID:SCR_005927). The BOLD time-series (including slice-timing correction when applied) were resampled onto their original, native space by applying the transforms to correct for head-motion. These resampled BOLD time-series will be referred to as preprocessed BOLD in original space, or just preprocessed BOLD. The BOLD

reference was then co-registered to the T1w reference using bbregister (FreeSurfer) which implements boundary-based registration (Greve & Fischl, 2009). Co-registration was configured with six degrees of freedom. Several confounding time-series were calculated based on the preprocessed BOLD: framewise displacement (FD), DVARS and three region-wise global signals. FD was computed using two formulations following Power (absolute sum of relative motions, (Power et al., 2014)) and Jenkinson (relative root mean square displacement between affines, (Jenkinson et al., 2002)). FD and DVARS are calculated for each functional run, both using their implementations in Nipype following the definitions by (Power et al., 2014).The three global signals are extracted within the CSF, the WM, and the whole-brain masks. Additionally, a set of physiological regressors were extracted to allow for component-based noise correction CompCor (Behzadi et al., 2007). Principal components are estimated after high-pass filtering the preprocessed BOLD time-series (using a discrete cosine filter with 128s cut-off) for the two CompCor variants: temporal (tCompCor) and anatomical (aCompCor).tCompCor components are then calculated from the top 2% variable voxels within the brain mask. For aCompCor, three probabilistic masks (CSF, WM and combined CSF+WM) are generated in anatomical space. The implementation differs from that of Behzadi et al. in that instead of eroding the masks by 2 pixels on BOLD space, the aCompCor masks are subtracted a mask of pixels that likely contain a volume fraction of GM. This mask is obtained by dilating a GM mask extracted from the FreeSurfer's aseg segmentation, and it ensures components are not extracted from voxels containing a minimal fraction of GM. Finally, these masks are resampled into BOLD space and binarized by thresholding at 0.99 (as in the original implementation). Components are also calculated separately within the WM and CSF masks. For each CompCor decomposition, the $\underline{k}$ components with the largest singular values are retained, such that the retained components' time series are sufficient to explain 50 percent of variance across the nuisance mask (CSF, WM, combined, or temporal). The remaining components are dropped from consideration. The head-motion estimates calculated in the correction step were also placed within the corresponding confounds file. The confound time series derived from head motion estimates and global signals were expanded with the inclusion of temporal derivatives and quadratic terms for each (Satterthwaite et al.,

2013). Frames that exceeded a threshold of 0.5 mm FD or 1.5 standardised DVARS were annotated as motion outliers. The BOLD time-series were resampled into standard space, generating a preprocessed BOLD run in MNI152NLin2009cAsym space. First, a reference volume and its skull-stripped version were generated using a custom methodology of fMRIPrep. All resamplings can be performed with a single interpolation step by composing all the pertinent transformations (i.e. head-motion transform matrices, susceptibility distortion correction when available, and co-registrations to anatomical and output spaces). Gridded (volumetric) resamplings were performed using antsApplyTransforms (ANTs), configured with Lanczos interpolation to minimize the smoothing effects of other kernels (Lanczos, 1964). Non-gridded (surface) resamplings were performed using mri_vol2surf (FreeSurfer).

Many internal operations of fMRIPrep use Nilearn 0.8.1 (Abraham et al., 2014, RRID:SCR_001362), mostly within the functional processing workflow. For more details of the pipeline, see the section corresponding to workflows in fMRIPrep's documentation.

The above boilerplate text was automatically generated by fMRIPrep with the express intention that users should copy and paste this text into their manuscripts unchanged. It is released under the CC0 license.

fMRI data analysis. The fMRI data were analysed with bidspm v3.1.0dev; https://github.com/cpp-lln-lab/bidspm; DOI: https://doi.org/10.5281/zenodo.3554331 - [@bidspm]) using statistical parametric mapping (SPM12 Wellcome Center for Neuroimaging, London, UK); using MATLAB (R2019b) on a Microsoft Windows computer (10.0.18363.1556).
fMRI Statistical Analyses Overview:

- Mass univariate analyses from the whole brain coverage data: contrasts between conditions at the subject level, extended to the group level
  - Functional response to biomotion and looming motion stimuli (contrasted with static catch trials or baseline), respectively
  - Stimulus presentation side comparison: impaired versus sighted fields for CVI participants, left versus right (and vice versa) for neurotypical controls.

— ROI analyses

  — Whole brain coverage data: middle temporal area, lateral occipital complex.

  — High-resolution fMRI data: thalamus, pulvinar.

Statistical model. The statistical model was designed following the BIDS stats model structure implemented within the bidspm app. We modeled the fMRI experiment in a block design with regressors entered into the run-specific design matrix. The onsets were convolved with SPM canonical hemodynamic response function for the following conditions, i.e. motion, static, biomotion repeated for the left and right hemispheres. Nuisance covariates included translation, rotation around the three directions, non-steady-state outlier and motion outliers to censor any time points flagged by fmriprep as outliers.

Subject level analysis. At the subject level, fMRI analyses were first performed on the data from the whole brain coverage. We conducted a spatial smoothing of the functional whole brain data using a three-dimensional isotropic Gaussian with a full width at half maximum of 8mm. Subsequent to fmriprep preprocessing steps and additional smoothing, fMRI model specification was performed. The input data were the fmriprep preprocessed BOLD images in MNI space for the task "motion". At the subject level, we performed a mass univariate analysis with a linear regression at each voxel of the brain, using generalized least squares with a global AR(1) model to account for temporal auto-correlation and a drift fit with discrete cosine transform basis (128 seconds cut-off). Image intensity scaling was done run-wide before statistical modeling such that the mean image would have a mean intracerebral intensity of 100. Each condition was explicitly modeled against baseline, such as motion > baseline. Contrasts were defined in terms of stimulus conditions. Between conditions contrasts were computed for each subject and included the following: motion greater than static, motion presented on the right greater than motion presented on the left (and vice versa), biomotion greater than baseline, biomotion presented on the right greater than biomotion presented on the left (and vice versa). The images from these between conditions contrasts were further passed at the group level.

Group level analysis. Group level analyses were performed to measure the collective patterns of brain activation across the neurotypical control group. Contrast for the following conditions were passed as summary statistics for a group level analysis: motion with static catch trials, biomotion, repeated for the left and right hemispheres. Statistical inferences were adjusted for multiple comparisons at the voxel-level using the family-wise error (FWE) correction with a threshold of $p<0.05$, a standard correction within the SPM12 software, and a cluster-level inference with a cluster-level forming threshold of $p<0.05$. Clusters over 15 voxels are presented for vizualisations purposes. Lesioned voxels were removed from the analysis for CVI participants. This method section was in part automatically generated using bidspm (v3.1.0dev; bidspm; DOI and octache)

ROI analysis. ROI based analyses were performed on unsmoothed data using the CPP-ROI toolbox, implemented within bidSPM, which uses the MarsBaR toolbox (Brett et al., 2002). To define the regions of interest (ROIs), we utilized two atlases: the Wang atlas (L. Wang et al., 2015) for specialized visual regions and the Neuromorphometric atlas for the remaining regions. Both atlases were inversely normalized to each participant's native space. Subsequently, individual ROIs were delineated based on the T1-weighted anatomical images in their respective native spaces. For all participants, the ROIs were carefully cleared of cerebrospinal fluid. In the case of participants with CVI, ROIs were further cleaned to exclude voxels affected by lesions. The input data for ROI analyses were the preprocessed BOLD images in T1w native space for the looming stimuli and the biomotion stimuli. ROI-specific data was extracted by computing the percent signal change within the individually subject-specific defined ROIs per condition per participant and compared across groups. Statistical analyses were then conducted on the extracted ROI data to assess the effects of the experimental manipulations. The cortical ROI analyses were done using data from the whole brain coverage (i.e., hMT, LOC) and the subcortcial ROI analyses (i.e., thalamus and pulvinar) were done using the high resolution data and the statistical significance was set at $p < 0.05$. Group level comparisons of the percent signal change mean were computed between the neurotypical control group and the participants with CVI independently for the ROIs. For hMT and LOC, we independently examined whether the intact hemisphere retained a

contralateral dominance in response to visual stimuli, to confirm a neurotypical-like motion representation after stimulation of the sighted hemifield. Next, we examined whether the lesioned hemisphere had less differential recruitment to presentation side than neurotypical controls, potentially facilitating residual visual abilities. For the thalamus, we independently examined whether the intact hemisphere displayed a stronger contralateral dominance in response to visual stimuli than neurotypical controls, showing an enhanced recruitment of this region post occipital cortex injury. For the pulvinar, we examined whether the intact hemisphere showed a contralateral dominance in response to visual stimuli.

3. Results

3.1. fMRI response to visual motion - Whole brain coverage

To investigate functional activation in response to looming and biomotion stimuli, we employed an exploratory whole brain analysis. We considered specific contrasts using stimuli presentations for neurotypical controls and CVI participants. CVI participants were initially categorized as high (>.20 threshold; corresponds to neurotypical visual abilities, as determined by the average score of all control participants), low (>.90; indicating an inability to discriminate motion direction or respond correctly across all coherence levels throughout the task and mid performers (everything in between). This classification was based on the motion discrimination threshold task, which served to underscore their residual visual motion processing abilities. This preliminary classification serves to simplify the reporting of findings, while conveying the range of neural responses to motion stimuli post occipital cortex injury across CVI participants.

Results of the looming motion greater than static contrast for neurotypical controls reveal activation in the right and left middle temporal gyri (V5/MT+), as expected. The contrasts between left and right visual field presentation, and vice versa, both show activation in contralateral visual processing areas, i.e. superior occipital gyrus and posterior calcarine sulcus. The whole brain activation patterns in CVI participants exhibited a broader distribution compared to the more focused activation seen in neurotypical controls, where activation

was more localized to visual and motion processing regions. Looming motion greater than static presented in the intact visual field revealed individual differences across participants encompassing the lateral occipital complex, superior temporal gyrus, middle temporal gyrus, middle frontal gyrus, superior parietal lobule. While there were notable similarities, such as the involvement of the lateral occipital complex, the whole brain analysis revealed variability across CVI participants. In response to looming motion greater than static presented in the impaired visual field, the activation patterns showed distinctive characteristics, such as the recruitment of the middle temporal area - though not exclusively - for high-performing CVI participants. Conversely, the activation patterns among low-performing CVI participants did not consistently align with any distinct clusters. The motion presentation in the impaired versus intact visual field elicited activation across different regions within the high and mid-CVI participants, encompassing areas such as the superior occipital gyrus, temporal occipital fusiform gyrus, and lateral occipital complex, whereas low performers did not exhibit any distinct activation.

fMRI group level results in response to looming motion for neurotypical controls and CVI participants are shown in Figure 4. Visualization includes three CVI participants representing varying levels of brain damage and performance (i.e., high, mid, low) in the motion discrimination threshold task. Visual motion fMRI responses of CVI participants for motion greater than static contrast for the intact and impaired visual fields respectively, as well as the impaired greater than intact visual field presentations, are displayed on axial slices of each participant's anatomical image. The latter is shown for CVI high and mid-performers, as no significant clusters remained for CVI8. Coordinates and cluster size of the activated brain regions for neurotypical controls are in Table 3 and for CVI participants are in Table 4.

Results of the biomotion presentation (biomotion > baseline) for neurotypical controls reveal activation in the right and left middle temporal gyri (V5/MT+). The contrasts between left and right visual field presentation, and vice versa, show activation in the contralateral lateral occipital cortex and calacarine cortex. The whole brain activation patterns exhibited a wider spatial distribution across CVI participants, contrasting the more localized activation

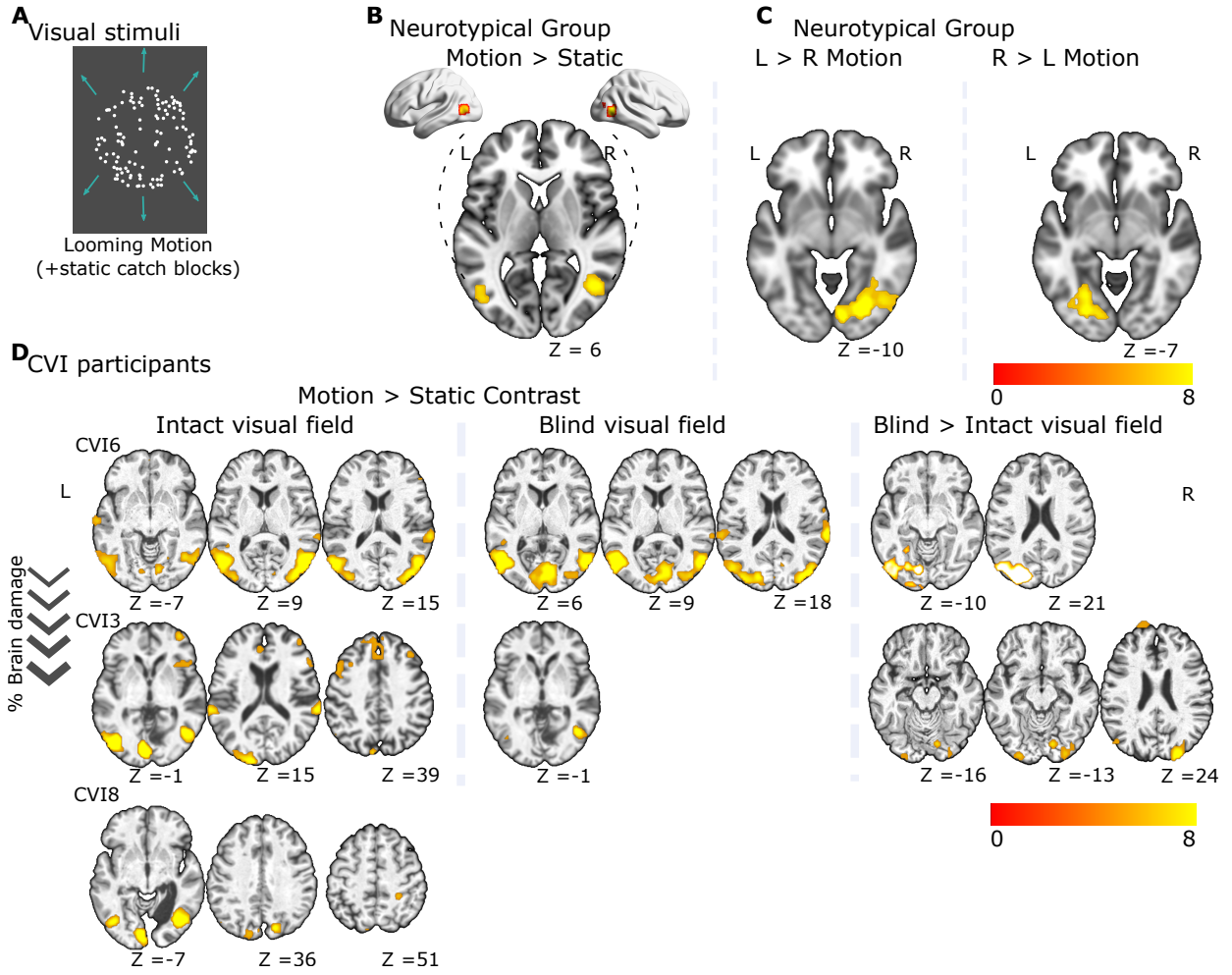

Figure 4 – fMRI response to looming motion for neurotypical controls (n=25) and CVI participants (n=8). (A) Visual looming stimuli with static catch trials. (B) Motion > static contrast group level results for neurotypical controls showing bilateral activation of hMT. Axial slices are displayed in MRIcroGL with MNI152 atlas, while inflated surface maps in BrainNet Viewer projected onto the MNI152 atlas. (C) Left > right visual field presentation (and vice versa) reveals contralateral activation with clusters identified in the superior occipital gyrus and the posterior calcarine sulcus. (D) CVI participants' fMRI response for looming motion greater than static contrast for the intact and impaired visual fields respectively are displayed on axial slices of each participant's anatomical image and reveal a more bilateral activation. Looming motion in the impaired vs. intact visual fields are shown for two CVI participants, no significant clusters remained for CVI8. Visualization includes three CVI participants representing varying levels of brain damage and performance (high, mid, low). Results are subjected to voxel-level thresholding using a FWE correction at $p<0.05$, alongside a cluster-defining threshold of $p<0.05$. Activation coordinates and cluster sizes for neurotypical controls are given in Table 3 and CVI participants' data are in Table 4.

in visual and motion processing regions in the neurotypical controls, similar to what was observed for looming motion stimuli. For biomotion presentation in the intact versus impaired visual field, high-performing individuals exhibited activation primarily within visual areas, whereas mid and low-performing participants displayed a wider distribution, encompassing visual areas as well as the superior and inferior frontal gyrus. A similar trend emerged for biomotion presentation in the impaired versus intact visual field of CVI participants, with high-performing individuals primarily activating visual areas, while mid and low-performing participants showed recruitment of a broader set of regions, including visual areas in addition to the middle frontal gyrus and inferior temporal gyrus.

fMRI group level results of the biomotion presentation for neurotypical controls are shown in Figure 5. Visualization includes three CVI participants representing varying levels of brain damage and performance (high, mid, low) in the motion discrimination threshold task. Visual motion fMRI responses of CVI participants for intact biomotion presentation greater than impaired biomotion presentation (intact > impaired visual field [biomotion]) and vice versa (impaired > intact visual field [biomotion]) are displayed on axial slices of each participant's anatomical image. Coordinates of the activation and cluster size of the activated brain regions corresponding to the neurotypical controls are given in Table 5 and for the CVI participants are in Table 6. Unthresholded statistical maps are provided at the group level for the neurotypical control group and for all individual participants with CVI for both looming motion and biomotion presentation on the NeuroVault repository here.

3.2. Regions of interest analyses

We conducted independent regions of interest (ROI) analyses to investigate the percent of signal change within the middle temporal area (hMT), the lateral occipital complex (LOC), the thalamus and pulvinar, as selected a priori based on hypotheses, in response to visual looming motion and biomotion, respectively. We considered both contralateral and ipsilateral visual field motion stimuli presentations for neurotypical controls and CVI participants. The mean and standard error for each group are displayed for each panel. Among the CVI participants, those identified as high performers in the motion discrimination threshold

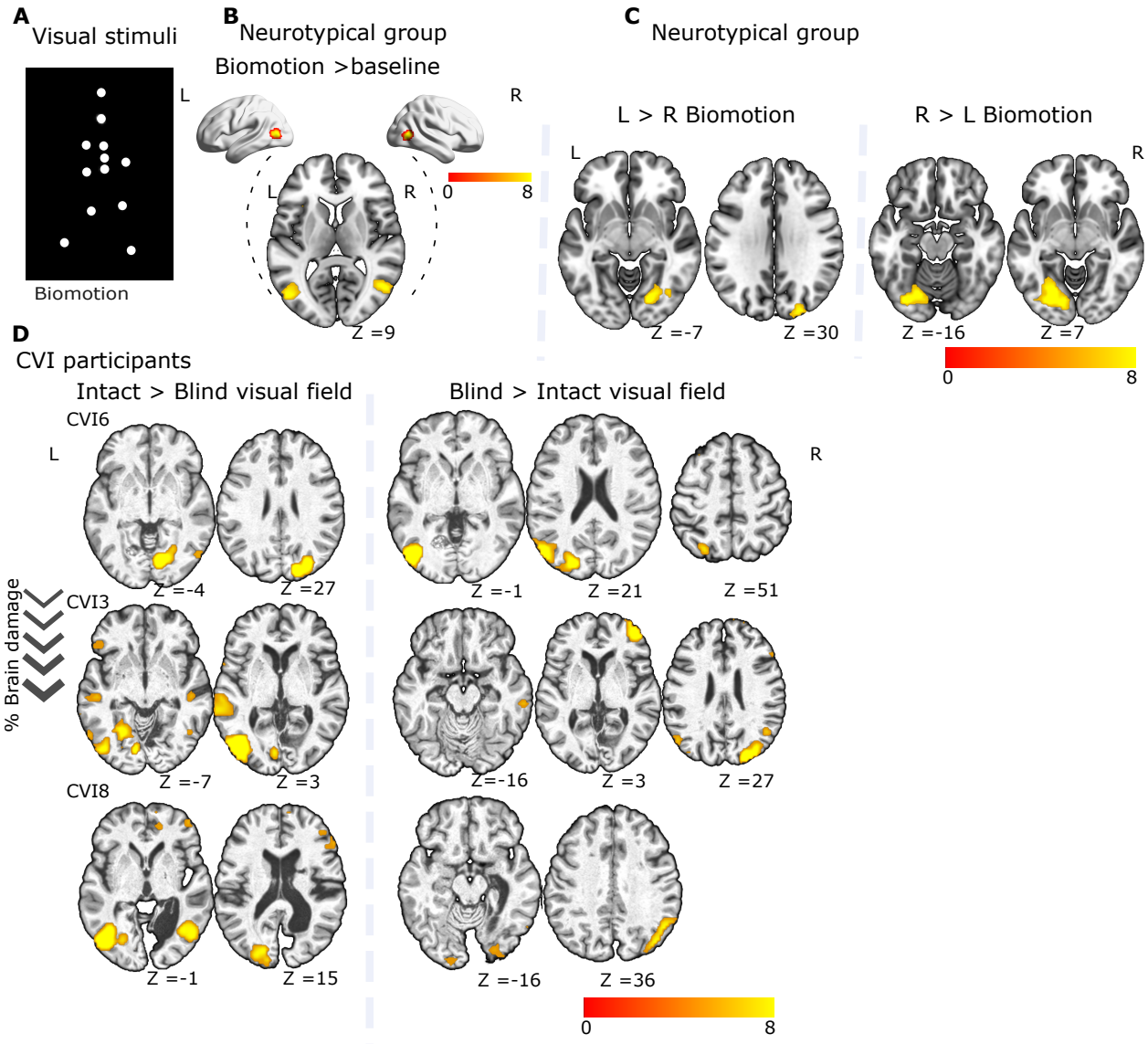

Figure 5 – fMRI responses to biomotion for neurotypical controls (n=25) and CVI participants (n=8). (A) Visual biomotion stimuli. (B) Group level results for neurotypical controls with both left and right visual field presentations showing activation in the middle temporal gyri. (C) Left vs. right visual field presentation (and vice versa) reveals contralateral acitvation in the lateral occipital cortex and calcarine cortex. Axial slices are displayed in MRIcroGL with MNI152 atlas, while inflated surface maps in BrainNet Viewer projected onto the MNI152 atlas for visualization. (D) CVI participants' results in the intact vs. impaired visual fields (and vice versa) are shown on axial slices of each participant's anatomical image. Visualization includes three CVI participants representing varying levels of brain damage and performance (high, mid, low). Results are subjected to voxel-level thresholding using a FWE correction at $p<0.05$, alongside a cluster-defining threshold of $p<0.05$. Activation coordinates and cluster sizes for neurotypical controls are given in Table 5 and CVI participants' data are in Table 6.148

task, equivalent to neurotypical controls, were singled out for their residual visual motion processing abilities and are represented in light red on all graphs.

Cortical ROIs representing visual motion information. The independent ROI analyses for hMT and LOC involved extracting data from whole brain coverage. For the response to visual looming motion, hMT signal change (%) exhibited a contralateral dominance in neurotypical controls, indicating increased contralateral activation compared to ipsilateral stimulation. Within the intact hemisphere of CVI participants, hMT signal change closely paralleled that of neurotypical controls, with a significant contralateral dominance (mean[contra-ipsi] = 0.53, SE = 0.16, p=0.03, t = 3.22). Conversely, the lesioned hemisphere of CVI participants displayed on average a more balanced bilateral activation, with similar signal changes in response to contralateral and ipsilateral motion presentation, contrasting the asymmetry in neurotypical controls and the intact hemisphere. This distinctive pattern resulted in a significantly smaller difference between contralateral and ipsilateral signal change compared to controls (mean difference controls[contra-ipsi] - CVI[contra-ipsi] = 0.56, SE = 0.23, p=0.02, t =2.45). The LOC findings mirror those of hMT, exhibiting similar trends. For neurotypical controls, a contralateral dominance was observed, accompanied by a slightly reduced average signal change compared to hMT. Within the intact hemisphere of CVI participants, though the LOC exhibited a lateralization in response to contralateral stimulation, the average ipsilateral response seems higher than that of controls, which corresponds to processing visual information in the impaired visual field. Within the lesioned hemisphere, the average LOC signal change showed a decrease in laterality, with a significantly reduced difference between contralateral and ipsilateral presentation compared to neurotypical controls (mean difference controls[contra-ipsi] - CVI[contra-ipsi] = 0.38, SE = 0.16, p=0.03, t =2.43). For biomotion presentation, hMT signal change displayed trends and significant differences similar to those of looming motion. This encompassed a contralateral dominance for neurotypical controls and the intact hemisphere of CVI participants (mean[contra-ipsi] = 0.38, SE = 0.18, p=0.05, t= 1.75), with less pronounced asymmetry in the lesioned hemisphere. This resulted in a significantly smaller difference between contralateral and ipsilateral signal change in the lesioned hemisphere compared to neurotypical

controls (mean difference controls[contra-ipsi] - CVI[contra-ipsi] = 0.45, SE = 0.19, p=0.05, t =2.42). For the LOC, the percent signal change appeared slightly lower than that of hMT in neurotypical controls. A contralateral dominance was also observed in the intact hemisphere of CVI participants (mean[contra-ipsi] = 0.38, SE = 0.11, p=0.03, t= 3.54). In the lesioned hemisphere, response to ipsilateral biomotion presentation also yielded what appears to be a higher signal change compared to neurotypical controls. See the corresponding Figure 6 for visualization of the percent signal change of hMT and LOC for looming motion and biomotion.

Subcortical ROIS representing visual motion information using high resolution fMRI. The ROI analysis targeting the thalamus and pulvinar involved extracting data from the high-resolution fMRI scans. The placement of the field of view was adapted for each participant prior to fMRI data acquisition to encompass these ROIs with optimal spatial resolution. For the response to visual looming motion presentation, within the intact hemisphere of CVI participants, the thalamus signal change (%) exhibited a contralateral dominance (mean[contra-ipsi] = 0.15, SE = 0.04, p=0.02, t = 1.38), signifying a pronounced discrepancy between contralateral and ipsilateral motion presentation. This difference was considerably larger than that observed in neurotypical controls (mean difference controls[contra-ipsi] - CVI[contra-ipsi] = -0.13, SE = 0.04 , p= 0.0055, t = -2.93). Conversely, the lesioned hemisphere of CVI participants displays an opposing trend, featuring an ipsilateral dominance in signal change on average (i.e., responding more to intact visual field presentation). This resulted in a significantly lower difference in signal change between contralateral and ipsilateral signal change compared to neurotypical controls (mean difference controls[contra-ipsi] - CVI[contra-ipsi] = 0.12, SE = 0.03 , p=0.0005, t = 4.09). However, within the lesioned hemisphere, those identified as high performers, displaying residual visual abilities comparable to neurotypical controls (i.e., below 20% motion coherence), exhibited a contralateral dominance in response to looming motion presentation. Similarly, the pulvinar signal change (%) paralleled the trends observed in the thalamus, with an average contralateral dominance in the intact hemisphere of CVI participants (mean

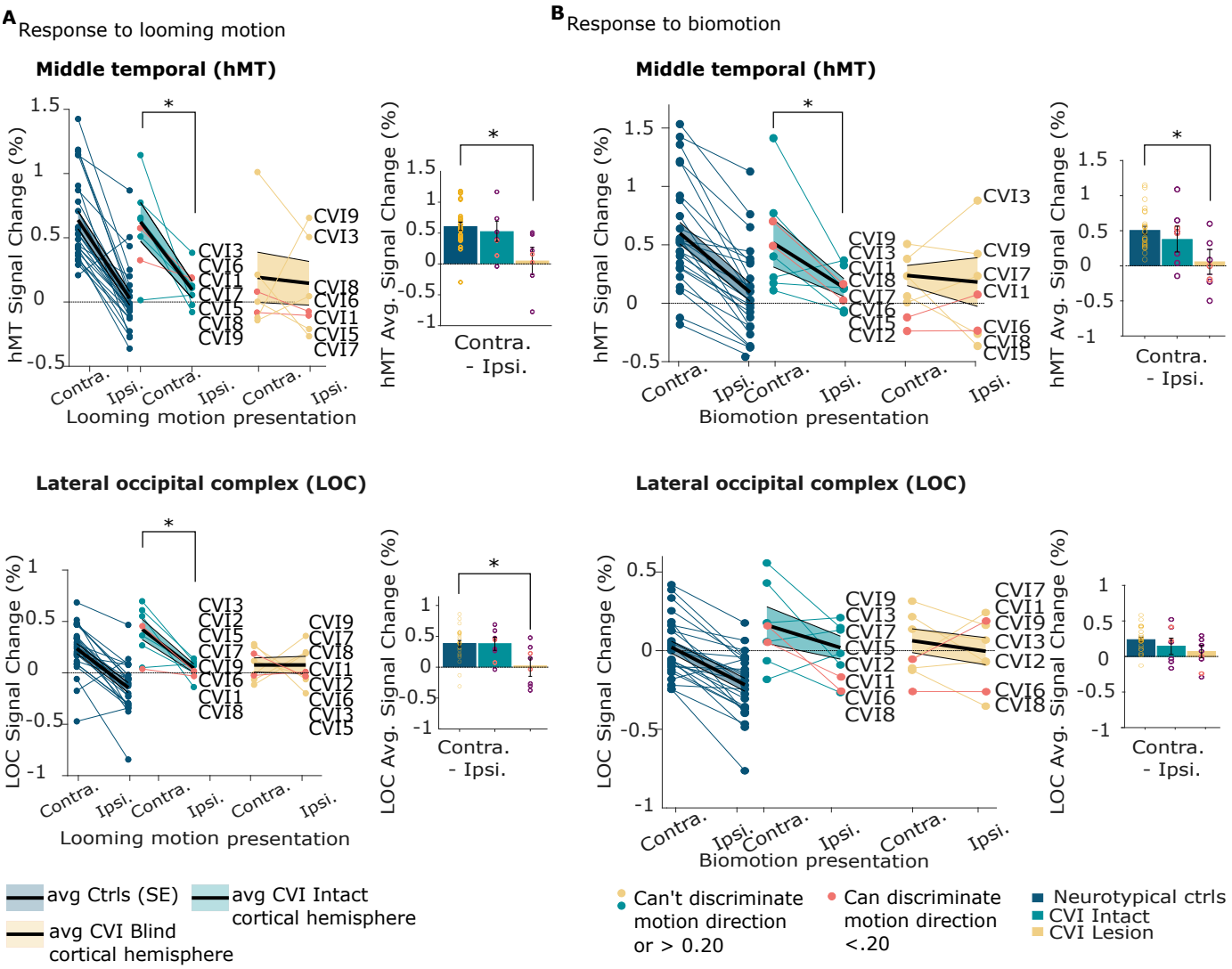

Figure 6 – Cortical ROIs percent signal change to visual motion presentation for neurotypical controls (n=25) and CVI participants (n=8).

difference controls[contra-ipsi] = 0.09, SE = 0.04, p=0.05, t = 0.83), accompanied by a tendency for higher ipsilateral signal change in the lesioned hemisphere. This disparity led to a significant difference between contralateral and ipsilateral presentation compared to controls (mean difference controls[contra-ipsi] - CVI[contra-ipsi] = 0.08, SE = 0.09, p = 0.03, t = 0.85). The high-performing CVI participants, however, displayed a distinct pattern by displaying a contralateral dominance in response to looming motion presentation.

Fig. 6 (continued). (A) Cortical ROIs response to looming motion. hMT signal change (%) shows a contralateral dominance for neurotypical controls. Within CVI participants' intact hemisphere, hMT shows a significant contralateral dominance, comparable to that of neurotypical controls. The ipsilesional hMT shows an average comparable signal change in response to controlateral and ipsilateral motion presentation, significantly more balanced than controls. The lateral occipital complex (LOC) echoes the hMT findings, showing similar trends. Within CVI participants' intact hemisphere, LOC appears to respond more than controls to ipsilateral presentation, corresponding to the impaired visual field presentation. The average ipsilesional LOC shows a delateralization, with a significantly smaller discrepancy between presentation side than neurotypical controls. (B) Cortical ROIs response to biomotion. hMT signal change presents similar trends and significant differences as for looming motion. Within CVI participants' intact hemisphere, LOC also seems to respond more than controls to ipsilateral presentation, corresponding to the impaired visual field presentation.*$p<0.05$

For biomotion presentation, thalamus signal change (%) displayed trends similar to those of looming motion, with an average contralateral dominance in the intact hemisphere and an ipsilateral dominance in the lesioned hemisphere, though these trends did not attain statistical significance. The pulvinar signal change (%) to biomotion did not exhibit comparable significant differences. See the corresponding Figure 7 for visualization of the percent signal change of the thalamus and pulvinar for looming motion and biomotion.

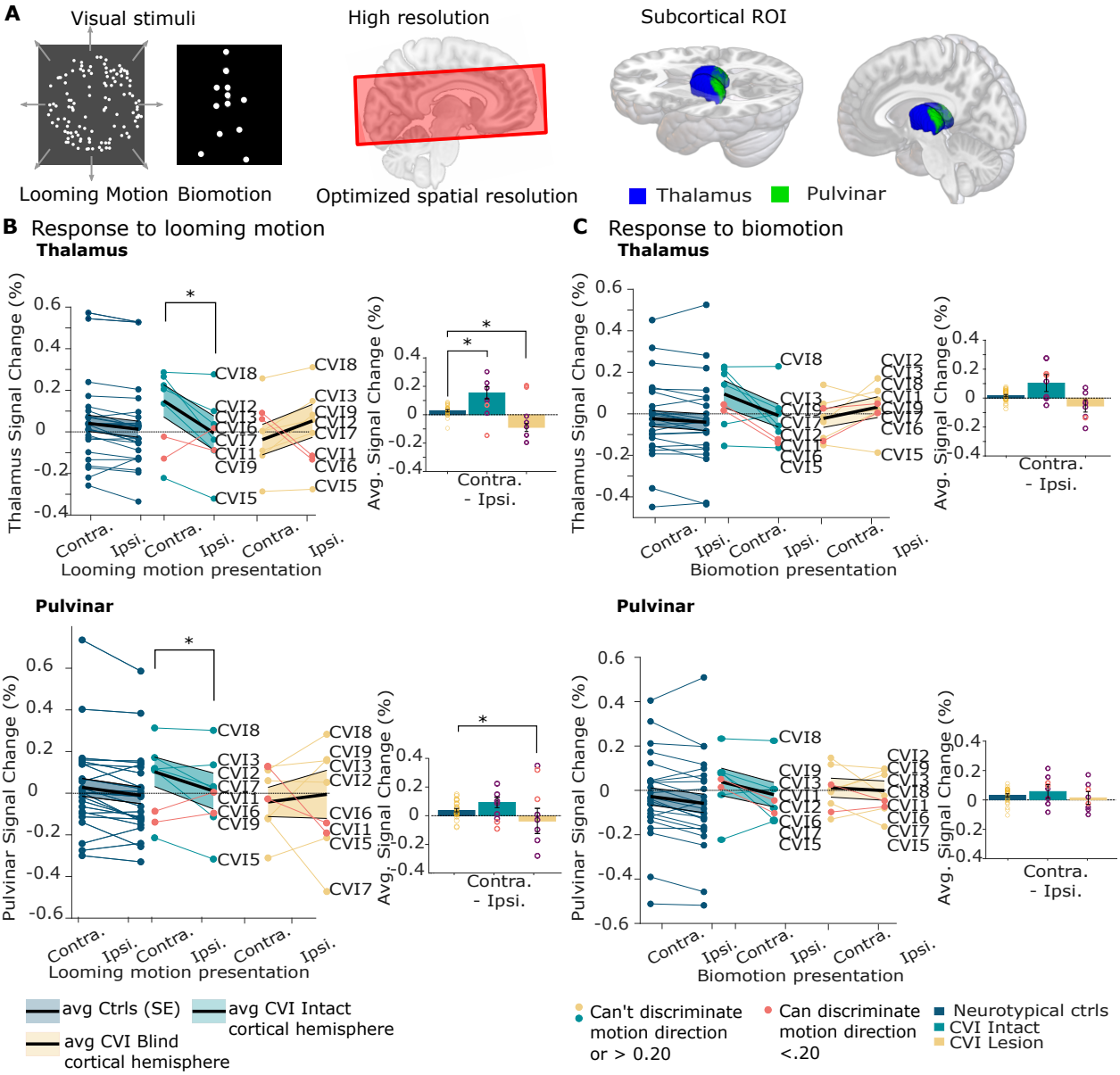

Figure 7 – Subcortical ROIs percent signal change in response to visual motion presentation for CVI participants (n =8) and neurotypical controls (n=25) from high resolution fMRI.

Fig. 7 (continued). (A) The visual looming motion and biomotion stimuli, the placement of the field of view to target ROIs, the location of the thalamus and pulvinar. (B) ROIs response to looming motion. The thalamus signal change (%) in the intact hemisphere exhibits an average contralateral dominance for CVI participants, significantly higher than controls. We observe an opposing ipsilateral dominant trend within the lesioned hemisphere, significantly different than neurotypical controls. High performing CVI participants (singled out in red) rather display a contralateral dominance. The pulvinar signal change (%) shows similar trends as the thalamus with an average contralateral dominance in the intact hemisphere of CVI participants. CVI participants displayed a tendency for higher ipsilateral signal change in the lesioned hemisphere, significantly different than controls, with high performers exhibiting a contralateral dominance. (C) ROIs response to biomotion. The thalamus signal change (%) shows a parallel trend as the response to looming motion, with an average contralateral dominance in the intact hemisphere and an ipsilateral dominance in the lesioned hemisphere, though we observe no comparable significant differences. The pulvinar signal change (%) shows no comparable significant differences. *$p<0.05$

4. Discussion

In the current study, we investigated the neural underpinnings of visual motion processing in neurotypical individuals and those with occipital cortex lesions resulting in cortical visual impairment (CVI) using functional neuroimaging techniques. The results show that the brain can process and integrate visual motion stimuli, including looming and biological motion, even in the absence of intact primary visual areas. Through exploratory whole-brain analyses, we observed a broader distribution of activated regions in CVI participants, contrasting the more focused activation observed in regions associated with visual and motion processing in neurotypical controls. The regions of interest (ROIs) analyses conducted within the lesioned hemisphere of CVI participants reveal a more synergistic activation pattern in the middle temporal area and lateral occipital complex in reponse to both contralateral and ipsilateral presentation, contrasting the asymmetry observed in neurotypical controls and the intact hemisphere. Within the intact hemisphere, the lateral occipital complex responds to ipsilateral motion presentation, corresponding to the impaired visual field. Within the lesioned hemisphere, the thalamus and pulvinar displayed an ipsilateral dominance in response to looming motion, which opposes the contralateral dominance in the intact hemisphere and in those CVI participants exhibiting residual visual abilities comparable to neurotypical controls.

4.1. Consequences of a V1 lesion on visual motion processing

The discrepancy in activation patterns between CVI participants and neurotypical controls underscores the pivotal role of the primary visual area and the impact of damage to this region on the neural mechanisms governing visual processing in individuals coping with visual impairment. In response to visual motion, the whole-brain analyses revealed extra-striate areas extending from the occipital to parietal and temporal regions, in line with previous work (for a meta-analysis see Celeghin et al., 2018), encompassing a broader distribution than the more specialized visual and motion processing areas consistently observed in neurotypical controls. This aligns with several fMRI studies indicating that topographic visual

representations can be found outside occipital regions in temporal, parietal, and even frontal areas (Hagler & Sereno, 2006; Hasson et al., 2003; Huk et al., 2002; Saygin & Sereno, 2008; Sereno et al., 2001; Silver et al., 2005). The activation in parietal and frontal regions could be tied to visual attention, especially shifts between the left and right hemifields (Saygin & Sereno, 2008), when considering the reduced visual input from the clinically blind field. Moreover, while individual differences in brain representations have been shown to predict object perception patterns (Charest et al., 2014), we believe the increased variability introduced by brain damage can further amplify these differences, leading to variations in residual perception.

Specifically, in the intact visual field of CVI participants, looming motion contrasted with static recruited a range of brain regions including the lateral occipital complex, superior and middle temporal gyrus, middle frontal gyrus, and superior parietal lobule. In the impaired visual field of high-performing CVI participants, activation in hMT highlights representation of motion, which coheres with prior research suggesting a non-striate visual input to hMT after a primary visual cortex injury (Barbur et al., 1993; Bridge et al., 2010; Rodman et al., 1989). This confirms that V1 is not necessary to process visual motion and implies that alternative pathways even extend to enable motion direction discrimination. Looming motion presented in the impaired versus intact visual field revealed varying activation patterns in high and mid-performing CVI participants, involving regions such as the superior occipital gyrus, temporal occipital fusiform gyrus, and lateral occipital complex, whereas low-performing CVI participants did not exhibit distinct activation. This coheres with studies bridging residual visual performances with functional activation patterns (Ajina & Bridge, 2017; Tamietto & Morrone, 2016). In response to biomotion in the intact visual field, high-performing CVI participants primarily activated visual areas, while mid and low-performing participants showed more distributed activation, including the inferior frontal gyrus and superior frontal gyrus. Similar trends were observed for impaired versus intact visual field, with high-performing participants predominantly activating visual areas and mid and low-performing participants engaging a broader set of regions, including visual areas, in addition to the middle frontal gyrus, and inferior temporal gyrus. Thus, varying patterns of

activation emerged for both looming and biomotion presentation across intact and impaired visual fields and performance levels. Future investigations with larger samples could assess these idiosyncrasies in brain representations, controlling for brain damage, to predict levels of residual visual abilities in motion processing.

4.2. Cortical regions for visual motion

The middle temporal area (hMT) and lateral occipital complex (LOC) were targeted as cortical ROIs to assess visual processing and motion representation despite lesioned primary visul areas. The middle temporal area is known to respond to motion presented in the impaired field of individuals with CVI Ajina and Bridge, 2017; Barbur et al., 1993; Bridge et al., 2010; Goebel et al., 2001; Morland et al., 1999; S. Zeki and Ffytche, 1998. The lateral occipital complex is associated with processing of simple visual features, object recognition, and visual awareness (Amedi et al., 2001; Grill-Spector et al., 2001; Hutchinson, 2019; Lindh et al., 2019; Pitts et al., 2012), yet has also been linked to perceptual processing during inattentional blindness (Hutchinson, 2019), implicit processes, (H. Kim, 2019) and, more recently, the neural correlates of unconscious processing (for a meta-analysis see MacLean et al., 2023). The findings in the current study first indicate that the hMT and LOC in both hemispheres can be activated by their respective contralateral visual hemifields, yet the signal's intensity differs across CVI participants and between their ipsilesional and intact hemispheres, as expected. In response to visual motion, the ipsilesional hMT and LOC display on average across CVI participants less differential recruitment between presentation sides, contrasting the asymmetry and contralateral dominance in neurotypical controls and the intact hemisphere. The hMT in the intact hemisphere of CVI participants that displayed neurotypical-like abilities to motion discrimination, though non exclusively, can also respond to looming motion in the ipsilateral impaired hemifield, though to a less degree. The hMT displayed similar trends and significant differences in response to biomotion. The response pattern of hMT has been shown to to undergo qualitative changes after V1 damage and become more similar to low-level visual cortex (Ajina & Bridge, 2017), which coheres with the observed difference between the CVI and neurotypical populations.

The average ipsilesional LOC shows less differential recruitment between presentation sides. The LOC in the intact hemisphere seems to respond more to ipsilateral visual motion than controls, corresponding to the impaired visual field. While this region is thought to receive feedforward visual input from the early visual cortex (Dijkstra et al., 2021), linked to unconscious processing, it may facilitate residual visual abilities, suggesting an alternative input that warrants additional investigation. For CVI participants, the overall trends for LOC ressemble hMT, although the LOC of neurotypical controls appeared to respond less robustly to visual motion than the hMT, suggesting more involvement of this region post occipital cortex injury, which would require further investigation. Additionally, LOC's seemingly higher general response in CVI participants' intact hemisphere compared to neurotypical controls could be driven by the more prominent subcortical input following damage to V1.

4.3. Subcortical regions for visual motion

To investigate the role of subcortical regions in motion processing following occipital cortex injury, we utilized high-resolution fMRI to conduct ROI analyses, focusing on the contributions of the thalamus and pulvinar. The pulvinar, the largest thalamic nucleus, is thought to receive visual input from the optic tract or through the superior colliculi, subsequently relaying this information to area MT (Ajina & Bridge, 2017; Berman & Wurtz, 2010; Warner et al., 2010). Recent findings have further identified a direct tract from the pulvinar to MT in neurotypical individuals (Rowe et al., 2023). In neurodevelopment, this pulvinar-mediated subcortical shortcut is thought to be crucial for the early maturation of MT (Warner et al., 2012; Warner et al., 2015), before regressing in prominence, and ceding to an increasingly dominant primary pathway that connects the lateral geniculate nucleus to the primary visual cortex, and on to MT(Mitchell & Leopold, 2015; Warner et al., 2010). Following V1 lesions, individuals with residual vision have been thought to atypically retain this early pulvinar-mediated visual pathway (Bridge et al., 2016). While the pulvinar-hMT pathway may be inherent to neurotypical processing, V1 damage offers a unique opportunity

to isolate its neuronal properties, and potentially observe an enhanced signal. Studies involving non-human primates and cats with occipital cortex lesions (Benevento & Standage, 1983; Berman & Wurtz, 2010; Ciaramitaro et al., 1997; H. Jiang et al., 2015; Piche et al., 2015; Saalmann & Kastner, 2011) have shown the involvement of these structures in visual motion processing, even in the absence of primary visual inputs. The involvement of the pulvinar has further been suggested in studies presenting biological and moving stimuli in the blind field (Bridge et al., 2016; Tamietto et al., 2010; Tran et al., 2019; Van den Stock et al., 2011). The current study provides evidence that presenting salient motion in the intact and impaired hemifield differentially activates these structures, showing the brain's adaptive ability to enable motion processing and involve the subcortical level in CVI individuals. Particularly with looming motion, the thalamus showed a contralateral dominance within the intact hemisphere with an opposing trend for an ipsilateral dominance within the lesioned hemisphere, both significantly different than neurotypical controls. High-performing individuals, with residual visual capacities echoing neurotypical controls, showed ipsilesional thalamic responses to contralateral impaired visual field presentation. This pattern may suggest a potential correlation between an increase in thalamic signal in response to stimulation in the clinically blind field and enhanced residual abilities — a hypothesis meriting more investigation. The pulvinar's average heightened signal response to looming motion aligns with prior research suggesting its role in rapidly processing salient motion signals, despite damage to V1(Furman, 2014; Tamietto & Morrone, 2016). Collectively, these findings reflect the ability of the thalamus and pulvinar in facilitating different spared visual functions, and in the subsequent functional reorganization after occipital cortex injury. A future avenue of investigation could involve examining the direct neural pathways between these structures and hMT using diffusion MRI as well as connectivity analyses, especially following occipital cortex lesions. Early lesions to V1 may facilitate retention of the pulvinar-mediated pathway, and this would merit further investigation with a larger cohort, controlling for age at lesion.

The relative strength of the signal increase in subcortical regions for biomotion and looming motion may be attributable to the inherent characteristics of the visual inputs. Looming

motion, characterized by objects rapidly approaching, typically induces a robust sense of visual flow, likely resulting in more prominent modulations in visual processing. Studies with neurotypical individuals as well as non-human primates with visual cortex lesions and in a patient with cortical visual impairment have shown specialized functional responses to these stimuli (Ball & Tronick, 1971; Billington et al., 2011; Hervais-Adelman et al., 2015; King & Cowey, 1992; Salay et al., 2018). Conversely, while biomotion is dynamic, facilitating the extraction of meaningful information from limited visual cues (Blake & Shiffrar, 2007; Johansson, 1973; Troje, 2013), extrastriate areas are known to be stimulus-selective (Desimone et al., 1984; Krause & Pack, 2014; Tsunoda et al., 2001), and this may result in more subtler changes in visual flow. Regions tasked with processing higher-level features, particularly those recognizing human motion, might rely less on the sheer intensity or vigour of the stimuli, and may rather prioritize the nature of the visual information. Analogous to the observed rise in firing rate of most MT cells with increases in motion strength (Hagan et al., 2020), the subcortical response may be selective to stimuli attributes, still capable of processing aspects of higher-level features independently of V1, albeit perhaps more challenging to detect. These findings emphasize the intricate interplay between stimulus characteristics and the level of engaged neural mechanisms, in addition to the brain's ability to adapt to varied visual inputs at the subcortical level following occipital cortex injury. While this study suggests that functional alterations within the visual and motion processing areas of the brain, specifically MT, LOC, pulvinar and thalamus, can be present after an occipital cortex injury, future studies need to investigate the nature of the dynamic interaction of the relative strength of the retained or enhanced pulvinar-mediated pathway, stimulus selectivity, sparing of the lateral occipital complex, and the extent of qualitative adaptation for low-level processing of visual features in hMT.

4.4. Strengths and limitations

The current study empirically shows functional activation patterns in response to visual motion stimuli in cortical and subcortical regions, despite damage to occipital cortex areas,

when compared to a neurotypical control group. The findings extend beyond previous research and contribute to our understanding of visual processing in individuals with CVI, a visual impairment that is gaining recognition, yet for which the underlying neural mechanisms remain obscure. We present a novel approach for automatic lesion mapping in this population allowing for reliable quantification of brain damage, in addition to categorizing individuals based on their residual visual abilities to single out high performers, focusing on two distinct stimuli to assess motion processing, in addition to employing high-resolution fMRI for targeted ROI analyses, and exploratory whole brain analyses. Nonetheless, important limitations need to be considered. Although the natural variability in human lesions might initially seem limiting (M. C. Schmid et al., 2009), such cases of brain damage challenge our understanding of brain-behaviour models and have been pivotal in advancing cognitive neuroscience theories (Medina & Fischer-Baum, 2017; Vaidya et al., 2019). The inherent variability in structural damage can, in fact, be a strength, particularly when assessing the diverse outcomes in residual vision (Ajina & Bridge, 2017). We preliminarily categorized participants as high, mid, or low performers and quantified brain damage, providing a foundation for future investigations to expand into the spectrum of visual motion processing alterations attributable to individual clinical profiles. While we believe the sample size is appropriate for functional neuroimaging empirical lesion studies given anatomical, behavioral, and clinical constraints (Roalf & Gur, 2017), we acknowledge that this may lead to reduced statistical power, potentially resulting in inflated effects (Button et al., 2013), requiring a more nuanced interpretation of the findings.

Unilateral occipital cortex lesions allow for visual stimuli presentation in both impaired and intact visual fields at different time points. This setup offers a matched control condition for each CVI individual, yielding valid statistical outcomes and enhancing the estimation of the true effect. Driven by theory and hypotheses, this study further reduces the risk of high false-positive rates. High-resolution scans were designed to focus on subcortical structures, and the visual stimuli were optimized to elicit robust activation in regions linked to the hypotheses.

Beyond the targeted approaches, we also conducted exploratory whole brain analyses, emphasizing the importance of minimizing researcher bias and comprehensively assessing all neural activation variations. The observed differences in activation patterns could be attributed in part due to oculomotor activation, including the planning of saccades toward the stimulus, in addition to increased visual responses to the stimulus. The regions are not mutually exclusively elicited and may rather exhibit differential activation patterns, which proves challenging to disentangle with the temporal resolution of fMRI. Despite these challenges, we are confident that the results are not merely artifacts or random fluctuations in the data. Moreover, our findings should be considered within the broader context of the human MT complex (hMT+/V5), encompassing MT along with adjacent motion-selective regions, notably the medial superior temporal cortex (MST). Visual information processed in MT is subsequently relayed to MST for specific functions like optic flow motion processing (Duffy & Wurtz, 1991; Komatsu & Wurtz, 1988b; Maunsell & Van Essen, 1983b; Ungerleider & Desimone, 1986). Given that MST tends to remain relatively unaffected after V1 lesions and considering that the representation of the visual field is bilateral, residual responses within the ipsilesional MT may partly originate from MST through feedback projections (Azzopardi et al., 2003; Huk et al., 2002). Future investigations utilizing dynamic causal modeling analyses could provide insights into these potential feedback mechanisms and enhance our understanding of the observed differences in functional response patterns across CVI participants, which may be attributed in part due to the differential involvement of area MST. The diverse response profiles across CVI participants underline the need for an in-depth understanding of the altered neural mechanisms for visual processing in CVI, while revealing the multifaceted impact of this condition on brain activation and residual visual function. This study provides a robust methodological framework and empirical foundation for future investigations into visual motion processing in the clinically blind population, potentially on the longitudinal impacts and individual differences of occipital brain damage.

5. Conclusion

The current study assessed visual motion processing of both neurotypical controls and individuals with cortical visual impairment using functional neuroimaging and reveals that visual motion of diverse stimuli, looming and biological stimuli, can be processed and integrated in the brain without intact primary visual areas. Whole brain exploratory results reveal a broader distribution of activated regions in CVI participants, contrasting the more focused activation observed in regions associated with visual and motion processing in neurotypical controls. Within the lesioned hemisphere, targeted cortical regions of interest, i.e., the middle temporal area and lateral occipital complex, display a more synergistic activation pattern to contralateral and ipsilateral visual motion, contrasting the contralateral dominance observed in neurotypical controls and the intact hemisphere. The lateral occipital complex within the intact hemisphere seems to display a higher response to ipsilateral motion presentation, corresponding to the impaired visual field. High-resolution fMRI further revealed the ipsilesional thalamus and pulvinar to display an ipsilateral dominance in response to looming motion, which opposes the contralateral dominance in the intact hemisphere and in those CVI participants exhibiting residual visual abilities comparable to neurotypical controls. These results shed light on the extent of neural modulation post CVI and suggest the nature of the visual stimuli to facilitate residual visual processing. The findings provide a methodological and empirical basis for future studies to assess the multi-faceted impact of an occipital cortex lesion on visual processing perhaps using combined neuroimaging-behavioral designs, diffusion MRI and connectivity analyses.

Table 3 – Brain regions showing consistent activation during looming motion for the neurotypical group. For each cluster, brain region label, hemisphere, K, number of voxels, MNI coordinates, peak Z and p values are provided.

Brain regions	**Hemi**	***K***	**p**	**x**	**y**	**z**	***Z***
Motion > static							
Middle temporal gyrus	R	54	0.001	49	-64	6	5.02
Middle temporal gyrus	L	26	0.005	-49	-73	6	4.69
Motion L > Motion R							
Superior occipital gyrus	R	155	0.001	19	-88	27	5.29
Posterior calcarine sulcus	R	23	0.0019	11	-88	3	4.83
Motion R > Motion L							
Posterior calcarine sulcus	L	135	0.002	-7	-88	-1	5.38
Superior occipital gyrus	L	172	0.001	-16	-91	21	5.15

Table 4 – Brain regions showing consistent activation during looming motion for the neurotypical group. For each cluster, brain region label, hemisphere, *K*, number of voxels, MNI coordinates, peak *Z* and *p* values are provided.

Brain regions	**Hemi**	***K***	**x**	**y**	**z**	**Z**	***p***
Intact [motion > static]							
CVI6							
Lateral occipital cortex	R	1528	>0.001	52	-70	9	Inf
Lateral occipital cortex	L	1183	>0.001	-52	-70	9	Inf
Superior temporal gyrus	R	62	>0.001	67	-37	15	Inf
Middle temporal gyrus	L	36	>0.001	-67	-17	-7	6.53
CVI3							
Posterior calcarine sulcus	L	220	>0.001	-7	-88	-1	Inf
Lateral occipital cortex	L	727	>0.001	-43	-76	-1	Inf
Lateral occipital cortex	R	166	>0.001	46	-64	-1	Inf
Superior temporal gyrus	R	68	>0.001	67	-34	15	Inf
Superior temporal gyrus	L	75	>0.001	-70	-37	15	7.78
Superior frontal gyrus	R	863	>0.001	5	22	66	7.36
Middle frontal gyrus	R	35	>0.001	37	58	-4	7.31
Temporal fusiform gyrus	R	219	>0.001	31	1	-40	7.31
Superior parietal lobule	R	31	>0.001	34	-43	63	7.18
Inferior frontal gyrus	L	116	>0.001	-49	34	-10	7.11
Inferior frontal gyrus	R	80	>0.001	49	25	-7	6.93
Angular gyrus	R	32	>0.001	58	-37	54	5.87
Middle frontal gyrus	L	72	>0.001	-52	13	39	5.82
Middle temporal gyrus	L	36	>0.001	-58	-5	-19	5.74
Temporal occipital fusiform gyrus	L	22	>0.001	-40	-46	-19	5.72
Middle temporal gyrus	R	26	>0.001	58	-2	-22	5.41
CVI8							
Lateral occipital cortex	R	280	>0.001	40	-73	-10	Inf
Calcarine cortex	L	564	>0.001	-7	-88	-7	Inf
Lateral occipital cortex	L	100	>0.001	-46	-73	-4	Inf
Precuneus	R	75	>0.001	16	-79	36	Inf
Superior parietal lobule	R	24	>0.001	28	-40	51	6.16

Table 4 *(continued)*

Brain regions	**Hemi**	***K***	***p***	**x**	**y**	**z**	**Z**
Impaired [motion > static]							
CVI6							
Middle temporal gyrus	L	1492	>0.001	-52	-64	9	Inf
Middle temporal gyrus	R	716	>0.001	55	-70	6	Inf
Posterior superior temporal gyrus	R	100	>0.001	70	-31	18	Inf
Supramarginal gyrus	R	87	>0.001	61	-31	51	Inf
Superior temporal gyrus	L	52	>0.001	-64	-34	15	7.19
LOC	L	251	>0.001	-7	-73	60	6.63
Occipital fusiform gyrus	L	28	0.001	-22	-85	-19	5.78
Postcentral gyrus	R	19	0.003	64	-5	21	5.66
Angular gyrus	R	39	>0.001	34	-67	54	5.51
CVI3							
Lateral occipital cortex	R	69	>0.001	43	-64	-1	Inf
Impaired > Intact [motion]							
CVI6							
Superior occipital gyrus	L	1591	>0.001	-22	-88	21	Inf
Temporal occipital fusiform gyrus	L	25	>0.001	-28	-55	-10	6.11
CVI3							
Lateral occipital complex	R	282	>0.001	28	-94	24	Inf
Occipital fusiform gyrus	R	28	>0.001	14	-79	-16	7.49
Lateral occipital complex	L	46	>0.001	-28	-94	-13	6.62

Table 5 – Brain regions showing consistent activation during motion visual processing of biomotion stimuli for the neurotypical group. For each cluster, brain region label, hemisphere, K, number of voxels, MNI coordinates, peak Z and p values are provided.

Brain regions	**Hemi**	***K***	**p**	**x**	**y**	**z**	***Z***
Biomotion > baseline							
Middle temporal gyrus	R	125	0.000	49	-64	6	6.03
Middle temporal gyrus	L	125	0.000	-49	-73	9	5.94
Biomotion L > Biomotion R							
Lateral occipital cortex (inferior)	R	166	0.000	46	-70	6	6.11
Calcarine cortex	R	31	0.010	11	-88	6	5.83
Superior occipital gyrus	R	130	0.001	25	-88	30	5.76
Biomotion R > Biomotion L							
Superior occipital gyrus	L	337	0.001	-25	-88	30	5.61
Calcarine cortex	L	141	0.010	-31	-79	-16	5.54

Table 6 – Brain regions showing consistent activation during biomotion for individuals with CVI. For each cluster, brain region label, hemisphere, K, number of voxels, MNI coordinates, peak Z and p values are provided.

Brain regions	**Hemi**	***K***	**x**	**y**	**z**	**Z**	***p***
Intact > Impaired [biomotion]							
CVI6							
Lingual gyrus	R	353	0.000	11	-76	-4	Inf
LOC superior (superior occipital gyrus)	R	700	0.000	19	-88	27	Inf
CVI3							
LOC inferior	L	702	0.000	-43	-76	3	Inf
Occipital pole	L	459	0.000	-25	-100	12	Inf
Precentral gyrus	R	86	0.000	52	-8	54	Inf
Precentral gyrus	L	174	0.000	-49	-2	54	Inf
Superior frontal gyrus	L	171	0.000	-10	-2	72	Inf
Middle temporal gyrus	L	407	0.000	-70	-43	12	Inf
Inferior frontal gyrus	L	272	0.000	-43	-10	27	Inf
Fusiform gyrus	L	18	0.000	-40	-46	-19	6.85
Middle temporal gyrus	R	17	0.000	49	-25	-7	6.14
CVI8							
Inferior occipital gyrus	L	639	0.000	-46	-76	-1	Inf
LOC	R	274	0.000	37	-67	-7	Inf
Superior occipital gyrus	L	221	0.000	-22	-88	24	Inf
Medial orbital gyrus	L	20	0.000	-7	52	-28	6.55
Inferior frontal gyrus	R	46	0.000	58	34	15	6.33
Frontal pole		85	0.000	49	55	-4	6.32
Middle frontal gyrus	R	17	0.001	46	43	12	5.50

Table 6 *(continued)*

Brain regions	**Hemi**	***K***	***p***	**x**	**y**	**z**	**Z**
Impaired > Intact [biomotion]							
CVI6							
LOC inferior	L	630	0.000	-46	-79	-1	Inf
LOC superior (superior occipital gyrus)	L	174	0.000	-22	-88	21	Inf
Angular gyrus	L	39	0.000	-28	-73	51	7.46
CVI3							
Superior occipital gyrus	R	373	0.000	25	-91	27	Inf
Middle frontal gyrus	R	538	0.000	43	49	3	Inf
Angular gyrus	R	200	0.000	49	-61	30	7.63
LOC superior	L	86	0.000	-55	-73	33	7.17
Middle temporal gyrus	R	20	0.000	64	-28	-16	6.14
CVI8							
Middle occipital gyrus	R	189	0.000	43	-76	36	Inf
Occipital fusiform gyrus	R	53	0.000	25	-85	-16	6.50
LOC (inferior)	R	16	0.000	37	-94	3	6.09
Occipital fusiform gyrus	L	40	0.000	-19	-97	-13	6.01
Inferior temporal gyrus	R	28	0.001	46	-2 -	37	5.50

Data and code availability statement

Data are available from the corresponding author upon request. All data were analyzed with software publicly available from: https://fmriprep.org/en/stable/ and https://bidspm.readthedocs.io/en/latest/index.html in addition to Matlab. Custom scripts for the visual tasks were created with Psychophysics Toolbox : http://psychtoolbox.org/ uploaded on Github and available from the corresponding author upon request. Computational work was further supported by resources provided by the High-performance Computing Platform Compute Canada and Calcul Québec.

Author Contributions

Michèle W. MacLean (Conceptualization, Methodology, Project administration, Investigation, Formal analysis, Data curation, Software, Validation, Visualization, Writing – Original Draft, Writing – Review & Editing); Remi Gau (Conceptualization, Methodology, Formal analysis, Data curation, Software, Validation, Writing – Review & Editing); Catherine Landry (Investigation); Mohamed Rezk (Software); Dang K. Nguyen (Resources, Writing – Review & Editing); Olivier Collignon (Conceptualization, Supervision); Franco Lepore (Funding acquisition, Supervision).

Funding

Project administration was supported by the Canada Research Chair Program RGPIN-8245-2014 [FL]; and the Natural Sciences and Engineering Research Council of Canada RGPIN/05053-2014 [FL]; and the Canadian Institutes of Health Research 166197 [FL] grants. MWM was supported by a salary award from Fonds de Recherche Nature et Technologies (FRQNT).

Declarations of interest

None.

Acknowledgements

We sincerely thank all participants for participating in this study. We thank the Functional Neuroimaging Unit (UNF) team at the Centre de recherche de l'Institut universitaire de gériatrie de Montréal (CRIUGM) for assistance in MRI data collection and experimental setup, in particular Carollyn Hurst, Basile Pinsard and Arnaud Boré as well as Prof Julien Cohen-Adad for advice on specifying MRI data acquisition parameters.

Supplementary materials

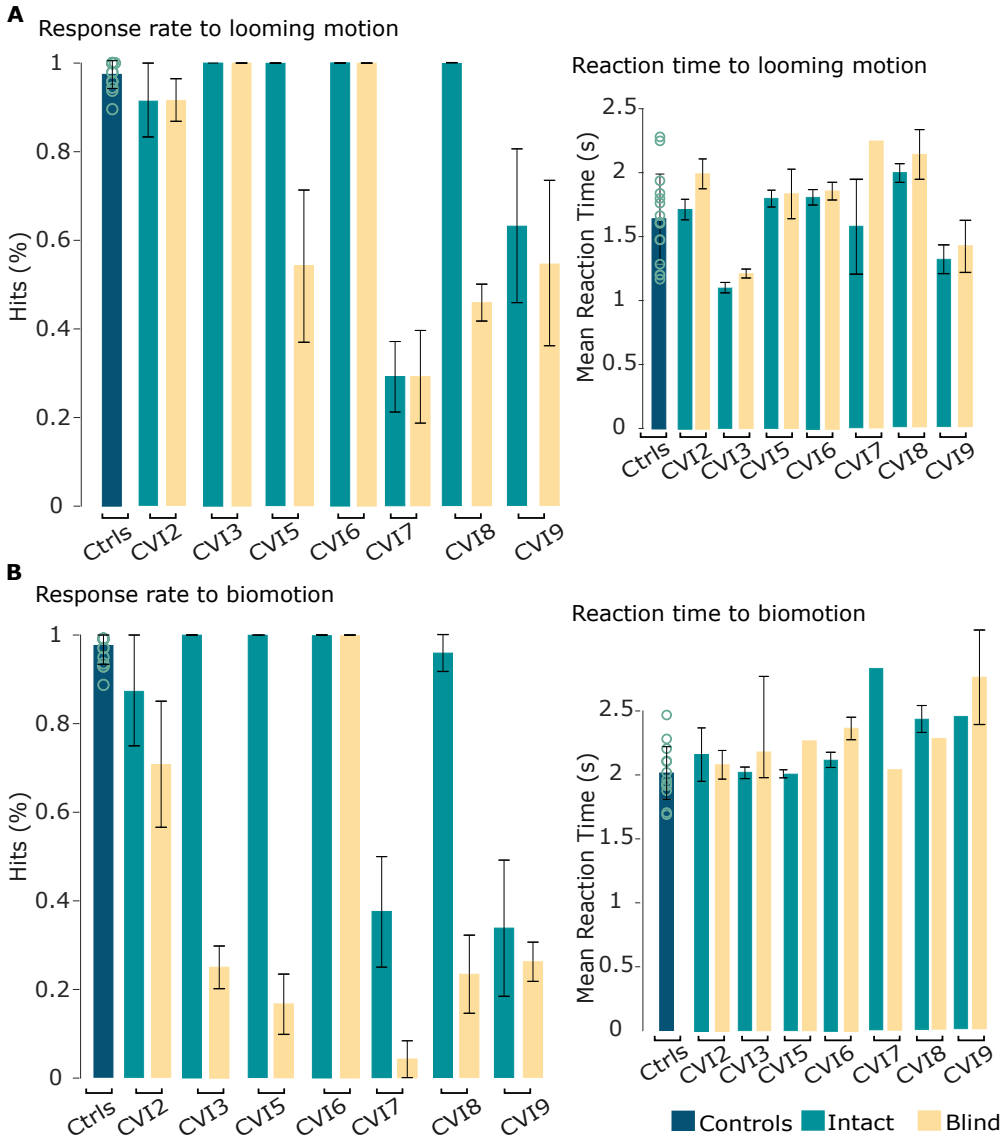

Figure S1 – Behavioral results of the peripheral motion processing task for neurotypical controls combining both left and right visual field and CVI participants while inside the MRI scanner.

Fig. S1 (continued). (A) Looming motion response rate (left) and reaction time (right) for neurotypical controls, and CVI participants for their intact and impaired visual fields. (B) Biomotion response rate (left) and reaction time (right) for neurotypical controls, and CVI participants for their intact and impaired visual fields. Mean performance corresponds to the percentage of correct responses (hits) and mean reaction time of correct responses (hits) for neurotypical controls and CVI participants.

Chapter 6

Discussion

Cortical visual impairment (CVI), resulting from damage to the visual cortex, can trigger a series of functional and structural alterations. CVI impacts the processing and representation of visual information within the brain, providing a unique clinical model to investigate how the visual system adapts in response to damage in primary visual areas. Changes in this neural architecture are intricately linked to understanding the neural underpinnings of conscious and unconscious visual perception. This thesis uses a multi-modal approach, integrating behavioral, structural and functional neuroimaging techniques, to characterize neural correlates of conscious and unconscious visual perception and implications of occipital cortex lesions. Article 1 aimed to conduct two quantitative meta-analyses to empirically identify convergent functional brain activity associated with conscious and unconscious visual processing in the intact brain. Article 2 aimed to investigate V1-independent pathways of visual motion detection in a patient with homonymous hemianopia and blindsight, using fMRI. Chapter 4 sought to compile an extensive high-resolution MRI dataset for visual motion perception, including CVI participants and neurotypical controls. In Article 3, a portion of the newly acquired dataset was used to investigate the alterations in neural correlates associated with diverse visual motion stimuli processing following occipital cortex injuries leading to CVI, in comparison to a neurotypical control group, using high-resolution fMRI.

6.1. Chapter Overview

The remaining of this chapter provides a summary of thesis findings (Sec 6.2), their interpretation (Sec 6.3), implications, including methodological contributions, strengths and limitations (Sec 6.4), future research avenues (Sec 6.5) and a conclusion (Sec 6.6).

6.2. Summary of findings

The first meta-analysis in the first article revealed significant activations associated with conscious visual perception across a constellation of regions comprising the bilateral inferior frontal junction, intraparietal sulcus, dorsal anterior cingulate, angular gyrus, temporo-occipital cortex and anterior insula. Conscious awareness was associated with attention, cognitive control and working memory, as evidenced by cognitive decoding using Neurosynth. The meta-analysis investigating unconscious percepts consistently revealed posterior activations in the lateral occipital complex, along with the intraparietal sulcus and precuneus.

The results from the second article present the neural mechanisms involved in motion detection in blindsight, observed in a patient with homonymous hemianopia. Intact visual hemifield stimulation led to significant contralateral activations in primary and secondary visual areas, motion-specific areas, and the thalamus. Conversely, blind hemifield stimulation resulted in bilateral activity in extrastriate and frontal areas, alongside activations within the superior colliculi. These results emphasize the significance of atypical secondary pathways that bypass primary visual areas, facilitating residual vision.

The findings from the third study show altered visual processing of looming and biological motion stimuli without intact primary visual areas. Whole brain analyses show a broader activation in CVI participants, contrasting the focused activation in visual motion processing regions in neurotypical controls. The regions of interest (ROIs) analyses conducted in the lesioned hemisphere reveal a more synergistic activation in the middle temporal area and lateral occipital complex, differing from the contralateral dominance to presentation side in controls. High-resolution fMRI shows the ipsilesional thalamus and pulvinar exhibiting an ipsilateral dominance in response to looming motion, which opposes the contralateral dominance in the intact hemisphere and in CVI participants exhibiting residual visual abilities comparable to neurotypical controls. The results identify functional modulation of visual pathways following occipital cortex damage, and the resulting impact on processing diverse stimuli, thereby offering insights on structures facilitating spared visual function.

6.3. Interpretation of thesis findings

6.3.1. Neural bases of conscious and unconscious visual processing

The first publication presents a neuroimaging meta-analysis identifying brain regions consistently associated with conscious visual awareness. This includes the following brain regions, each associated with broader cognitive tasks (Duncan & Owen, 2000): the inferior frontal junction for top-down attention modulation, cognitive control and working memory (Baldauf & Desimone, 2014; Bedini & Baldauf, 2021; Sundermann & Pfleiderer, 2012; Zanto et al., 2011); the intraparietal sulcus which plays a role in higher visual functions, the dorsal attention system, working memory and numerical cognition (Dehaene et al., 2003; Gillebert et al., 2011; Power et al., 2011; Velenosi et al., 2020; Yantis et al., 2002; Yokoi & Komatsu, 2009); the angular gyrus contributing to attention, memory retrieval and semantic cognition (Humphreys et al., 2021; Seghier, 2013); the dorsal anterior cingulate cortex, involved in executive control and reward-based decision-making (Rushworth et al., 2012; Shenhav et al., 2013; Shenhav et al., 2016); and the insula, known to process visually salient stimuli, also involved in cognitive control and decision-making (Engstrom et al., 2014; Uddin et al., 2017; Ullsperger et al., 2010). These regions are part of the brain's "multiple-demand" system (Assem et al., 2020; Duncan, 2010; Fedorenko et al., 2013), capable of integrating a range of cognitive operations and suggesting a convergence between conscious perception and higher cognitive processes such as visual attention, cognitive control, and working memory (for review see Martin-Signes et al., 2019; Persuh et al., 2018; Pitts et al., 2018; Soto & Silvanto, 2014). Moreover, the findings align with a previous study which reviewed evidence for two partially segregated networks contributing to distinct attentional functions (Corbetta Shulmann, 2002). The first network, involving the intraparietal and superior frontal cortex, is associated with cognitive, top-down selection of stimuli and responses, whereas the second network, consisting of the temporoparietal and inferior frontal cortex, specializes in detecting salient or unexpected stimuli. This further supports the association between conscious visual awareness and attention, as revealed through functional decoding using Neurosynth, which, considering the previous study, suggests potential intersections with goal-oriented, top-down

attention. The overlap between the meta-analysis results and the networks described by Corbetta et al. corroborates them as relevant avenues for further investigation into the intricate relationship between perceptual awareness and attention in visual processing, to understand how the regions may be differentially involved across these cognitive processes. Our findings, derived from different experimental contrasts, provide insight on their nuanced roles in different representations of the conscious state. For instance, conscious versus unconscious processing contrasts highlight the role of frontal regions (for review see Mashour et al., 2020; Tsuchiya et al., 2015), competing conscious percepts contrasts emphasize the intraparietal sulcus and its potential involvement in attentional shifts (Yantis et al., 2002), whereas conscious versus preconscious perception contrasts display greater occipital cortex involvement. The results also suggest differential engagement of neural resources associated with the conscious states required to complete specific experimental tasks. Overall, the results present reliably activated regions across independent studies, highlight a common ground with higher-level cognitive processes and account for a more comprehensive framework of conscious visual awareness.

The second meta-analysis on unconscious visual processing highlighted consistent activity in the lateral occipital cortex, precuneus, and intraparietal sulcus, emcompassing regions beyond primary visual areas. Known for implicit processes and inattentional blindness (Hutchinson, 2019; H. Kim, 2019), the lateral occipital cortex seems to show differential recruitment of its inferior and superior divisions for conscious and unconscious processing, respectively, which would gain from further investigation. The precuneus and intraparietal sulcus, also linked to unconscious perception in blindsight (Celeghin et al., 2018), contribute to various facets of visual processing including object priming, unconsciously storing abstract intentions, episodic memory retrieval, among others, despite a propensity for task-induced deactivation (Cavanna & Trimble, 2006; Gusnard & Raichle, 2001; Koutstaal et al., 2001; Soon et al., 2008; Soon et al., 2013). The intraparietal sulcus, central to the dorsal attention system, was activated in both conscious and unconscious perception, implying these states are not mutually exclusive. The results suggest that regions may adjust their functional activity according to the extent of conscious or unconscious processing, a possibility that needs

exploration. As expected, primary visual areas were not prominently activated, as they are fundamental to both conscious and unconscious processing, and thus factored out in the study contrasts (de Graaf et al., 2012). Given our limited understanding of unconscious processing and the weaker correlation with Neurosynth, our findings reveal the necessity for research to investigate how unconscious processing is related to rest, memory retrieval, etc.

6.3.2. Findings in light of prominent theories of consciousness

Theories addressing conscious awareness, such as Global Neuronal Workspace Theory (GWT) (Dehaene & Naccache, 2001), Recurrent Processing Theory (RP) (V. A. Lamme, 2010, 2006a), Higher-Order Thought Theory (HOT) (Brown et al., 2019; Lau & Rosenthal, 2011), and Integrated Information Theory (IIT) (Tononi, 2008, 2012; Tononi et al., 2016), provide diverse insights about how sensory areas encode stimulus content and whether broadcasting takes place to elicit a conscious percept. Our meta-analytical findings associated with conscious visual processing seem empirically consistent with the GWT. This theory describes a network of regions, including the prefrontal and parietal cortices, engaged during conscious access, via a network 'ignition' involving the rapid amplification and maintenance of neural representations (Dehaene & Naccache, 2001). Visual information is broadcast past sensory cortices and involves higher-level cortical association areas, which seems consistent with our results. For unconscious processing, the activation appears to drive outside primary sensory cortices, with weakening neural signals possibly due to absent long-range synchrony (Dehaene et al., 2006; Melloni et al., 2007). Conscious and unconscious visual processing appear to be modulated by the attentional load and visual input content (Fang & He, 2005; Y. Jiang & He, 2006; Levinson et al., 2021; Mashour et al., 2020; Song & Yao, 2016). RP and GWT emphasize feedforward and feedback loops in conscious processing, with the latter suggesting a more extensive loop (V. A. Lamme, 2010; V. A. F. Lamme, 2006b; Mashour et al., 2020). The findings suggest certain regions to be differentially activated for conscious and unconscious perception, like the intraparietal sulcus, which suggests that recurrent neurocognitive circuits amplify the strength of neuronal representations within this region for conscious access. HOT proposes the entrance of lower-order representations into higher-order

meta-representations, mainly associated with the prefrontal and parietal cortex (Brown et al., 2019; Lau & Rosenthal, 2011). IIT offers a mathematical framework to understand phenomenology, although the study's design doesn't provide direct insight into this (Tononi, 2008, 2012; Tononi et al., 2016).

Despite inconsistencies (Mashour et al., 2020; Seth & Bayne, 2022), these theories are not mutually exclusive and certain features could be integrated into a comprehensive model of conscious awareness, viewing them as describing different states of the same underlying process. This could involve activation of prefrontal and parietal cortices which rely in part on attentional processes (GWT), amplification of neuronal representations within these regions for conscious access via recurrent processing (RP), accompanied by appropriate higher-order meta-representational states (HOT), and incorporation into information complexes when content is conscious (IIT).

6.3.3. Visual pathways and residual visual abilities after occipital cortex lesions

The second published empirical study adopted a novel approach to explore Type II blindsight in a participant with a V1 lesion, using an event-related motion detection fMRI design. Presenting motion in the intact visual field elicited functional activation in the primary visual and contralateral MT areas, as expected, along with bilateral activation in parietal regions, potentially associated with attentional shifts (Saygin & Sereno, 2008). However, presenting motion in the impaired visual field elicited activation in the contralateral striate, extrastriate visual areas, such as the inferior and middle occipital gyri, and ipsilateral MT, indicating regions potentially involved in implicit visual motion processing. Common regions for intact and impaired visual field stimulation included the right calcarine, left inferior occipital gyrus, and right MT area, highlighting regions that may be involved in facilitating information processing, or compensating for the brain injury, when the impaired visual field is stimulated, consistent with previous research (Celeghin et al., 2017). Despite observing contralateral activation when stimulating either the intact or impaired visual field, we consistently detected area MT activation in the right hemisphere in response to motion

stimuli in either visual field, as indicated by the main effects of visual motion. This finding does not imply a hemispheric directional bias or a lateralized response to motion presentation, rather it suggests an involvement of the intact hemisphere in residual vision processes, which is supported by previous research (Celeghin et al., 2017, 2018). Given the correlational nature of fMRI data, the same brain region recruited for both impaired and intact visual field presentations may exhibit fundamentally different response patters, which could be driven by a subcortical input (Ajina et al., 2015). Moreover, the activation within the right inferior parietal lobe, independent of visual hemifield presentation, could be linked to attentional capture even without awareness (Dupont et al., 1994; Hervais-Adelman et al., 2015). Activation of frontal areas and the insula could help explain the patient's sense of activity within the impaired visual field and the accurate performance on the task (Craig, 2009; Persaud et al., 2011; Van den Stock et al., 2014). Differential activation patterns in the superior colliculi and pulvinar regions were observed depending on the stimulated field. Atypical ipsilateral activation for intact hemifield stimulation suggests an adaptive increase in colliculus activation, which would require further research. These observations highlight that damage to the visual cortex significantly influences how visual information is processed and represented within the brain, both in the intact and impaired visual field, corresponding to conscious and nonconscious perception.

Building on the insights and findings of the second study, which provided empirical evidence of changes in neural engagement post-brain injury, the third empirical study extends further showing a broader landscape of visual processing alterations in a cohort of CVI participants after damage to the occipital cortex, compared to a group of neurotypical controls. This study also accounts for variability of signal change after injury, quantifies lesion extent and residual abilities, presents more complex and rigorous visual motion stimulation and employs high-resolution fMRI. Whole-brain analyses in response to visual motion showed activation in extra-striate areas spanning from the occipital to parietal and temporal regions, consistent with previous work (for a meta-analysis see Celeghin et al., 2018), differing from the focused activation observed in controls. While visual representations exist beyond occipital regions (Hagler & Sereno, 2006; Huk et al., 2002; Saygin & Sereno, 2008; Sereno

et al., 2001), variability of brain lesions might amplify inherent individual representation differences, affecting residual perception. Studies have started to associate residual vision with functional activation patterns (Ajina & Bridge, 2017; Tamietto & Morrone, 2016).

We selected the hMT and lateral occipital complex as cortical ROIs due to hMT's established role in visual motion processing as well as the observed activation in Article 2, in addition to the lateral occipital complex's primary association with unconscious processing- yet also conscious processing, as highlighted in Article 1. The ROI analyses first showed that both regions in CVI participants can be activated by contralateral visual hemifields, yet with seemingly varying intensity. The ipsilesional hMT and lateral occipital complex respond less asymmetrically to visual field presentation compared to neurotypical controls. In the intact hemisphere, the hMT of CVI participants with neurotypical-like residual visual abilities can respond to looming motion in the impaired hemifield, supporting prior research (Barbur et al., 1993; Bridge et al., 2010; Rodman et al., 1989), and suggesting alternate visual processing pathways transmitting information to this region. This result is consistent with the intact hMT activation following impaired visual field stimulation observed in the second study where the participant also had strong residual visual abilities. Moreover, in the intact hemisphere, the lateral occipital complex seems to respond more to ipsilateral - impaired - visual field presentation than controls. Given this observed response and its previously suggested link to unconscious processing (Dijkstra et al., 2021), further research could explore the role of this region. Specifically, investigations could determine if the altered response after damage to primary visual areas stems from increased subcortical contributions and/or feedback processes.

The high-resolution fMRI was used to target the subcortical regions observed in the second article. The results indicate that the thalamus and pulvinar adaptively process salient motion at the subcortical level in CVI individuals. Specifically, the thalamus exhibits contrasting activation trends in intact and lesioned hemispheres, with a contralateral and ipsilateral dominance, respectively, significantly different than controls. High-performing CVI individuals displayed ipsilesional thalamic responses to the contralateral impaired visual field, suggesting a potential link between heightened thalamic responses to clinically blind

field stimulation and enhanced residual visual abilities, warranting further research. The pulvinar's amplified response to looming motion corroborates previous findings of its role in processing salient motion, even post V1 damage (Furman, 2014; Tamietto & Morrone, 2016). The pulvinar-mediated pathway is thought to be crucial for the early maturation of hMT (Warner et al., 2012; Warner et al., 2015), before giving way to a primary pathway linking the lateral geniculate nucleus to the primary visual cortex and MT (Mitchell & Leopold, 2015; Warner et al., 2010). After V1 lesions, individuals with residual vision have been thought to atypically retain this early pulvinar-mediated route(Bridge et al., 2016). While the pulvinar-hMT route may be inherent to neurotypical processing, V1 damage offers a unique opportunity to isolate its neuronal properties, and potentially observe an enhanced signal. These results underscore the thalamus and pulvinar's role in retaining visual functions after occipital cortex injury. Future research could explore the direct neural pathways between these regions and hMT, particularly post-injury, and whether early V1 lesions bolster the pulvinar-mediated pathway. In addition, recent research suggests that midbrain structures are involved in higher-level perceptual processes such as attention-related modulation, event detection, and object selectivity, as observed in intact models, extending beyond their role of projecting to the cortex (Bogadhi et al., 2021). This warrants further exploration into the potential link between the higher-level perceptual functions of midbrain structures in intact settings and the degree of residual vision that individuals may retain following injury.

Extra-striate regions are known to be stimulus selective, with MT neurons exhibiting selectivity not only for motion but also for other stimuli such as pattern-direction, bars, contrast and naturalistic movies at the single-cell level (Britten et al., 1992; Desimone et al., 1984; Krause & Pack, 2014; Movshon et al., 1985; Nishimoto & Gallant, 2011; Pack & Born, 2001; Pack et al., 2005; Tsunoda et al., 2001). Much like this stimulus-selectivity, the relative signal increase in cortical and subcortical regions might stem from the nature of the visual inputs, with looming motion inducing a stronger visual flow than biomotion stimuli, resulting in modulations in visual processing. Regions focusing on higher-level features, such as human motion recognition, might emphasize the quality of visual data rather than

its intensity. Neurons exhibit differential activation within a region in response to various modulated stimuli, including changes in stimulus location, motion direction, frequency variations, and patterns like gratings Borst and Egelhaaf, 1989; Bremmer et al., 2002; Duffy and Wurtz, 1995. The representation of motion in MT can be influenced by stimulus properties, with a substantial proportion of directionally selective neurons observed in primate models (Maunsell & Van Essen, 1983a; Miura et al., 2014; Tanaka & Saito, 1989). Moreover, visual pathways are characterized by bidirectional communication, where each feedforward connection is coupled with a feedback connection capable of modulating the response (Sillito et al., 2006). Top-down influences consider the nature of stimulus-dependent properties in sensory cortical areas and can dynamically tune the neuronal response to align with current perceptual demands (Gilbert & Li, 2013). As stimulus complexity increases, the role of attentional influences becomes more prominent, which can result in signal amplification (Motter, 1993). Thus, it is expected that the type and complexity of stimuli used can impact neural responses. While studies 2 and 3 focused on the human MT complex (hMT+/V5), which includes the medial superior temporal cortex (MST), the differences in response patterns between biological and looming stimuli could also be linked to the differential involvement of MST. MST receives direct feedforward input from MT, has a bilateral visual field representation, and is specialized in processing optic flow stimuli (Azzopardi et al., 2003; Duffy & Wurtz, 1991; Huk et al., 2002; Komatsu & Wurtz, 1988b; Maunsell & Van Essen, 1983b; Ungerleider & Desimone, 1986). MST has been suggested to send feedback projections to MT, which could potentially amplify the signal following the presentation of looming stimuli. Investigating the potential interplay between these two regions could offer valuable insights into the observed differences in our findings. This emphasizes the complex interaction between stimulus attributes and neural engagement, showcasing the brain's adaptability to diverse visual inputs post occipital cortex damage. While our study highlights possible functional changes in regions like hMT, lateral occipital complex, pulvinar, and thalamus after injury, future research should investigate further the interactions of regions within the pulvinar-mediated pathway and the extent of qualitative adaptation for processing of various visual features.

6.4. Implication of thesis findings

6.4.1. Methodological contributions

This thesis follows key sequential - yet standalone- steps in empirical science, beginning with a proof-of-concept case study (Article 2), to generating a unique dataset (Chapter 4), advancing to a high-resolution fMRI study incorporating a larger sample size with group analyses (Article 3), and further extending its scope by including meta-analyses (Article 1). Each experimental framework offers valuable and distinct contributions to help capture the complexity of visual conscious awareness and unconscious visual perception more effectively, collectively enhancing the overall robustness and applicability of the research. In addition, the work from this thesis contributed to the development of the bidspm statistical analysis processing pipeline, a key methodological contribution, and supports its usage for future studies. This includes the incorporation of a refined algorithm for automated lesion mapping, underlining the need for standardized analysis methods. Moreover, having used this now openly available standardized pipeline for statistical procedures increases reproducibility of the thesis results.

The first article (published April 2023) underscores the significance of conducting meta-analyses, particularly within the field of conscious and unconscious visual perception. This study not only consolidates a vast amount of data, but also serves as a milestone in asserting the fundamental results in the field. The rise of interdisciplinary cognitive neuroscience has catalyzed the interest in understanding the neural underpinnings of conscious perception, driving numerous new studies. The ALE meta-analysis successfully discerned patterns and trends, that may not have been evident in individual studies, while mitigating false positives, enhancing statistical power, and revealing the true effect size. It assessed consistency across studies by examining the convergence of activation across brain regions (Eickhoff et al., 2009; Salimi-Khorshidi et al., 2009; Wager et al., 2009), ensuring robust and reliable outcomes and strengthened the confidence in the results. Standardizing measures across studies, prior to the main analyses, enhanced comparability, and attests to the meta-analysis's methodological value. The meta-analysis also highlighted areas requiring further exploration, such as

unconscious processing, differential activation within the same structures, temporal information processing, and the association with higher-order cognitive processes. While associations with other cognitive processes have been previously suggested, the meta-analysis goes beyond by not only quantitatively identifying consistent activation across multiple independent neuroimaging studies but also conducting functional decoding to reveal the cognitive processes associated with the results by comparing to over 14,300 fMRI studies. This consolidating approach adds a robust and data-driven dimension to understanding the interplay of cognitive processes with conscious and unconscious perception.

Moreover, mapping reliable neural correlates associated with visual conscious awareness in the intact brain could potentially ultimately benefit various clinical populations with visual impairments by facilitating the identification of main differences and targeting regions needing more investigation. Understanding visual conscious awareness is also a timely effort in current scientific pursuits especially when considering the rise of Neuro-AI. In April 2023, researchers emphasised the urgent need for consciousness research to align with the artificial intelligence (AI) advancements in an open letter, entitled "The responsible development of AI agenda needs to include consciousness research" by The Association for Mathematical Consciousness Science, here. The rapid pace of research in this area will undoubtedly warrant future meta-analyses and this study sets a precedent for future investigations. Subsequent meta-analyses will be able to leverage the data points from our meta-analytical work as a starting point, thus accelerating continuous progress.

6.4.2. Strengths and limitations

The findings from the current neuroimaging thesis extend beyond previous research and contribute to our understanding of visual processing in neurotypical individuals and those with CVI, yet important methodological limitations need to be addressed. Studies 2 and 4 are limited by the modest sample sizes, which restrict their statistical power. In cognitive neuroscience, sufficient power enables to detect significant effects and establish reliable associations between brain regions and behavior. (Button et al., 2013) highlighted the widespread issue of underpowered neuroscience studies, particularly fMRI studies, which typically

have a median power around 8%, whereas the median power for neuroscience studies is 21%. Consequently, low-powered studies are prone to false negatives and are likely to capture only the largest effects, often missing smaller, yet still relevant, brain-behavior relationships (Yarkoni, 2009; Zuo et al., 2019). Despite these constraints, the brain lesion case-study presented in the second article offers unique advantages. Historically, case studies with focal brain damage have significantly contributed to cognitive neuroscience theories, providing robust inferential strengths, over those of temporary manipulations and challenging brain-behavior models (Deifelt Streese & Tranel, 2021; Medina & Fischer-Baum, 2017). The study introduces a unique case, ML, characterized by right homonymous hemianopia acquired relatively young at age 17, strong residual visual motion abilities, advanced education, excellent health, absence of prior neurological or psychological disorders, and a fully intact left visual field. Her responsiveness to stimuli in both hemifields was remarkably not significantly different, employing a conservative response strategy. While she lacked awareness of blind field stimuli, she clearly perceived those in her intact hemifield. The study was designed with the assumption of observing MT activation, given pre-fMRI behavioral tests, to enable to delve into the complexities of visual motion representation despite a V1-lesion. ML's case offers a rich opportunity to explore in detail the effects of this specific lesion with minimal confounding factors, reaffirming previous findings and revealing nuanced insights within functionally activated regions. Rigorous experimental designs and analyses were used to further aim to offset the limitations (Amaro & Barker, 2006; Celeghin et al., 2018; Wall et al., 2009). The theory-driven analyses in this second article reduced the risk of inflated false-positive rates, and served as a foundation for the third study. The experimental tasks used stimuli known to probe visual processing in individuals with damage to the visual cortex, relevant to our hypotheses. This involved employing motion detection and discrimination, looming, biomotion stimuli, etc. - all of which the code is available for secondary usage. An independent neurotypical control group was utilized to validate and optimize the behavioral tasks prior to the main experiment, strengthening the validity of the results in the third study. By presenting visual stimuli in both intact and impaired visual fields at different time points, matched control conditions were established for each CVI participant, in addition to the

neurotypical control group in the third study, thereby enhancing the reliability of statistical outcomes and effect estimation. Efforts were made to address light scatter artifacts, where light from stimuli directed towards the impaired visual field could inadvertently reach the intact field, potentially simulating residual visual abilities (Cowey Weiskrantz, 1963). To minimize the potential impact of light scatter during the motion direction discrimination task performed outside the scanner, we maintained a background luminance of 60 lux. Nonetheless, we recognize that utilizing white dots on a grey background in an illuminated room could have ensured a light scatter-safe stimulus condition, potentially preventing the need for additional tests, in alignment with the recommendations from (D. Schmid et al., 2022). Inside the scanner, where controlling lighting conditions is challenging, we employed looming motion stimuli with white dots on a grey background, consistent with these recommended practices. For biological motion stimuli, which featured fewer dots, we increased the contrast between point-lights and the background to optimize the balance between visibility and the associated MRI signal. Prior to each experiment, we assessed blind field stimulus presentations, with participants confirming the absence of visible stimuli in the impaired visual field and any related effects in the intact visual field. Despite this limitation, given our a priori blind field testing as well as the stimulus conditions, we believe that our results regarding residual visual abilities are not driven by potential light-scatter effects in the intact visual field. Future studies might benefit from adhering to these recommendations (D. Schmid et al., 2022) to streamline the experimental setup and save time on additional testing. The use of high resolution fMRI with ROI analyses enabled to target and enhance anatomical specificity of subcortical regions, advancing our understanding of the impact of CVI. MRI acquisition parameters were meticulously optimized through pilot sessions to enhance resolution of subcortical structures associated with the hypotheses. To mitigate potential confirmation bias, exploratory whole-brain analyses in the second and fourth studies were also performed, a practice seemingly in decline with recent articles predominantly reporting exclusively pre-defined ROI analyses. Moreover, while previous studies have explored regions like MT, our ROI results provide a clear depiction of percent signal change across individual participants following motion presentations in both hemifields (along with the

difference between them) for both hemispheres, and simultaneously allow visualizing them as a group. The results also highlight high performers, allowing for a nuanced representation of brain-behavior relationships. Consequently, our findings offer a valuable perspective into the involvement of MT, the lateral occipital cortex, thalamus, and pulvinar in CVI, further enriching the understanding of reorganization in motion-selective regions post brain injury in the primary visual area that may facilitate spared visual function.

Meta-analyses may be subject to publication bias and the limitations inherent in the individual included studies. Moreover, including in the meta-analyses various designs, stimuli, fMRI acquisition parameters and analysis pipelines should be considered when interpreting results. Nevertheless, neuroimaging meta-analyses commonly compare studies across different control conditions or baselines (Salimi-Khorshidi et al., 2009; Wager et al., 2009). Moreover, in the first article, results from small sample size studies are represented with wider Gaussian distribution properties as opposed to results from larger sample size studies (Eickhoff et al., 2009). Performing a meta-analysis remains the most efficient approach to consolidate significant activated regions across independent studies and provide a more accurate of the true effect.

6.5. Future research avenues

Multi-center collaboration for larger sample sizes. Replication of the methodology and findings from this thesis, both through the data already acquired and via independent cohorts, is a crucial next step to ensure reliability. Future studies will greatly benefit from expanding sample sizes to strengthen the statistical power, robustness and generalizability of the findings. Larger cohorts can help identify subtle differences in brain activation post CVI and how this relates to residual visual processing, potentially uncovering neural features that were not detectable with a smaller population. However, most hemianopia studies have five participants or less (Bridge, 2020; Bridge et al., 2008; Papanikolaou et al., 2014; Tamietto et al., 2010). As it is challenging for one laboratory to acquire large sample sizes, multi-lab or multi-center collaboration initiatives can be beneficial to the field for larger and more diverse sample sizes as well as conducting functional neuroimaging meta-analyses specific to

the impact of CVI. Detailed descriptions of the meta-data of each individual study will be crucial to better aggregate the results, which can be done following the BIDS specification guidelines, including patient descriptions, acquisition parameters, pre-processing specification, etc. Moreover, a large-scale project to reproduce brain-behavior correlations could address the idiosyncrasies across CVI individuals, and attest to the generalizability of fMRI findings across studies.

A comprehensive analysis of the MRI dataset. Moreover, the experimental effort of my doctoral research has generated a wealth of data that remain largely unexplored. A thorough analysis of the remaining data includes structural based analyses such as voxel based morphometry, diffusion MRI, resting state fMRI, effective connectivity analyses from tasked-based fMRI, electrophysiological analyses of the neurotypical control group and CVI individuals, among others. This database, including preprocessed fMRI data and quality control metrics, was documented as a chapter, considering ethical limitations, in the hopes to encourage the neuroimaging community's ability to adopt practices promoting transparency and secondary usage of data. For instance, the resting state fMRI data could be used to evaluate spontaneous brain activity in individuals with CVI compared to the neurotypical control group. This technique could identify changes in large scale resting state networks—distinct spatial regions of the brain that display synchronous BOLD fluctuations at rest(Lee et al., 2013), and understand how occipital cortex lesions alter intrinsic neural interactions. While one study has investigated functional interactions in 10 individuals with chronic visual impairment, showing a significant alteration in the intrinsic architecture of a large-scale brain system (Pedersini et al., 2020), further rsfMRI analyses could potentially reveal reduced connectivity in brain circuits serving neurotypical visual processing. There might also be an increase in connectivity between the alternative visual pathways highlighted in our articles, i.e., encompassing the superior colliculus, pulvinar, LGN, and V5/MT+ structures. To investigate the functional connectivity between these regions, ROI to ROI analyses could be performed. Moreover, diffusion MRI offers the possibility of analyzing the brain's structural connectivity by tracking the diffusion of water molecules, which primarily occurs along the

axons of neurons. This provides a way to map the white matter tracts, the structural pathways through which information travels between different brain areas. This neuroimaging technique could be used to chart the integrity and functionality of neurotypical visual processing pathways and understand the specific structural disruptions that result in CVI. For example, previous work employed diffusion imaging to show that the fractional anisotropy metric—a measure of white matter microstructure—of the tract between LGN and MT+ of CVI participants with blindsight was comparable to those of neurotypical controls, and significantly lower for those without blindsight (Ajina et al., 2015b). The outcomes of these subsequent analyses may either reveal new patterns or strengthen the observations made during the studies included in this thesis.

Assessing peripheral factors on the BOLD signal. Future research could address and account for peripheral factors, such as heart-rate and eye movements, into their investigations of the neural correlates associated with both conscious awareness and unconscious perception. Although cognitive neuroscience mainly explores the processing of external stimuli, the brain also receives significant internal input from the body. General body-brain interactions can shape our cognition and it has become increasingly evident that brain-heart interactions play a role in the neurobiology of consciousness or perceptual awareness (for a recent review see Candia-Rivera, 2022). For instance, heartbeat-evoked responses have been shown to predict perception in a visual detection task and lead to differential activation in cortical areas, suggesting they shape visual conscious experience (Park et al., 2014). Stimulus timing, along the cardiac cycle, has been shown to modulate perception and conscious access to the stimulus (Al et al., 2020). Fluctuations in heart rate have been shown to be partially driven by conscious processing and associated with the attentional state (P. Perez et al., 2021). Moreover, the autonomous nervous system has been shown to modulate brain-state dynamics, ultimately supporting shifts in conscious awareness (Munn et al., 2021; Wainstein et al., 2021). To what extent brain-heart interactions are a consequence of the brain processing the contents of visual awareness or have causal role in perception is yet to be fully understood. As neural and behavioural responses can be influenced by factors related to cardiac signals, analyzing them alongside brain activity would be relevant for future

research (Azzalini et al., 2019). Furthermore, experimental tasks that involve eye movements may affect fMRI findings. Alongside signals specific to conscious visual perception, eye movement-related signals may align with neural activity and reflect changes associated with i) the conscious perception state unrelated to visual stimuli or 2) eye movement motor control (DiNuzzo et al., 2019; Guipponi et al., 2015; Kronemer et al., 2022; Maki-Marttunen, 2021; Tse et al., 2010). Nevertheless, a recent study observed that visual consciousness remained broadly distributed across cortical and subcortical regions even after removing eye movement-based confounds (Kronemer et al., 2022), indicating that eye movements should not lead to the exclusion of specific brain regions. Despite the main association between visual perception and eye movements, accumulating evidence reveals a dissociation between the contents of perceptual awareness and different types of eye movements. For example, eye movements have shown that individuals are processing visual information in the absence of awareness, potentially involving subcortical pathways (for review see Spering & Carrasco, 2015). Understanding these distinctions between eye movements and perceptual awareness can provide valuable insights into how they influence BOLD activity. Nonetheless, future studies should recognize eye-movement related signals as potential confounding factors when interpreting results. Adopting an approach that explores multiple overlapping systems may facilitate a more comprehensive understanding of the neurophysiological complexity associated with conscious perception. The collected physiological measurements described in Chapter 4 of this thesis, could be leveraged in future studies to investigate these influencing peripheral factors.

Assessing individual factors associated with brain activation patterns in CVI. Further studies could investigate the role of individual differences, along with factors such as age, gender, age at lesion, variable duration of disease and level of brain damage in the patterns of brain activation related to the impact of CVI and residual visual abilities. The extent and localization of the lesion and the resulting altered visual experience can lead to varying connectivity and structural changes across different regions (Clarkson et al., 2010; Cramer, 2008; Li et al., 2010), potentially resulting in diverse clinical subtypes. Future research could benefit from the implementation of machine learning methods to analyze neuroimaging data

and assess these multifaceted contributing factors at a larger scale. Advanced algorithms could also potentially identify complex patterns or interactions among brain regions during visual perception tasks that might not be evident through traditional statistical analyses. Incorporating machine learning techniques holds promise to develop individually-based imaging indices to help establish biomarkers and enhance prognostic models (Davatzikos, 2019). However, the reliable application of machine learning techniques in clinical neuroscience is currently in its early stages, with initial studies primarily focusing on accurately classifying patients from neurotypical controls, which in practice has limited value. Future research could build upon these studies and shift towards more clinically relevant investigations, such as detecting subtle imaging signatures or sub-types and refining clinical categories, according to these imaging phenotypes (Rathore et al., 2018). For instance, in the context of CVI, these subtypes could perhaps be reflected in the diverse engagement of alternative visual processing pathways and the associated residual visual function along with differential clinical characteristics. The use of semi-supervised learning methods might help address heterogeneity and enable this subcategorization of a patient into a subtype to be estimated in a data driven way, thus contributing to more precise diagnostics (Bzdok et al., 2015; Filipovych et al., 2011; Varol et al., 2017).

Multisensory approaches for investigation of cross-modal interactions in visual impairments. Future research could explore multisensory approaches to enhance our understanding of cross-modal interactions, studying the recruitment of non-visual areas to compensate for lesioned brain tissue. This would involve investigating the interplay between visual perception and other sensory modalities (e.g., auditory), and how these interactions affect functional, structural and connectivity alterations post-lesion. Research in visual deprivation conditions, such as blindness, has shed light on the brain's remarkable ability to adapt through cross-modal reorganization, where the visual cortex gets functionally repurposed to process non-visual sensory information (Amedi et al., 2010; Burton, 2003; Collignon et al., 2011; Collignon et al., 2009; M. Ptito & Kupers, 2005). Moreover, our systematic review revealed alterations in both auditory and non-auditory regions' white and grey matter in deaf individuals (Simon et al., 2020). Multisensory integrative mechanisms have been

shown to bolster detection and localization of audio-visual pairs, especially when unisensory stimuli are degraded (Dundon et al., 2015b; Frassinetti et al., 2005). These mechanisms may remain intact after stroke and operate within the blind visual field. This could be relevant from a rehabilitative perspective, as non-visual stimuli may facilitate impaired visual functions (Bolognini, 2019). Crossmodal localization capacities have also been shown in hemianopia, indicating that distinct neural pathways may operate within the intact versus blind field (Leo et al., 2008). A key focus could be the superior colliculus, a structure containing multisensory neurons (Stein, 1998) and thought to mediate unconscious visual pathways post-injury.

Neuro-rehabilitation of the impaired visual field. Understanding how the neuroplastic mechanisms unfold following a lesion is critical, particularly in distinguishing between adaptive and maladaptive neural reorganization. This can help facilitate the development of rational, evidence-based strategies to boost functional recovery. Research involving patients with visual field defects have shown reorganization of cerebral neural networks after consistent specialized visual training, indicating that repetitive training or visual stimulation can improve visual abilities long-term (for review see Gall et al., 2015; C. Perez & Chokron, 2014; Sabel, 2017; Weill-Chounlamountry et al., 2012). Perceptual visual training with complex motion stimuli in the blind-field has shown promise in rehabilitating cortically blind patients (Cavanaugh et al., 2017; Chokron et al., 2008; Das et al., 2014; Huxlin, 2008; Pandey et al., 2022). However, current clinical rehabilitation methods present limitations, as they primarily focus on adaptive visual strategies and lifestyle habits to cope with vision loss (Lam & Leat, 2013; Leat, 2016), or substitution techniques involving prism lenses to expand the visual field (Bowers et al., 2014; Peli, 2000). For most individuals, cortical blindness persists despite this period of clinical rehabilitation. Residual plasticity has been observed in the adult visual system, further suggesting that rehabilitation programs could potentially harness this latent adaptability (Castaldi et al., 2020). Specifically, perceptual training has been shown to dynamically modulate the function of the MT region in visual motion perception, suggesting that this region can exhibit considerable plasticity depending on recent perceptual

experience (L. D. Liu & Pack, 2017). Future research could explore neurostimulation techniques, targeting structures to facilitate a certain degree of recovery of visual function, such as V5/MT+ and LOC, as discussed in this thesis. Initiatives like the Lightup Project DOI offer a compelling direction, proposing to use non-invasive transcranial magnetic stimulation (TMS) to selectively stimulate cortical circuits to enhance visual awareness in the cortically blind brain. Such novel approaches aim to strengthen alternative pathways or selectively enhance the direction of pre-existing connections, thereby advancing the field toward more effective neuro-rehabilitation therapies. These interventions could be combined with visual training programs, such as those designed to enhance visual search strategies or saccades to the impaired visual field and incorporating multisensory integration (Dundon et al., 2015a; Dundon et al., 2015b). Moreover, using real-time fMRI neuralfeedback to give participants immediate feedback about their brain activity during visual tasks could allow participants to self-regulate brain function (Watanabe et al., 2017). Advanced fMRI neurofeedback enables to investigate causal brain/behaviour relationships via implicit protocols. For example, fMRI neurofeedback has been shown to modify the activation of the visual cortex resulting in improved performance on a visual task (Shibata et al., 2011). This could lead to new insights about the neural mechanisms of visual conscious awareness and causal improvements in the context of CVI. Future studies could use longitudinal designs with functional neuroimaging, before and after such rehabilitation programs, to track changes in brain activation patterns over time, ultimately to effectively encourage adaptive changes and mitigate maladaptive ones. Expanding fundamental research in this area has the potential to not only refine clinical rehabilitation strategies but also to inspire the development of innovative technologies and devices designed to assist visually impaired individuals, improving long-term patient outcomes and significantly contributing to a field of growing public interest and need.

Open science to enhance research transparency and impact. Moreover, promoting open science can help enhance transparency, reproducibility and accessibility in research. Future studies could preregister research protocols, on platforms like the Open Science Framework, to prevent post-hoc changes in hypotheses, or use open source software

for data analysis to understand how data were analyzed, and facilitate replicating or extending the work. Sharing raw and processed datasets, within ethical considerations, in addition to collaborating on or using data organization and management standards (e.g., BIDS), could facilitate a more comprehensive use of data. Adhering to methodological standards and conventions could increase the quality and precision of future studies, including meta-analyses, and further clarify brain-behaviour relationships (Muller et al., 2018; Nichols et al., 2017; Uddin et al., 2019). Open science practices can help accelerate the dissemination of research findings and, in the context of the current research, ultimately raise awareness about visual health and the impact of visual cortex damage, thus opening avenues for intervention.

6.6. Conclusion

Our sensory visual experience is subject to dynamic modifications, through experience or as a consequence of brain damage. Occipital cortex lesions leading to cortical visual impairment (CVI), can precipitate functional and structural changes in neurotypical visual pathways and alter how visual information is processed and represented within the brain. Comprehensively understanding the neural mechanisms involved in generating a conscious perception and how they can be modulated by damage to the visual cortex resulting in CVI, and the association with residual visual abilities, remains an ongoing challenge. This thesis leveraged a multi-layer research framework, incorporating behavioral assessments alongside structural and functional neuroimaging techniques. By integrating a proof-of-concept case study, group analysis, and meta-analysis, and introducing a novel dataset, this thesis contributes to the improvement of methods and experimental approaches to investigate visual processing in both neurotypical individuals and those with clinical blindness resulting from brain injury. The results from the two quantitative meta-analyses empirically identify consistent functional brain activity associated with conscious and unconscious visual processing in the intact brain across the wealth of acquired functional magnetic resonance imaging (fMRI) data. The studies on CVI show functional modulation of visual pathways in the brain following occipital cortex injuries, using pyschophysical visual motion tasks coupled with neuroimaging. Neural alterations were observed in cortical and subcortical regions, thereby offering insights into how regions such as the middle temporal area, lateral occipital complex, thalamus and pulvinar may contribute to facilitating spared visual function. The contribution of these regions in visual processing following brain injury appears highly plastic, and could be leveraged in future studies investigating neuro-rehabilitation in the impaired visual field. Collectively, this thesis further serves as a comprehensive empirical foundation for future cognitive neuroscience investigations into the brain-behaviour relationships associated with visual motion processing, conscious and unconscious visual perception.

References

Abraham, A., Pedregosa, F., Eickenberg, M., Gervais, P., Mueller, A., Kossaifi, J., Gramfort, A., Thirion, B., & Varoquaux, G. (2014). Machine learning for neuroimaging with scikit-learn. Frontiers in Neuroinformatics, 8. https://doi.org/10.3389/fninf.2014.00014

Aguirre, G. K., Zarahn, E., & D'Esposito, M. (1998). An area within human ventral cortex sensitive to "building" stimuli: Evidence and implications. Neuron, 21(2), 373–83. https://doi.org/10.1016/s0896-6273(00)80546-2

Ajina, S., & Bridge, H. (2017). Blindsight and unconscious vision: What they teach us about the human visual system. Neuroscientist, 23(5), 529–541. https://doi.org/10.1177/1073858416673817

Ajina, S., & Bridge, H. (2018). Subcortical pathways to extrastriate visual cortex underlie residual vision following bilateral damage to v1. Neuropsychologia. https://doi.org/10.1016/j.neuropsychologia.2018.01.007

Ajina, S., Kennard, C., Rees, G., & Bridge, H. (2015a). Motion area v5/mt+ response to global motion in the absence of v1 resembles early visual cortex. Brain, 138(Pt 1), 164–78. https://doi.org/10.1093/brain/awu328

Ajina, S., Pestilli, F., Rokem, A., Kennard, C., & Bridge, H. (2015b). Human blindsight is mediated by an intact geniculo-extrastriate pathway. Elife, 4. https://doi.org/10.7554/eLife.08935

Al, E., Iliopoulos, F., Forschack, N., Nierhaus, T., Grund, M., Motyka, P., Gaebler, M., Nikulin, V. V., & Villringer, A. (2020). Heart-brain interactions shape somatosensory perception and evoked potentials. Proc Natl Acad Sci U S A, 117(19), 10575–10584. https://doi.org/10.1073/pnas.1915629117

Allman, J., Miezin, F., & McGuinness, E. (1985). Direction- and velocity-specific responses from beyond the classical receptive field in the middle temporal visual area (mt). Perception, 14(2), 105–26. https://doi.org/10.1068/p140105

Allman, J. M., & Kaas, J. H. (1971). Representation of the visual field in striate and adjoining cortex of the owl monkey (aotus trivirgatus). Brain Res, 35(1), 89–106. https://doi.org/10.1016/0006-8993(71)90596-8

Amaro, J., E., & Barker, G. J. (2006). Study design in fmri: Basic principles. Brain Cogn, 60(3), 220–32. https://doi.org/10.1016/j.bandc.2005.11.009

Amedi, A., Malach, R., Hendler, T., Peled, S., & Zohary, E. (2001). Visuo-haptic object-related activation in the ventral visual pathway. Nat Neurosci, 4(3), 324–30. https://doi.org/10.1038/85201

Amedi, A., Raz, N., Azulay, H., Malach, R., & Zohary, E. (2010). Cortical activity during tactile exploration of objects in blind and sighted humans. Restor Neurol Neurosci, 28(2), 143–56. https://doi.org/10.3233/RNN-2010-0503

Antonietti, A. (2011). Introspecting a conscious decision or the consciousness of a decision? Conscious Cogn, 20(4), 1916–7, author reply 1918–9. https://doi.org/10.1016/j.concog.2011.04.011

Aru, J., Bachmann, T., Singer, W., & Melloni, L. (2012). Distilling the neural correlates of consciousness. Neurosci Biobehav Rev, 36(2), 737–46. https://doi.org/10.1016/j.neubiorev.2011.12.003

Assem, M., Glasser, M. F., Van Essen, D. C., & Duncan, J. (2020). A domain-general cognitive core defined in multimodally parcellated human cortex. Cereb Cortex, 30(8), 4361–4380. https://doi.org/10.1093/cercor/bhaa023

Avants, B., Epstein, C., Grossman, M., & Gee, J. (2008). Symmetric diffeomorphic image registration with cross-correlation: Evaluating automated labeling of elderly and neurodegenerative brain. Medical Image Analysis, 12(1), 26–41. https://doi.org/10.1016/j.media.2007.06.004

Azouvi, P., Bartolomeo, P., Beis, J. M., Perennou, D., Pradat-Diehl, P., & Rousseaux, M. (2006). A battery of tests for the quantitative assessment of unilateral neglect. Restor Neurol Neurosci, 24(4-6), 273–85.

Azzalini, D., Rebollo, I., & Tallon-Baudry, C. (2019). Visceral signals shape brain dynamics and cognition. Trends Cogn Sci, 23(6), 488–509. https://doi.org/10.1016/j.tics.2019.03.007

Azzopardi, P., Fallah, M., Gross, C. G., & Rodman, H. R. (2003). Response latencies of neurons in visual areas mt and mst of monkeys with striate cortex lesions. Neuropsychologia, 41(13), 1738–56. https://doi.org/10.1016/s0028-3932(03)00176-3

Baars, B. (1993). A cognitive theory of consciousness. Cambridge University Press.

Bach, M. (1996). The freiburg visual acuity test–automatic measurement of visual acuity. Optom Vis Sci, 73(1), 49–53.

Bach, M. (2007). The freiburg visual acuity test – variability unchanged by post-hoc re-analysis. Graefe's Arch Clin Exp Ophthalmol, 245:965–971.

Baker, J. F., Petersen, S. E., Newsome, W. T., & Allman, J. M. (1981). Visual response properties of neurons in four extrastriate visual areas of the owl monkey (aotus trivirgatus): A quantitative comparison of medial, dorsomedial, dorsolateral, and middle temporal areas. J Neurophysiol, 45(3), 397–416. https://doi.org/10.1152/jn.1981.45.3.397

Baldauf, D., & Desimone, R. (2014). Neural mechanisms of object-based attention. Science, 344(6182), 424–7. https://doi.org/10.1126/science.1247003

Balint, R. (1909). R. seelenlahmung des "schauens" optische ataxie raumliche, storung der aufmerksamkeit psychiat. Monatsschr Psychiatr Neurol, 51–81.

Ball, W., & Tronick, E. (1971). Infant responses to impending collision: Optical and real. Science, 171(3973), 818–20. https://doi.org/10.1126/science.171.3973.818

Barbur, J. L., Watson, J. D., Frackowiak, R. S., & Zeki, S. (1993). Conscious visual perception without v1. Brain, 116 (Pt 6), 1293–302.

Baria, A. T., Maniscalco, B., & He, B. J. (2017). Initial-state-dependent, robust, transient neural dynamics encode conscious visual perception. PLoS Comput Biol, 13(11), e1005806. https://doi.org/10.1371/journal.pcbi.1005806

Barleben, M., Stoppel, C. M., Kaufmann, J., Merkel, C., Wecke, T., Goertler, M., Heinze, H. J., Hopf, J. M., & Schoenfeld, M. A. (2015). Neural correlates of visual motion processing without awareness in patients with striate cortex and pulvinar lesions. Hum Brain Mapp, 36(4), 1585–94. https://doi.org/10.1002/hbm.22725

Beck, D. M., Rees, G., Frith, C. D., & Lavie, N. (2001). Neural correlates of change detection and change blindness. Nature Neuroscience, 4(6), 645–50.

Beckers, G., & Zeki, S. (1995). The consequences of inactivating areas v1 and v5 on visual motion perception. Brain, 118 (Pt 1), 49–60. https://doi.org/10.1093/brain/118.1.49

Bedini, M., & Baldauf, D. (2021). Structure, function and connectivity fingerprints of the frontal eye field versus the inferior frontal junction: A comprehensive comparison. Eur J Neurosci, 54(4), 5462–5506. https://doi.org/10.1111/ejn.15393

Behzadi, Y., Restom, K., Liau, J., & Liu, T. T. (2007). A component based noise correction method (CompCor) for BOLD and perfusion based fmri. NeuroImage, 37(1), 90–101. https://doi.org/10.1016/j.neuroimage.2007.04.042

Benevento, L. A., & Standage, G. P. (1983). The organization of projections of the retinorecipient and nonretinorecipient nuclei of the pretectal complex and layers of the superior colliculus to the lateral pulvinar and medial pulvinar in the macaque monkey. J Comp Neurol, 217(3), 307–36. https://doi.org/10.1002/cne.902170307

Berlucchi, G. (2017). Wandering thoughts about consciousness, the brain, and the commentary system of larry weiskrantz. Neuropsychologia. https://doi.org/10.1016/j.neuropsychologia.2017.10.011

Berman, R. A., & Wurtz, R. H. (2010). Functional identification of a pulvinar path from superior colliculus to cortical area mt. J Neurosci, 30(18), 6342–54. https://doi.org/10.1523/JNEUROSCI.6176-09.2010

Bertini, C., Cecere, R., & Ladavas, E. (2013). I am blind, but i "see" fear. Cortex, 49(4), 985–93.

Billington, J., Wilkie, R. M., Field, D. T., & Wann, J. P. (2011). Neural processing of imminent collision in humans. Proc Biol Sci, 278(1711), 1476–81. https://doi.org/10.1098/rspb.2010.1895

Binda, P., Thomas, J. M., Boynton, G. M., & Fine, I. (2013). Minimizing biases in estimating the reorganization of human visual areas with bold retinotopic mapping. J Vis, 13(7), 13. https://doi.org/10.1167/13.7.13

Binder, M., Gociewicz, K., Windey, B., Koculak, M., Finc, K., Nikadon, J., Derda, M., & Cleeremans, A. (2017). The levels of perceptual processing and the neural correlates of increasing subjective visibility. Consciousness Cognition, 55, 106–125.

Bisenius, S., Trapp, S., Neumann, J., & Schroeter, M. L. (2015). Identifying neural correlates of visual consciousness with ale meta-analyses. Neuroimage, 122, 177–87. https://doi.org/doi.org/10.1016/j.neuroimage.2015.07.070

Blake, R., & Logothetis, N. (2002). Visual competition. Nat Rev Neurosci, 3(1), 13–21. https://doi.org/10.1038/nrn701

Blake, R., & Shiffrar, M. (2007). Perception of human motion. Annu Rev Psychol, 58, 47–73. https://doi.org/10.1146/annurev.psych.57.102904.190152

Bogadhi, A. R., Katz, L. N., Bollimunta, A., Leopold, D. A., & Krauzlis, R. J. (2021). Midbrain activity shapes high-level visual properties in the primate temporal cortex. Neuron, 109(4), 690–699 e5. https://doi.org/10.1016/j.neuron.2020.11.023

Bolognini, V. (2019). Chapter 19 - hemianopia, spatial neglect, and their multisensory rehabilitation. Multisensory Perception, 423–447. https://doi.org/https://doi.org/10.1016/B978-0-12-812492-5.00019-X

Boly, M., Massimini, M., Tsuchiya, N., Postle, B. R., Koch, C., & Tononi, G. (2017). Are the neural correlates of consciousness in the front or in the back of the cerebral cortex? clinical and neuroimaging evidence. J Neurosci, 37(40), 9603–9613. https://doi.org/10.1523/JNEUROSCI.3218-16.2017

Bor, D., & Seth, A. K. (2012). Consciousness and the prefrontal parietal network: Insights from attention, working memory, and chunking. Front Psychol, 3, 63. https://doi.org/10.3389/fpsyg.2012.00063

Born, R. T., & Bradley, D. C. (2005). Structure and function of visual area mt. Annu Rev Neurosci, 28, 157–89. https://doi.org/10.1146/annurev.neuro.26.041002.131052

Borst, A., & Egelhaaf, M. (1989). Principles of visual motion detection. Trends Neurosci, 12(8), 297–306. https://doi.org/10.1016/0166-2236(89)90010-6

Bourne, J. A., & Morrone, M. C. (2017). Plasticity of visual pathways and function in the developing brain: Is the pulvinar a crucial player? Front Syst Neurosci, 11, 3. https://doi.org/10.3389/fnsys.2017.00003

Bowers, A. R., Keeney, K., & Peli, E. (2014). Randomized crossover clinical trial of real and sham peripheral prism glasses for hemianopia. JAMA Ophthalmol, 132(2), 214–22. https://doi.org/10.1001/jamaophthalmol.2013.5636

Brainard, D. H. (1997). The psychophysics toolbox. Spat Vis, 10(4), 433–6.

Breitmeyer, B. G., & Ogmen, H. (2000). Recent models and findings in visual backward masking: A comparison, review, and update. Percept Psychophys, 62(8), 1572–95. https://doi.org/10.3758/bf03212157

Bremmer, F., Duhamel, J. R., Ben Hamed, S., & Graf, W. (2002). Heading encoding in the macaque ventral intraparietal area (vip). Eur J Neurosci, 16(8), 1554–68. https://doi.org/10.1046/j.1460-9568.2002.02207.x

Brett, M., Anton, J. L., Valabregue, R., & Poline, J. B. (2002). Region of interest analysis using an spm toolbox [abstract] presented at the 8th international conference on functional mapping of the human brain. NeuroImage, Vol 16, No 2.

Bridge, H. (2020). Loss of visual cortex and its consequences for residual vision. Current Opinion in Physiology, 16, 21–26. https://doi.org/doi.org/10.1016/j.cophys.2020.05.002

Bridge, H., Hicks, S. L., Xie, J., Okell, T. W., Mannan, S., Alexander, I., Cowey, A., & Kennard, C. (2010). Visual activation of extra-striate cortex in the absence of v1 activation. Neuropsychologia, 48(14), 4148–54. https://doi.org/10.1016/j.neuropsychologia.2010.10.022

Bridge, H., Leopold, D. A., & Bourne, J. A. (2016). Adaptive pulvinar circuitry supports visual cognition. Trends Cogn Sci, 20(2), 146–157. https://doi.org/10.1016/j.tics.2015.10.003

Bridge, H., Thomas, O., Jbabdi, S., & Cowey, A. (2008). Changes in connectivity after visual cortical brain damage underlie altered visual function. Brain, 131(Pt 6), 1433–44. https://doi.org/10.1093/brain/awn063

Bridge, H., Thomas, O. M., Minini, L., Cavina-Pratesi, C., Milner, A. D., & Parker, A. J. (2013). Structural and functional changes across the visual cortex of a patient with visual form agnosia. J Neurosci, 33(31), 12779–91. https://doi.org/10.1523/JNEUROSCI.4853-12.2013

Briggs, F., & Usrey, W. M. (2011). Corticogeniculate feedback and visual processing in the primate. J Physiol, 589(Pt 1), 33–40. https://doi.org/10.1113/jphysiol.2010.193599

Britten, K. H., Shadlen, M. N., Newsome, W. T., & Movshon, J. A. (1992). The analysis of visual motion: A comparison of neuronal and psychophysical performance. J Neurosci, 12(12), 4745–65. https://doi.org/10.1523/JNEUROSCI.12-12-04745.1992

Brown, R., Lau, H., & LeDoux, J. E. (2019). Understanding the higher-order approach to consciousness. Trends Cogn Sci, 23(9), 754–768. https://doi.org/10.1016/j.tics.2019.06.009

Buonomano, D. V., & Merzenich, M. M. (1998). Cortical plasticity: From synapses to maps. Annu Rev Neurosci, 21, 149–86. https://doi.org/10.1146/annurev.neuro.21.1.149

Burra, N., Hervais-Adelman, A., Celeghin, A., de Gelder, B., & Pegna, A. J. (2017). Affective blindsight relies on low spatial frequencies. Neuropsychologia. https://doi.org/10.1016/j.neuropsychologia.2017.10.009

Burra, N., Hervais-Adelman, A., Kerzel, D., Tamietto, M., de Gelder, B., & Pegna, A. J. (2013). Amygdala activation for eye contact despite complete cortical blindness. J Neurosci, 33(25), 10483–9. https://doi.org/10.1523/JNEUROSCI.3994-12.2013

Burton, H. (2003). Visual cortex activity in early and late blind people. J Neurosci, 23(10), 4005–11. https://doi.org/10.1523/JNEUROSCI.23-10-04005.2003

Button, K. S., Ioannidis, J. P., Mokrysz, C., Nosek, B. A., Flint, J., Robinson, E. S., & Munafo, M. R. (2013). Power failure: Why small sample size undermines the reliability of neuroscience. Nat Rev Neurosci, 14(5), 365–76. https://doi.org/10.1038/nrn3475

Bzdok, D., Eickenberg, M., Grisel, O., Thirion, B., & Varoquaux, G. (2015). Semi-supervised factored logistic regression for high-dimensional neuroimaging data. NIPS.

Candia-Rivera, D. (2022). Brain-heart interactions in the neurobiology of consciousness. Curr Res Neurobiol, 3, 100050. https://doi.org/10.1016/j.crneur.2022.100050

Castaldi, E., Lunghi, C., & Morrone, M. C. (2020). Neuroplasticity in adult human visual cortex. Neurosci Biobehav Rev, 112, 542–552. https://doi.org/10.1016/j.neubiorev.2020.02.028

Cavanaugh, M. R., Barbot, A., Carrasco, M., & Huxlin, K. R. (2017). Feature-based attention potentiates recovery of fine direction discrimination in cortically blind patients. Neuropsychologia. https://doi.org/10.1016/j.neuropsychologia.2017.12.010

Cavanna, A. E., & Trimble, M. R. (2006). The precuneus: A review of its functional anatomy and behavioural correlates. Brain, 129(Pt 3), 564–83. https://doi.org/10.1093/brain/awl004

Celeghin, A., Bagnis, A., Diano, M., Mendez, C. A., Costa, T., & Tamietto, M. (2018). Functional neuroanatomy of blindsight revealed by activation likelihood estimation meta-analysis. Neuropsychologia. https://doi.org/10.1016/j.neuropsychologia.2018.06.007

Celeghin, A., de Gelder, B., & Tamietto, M. (2015). From affective blindsight to emotional consciousness. Conscious Cogn, 36, 414–25. https://doi.org/10.1016/j.concog.2015.05.007

Celeghin, A., Diano, M., de Gelder, B., Weiskrantz, L., Marzi, C. A., & Tamietto, M. (2017). Intact hemisphere and corpus callosum compensate for visuomotor functions after early visual cortex damage. Proc Natl Acad Sci U S A, 114(48), E10475–E10483. https://doi.org/10.1073/pnas.1714801114

Charest, I., Kievit, R. A., Schmitz, T. W., Deca, D., & Kriegeskorte, N. (2014). Unique semantic space in the brain of each beholder predicts perceived similarity. Proc Natl Acad Sci U S A, 111(40), 14565–70. https://doi.org/10.1073/pnas.1402594111

Chokron, S., Perez, C., Obadia, M., Gaudry, I., Laloum, L., & Gout, O. (2008). From blindsight to sight: Cognitive rehabilitation of visual field defects. Restorative Neurology Neuroscience, 26(4-5), 305–20.

Ciaramitaro, V. M., Todd, W. E., & Rosenquist, A. C. (1997). Disinhibition of the superior colliculus restores orienting to visual stimuli in the hemianopic field of the cat. J Comp Neurol, 387(4), 568–87.

Clarkson, A. N., Huang, B. S., Macisaac, S. E., Mody, I., & Carmichael, S. T. (2010). Reducing excessive gaba-mediated tonic inhibition promotes functional recovery after stroke. Nature, 468(7321), 305–9. https://doi.org/10.1038/nature09511

Collignon, O., Champoux, F., Voss, P., & Lepore, F. (2011). Sensory rehabilitation in the plastic brain. Prog Brain Res, 191, 211–31. https://doi.org/10.1016/B978-0-444-53752-2.00003-5

Collignon, O., Dormal, G., Albouy, G., Vandewalle, G., Voss, P., Phillips, C., & Lepore, F. (2013). Impact of blindness onset on the functional organization and the connectivity of the occipital cortex. Brain, 136(Pt 9), 2769–83. https://doi.org/10.1093/brain/awt176

Collignon, O., Voss, P., Lassonde, M., & Lepore, F. (2009). Cross-modal plasticity for the spatial processing of sounds in visually deprived subjects. Exp Brain Res, 192(3), 343–58. https://doi.org/10.1007/s00221-008-1553-z

Cowey, A. (2010). The blindsight saga. Experimental brain research, 200, 3–24. https://doi.org/10.1007/s00221-009-1914-2

Cox, R. W., Chen, G., Glen, D. R., Reynolds, R. C., & Taylor, P. A. (2017). Fmri clustering in afni: False-positive rates redux. Brain Connect, 7(3), 152–171. https://doi.org/10.1089/brain.2016.0475

Cox, R. W., & Hyde, J. S. (1997). Software tools for analysis and visualization of fmri data. NMR in Biomedicine, 10(4-5), 171–178. https://doi.org/10.1002/(SICI)1099-1492(199706/08)10:4/5<171::AID-NBM453>3.0.CO;2-L

Craig, A. D. (2009). How do you feel–now? the anterior insula and human awareness. Nat Rev Neurosci, 10(1), 59–70. https://doi.org/10.1038/nrn2555

Cramer, S. C. (2008). A window into the molecular basis of human brain plasticity. J Physiol, 586(23), 5601. https://doi.org/10.1113/jphysiol.2008.165183

Dale, A. M., Fischl, B., & Sereno, M. I. (1999). Cortical surface-based analysis: I. segmentation and surface reconstruction. NeuroImage, 9(2), 179–194. https://doi.org/10.1006/nimg.1998.0395

Danckert, J., & Rossetti, Y. (2005). Blindsight in action: What can the different sub-types of blindsight tell us about the control of visually guided actions? Neuroscience Biobehavioral Reviews, 29, 1035–1046. https://doi.org/10.1016/j.neubiorev.2005.02.001

Danziger, S., Fendrich, R., & Rafal, R. D. (1997). Inhibitory tagging of locations in the blind field of hemianopic patients. Conscious Cogn, 6(2-3), 291–307. https://doi.org/10.1006/ccog.1997.0312

Das, A., Tadin, D., & Huxlin, K. R. (2014). Beyond blindsight: Properties of visual relearning in cortically blind fields. The Journal of neuroscience, Society for Neuroscience, 34, 11652–64. https://doi.org/10.1523/JNEUROSCI.1076-14.2014

Davatzikos, C. (2019). Machine learning in neuroimaging: Progress and challenges. Neuroimage, 197, 652–656. https://doi.org/10.1016/j.neuroimage.2018.10.003

DeAngelis, G. C., Cumming, B. G., & Newsome, W. T. (1998). Cortical area mt and the perception of stereoscopic depth. Nature, 394(6694), 677–80. https://doi.org/10.1038/29299

de Gelder, B., & Hadjikhani, N. (2006). Non-conscious recognition of emotional body language. Neuroreport, 17(6), 583–6.

de Gelder, B., Tamietto, M., Pegna, A. J., & Van den Stock, J. (2015). Visual imagery influences brain responses to visual stimulation in bilateral cortical blindness. Cortex, 72, 15–26. https://doi.org/10.1016/j.cortex.2014.11.009

de Gelder, B., Tamietto, M., van Boxtel, G., Goebel, R., Sahraie, A., van den Stock, J., Stienen, B. M., Weiskrantz, L., & Pegna, A. (2008). Intact navigation skills after bilateral loss of striate cortex. Curr Biol, 18(24), R1128–9. https://doi.org/10.1016/j.cub.2008.11.002

de Gelder, B., Vroomen, J., Pourtois, G., & Weiskrantz, L. (1999). Non-conscious recognition of affect in the absence of striate cortex. Neuroreport, 10(18), 3759–63.

de Graaf, T. A., Hsieh, P. J., & Sack, A. T. (2012). The 'correlates' in neural correlates of consciousness. Neurosci Biobehav Rev, 36(1), 191–7. https://doi.org/10.1016/j.neubiorev.2011.05.012

de Haan, E. H., & Cowey, A. (2011). On the usefulness of 'what' and 'where' pathways in vision. Trends Cogn Sci, 15(10), 460–6. https://doi.org/10.1016/j.tics.2011.08.005

de Haan, G. A., Heutink, J., Melis-Dankers, B. J., Tucha, O., & Brouwer, W. H. (2014). Spontaneous recovery and treatment effects in patients with homonymous visual field defects: A meta-analysis of existing literature in terms of the icf framework. Surv Ophthalmol, 59(1), 77–96. https://doi.org/10.1016/j.survophthal.2013.02.006

Dehaene, S., & Changeux, J. P. (2011). Experimental and theoretical approaches to conscious processing. Neuron, 70(2), 200–27. https://doi.org/10.1016/j.neuron.2011.03.018

Dehaene, S., Changeux, J. P., Naccache, L., Sackur, J., & Sergent, C. (2006). Conscious, preconscious, and subliminal processing: A testable taxonomy. Trends in Cognitive Sciences, 10(5), 204–11. https://doi.org/10.1016/j.tics.2006.03.007

Dehaene, S., & Naccache, L. (2001). Towards a cognitive neuroscience of consciousness: Basic evidence and a workspace framework. Cognition, 79(1-2), 1–37. https://doi.org/doi.org/10.1016/S0010-0277(00)00123-2

Dehaene, S., Piazza, M., Pinel, P., & Cohen, L. (2003). Three parietal circuits for number processing. Cogn Neuropsychol, 20(3), 487–506. https://doi.org/10.1080/02643290244000239

Deifelt Streese, C., & Tranel, D. (2021). Combined lesion-deficit and fmri approaches in single-case studies: Unique contributions to cognitive neuroscience. Curr Opin Behav Sci, 40, 58–63. https://doi.org/10.1016/j.cobeha.2021.01.004

de Lange, F. P., Heilbron, M., & Kok, P. (2018). How do expectations shape perception? Trends Cogn Sci, 22(9), 764–779. https://doi.org/10.1016/j.tics.2018.06.002

Desimone, R., Albright, T. D., Gross, C. G., & Bruce, C. (1984). Stimulus-selective properties of inferior temporal neurons in the macaque. J Neurosci, 4(8), 2051–62. https://doi.org/10.1523/JNEUROSCI.04-08-02051.1984

Dijkstra, N., van Gaal, S., Geerligs, L., Bosch, S. E., & van Gerven, M. A. J. (2021). No evidence for neural overlap between unconsciously processed and imagined stimuli. eNeuro, 8(5). https://doi.org/10.1523/ENEURO.0228-21.2021

DiNuzzo, M., Mascali, D., Moraschi, M., Bussu, G., Maugeri, L., Mangini, F., Fratini, M., & Giove, F. (2019). Brain networks underlying eye's pupil dynamics. Front Neurosci, 13, 965. https://doi.org/10.3389/fnins.2019.00965

Downing, P. E., Jiang, Y., Shuman, M., & Kanwisher, N. (2001). A cortical area selective for visual processing of the human body. Science, 293(5539), 2470–3. https://doi.org/10.1126/science.1063414

Dreher, B., Djavadian, R. L., Turlejski, K. J., & Wang, C. (1996). Areas pmls and 21a of cat visual cortex are not only functionally but also hodologically distinct. Prog Brain Res, 112, 251–76. https://doi.org/10.1016/s0079-6123(08)63334-8

Dubner, R., & Zeki, S. M. (1971). Response properties and receptive fields of cells in an anatomically defined region of the superior temporal sulcus in the monkey. Brain Res, 35(2), 528–32. https://doi.org/10.1016/0006-8993(71)90494-x

Duffy, C. J., & Wurtz, R. H. (1991). Sensitivity of mst neurons to optic flow stimuli. i. a continuum of response selectivity to large-field stimuli. J Neurophysiol, 65(6), 1329–45. https://doi.org/10.1152/jn.1991.65.6.1329

Duffy, C. J., & Wurtz, R. H. (1995). Response of monkey mst neurons to optic flow stimuli with shifted centers of motion. J Neurosci, 15(7 Pt 2), 5192–208. https://doi.org/10.1523/JNEUROSCI.15-07-05192.1995

Dukelow, S. P., DeSouza, J. F., Culham, J. C., van den Berg, A. V., Menon, R. S., & Vilis, T. (2001). Distinguishing subregions of the human mt+ complex using visual fields and pursuit eye movements. J Neurophysiol, 86(4), 1991–2000. https://doi.org/10.1152/jn.2001.86.4.1991

Duncan, J. (2010). The multiple-demand (md) system of the primate brain: Mental programs for intelligent behaviour. Trends Cogn Sci, 14(4), 172–9. https://doi.org/10.1016/j.tics.2010.01.004

Duncan, J., & Owen, A. M. (2000). Common regions of the human frontal lobe recruited by diverse cognitive demands. Trends Neurosci, 23(10), 475–83. https://doi.org/10.1016/s0166-2236(00)01633-7

Dundon, N. M., Bertini, C., Ladavas, E., Sabel, B. A., & Gall, C. (2015a). Visual rehabilitation: Visual scanning, multisensory stimulation and vision restoration trainings. Front Behav Neurosci, 9, 192. https://doi.org/10.3389/fnbeh.2015.00192

Dundon, N. M., Ladavas, E., Maier, M. E., & Bertini, C. (2015b). Multisensory stimulation in hemianopic patients boosts orienting responses to the hemianopic field and reduces attentional resources to the intact field. Restor Neurol Neurosci, 33(4), 405–19. https://doi.org/10.3233/RNN-140457

Dupont, P., Orban, G. A., De Bruyn, B., Verbruggen, A., & Mortelmans, L. (1994). Many areas in the human brain respond to visual motion. J Neurophysiol, 72(3), 1420–4. https://doi.org/10.1152/jn.1994.72.3.1420

Eickhoff, S. B., Bzdok, D., Laird, A. R., Kurth, F., & Fox, P. T. (2012). Activation likelihood estimation meta-analysis revisited. Neuroimage, 59(3), 2349–61. https://doi.org/10.1016/j.neuroimage.2011.09.017

Eickhoff, S. B., Laird, A. R., Grefkes, C., Wang, L. E., Zilles, K., & Fox, P. T. (2009). Coordinate-based activation likelihood estimation meta-analysis of neuroimaging data: A random-effects approach based on empirical estimates of spatial uncertainty. Hum Brain Mapp, 30(9), 2907–26. https://doi.org/10.1002/hbm.20718

Eickhoff, S. B., Nichols, T. E., Laird, A. R., Hoffstaedter, F., Amunts, K., Fox, P. T., Bzdok, D., & Eickhoff, C. R. (2016). Behavior, sensitivity, and power of activation likelihood estimation characterized by massive empirical simulation. Neuroimage, 137, 70–85. https://doi.org/10.1016/j.neuroimage.2016.04.072

Eklund, A., Nichols, T. E., & Knutsson, H. (2016). Cluster failure: Why fmri inferences for spatial extent have inflated false-positive rates. Proc Natl Acad Sci U S A, 113(28), 7900–5. https://doi.org/10.1073/pnas.1602413113

Engstrom, M., Karlsson, T., Landtblom, A. M., & Craig, A. D. (2014). Evidence of conjoint activation of the anterior insular and cingulate cortices during effortful tasks. Front Hum Neurosci, 8, 1071. https://doi.org/10.3389/fnhum.2014.01071

Epstein, R., & Kanwisher, N. (1998). A cortical representation of the local visual environment. Nature, 392(6676), 598–601. https://doi.org/10.1038/33402

Eriksson, J., Larsson, A., Ahlstrom, K. R., & Nyberg, L. (2007). Similar frontal and distinct posterior cortical regions mediate visual and auditory perceptual awareness. Cerebral Cortex, 17(4), 760–765.

Esteban, O., Birman, D., Schaer, M., Koyejo, O. O., Poldrack, R. A., & Gorgolewski, K. J. (2017). Mriqc: Advancing the automatic prediction of image quality in mri from unseen sites. PLoS One, 12(9), e0184661. https://doi.org/10.1371/journal.pone.0184661

Esteban, O., Markiewicz, C. J., Blair, R. W., Moodie, C. A., Isik, A. I., Erramuzpe, A., Kent, J. D., Goncalves, M., DuPre, E., Snyder, M., Oya, H., Ghosh, S. S., Wright, J., Durnez, J., Poldrack, R. A., & Gorgolewski, K. J. (2019). Fmriprep: A robust preprocessing pipeline for functional mri. Nat Methods, 16(1), 111–116. https://doi.org/10.1038/s41592-018-0235-4

Fang, F., & He, S. (2005). Cortical responses to invisible objects in the human dorsal and ventral pathways. Nat Neurosci, 8(10), 1380–5. https://doi.org/10.1038/nn1537

Fedorenko, E., Duncan, J., & Kanwisher, N. (2013). Broad domain generality in focal regions of frontal and parietal cortex. Proc Natl Acad Sci U S A, 110(41), 16616–21. https://doi.org/10.1073/pnas.1315235110

Felleman, D. J., & Van Essen, D. C. (1991). Distributed hierarchical processing in the primate cerebral cortex. Cereb Cortex, 1(1), 1–47. https://doi.org/10.1093/cercor/1.1.1-a

Filipovych, R., Resnick, S. M., & Davatzikos, C. (2011). Semi-supervised cluster analysis of imaging data. Neuroimage, 54(3), 2185–97. https://doi.org/10.1016/j.neuroimage.2010.09.074

Flounders, M. W., Gonzalez-Garcia, C., Hardstone, R., & He, B. J. (2019). Neural dynamics of visual ambiguity resolution by perceptual prior. Elife, 8. https://doi.org/10.7554/eLife.41861

Fonov, V., Evans, A., McKinstry, R., Almli, C., & Collins, D. (2009). Unbiased nonlinear average age-appropriate brain templates from birth to adulthood. NeuroImage, 47, Supplement 1, S102. https://doi.org/10.1016/S1053-8119(09)70884-5

Francis, G. (2000). Quantitative theories of metacontrast masking. Psychol Rev, 107(4), 768–85. https://doi.org/10.1037/0033-295x.107.4.768

Frassinetti, F., Bolognini, N., Bottari, D., Bonora, A., & Ladavas, E. (2005). Audiovisual integration in patients with visual deficit. J Cogn Neurosci, 17(9), 1442–52. https://doi.org/10.1162/0898929054985446

Furman, M. (2014). Visual network in neuronal networks in brain function, cns disorders, and therapeutics. Academic Press. https://doi.org/doi.org/10.1016/B978-0-12-415804-7.00019-8

Gall, C., Silvennoinen, K., Granata, G., de Rossi, F., Vecchio, F., Brosel, D., Bola, M., Sailer, M., Waleszczyk, W. J., Rossini, P. M., Tatlisumak, T., & Sabel, B. A. (2015). Non-invasive electric current stimulation for restoration of vision after unilateral occipital stroke. Contemp Clin Trials, 43, 231–6. https://doi.org/10.1016/j.cct.2015.06.005

Gaymard, B., & Pierrot-Deseilligny, C. (1999). Neurology of saccades and smooth pursuit. Curr Opin Neurol, 12(1), 13–9.

Georgy, L., Celeghin, A., Marzi, C. A., Tamietto, M., & Ptito, A. (2016). The superior colliculus is sensitive to gestalt-like stimulus configuration in hemispherectomy patients. Cortex, 81, 151–61. https://doi.org/10.1016/j.cortex.2016.04.018

Gerbella, M., Caruana, F., & Rizzolatti, G. (2017). Pathways for smiling, disgust and fear recognition in blindsight patients. Neuropsychologia. https://doi.org/10.1016/j.neuropsychologia.2017.08.028

Ghorbani, S., Mahdaviani, K., Thaler, A., Kording, K., Cook, D. J., Blohm, G., & Troje, N. F. (2021). Movi: A large multi-purpose human motion and video dataset. PLoS One, 16(6), e0253157. https://doi.org/10.1371/journal.pone.0253157

Giese, M. A., & Poggio, T. (2003). Neural mechanisms for the recognition of biological movements. Nat Rev Neurosci, 4(3), 179–92. https://doi.org/10.1038/nrn1057

Gilbert, C. D., & Li, W. (2013). Top-down influences on visual processing. Nat Rev Neurosci, 14(5), 350–63. https://doi.org/10.1038/nrn3476

Gillebert, C. R., Mantini, D., Thijs, V., Sunaert, S., Dupont, P., & Vandenberghe, R. (2011). Lesion evidence for the critical role of the intraparietal sulcus in spatial attention. Brain, 134(Pt 6), 1694–709. https://doi.org/10.1093/brain/awr085

Girard, P., Salin, P. A., & Bullier, J. (1992). Response selectivity of neurons in area mt of the macaque monkey during reversible inactivation of area v1. J Neurophysiol, 67(6), 1437–46. https://doi.org/10.1152/jn.1992.67.6.1437

Glover, G. H. (1999). Deconvolution of impulse response in event-related bold fmri. Neuroimage, 9(4), 416–29.

Goebel, R., Muckli, L., Zanella, F. E., Singer, W., & Stoerig, P. (2001). Sustained extrastriate cortical activation without visual awareness revealed by fmri studies of hemianopic patients. Vision Res, 41(10-11), 1459–74. https://doi.org/10.1016/s0042-6989(01)00069-4

Goodale, M. A. (2008). Action without perception in human vision. Cogn Neuropsychol, 25(7-8), 891–919. https://doi.org/10.1080/02643290801961984

Goodale, M. A., & Milner, A. D. (1992). Separate visual pathways for perception and action. Trends Neurosci, 15(1), 20–5.

Goodwin, D. (2014). Homonymous hemianopia : Challenges and solutions, 1919–1927.

Gorgolewski, K. J., Auer, T., Calhoun, V. D., Craddock, R. C., Das, S., Duff, E. P., Flandin, G., Ghosh, S. S., Glatard, T., Halchenko, Y. O., Handwerker, D. A., Hanke, M., Keator, D., Li, X., Michael, Z., Maumet, C., Nichols, B. N., Nichols, T. E., Pellman, J., ... Poldrack, R. A. (2016). The brain imaging data structure, a format for organizing and describing outputs of neuroimaging experiments. Sci Data, 3, 160044. https://doi.org/10.1038/sdata.2016.44

Gorgolewski, K. J., Varoquaux, G., Rivera, G., Schwarz, Y., Ghosh, S. S., Maumet, C., Sochat, V. V., Nichols, T. E., Poldrack, R. A., Poline, J. B., Yarkoni, T., & Margulies, D. S. (2015). Neurovault.org: A web-based repository for collecting and sharing unthresholded statistical maps of the human brain. Front Neuroinform, 9, 8. https://doi.org/10.3389/fninf.2015.00008

Grasso, P. A., Pietrelli, M., Zanon, M., Ladavas, E., & Bertini, C. (2018). Alpha oscillations reveal implicit visual processing of motion in hemianopia. Cortex. https://doi.org/10.1016/j.cortex.2018.08.009

Grefkes, C., Nowak, D. A., Eickhoff, S. B., Dafotakis, M., Kust, J., Karbe, H., & Fink, G. R. (2008). Cortical connectivity after subcortical stroke assessed with functional magnetic resonance imaging. Ann Neurol, 63(2), 236–46. https://doi.org/10.1002/ana.21228

Greve, D. N., & Fischl, B. (2009). Accurate and robust brain image alignment using boundary-based registration. NeuroImage, 48(1), 63–72. https://doi.org/10.1016/j.neuroimage.2009.06.060

Grill-Spector, K., Kourtzi, Z., & Kanwisher, N. (2001). The lateral occipital complex and its role in object recognition. Vision Res, 41(10-11), 1409–22. https://doi.org/10.1016/s0042-6989(01)00073-6

Gross, C. G. (1991). Contribution of striate cortex and the superior colliculus to visual function in area mt, the superior temporal polysensory area and the inferior temporal cortex. Neuropsychologia, 29(6), 497–515. https://doi.org/10.1016/0028-3932(91)90007-u

Guipponi, O., Odouard, S., Pinede, S., Wardak, C., & Ben Hamed, S. (2015). Fmri cortical correlates of spontaneous eye blinks in the nonhuman primate. Cereb Cortex, 25(9), 2333–45. https://doi.org/10.1093/cercor/bhu038

Gusnard, D. A., & Raichle, M. E. (2001). Searching for a baseline: Functional imaging and the resting human brain. Nat Rev Neurosci, 2(10), 685–94. https://doi.org/10.1038/35094500

Hadid, V., & Lepore, F. (2017). From cortical blindness to conscious visual perception: Theories on neuronal networks and visual training strategies. Frontiers in Systems Neuroscience, 11 (no pagination).

Hagan, M. A., Chaplin, T. A., Huxlin, K. R., Rosa, M. G. P., & Lui, L. L. (2020). Altered sensitivity to motion of area mt neurons following long-term v1 lesions. Cereb Cortex, 30(2), 451–464. https://doi.org/10.1093/cercor/bhz096

Hagberg, G. E., Zito, G., Patria, F., & Sanes, J. N. (2001). Improved detection of event-related functional mri signals using probability functions. Neuroimage, 14(5), 1193–205. https://doi.org/10.1006/nimg.2001.0880

Hagler, J., D. J., & Sereno, M. I. (2006). Spatial maps in frontal and prefrontal cortex. Neuroimage, 29(2), 567–77. https://doi.org/10.1016/j.neuroimage.2005.08.058

Hasson, U., Harel, M., Levy, I., & Malach, R. (2003). Large-scale mirror-symmetry organization of human occipito-temporal object areas. Neuron, 37(6), 1027–41. https://doi.org/10.1016/s0896-6273(03)00144-2

Heeks, F., & Azzopardi, P. (2015). Thresholds for detection and awareness of masked facial stimuli. Conscious Cogn, 32, 68–78. https://doi.org/10.1016/j.concog.2014.09.009

Hendrickson, A. E., Wilson, J. R., & Ogren, M. P. (1978). The neuroanatomical organization of pathways between the dorsal lateral geniculate nucleus and visual cortex in old world and new world primates. J Comp Neurol, 182(1), 123–36. https://doi.org/10.1002/cne.901820108

Hervais-Adelman, A., Legrand, L. B., Zhan, M., Tamietto, M., de Gelder, B., & Pegna, A. J. (2015). Looming sensitive cortical regions without v1 input: Evidence from a patient with bilateral cortical blindness. Front Integr Neurosci, 9, 51. https://doi.org/10.3389/fnint.2015.00051

Heuninckx, S., Wenderoth, N., & Swinnen, S. P. (2008). Systems neuroplasticity in the aging brain: Recruiting additional neural resources for successful motor performance in elderly persons. J Neurosci, 28(1), 91–9. https://doi.org/10.1523/JNEUROSCI.3300-07.2008

Hirai, M., & Senju, A. (2020). The two-process theory of biological motion processing. Neurosci Biobehav Rev, 111, 114–124. https://doi.org/10.1016/j.neubiorev.2020.01.010

Holmes, G. (1918). Disturbances of vision by cerebral lesions. Br J Ophthalmol, 2(7), 353–84. https://doi.org/10.1136/bjo.2.7.353

Hubel, D. H., & Wiesel, T. N. (1959). Receptive fields of single neurones in the cat's striate cortex. J Physiol, 148(3), 574–91. https://doi.org/10.1113/jphysiol.1959.sp006308

Hubel, D. H., & Wiesel, T. N. (1970). Stereoscopic vision in macaque monkey. cells sensitive to binocular depth in area 18 of the macaque monkey cortex. Nature, 225(5227), 41–2.

Hubel, D. H., & Wiesel, T. N. (1972). Laminar and columnar distribution of geniculo-cortical fibers in the macaque monkey. J Comp Neurol, 146(4), 421–50. https://doi.org/10.1002/cne.901460402

Huk, A. C., Dougherty, R. F., & Heeger, D. J. (2002). Retinotopy and functional subdivision of human areas mt and mst. J Neurosci, 22(16), 7195–205. https://doi.org/10.1523/JNEUROSCI.22-16-07195.2002

Humphreys, G. F., Lambon Ralph, M. A., & Simons, J. S. (2021). A unifying account of angular gyrus contributions to episodic and semantic cognition. Trends Neurosci, 44(6), 452–463. https://doi.org/10.1016/j.tins.2021.01.006

Hutchinson, B. T. (2019). Toward a theory of consciousness: A review of the neural correlates of inattentional blindness. Neuroscience and Biobehavioral Reviews, 104, 87–99. https://doi.org/10.1016/j.neubiorev.2019.06.003

Huxlin, K. R. (2008). Perceptual plasticity in damaged adult visual systems. Vision Research, 48, 2154–2166. https://doi.org/10.1016/j.visres.2008.05.022

Imamoglu, F., Kahnt, T., Koch, C., & Haynes, J.-D. (2012). Changes in functional connectivity support conscious object recognition. NeuroImage, 63(4), 1909–1917.

Jackson, S. R. (1999). Pathological perceptual completion in hemianopia extends to the control of reach-to-grasp movements. Neuroreport, 10(12), 2461–6.

James, T. W., Culham, J., Humphrey, G. K., Milner, A. D., & Goodale, M. A. (2003). Ventral occipital lesions impair object recognition but not object-directed grasping: An fmri study. Brain, 126(Pt 11), 2463–75. https://doi.org/10.1093/brain/awg248

Jenkinson, M., Beckmann, C. F., Behrens, T. E., Woolrich, M. W., & Smith, S. M. (2012). Fsl. Neuroimage, 62(2), 782–90. https://doi.org/10.1016/j.neuroimage.2011.09.015

Jenkinson, M., Bannister, P., Brady, M., & Smith, S. (2002). Improved optimization for the robust and accurate linear registration and motion correction of brain images. NeuroImage, 17(2), 825–841. https://doi.org/10.1006/nimg.2002.1132

Jiang, H., Stein, B. E., & McHaffie, J. G. (2015). Multisensory training reverses midbrain lesion-induced changes and ameliorates haemianopia. Nature communications, 6, 7263. https://doi.org/10.1038/ncomms8263

Jiang, Y., & He, S. (2006). Cortical responses to invisible faces: Dissociating subsystems for facial-information processing. Curr Biol, 16(20), 2023–9. https://doi.org/10.1016/j.cub.2006.08.084

Johansson, G. (1973). Visual perception of biological motion and a model for its analysis. Perception Psychophysics, 14, 201–211. https://doi.org/https://doi.org/10.3758/BF03212378

Kamitani, Y., & Tong, F. (2006). Decoding seen and attended motion directions from activity in the human visual cortex. Curr Biol, 16(11), 1096–102. https://doi.org/10.1016/j.cub.2006.04.003

Kang, Y. H. R., Petzschner, F. H., Wolpert, D. M., & Shadlen, M. N. (2017). Piercing of consciousness as a threshold-crossing operation. Curr Biol, 27(15), 2285–2295 e6. https://doi.org/10.1016/j.cub.2017.06.047

Kanwisher, N., McDermott, J., & Chun, M. M. (1997). The fusiform face area: A module in human extrastriate cortex specialized for face perception. J Neurosci, 17(11), 4302–11. https://doi.org/10.1523/JNEUROSCI.17-11-04302.1997

Kentridge, R. W., Heywood, C. A., & Weiskrantz, L. (2007). Color contrast processing in human striate cortex. Proc Natl Acad Sci U S A, 104(38), 15129–31. https://doi.org/10.1073/pnas.0706603104

Kim, C. Y., & Blake, R. (2005). Psychophysical magic: Rendering the visible 'invisible'. Trends Cogn Sci, 9(8), 381–8. https://doi.org/10.1016/j.tics.2005.06.012

Kim, H. (2019). Neural correlates of explicit and implicit memory at encoding and retrieval: A unified framework and meta-analysis of functional neuroimaging studies. Biol Psychol, 145, 96–111. https://doi.org/10.1016/j.biopsycho.2019.04.006

King, S. M., & Cowey, A. (1992). Defensive responses to looming visual stimuli in monkeys with unilateral striate cortex ablation. Neuropsychologia, 30(11), 1017–24. https://doi.org/10.1016/0028-3932(92)90053-o

Kinoshita, M., Kato, R., Isa, K., Kobayashi, K., Kobayashi, K., Onoe, H., & Isa, T. (2019). Dissecting the circuit for blindsight to reveal the critical role of pulvinar and superior colliculus. Nat Commun, 10(1), 135. https://doi.org/10.1038/s41467-018-08058-0

Klein, A., Ghosh, S. S., Bao, F. S., Giard, J., Häme, Y., Stavsky, E., Lee, N., Rossa, B., Reuter, M., Neto, E. C., & Keshavan, A. (2017). Mindboggling morphometry of human brains. PLOS Computational Biology, 13(2), e1005350. https://doi.org/10.1371/journal.pcbi.1005350

Kleinschmidt, A., Buchel, C., Zeki, S., & Frackowiak, R. S. J. (1998). Human brain activity during spontaneously reversing perception of ambiguous figures. Proceedings of the Royal Society B: Biological Sciences, 265(1413), 2427–2433. https://doi.org/10.1098/rspb.1998.0594

Koch, C. (2004). The quest for consciousness: A neurobiological approach. Co: Roberts; Company.

Koch, C., Massimini, M., Boly, M., & Tononi, G. (2016). Neural correlates of consciousness: Progress and problems. Nature Reviews Neuroscience, 17, 307–321. https://doi.org/10.1038/nrn.2016.22

Koivisto, M., & Revonsuo, A. (2010). Event-related brain potential correlates of visual awareness. Neurosci Biobehav Rev, 34(6), 922–34. https://doi.org/10.1016/j.neubiorev.2009.12.002

Kolster, H., Peeters, R., & Orban, G. A. (2010). The retinotopic organization of the human middle temporal area mt/v5 and its cortical neighbors. J Neurosci, 30(29), 9801–20. https://doi.org/10.1523/JNEUROSCI.2069-10.2010

Komatsu, H., & Wurtz, R. H. (1988b). Relation of cortical areas mt and mst to pursuit eye movements. i. localization and visual properties of neurons. J Neurophysiol, 60(2), 580–603. https://doi.org/10.1152/jn.1988.60.2.580

Kouider, S. (2009). Neurobiological theories of consciousness.

Kouider, S., de Gardelle, V., Sackur, J., & Dupoux, E. (2010). How rich is consciousness? the partial awareness hypothesis. Trends Cogn Sci, 14(7), 301–7. https://doi.org/10.1016/j.tics.2010.04.006

Koutstaal, W., Wagner, A. D., Rotte, M., Maril, A., Buckner, R. L., & Schacter, D. L. (2001). Perceptual specificity in visual object priming: Functional magnetic resonance imaging evidence for a laterality difference in fusiform cortex. Neuropsychologia, 39(2), 184–199. https://doi.org/10.1016/s0028-3932(00)00087-7

Kranczioch, C., Debener, S., Schwarzbach, J., Goebel, R., & Engel, A. K. (2005). Neural correlates of conscious perception in the attentional blink. Neuroimage, 24(3), 704–714. https://doi.org/10.1016/j.neuroimage.2004.09.024

Krause, M. R., & Pack, C. C. (2014). Contextual modulation and stimulus selectivity in extrastriate cortex. Vision Res, 104, 36–46. https://doi.org/10.1016/j.visres.2014.10.006

Kronemer, S. I., Aksen, M., Ding, J. Z., Ryu, J. H., Xin, Q., Ding, Z., Prince, J. S., Kwon, H., Khalaf, A., Forman, S., Jin, D. S., Wang, K., Chen, K., Hu, C., Agarwal, A., Saberski, E., Wafa, S. M. A., Morgan, O. P., Wu, J., ... Blumenfeld, H. (2022). Human visual consciousness involves large scale cortical and subcortical networks independent of task report and eye movement activity. Nat Commun, 13(1), 7342. https://doi.org/10.1038/s41467-022-35117-4

Ladd, G. T. (1894). Direct control of the retinal field. Psychological Review, 1(4).

Laird, A. R., Eickhoff, S. B., Li, K., Robin, D. A., Glahn, D. C., & Fox, P. T. (2009). Investigating the functional heterogeneity of the default mode network using coordinate-based meta-analytic modeling. J Neurosci, 29(46), 14496–505. https://doi.org/10.1523/JNEUROSCI.4004-09.2009

Lam, N., & Leat, S. J. (2013). Barriers to accessing low-vision care: The patient's perspective. Can J Ophthalmol, 48(6), 458–62. https://doi.org/10.1016/j.jcjo.2013.02.014

Lamme, V. A. (2003). Why visual attention and awareness are different. Trends Cogn Sci, 7(1), 12–18. https://doi.org/10.1016/s1364-6613(02)00013-x

Lamme, V. A. (2010). How neuroscience will change our view on consciousness. Cogn Neurosci, 1(3), 204–20. https://doi.org/10.1080/17588921003731586

Lamme, V. A. (2006a). Towards a true neural stance on consciousness. Trends Cogn Sci, 10(11), 494–501. https://doi.org/10.1016/j.tics.2006.09.001

Lamme, V. A. F. (2018). Challenges for theories of consciousness: Seeing or knowing, the missing ingredient and how to deal with panpsychism. Philos Trans R Soc Lond B Biol Sci, 373(1755). https://doi.org/10.1098/rstb.2017.0344

Lamme, V. A. F. (2006b). Zap! magnetic tricks on conscious and unconscious vision. Trends in Cognitive Sciences, 10(5), 193–195. https://doi.org/10.1016/j.tics.2006.03.002

Lancaster, J. L., Tordesillas-Gutierrez, D., Martinez, M., Salinas, F., Evans, A., Zilles, K., Mazziotta, J. C., & Fox, P. T. (2007). Bias between mni and talairach coordinates analyzed using the icbm-152 brain template. Hum Brain Mapp, 28(11), 1194–205. https://doi.org/10.1002/hbm.20345

Lanczos, C. (1964). Evaluation of noisy data. SIAM Journal on Numerical Analysis, 1(1), 76–85. https://doi.org/10.1137/0701007

Lau, H., & Rosenthal, D. (2011). Empirical support for higher-order theories of conscious awareness. Trends Cogn Sci, 15(8), 365–73. https://doi.org/10.1016/j.tics.2011.05.009

Laureys, S. (2005). The neural correlate of (un)awareness: Lessons from the vegetative state. Trends Cogn Sci, 9(12), 556–9. https://doi.org/10.1016/j.tics.2005.10.010

Lazar, N. (2008). The statistical analysis of functional mri data.

Leat, S. J. (2016). A proposed model for integrated low-vision rehabilitation services in canada. Optom Vis Sci, 93(1), 77–84. https://doi.org/10.1097/OPX.0000000000000750

Lee, M. H., Smyser, C. D., & Shimony, J. S. (2013). Resting-state fmri: A review of methods and clinical applications. AJNR Am J Neuroradiol, 34(10), 1866–72. https://doi.org/10.3174/ajnr.A3263

Leh, S. E., Chakravarty, M. M., & Ptito, A. (2008). The connectivity of the human pulvinar: A diffusion tensor imaging tractography study. Int J Biomed Imaging, 2008, 789539. https://doi.org/10.1155/2008/789539

Leh, S. E., Johansen-Berg, H., & Ptito, A. (2006). Unconscious vision: New insights into the neuronal correlate of blindsight using diffusion tractography. Brain, 129(Pt 7), 1822–32. https://doi.org/10.1093/brain/awl111

Leh, S. E., Ptito, A., Schonwiesner, M., Chakravarty, M. M., & Mullen, K. T. (2010). Blindsight mediated by an s-cone-independent collicular pathway: An fmri study in hemispherectomized subjects. Journal of Cognitive Neuroscience, 22(4), 670–682. https://doi.org/10.1162/jocn.2009.21217

Leo, F., Bolognini, N., Passamonti, C., Stein, B. E., & Ladavas, E. (2008). Cross-modal localization in hemianopia: New insights on multisensory integration. Brain, 131(Pt 3), 855–65. https://doi.org/10.1093/brain/awn003

Leopold, D. A. (2012). Primary visual cortex: Awareness and blindsight. Annu Rev Neurosci, 35, 91–109. https://doi.org/10.1146/annurev-neuro-062111-150356

Levinson, M., Podvalny, E., Baete, S. H., & He, B. J. (2021). Cortical and subcortical signatures of conscious object recognition. Nat Commun, 12(1), 2930. https://doi.org/10.1038/s41467-021-23266-x

Li, S., Overman, J. J., Katsman, D., Kozlov, S. V., Donnelly, C. J., Twiss, J. L., Giger, R. J., Coppola, G., Geschwind, D. H., & Carmichael, S. T. (2010). An age-related

sprouting transcriptome provides molecular control of axonal sprouting after stroke. Nature Neuroscience, 13, 1496. https://doi.org/10.1038/nn.2674https://www.nature.com/articles/nn.2674#supplementary-information

Lindh, D., Sligte, I. G., Assecondi, S., Shapiro, K. L., & Charest, I. (2019). Conscious perception of natural images is constrained by category-related visual features. Nat Commun, 10(1), 4106. https://doi.org/10.1038/s41467-019-12135-3

Lindquist, M. (2008). The statistical analysis of fmri data. Statistical Science, 23, 439–464.

Liu, D., Li, S., Ren, L., Li, X., & Wang, Z. (2022). The superior colliculus/lateral posterior thalamic nuclei in mice rapidly transmit fear visual information through the theta frequency band. Neuroscience, 496, 230–240. https://doi.org/10.1016/j.neuroscience.2022.06.021

Liu, L. D., & Pack, C. C. (2017). The contribution of area mt to visual motion perception depends on training. Neuron, 95(2), 436–446 e3. https://doi.org/10.1016/j.neuron.2017.06.024

Liu, Y. J., Wang, Q., & Li, B. (2011). Neuronal responses to looming objects in the superior colliculus of the cat. Brain Behav Evol, 77(3), 193–205. https://doi.org/10.1159/000327045

Lotze, M., Markert, J., Sauseng, P., Hoppe, J., Plewnia, C., & Gerloff, C. (2006). The role of multiple contralesional motor areas for complex hand movements after internal capsular lesion. J Neurosci, 26(22), 6096–102. https://doi.org/10.1523/JNEUROSCI.4564-05.2006

Lumer, E. D., Friston, K. J., & Rees, G. (1998). Neural correlates of perceptual rivalry in the human brain. Science, 280(5371), 1930–4. https://doi.org/10.1126/science.280.5371.1930

Lutkenhoff, E. S., Rosenberg, M., Chiang, J., Zhang, K., Pickard, J. D., Owen, A. M., & Monti, M. M. (2014). Optimized brain extraction for pathological brains (optibet). PLoS One, 9(12), e115551. https://doi.org/10.1371/journal.pone.0115551

MacLean, M. W., Hadid, V., Spreng, R. N., & Lepore, F. (2023). Revealing robust neural correlates of conscious and unconscious visual processing: Activation likelihood

estimation meta-analyses. Neuroimage, 273, 120088. https://doi.org/10.1016/j.neuroimage.2023.120088

Maki-Marttunen, V. (2021). Pupil-based states of brain integration across cognitive states. Neuroscience, 471, 61–71. https://doi.org/10.1016/j.neuroscience.2021.07.016

Malikovic, A., Amunts, K., Schleicher, A., Mohlberg, H., Kujovic, M., Palomero-Gallagher, N., Eickhoff, S. B., & Zilles, K. (2016). Cytoarchitecture of the human lateral occipital cortex: Mapping of two extrastriate areas hoc4la and hoc4lp. Brain Struct Funct, 221(4), 1877–97. https://doi.org/10.1007/s00429-015-1009-8

Mamassian, P., & Goutcher, R. (2005). Temporal dynamics in bistable perception. J Vis, 5(4), 361–75. https://doi.org/10.1167/5.4.7

Margalit, E., Biederman, I., Tjan, B. S., & Shah, M. P. (2017). What is actually affected by the scrambling of objects when localizing the lateral occipital complex? J Cogn Neurosci, 29(9), 1595–1604. https://doi.org/10.1162/jocn_a_01144

Martin, P. R., & Solomon, S. G. (2011). Information processing in the primate visual system. J Physiol, 589(Pt 1), 29–31. https://doi.org/10.1113/jphysiol.2010.201798

Martin-Signes, M., Paz-Alonso, P. M., & Chica, A. B. (2019). Connectivity of frontoparietal regions reveals executive attention and consciousness interactions. Cerebral Cortex, 29(11), 4539–4550. https://doi.org/10.1093/cercor/bhy332

Mashour, G. A., Roelfsema, P., Changeux, J. P., & Dehaene, S. (2020). Conscious processing and the global neuronal workspace hypothesis. Neuron, 105(5), 776–798. https://doi.org/10.1016/j.neuron.2020.01.026

Mather, G., Pavan, A., Bellacosa Marotti, R., Campana, G., & Casco, C. (2013). Interactions between motion and form processing in the human visual system. Front Comput Neurosci, 7, 65. https://doi.org/10.3389/fncom.2013.00065

Maunsell, J. H., & Van Essen, D. C. (1983). Functional properties of neurons in middle temporal visual area of the macaque monkey. i. selectivity for stimulus direction, speed, and orientation. J Neurophysiol, 49(5), 1127–47. https://doi.org/10.1152/jn.1983.49.5.1127

Maunsell, J. H., & Van Essen, D. C. (1987). Topographic organization of the middle temporal visual area in the macaque monkey: Representational biases and the relationship to callosal connections and myeloarchitectonic boundaries. J Comp Neurol, 266(4), 535–55. https://doi.org/10.1002/cne.902660407

Maunsell, J. H., & Van Essen, D. C. (1983a). Functional properties of neurons in middle temporal visual area of the macaque monkey. i. selectivity for stimulus direction, speed, and orientation. J Neurophysiol, 49(5), 1127–47. https://doi.org/10.1152/jn.1983.49.5.1127

Maunsell, J. H., & Van Essen, D. C. (1983b). Functional properties of neurons in middle temporal visual area of the macaque monkey. ii. binocular interactions and sensitivity to binocular disparity. J Neurophysiol, 49(5), 1148–67. https://doi.org/10.1152/jn.1983.49.5.1148

May, P. J. (2006). The mammalian superior colliculus: Laminar structure and connections. Prog Brain Res, 151, 321–78. https://doi.org/10.1016/S0079-6123(05)51011-2

Mazzi, C., Mancini, F., & Savazzi, S. (2014). Can ips reach visual awareness without v1? evidence from tms in healthy subjects and hemianopic patients. Neuropsychologia, 64, 134–44.

Mazzi, C., Savazzi, S., & Silvanto, J. (2017). On the "blindness" of blindsight: What is the evidence for phenomenal awareness in the absence of primary visual cortex (v1)? Neuropsychologia. https://doi.org/10.1016/j.neuropsychologia.2017.10.029

Mazzi, C., Savazzi, S., & Silvanto, J. (2019). On the "blindness" of blindsight: What is the evidence for phenomenal awareness in the absence of primary visual cortex (v1)? Neuropsychologia, 128, 103–108. https://doi.org/10.1016/j.neuropsychologia.2017.10.029

McCarthy, G., Puce, A., Gore, J. C., & Allison, T. (1997). Face-specific processing in the human fusiform gyrus. J Cogn Neurosci, 9(5), 605–10. https://doi.org/10.1162/jocn.1997.9.5.605

Medina, J., & Fischer-Baum, S. (2017). Single-case cognitive neuropsychology in the age of big data. Cogn Neuropsychol, 34(7-8), 440–448. https://doi.org/10.1080/02643294.2017.1321537

Meijs, E. L., Slagter, H. A., de Lange, F. P., & van Gaal, S. (2018). Dynamic interactions between top-down expectations and conscious awareness. J Neurosci, 38(9), 2318–2327. https://doi.org/10.1523/JNEUROSCI.1952-17.2017

Melloni, L., Molina, C., Pena, M., Torres, D., Singer, W., & Rodriguez, E. (2007). Synchronization of neural activity across cortical areas correlates with conscious perception. J Neurosci, 27(11), 2858–65. https://doi.org/10.1523/JNEUROSCI.4623-06.2007

Melloni, L., Schwiedrzik, C. M., Muller, N., Rodriguez, E., & Singer, W. (2011). Expectations change the signatures and timing of electrophysiological correlates of perceptual awareness. J Neurosci, 31(4), 1386–96. https://doi.org/10.1523/JNEUROSCI.4570-10.2011

Miller, S. M. (2014). Closing in on the constitution of consciousness. Front Psychol, 5, 1293. https://doi.org/10.3389/fpsyg.2014.01293

Mishkin, M., Ungerleider, L. G., & Macko, K. A. (1983). Object vision and spatial vision: Two cortical pathways. Trends in neurosciences, 6, 414–417.

Mitchell, J. F., & Leopold, D. A. (2015). The marmoset monkey as a model for visual neuroscience. Neurosci Res, 93, 20–46. https://doi.org/10.1016/j.neures.2015.01.008

Miura, K., Inaba, N., Aoki, Y., & Kawano, K. (2014). Difference in visual motion representation between cortical areas mt and mst during ocular following responses. J Neurosci, 34(6), 2160–8. https://doi.org/10.1523/JNEUROSCI.3797-13.2014

Moher, D., Liberati, A., Tetzlaff, J., Altman, D. G., & Group, P. (2009). Preferred reporting items for systematic reviews and meta-analyses: The prisma statement. J Clin Epidemiol, 62(10), 1006–12. https://doi.org/10.1016/j.jclinepi.2009.06.005

Morland, A. B., Jones, S. R., Finlay, A. L., Deyzac, E., Le, S., & Kemp, S. (1999). Visual perception of motion, luminance and colour in a human hemianope. Brain, 122 (Pt 6), 1183–98.

Morland, A. B., Le, S., Carroll, E., Hoffmann, M. B., & Pambakian, A. (2004). The role of spared calcarine cortex and lateral occipital cortex in the responses of human hemianopes to visual motion. J Cogn Neurosci, 16(2), 204–18. https://doi.org/10.1162/089892904322984517

Motter, B. C. (1993). Focal attention produces spatially selective processing in visual cortical areas v1, v2, and v4 in the presence of competing stimuli. J Neurophysiol, 70(3), 909–19. https://doi.org/10.1152/jn.1993.70.3.909

Movshon, J., Adelson, E., Gizzi, M., & Newsome, W. (1985). The analysis of moving visual patterns. Pontificia Academica Scripta Varia, 54, 117–151.

Muller, V. I., Cieslik, E. C., Laird, A. R., Fox, P. T., Radua, J., Mataix-Cols, D., Tench, C. R., Yarkoni, T., Nichols, T. E., Turkeltaub, P. E., Wager, T. D., & Eickhoff, S. B. (2018). Ten simple rules for neuroimaging meta-analysis. Neurosci Biobehav Rev, 84, 151–161. https://doi.org/10.1016/j.neubiorev.2017.11.012

Mundinano, I. C., Chen, J., de Souza, M., Sarossy, M. G., Joanisse, M. F., Goodale, M. A., & Bourne, J. A. (2017). More than blindsight: Case report of a child with extraordinary visual capacity following perinatal bilateral occipital lobe injury. Neuropsychologia. https://doi.org/10.1016/j.neuropsychologia.2017.11.017

Munn, B. R., Muller, E. J., Wainstein, G., & Shine, J. M. (2021). The ascending arousal system shapes neural dynamics to mediate awareness of cognitive states. Nat Commun, 12(1), 6016. https://doi.org/10.1038/s41467-021-26268-x

Nani, A., Manuello, J., Mancuso, L., Liloia, D., Costa, T., & Cauda, F. (2019). The neural correlates of consciousness and attention: Two sister processes of the brain. Front Neurosci, 13, 1169. https://doi.org/10.3389/fnins.2019.01169

Nassi, J. J., & Callaway, E. M. (2009). Parallel processing strategies of the primate visual system. Nat Rev Neurosci, 10(5), 360–72. https://doi.org/10.1038/nrn2619

Newsome, W. T., & Pare, E. B. (1988). A selective impairment of motion perception following lesions of the middle temporal visual area (mt). J Neurosci, 8(6), 2201–11. https://doi.org/10.1523/JNEUROSCI.08-06-02201.1988

Nguyen, M. N., Nishimaru, H., Matsumoto, J., Van Le, Q., Hori, E., Maior, R. S., Tomaz, C., Ono, T., & Nishijo, H. (2016). Population coding of facial information in the monkey superior colliculus and pulvinar. Front Neurosci, 10, 583. https://doi.org/10.3389/fnins.2016.00583

Nichols, T. E., Das, S., Eickhoff, S. B., Evans, A. C., Glatard, T., Hanke, M., Kriegeskorte, N., Milham, M. P., Poldrack, R. A., Poline, J. B., Proal, E., Thirion, B., Van Essen, D. C., White, T., & Yeo, B. T. (2017). Best practices in data analysis and sharing in neuroimaging using mri. Nat Neurosci, 20(3), 299–303. https://doi.org/10.1038/nn.4500

Nishimoto, S., & Gallant, J. L. (2011). A three-dimensional spatiotemporal receptive field model explains responses of area mt neurons to naturalistic movies. J Neurosci, 31(41), 14551–64. https://doi.org/10.1523/JNEUROSCI.6801-10.2011

Ogawa, S., Lee, T. M., Kay, A. R., & Tank, D. W. (1990). Brain magnetic resonance imaging with contrast dependent on blood oxygenation. Proc Natl Acad Sci U S A, 87(24), 9868–72. https://doi.org/10.1073/pnas.87.24.9868

Ogawa, S., Tank, D. W., Menon, R., Ellermann, J. M., Kim, S. G., Merkle, H., & Ugurbil, K. (1992). Intrinsic signal changes accompanying sensory stimulation: Functional brain mapping with magnetic resonance imaging. Proc Natl Acad Sci U S A, 89(13), 5951–5. https://doi.org/10.1073/pnas.89.13.5951

Oldfield, R. C. (1971). The assessment and analysis of handedness: The edinburgh inventory. Neuropsychologia, 9(1), 97–113. https://doi.org/10.1016/0028-3932(71)90067-4

Overgaard, M. (2012). Blindsight: Recent and historical controversies on the blindness of blindsight. Wiley Interdiscip Rev Cogn Sci, 3(6), 607–614. https://doi.org/10.1002/wcs.1194

Pack, C. C., & Born, R. T. (2001). Temporal dynamics of a neural solution to the aperture problem in visual area mt of macaque brain. Nature, 409(6823), 1040–2. https://doi.org/10.1038/35059085

Pack, C. C., Hunter, J. N., & Born, R. T. (2005). Contrast dependence of suppressive influences in cortical area mt of alert macaque. J Neurophysiol, 93(3), 1809–15. https://doi.org/10.1152/jn.00629.2004

Palczewski, K. (2012). Chemistry and biology of vision. J Biol Chem, 287(3), 1612–9. https://doi.org/10.1074/jbc.R111.301150

Pandey, A., Neupane, S., Adhikary, S., Vaidya, K., & Pack, C. C. (2022). Cortical visual impairment at birth can be improved rapidly by vision training in adulthood: A case study. Restorative Neurology and Neuroscience, 40(4-6), 261–270. https://doi.org/10.3233/RNN-221294

Papanikolaou, A., Keliris, G. A., Papageorgiou, T. D., Shao, Y., Krapp, E., Papageorgiou, E., Stingl, K., Bruckmann, A., Schiefer, U., Logothetis, N. K., & Smirnakis, S. M. (2014). Population receptive field analysis of the primary visual cortex complements perimetry in patients with homonymous visual field defects. Proceedings of the National Academy of Sciences of the United States of America, 111(16), E1656–65.

Park, H. D., Correia, S., Ducorps, A., & Tallon-Baudry, C. (2014). Spontaneous fluctuations in neural responses to heartbeats predict visual detection. Nat Neurosci, 17(4), 612–8. https://doi.org/10.1038/nn.3671

Pascual-Leone, A., Amedi, A., Fregni, F., & Merabet, L. B. (2005). The plastic human brain cortex. Annu Rev Neurosci, 28, 377–401. https://doi.org/10.1146/annurev.neuro.27.070203.144216

Payne, B. R. (1993). Evidence for visual cortical area homologs in cat and macaque monkey. Cereb Cortex, 3(1), 1–25. https://doi.org/10.1093/cercor/3.1.1

Pedersini, C. A., Guardia-Olmos, J., Montala-Flaquer, M., Cardobi, N., Sanchez-Lopez, J., Parisi, G., Savazzi, S., & Marzi, C. A. (2020). Functional interactions in patients with hemianopia: A graph theory-based connectivity study of resting fmri signal. PLoS ONE [Electronic Resource], 15(1), e0226816.

Pegna, A. J., Khateb, A., Lazeyras, F., & Seghier, M. L. (2005). Discriminating emotional faces without primary visual cortices involves the right amygdala. Nat Neurosci, 8(1), 24–5. https://doi.org/10.1038/nn1364

Peli, E. (2000). Field expansion for homonymous hemianopia by optically induced peripheral exotropia. Optom Vis Sci, 77(9), 453–64.

Pelli, D. G. (1997). The videotoolbox software for visual psychophysics: Transforming numbers into movies. Spat Vis, 10(4), 437–42.

Pelli, D. G., & Bex, P. (2013). Measuring contrast sensitivity. Vision Res, 90, 10–4. https://doi.org/10.1016/j.visres.2013.04.015

Perez, C., & Chokron, S. (2014). Rehabilitation of homonymous hemianopia: Insight into blindsight. Frontiers in integrative neuroscience, 8, 82. https://doi.org/10.3389/fnint.2014.00082

Perez, P., Madsen, J., Banellis, L., Turker, B., Raimondo, F., Perlbarg, V., Valente, M., Nierat, M. C., Puybasset, L., Naccache, L., Similowski, T., Cruse, D., Parra, L. C., & Sitt, J. D. (2021). Conscious processing of narrative stimuli synchronizes heart rate between individuals. Cell Rep, 36(11), 109692. https://doi.org/10.1016/j.celrep.2021.109692

Perry, V. H., & Cowey, A. (1984). Retinal ganglion cells that project to the superior colliculus and pretectum in the macaque monkey. Neuroscience, 12(4), 1125–37.

Persaud, N., Davidson, M., Maniscalco, B., Mobbs, D., Passingham, R. E., Cowey, A., & Lau, H. (2011). Awareness-related activity in prefrontal and parietal cortices in blindsight reflects more than superior visual performance. Neuroimage, 58(2), 605–11.

Persuh, M., LaRock, E., & Berger, J. (2018). Working memory and consciousness: The current state of play. Front Hum Neurosci, 12, 78. https://doi.org/10.3389/fnhum.2018.00078

Piche, M., Thomas, S., & Casanova, C. (2015). Spatiotemporal profiles of receptive fields of neurons in the lateral posterior nucleus of the cat lp-pulvinar complex. J Neurophysiol, 114(4), 2390–403. https://doi.org/10.1152/jn.00649.2015

Pitts, M. A., Lutsyshyna, L. A., & Hillyard, S. A. (2018). The relationship between attention and consciousness: An expanded taxonomy and implications for 'no-report' paradigms. Philos Trans R Soc Lond B Biol Sci, 373(1755). https://doi.org/10.1098/rstb.2017.0348

Pitts, M. A., Martinez, A., & Hillyard, S. A. (2012). Visual processing of contour patterns under conditions of inattentional blindness. J Cogn Neurosci, 24(2), 287–303. https://doi.org/10.1162/jocn_a_00111

Podvalny, E., Flounders, M. W., King, L. E., Holroyd, T., & He, B. J. (2019). A dual role of prestimulus spontaneous neural activity in visual object recognition. Nat Commun, 10(1), 3910. https://doi.org/10.1038/s41467-019-11877-4

Poldrack, R., Mumford, J., & Nichols, T. (2011). Handbook of functional mri data analysis.

Portas, C. M., Strange, B. A., Friston, K. J., Dolan, R. J., & Frith, C. D. (2000). How does the brain sustain a visual percept? Proceedings of the Royal Society of London, 267(1446), 845–50. https://doi.org/10.1098/rspb.2000.1080

Power, J. D., Cohen, A. L., Nelson, S. M., Wig, G. S., Barnes, K. A., Church, J. A., Vogel, A. C., Laumann, T. O., Miezin, F. M., Schlaggar, B. L., & Petersen, S. E. (2011). Functional network organization of the human brain. Neuron, 72(4), 665–78. https://doi.org/10.1016/j.neuron.2011.09.006

Power, J. D., Mitra, A., Laumann, T. O., Snyder, A. Z., Schlaggar, B. L., & Petersen, S. E. (2014). Methods to detect, characterize, and remove motion artifact in resting state fmri. NeuroImage, 84(Supplement C), 320–341. https://doi.org/10.1016/j.neuroimage.2013.08.048

Ptito, A., Lepore, F., Ptito, M., & Lassonde, M. (1991). Target detection and movement discrimination in the blind field of hemispherectomized patients. Brain, 114 (Pt 1B), 497–512.

Ptito, M., & Kupers, R. (2005). Cross-modal plasticity in early blindness. J Integr Neurosci, 4(4), 479–88. https://doi.org/10.1142/s0219635205000951

Rathore, S., Akbari, H., Rozycki, M., Abdullah, K. G., Nasrallah, M. P., Binder, Z. A., Davuluri, R. V., Lustig, R. A., Dahmane, N., Bilello, M., O'Rourke, D. M., & Davatzikos,

C. (2018). Radiomic mri signature reveals three distinct subtypes of glioblastoma with different clinical and molecular characteristics, offering prognostic value beyond idh1. Sci Rep, 8(1), 5087. https://doi.org/10.1038/s41598-018-22739-2

Reuter, M., Rosas, H. D., & Fischl, B. (2010). Highly accurate inverse consistent registration: A robust approach. NeuroImage, 53(4), 1181–1196. https://doi.org/10.1016/j.neuroimage.2010.07.020

Riddoch, G. (1917). Dissociation of visual perceptions due to occipital injuries, with especial reference to appreciation of movement. Brain, 40, 15–57.

Roalf, D. R., & Gur, R. C. (2017). Functional brain imaging in neuropsychology over the past 25 years. Neuropsychology, 31(8), 954–971. https://doi.org/10.1037/neu0000426

Rodieck, R. (1998). The first steps in seeing. Sinauer Associates.

Rodman, H. R., Gross, C. G., & Albright, T. D. (1989). Afferent basis of visual response properties in area mt of the macaque. i. effects of striate cortex removal. J Neurosci, 9(6), 2033–50. https://doi.org/10.1523/JNEUROSCI.09-06-02033.1989

Rosa, M. G., Tweedale, R., & Elston, G. N. (2000). Visual responses of neurons in the middle temporal area of new world monkeys after lesions of striate cortex. J Neurosci, 20(14), 5552–63. https://doi.org/10.1523/JNEUROSCI.20-14-05552.2000

Rowe, E. G., Zhang, Y., & Garrido, M. I. (2023). Evidence for adaptive myelination of subcortical shortcuts for visual motion perception in healthy adults. Hum Brain Mapp. https://doi.org/10.1002/hbm.26467

Rushworth, M. F., Kolling, N., Sallet, J., & Mars, R. B. (2012). Valuation and decision-making in frontal cortex: One or many serial or parallel systems? Curr Opin Neurobiol, 22(6), 946–55. https://doi.org/10.1016/j.conb.2012.04.011

Saalmann, Y. B., & Kastner, S. (2011). Cognitive and perceptual functions of the visual thalamus. Neuron, 71(2), 209–23. https://doi.org/10.1016/j.neuron.2011.06.027

Sabel, B. A. (2017). [are visual field defects reversible? - visual rehabilitation with brains]. Klin Monbl Augenheilkd, 234(2), 194–204. https://doi.org/10.1055/s-0042-104588

Salay, L. D., Ishiko, N., & Huberman, A. D. (2018). A midline thalamic circuit determines reactions to visual threat. Nature, 557(7704), 183–189. https://doi.org/10.1038/s41586-018-0078-2

Salimi-Khorshidi, G., Smith, S. M., Keltner, J. R., Wager, T. D., & Nichols, T. E. (2009). Meta-analysis of neuroimaging data: A comparison of image-based and coordinate-based pooling of studies. Neuroimage, 45(3), 810–23. https://doi.org/10.1016/j.neuroimage.2008.12.039

Salzman, C. D., Murasugi, C. M., Britten, K. H., & Newsome, W. T. (1992). Microstimulation in visual area mt: Effects on direction discrimination performance. J Neurosci, 12(6), 2331–55. https://doi.org/10.1523/JNEUROSCI.12-06-02331.1992

Sanders, M. D., Warrington, E. K., Marshall, J., & Wieskrantz, L. (1974). "blindsight": Vision in a field defect. Lancet, 1(7860), 707–8.

Sanjuan, A., Price, C. J., Mancini, L., Josse, G., Grogan, A., Yamamoto, A. K., Geva, S., Leff, A. P., Yousry, T. A., & Seghier, M. L. (2013). Automated identification of brain tumors from single mr images based on segmentation with refined patient-specific priors. Front Neurosci, 7, 241. https://doi.org/10.3389/fnins.2013.00241

Satterthwaite, T. D., Elliott, M. A., Gerraty, R. T., Ruparel, K., Loughead, J., Calkins, M. E., Eickhoff, S. B., Hakonarson, H., Gur, R. C., Gur, R. E., & Wolf, D. H. (2013). An improved framework for confound regression and filtering for control of motion artifact in the preprocessing of resting-state functional connectivity data. NeuroImage, 64(1), 240–256. https://doi.org/10.1016/j.neuroimage.2012.08.052

Saygin, A. P., & Sereno, M. I. (2008). Retinotopy and attention in human occipital, temporal, parietal, and frontal cortex. Cereb Cortex, 18(9), 2158–68. https://doi.org/10.1093/cercor/bhm242

Schmid, D., Schneider, S., & Schenk, T. (2022). How to test blindsight without light scatter artefacts? Neuropsychologia, 173, 108308. https://doi.org/10.1016/j.neuropsychologia.2022.108308

Schmid, M. C., Panagiotaropoulos, T., Augath, M. A., Logothetis, N. K., & Smirnakis, S. M. (2009). Visually driven activation in macaque areas v2 and v3 without input from

the primary visual cortex. PLoS One, 4(5), e5527. https://doi.org/10.1371/journal.pone.0005527

Schmid, M. C., Schmiedt, J. T., Peters, A. J., Saunders, R. C., Maier, A., & Leopold, D. A. (2013). Motion-sensitive responses in visual area v4 in the absence of primary visual cortex. J Neurosci, 33(48), 18740–5. https://doi.org/10.1523/JNEUROSCI.3923-13.2013

Schoenfeld, M. A., Heinze, H. J., & Woldorff, M. G. (2002). Unmasking motion-processing activity in human brain area v5/mt+ mediated by pathways that bypass primary visual cortex. Neuroimage, 17(2), 769–79.

Seghier, M. L. (2013). The angular gyrus: Multiple functions and multiple subdivisions. Neuroscientist, 19(1), 43–61. https://doi.org/10.1177/1073858412440596

Sereno, M. I., Pitzalis, S., & Martinez, A. (2001). Mapping of contralateral space in retinotopic coordinates by a parietal cortical area in humans. Science, 294(5545), 1350–4. https://doi.org/10.1126/science.1063695

Seth, A. K., & Bayne, T. (2022). Theories of consciousness. Nat Rev Neurosci, 23(7), 439–452. https://doi.org/10.1038/s41583-022-00587-4

Shang, C., Chen, Z., Liu, A., Li, Y., Zhang, J., Qu, B., Yan, F., Zhang, Y., Liu, W., Liu, Z., Guo, X., Li, D., Wang, Y., & Cao, P. (2018). Divergent midbrain circuits orchestrate escape and freezing responses to looming stimuli in mice. Nat Commun, 9(1), 1232. https://doi.org/10.1038/s41467-018-03580-7

Shenhav, A., Botvinick, M. M., & Cohen, J. D. (2013). The expected value of control: An integrative theory of anterior cingulate cortex function. Neuron, 79(2), 217–40. https://doi.org/10.1016/j.neuron.2013.07.007

Shenhav, A., Cohen, J. D., & Botvinick, M. M. (2016). Dorsal anterior cingulate cortex and the value of control. Nat Neurosci, 19(10), 1286–91. https://doi.org/10.1038/nn.4384

Shibata, K., Watanabe, T., Sasaki, Y., & Kawato, M. (2011). Perceptual learning incepted by decoded fmri neurofeedback without stimulus presentation. Science, 334(6061), 1413–5. https://doi.org/10.1126/science.1212003

Shipp, S., & Zeki, S. (1989). The organization of connections between areas v5 and v1 in macaque monkey visual cortex. Eur J Neurosci, 1(4), 309–32. https://doi.org/10.1111/j.1460-9568.1989.tb00798.x

Sillito, A. M., Cudeiro, J., & Jones, H. E. (2006). Always returning: Feedback and sensory processing in visual cortex and thalamus. Trends Neurosci, 29(6), 307–16. https://doi.org/10.1016/j.tins.2006.05.001

Silvanto, J. (2015). Why is "blindsight" blind? a new perspective on primary visual cortex, recurrent activity and visual awareness. Conscious Cogn, 32, 15–32. https://doi.org/10.1016/j.concog.2014.08.001

Silvanto, J., Cowey, A., Lavie, N., & Walsh, V. (2007). Making the blindsighted see. Neuropsychologia, 45(14), 3346–50. https://doi.org/10.1016/j.neuropsychologia.2007.06.008

Silver, M. A., Ress, D., & Heeger, D. J. (2005). Topographic maps of visual spatial attention in human parietal cortex. J Neurophysiol, 94(2), 1358–71. https://doi.org/10.1152/jn.01316.2004

Simon, M., Campbell, E., Genest, F., MacLean, M. W., Champoux, F., & Lepore, F. (2020). The impact of early deafness on brain plasticity: A systematic review of the white and gray matter changes. Front Neurosci, 14, 206. https://doi.org/10.3389/fnins.2020.00206

Sincich, L. C., Park, K. F., Wohlgemuth, M. J., & Horton, J. C. (2004). Bypassing v1: A direct geniculate input to area mt. Nat Neurosci, 7(10), 1123–8. https://doi.org/10.1038/nn1318

Smits, A. R., Seijdel, N., Scholte, H. S., Heywood, C. A., Kentridge, R. W., & de Haan, E. H. F. (2018). Action blindsight and antipointing in a hemianopic patient. Neuropsychologia. https://doi.org/10.1016/j.neuropsychologia.2018.03.029

Song, C., & Yao, H. (2016). Unconscious processing of invisible visual stimuli. Sci Rep, 6, 38917. https://doi.org/10.1038/srep38917

Soon, C. S., Brass, M., Heinze, H. J., & Haynes, J. D. (2008). Unconscious determinants of free decisions in the human brain. Nat Neurosci, 11(5), 543–5. https://doi.org/10.1038/nn.2112

Soon, C. S., He, A. H., Bode, S., & Haynes, J. D. (2013). Predicting free choices for abstract intentions. Proc Natl Acad Sci U S A, 110(15), 6217–22. https://doi.org/10.1073/pnas.1212218110

Soto, D., & Silvanto, J. (2014). Reappraising the relationship between working memory and conscious awareness. Trends Cogn Sci, 18(10), 520–5. https://doi.org/10.1016/j.tics.2014.06.005

Spear, P. D., & Baumann, T. P. (1975). Receptive-field characteristics of single neurons in lateral suprasylvian visual area of the cat. J Neurophysiol, 38(6), 1403–20. https://doi.org/10.1152/jn.1975.38.6.1403

Spear, P. D., & Baumann, T. P. (1979). Effects of visual cortex removal on receptive-field properties of neurons in lateral suprasylvian visual area of the cat. J Neurophysiol, 42(1 Pt 1), 31–56. https://doi.org/10.1152/jn.1979.42.1.31

Spering, M., & Carrasco, M. (2015). Acting without seeing: Eye movements reveal visual processing without awareness. Trends Neurosci, 38(4), 247–58. https://doi.org/10.1016/j.tins.2015.02.002

Stein, B. E. (1998). Neural mechanisms for synthesizing sensory information and producing adaptive behaviors. Exp Brain Res, 123(1-2), 124–35. https://doi.org/10.1007/s002210050553

Sundermann, B., & Pfleiderer, B. (2012). Functional connectivity profile of the human inferior frontal junction: Involvement in a cognitive control network. BMC Neurosci, 13, 119. https://doi.org/10.1186/1471-2202-13-119

Swienton, D. J., & Thomas, A. G. (2014). The visual pathway–functional anatomy and pathology. Semin Ultrasound CT MR, 35(5), 487–503. https://doi.org/10.1053/j.sult.2014.06.007

Tamietto, M., Cauda, F., Corazzini, L. L., Savazzi, S., Marzi, C. A., Goebel, R., Weiskrantz, L., & de Gelder, B. (2010). Collicular vision guides nonconscious behavior. J Cogn Neurosci, 22(5), 888–902. https://doi.org/10.1162/jocn.2009.21225

Tamietto, M., & Morrone, M. C. (2016). Visual plasticity: Blindsight bridges anatomy and function in the visual system. Curr Biol, 26(2), R70–R73. https://doi.org/10.1016/j.cub.2015.11.026

Tanaka, K., & Saito, H. (1989). Analysis of motion of the visual field by direction, expansion/contraction, and rotation cells clustered in the dorsal part of the medial superior temporal area of the macaque monkey. J Neurophysiol, 62(3), 626–41. https://doi.org/10.1152/jn.1989.62.3.626

Tao, D., He, Z., Lin, Y., Liu, C., & Tao, Q. (2021). Where does fear originate in the brain? a coordinate-based meta-analysis of explicit and implicit fear processing. Neuroimage, 227, 117686. https://doi.org/10.1016/j.neuroimage.2020.117686

Thakral, P. P. (2011). The neural substrates associated with inattentional blindness. Consciousness and Cognition, 20(4), 1768–1775. https://doi.org/10.1016/j.concog.2011.03.013

Tong, F. (2003). Primary visual cortex and visual awareness. Nat Rev Neurosci, 4(3), 219–29. https://doi.org/10.1038/nrn1055

Tononi, G. (2008). Consciousness as integrated information: A provisional manifesto. Biol Bull, 215(3), 216–42. https://doi.org/10.2307/25470707

Tononi, G. (2012). Integrated information theory of consciousness: An updated account. Arch Ital Biol, 150(4), 293–329. https://doi.org/10.4449/aib.v149i5.1388

Tononi, G., Boly, M., Massimini, M., & Koch, C. (2016). Integrated information theory: From consciousness to its physical substrate. Nat Rev Neurosci, 17(7), 450–61. https://doi.org/10.1038/nrn.2016.44

Tootell, R. B., Reppas, J. B., Kwong, K. K., Malach, R., Born, R. T., Brady, T. J., Rosen, B. R., & Belliveau, J. W. (1995b). Functional analysis of human mt and related visual cortical areas using magnetic resonance imaging. J Neurosci, 15(4), 3215–30.

Tran, A., MacLean, M. W., Hadid, V., Lazzouni, L., Nguyen, D. K., Tremblay, J., Dehaes, M., & Lepore, F. (2019). Neuronal mechanisms of motion detection underlying blindsight assessed by functional magnetic resonance imaging (fmri). Neuropsychologia. https://doi.org/10.1016/j.neuropsychologia.2019.02.012

Trevethan, C. T., Sahraie, A., & Weiskrantz, L. (2007). Form discrimination in a case of blindsight. Neuropsychologia, 45(9), 2092–103. https://doi.org/10.1016/j.neuropsychologia.2007.01.022

Troje, N. F. (2013). What is biological motion? definition, stimuli, and paradigms. (MD Rutherford, VA Kuhlmeie). MIT Press. https://doi.org/doi.org/10.7551/mitpress/9780262019279.003.0002

Tse, P. U., Baumgartner, F. J., & Greenlee, M. W. (2010). Event-related functional mri of cortical activity evoked by microsaccades, small visually-guided saccades, and eyeblinks in human visual cortex. Neuroimage, 49(1), 805–16. https://doi.org/10.1016/j.neuroimage.2009.07.052

Tsuchiya, N., & Koch, C. (2005). Continuous flash suppression reduces negative afterimages. Nat Neurosci, 8(8), 1096–101. https://doi.org/10.1038/nn1500

Tsuchiya, N., Wilke, M., Frassle, S., & Lamme, V. A. F. (2015). No-report paradigms: Extracting the true neural correlates of consciousness. Trends Cogn Sci, 19(12), 757–770. https://doi.org/10.1016/j.tics.2015.10.002

Tsunoda, K., Yamane, Y., Nishizaki, M., & Tanifuji, M. (2001). Complex objects are represented in macaque inferotemporal cortex by the combination of feature columns. Nat Neurosci, 4(8), 832–8. https://doi.org/10.1038/90547

Tustison, N. J., Avants, B. B., Cook, P. A., Zheng, Y., Egan, A., Yushkevich, P. A., & Gee, J. C. (2010). N4itk: Improved n3 bias correction. IEEE Transactions on Medical Imaging, 29(6), 1310–1320. https://doi.org/10.1109/TMI.2010.2046908

Uddin, L. Q., Nomi, J. S., Hebert-Seropian, B., Ghaziri, J., & Boucher, O. (2017). Structure and function of the human insula. J Clin Neurophysiol, 34(4), 300–306. https://doi.org/10.1097/WNP.0000000000000377

Uddin, L. Q., Yeo, B. T. T., & Spreng, R. N. (2019). Towards a universal taxonomy of macro-scale functional human brain networks. Brain Topogr, 32(6), 926–942. https://doi.org/10.1007/s10548-019-00744-6

Ullsperger, M., Harsay, H. A., Wessel, J. R., & Ridderinkhof, K. R. (2010). Conscious perception of errors and its relation to the anterior insula. Brain Struct Funct, 214(5-6), 629–43. https://doi.org/10.1007/s00429-010-0261-1

Ungerleider, L. G., & Desimone, R. (1986). Cortical connections of visual area mt in the macaque. J Comp Neurol, 248(2), 190–222. https://doi.org/10.1002/cne.902480204

Ungerleider, L. G., & Haxby, J. V. (1994). 'what' and 'where' in the human brain. Curr Opin Neurobiol, 4(2), 157–65. https://doi.org/10.1016/0959-4388(94)90066-3

Urbanski, M., Coubard, O. A., & Bourlon, C. (2014). Visualizing the blind brain: Brain imaging of visual field defects from early recovery to rehabilitation techniques. Frontiers in integrative neuroscience, 8, 74. https://doi.org/10.3389/fnint.2014.00074

Vaidya, A. R., Pujara, M. S., Petrides, M., Murray, E. A., & Fellows, L. K. (2019). Lesion studies in contemporary neuroscience. Trends Cogn Sci, 23(8), 653–671. https://doi.org/10.1016/j.tics.2019.05.009

Van den Stock, J., Tamietto, M., Hervais-Adelman, A., Pegna, A. J., & de Gelder, B. (2015). Body recognition in a patient with bilateral primary visual cortex lesions. Biol Psychiatry, 77(7), e31–3. https://doi.org/10.1016/j.biopsych.2013.06.023

Van den Stock, J., Tamietto, M., Sorger, B., Pichon, S., Grezes, J., & de Gelder, B. (2011). Cortico-subcortical visual, somatosensory, and motor activations for perceiving dynamic whole-body emotional expressions with and without striate cortex (v1). Proceedings of the National Academy of Sciences of the United States of America, 108(39), 16188–93.

Van den Stock, J., Tamietto, M., Zhan, M., Heinecke, A., Hervais-Adelman, A., Legrand, L. B., Pegna, A. J., & de Gelder, B. (2014). Neural correlates of body and face perception following bilateral destruction of the primary visual cortices. Frontiers in Behavioral Neuroscience, 8(FEB).

van Vugt, B., Dagnino, B., Vartak, D., Safaai, H., Panzeri, S., Dehaene, S., & Roelfsema, P. R. (2018). The threshold for conscious report: Signal loss and response bias in visual and frontal cortex. Science, 360(6388), 537–542. https://doi.org/10.1126/science.aar7186

Varol, E., Sotiras, A., Davatzikos, C., & Alzheimer's Disease Neuroimaging, I. (2017). Hydra: Revealing heterogeneity of imaging and genetic patterns through a multiple max-margin discriminative analysis framework. Neuroimage, 145(Pt B), 346–364. https://doi.org/10.1016/j.neuroimage.2016.02.041

Velenosi, L. A., Wu, Y. H., Schmidt, T. T., & Blankenburg, F. (2020). Intraparietal sulcus maintains working memory representations of somatosensory categories in an adaptive, context-dependent manner. Neuroimage, 221, 117146. https://doi.org/10.1016/j.neuroimage.2020.117146

Wada, Y., & Yamamoto, T. (2001). Selective impairment of facial recognition due to a haematoma restricted to the right fusiform and lateral occipital region. J Neurol Neurosurg Psychiatry, 71(2), 254–7. https://doi.org/10.1136/jnnp.71.2.254

Wager, T. D., Lindquist, M. A., Nichols, T. E., Kober, H., & Van Snellenberg, J. X. (2009). Evaluating the consistency and specificity of neuroimaging data using meta-analysis. Neuroimage, 45(1 Suppl), S210–21. https://doi.org/10.1016/j.neuroimage.2008.10.061

Wainstein, G., Rojas-Libano, D., Medel, V., Alnaes, D., Kolskar, K. K., Endestad, T., Laeng, B., Ossandon, T., Crossley, N., Matar, E., & Shine, J. M. (2021). The ascending arousal system promotes optimal performance through mesoscale network integration in a visuospatial attentional task. Netw Neurosci, 5(4), 890–910. https://doi.org/10.1162/netn_a_00205

Walker, R., Mannan, S., Maurer, D., Pambakian, A. L., & Kennard, C. (2000). The oculomotor distractor effect in normal and hemianopic vision. Proc Biol Sci, 267(1442), 431–8. https://doi.org/10.1098/rspb.2000.1018

Wall, M. B., Walker, R., & Smith, A. T. (2009). Functional imaging of the human superior colliculus: An optimised approach. Neuroimage, 47(4), 1620–7. https://doi.org/10.1016/j.neuroimage.2009.05.094

Wang, L., Mruczek, R. E., Arcaro, M. J., & Kastner, S. (2015). Probabilistic maps of visual topography in human cortex. Cereb Cortex, 25(10), 3911–31. https://doi.org/10.1093/cercor/bhu277

Wang, M. G., Arteaga, D., & He, B. J. J. (2013). Brain mechanisms for simple perception and bistable perception. PNAS, 110(35), E3350–E3359. https://doi.org/10.1073/pnas.1221945110

Warner, C. E., Goldshmit, Y., & Bourne, J. A. (2010). Retinal afferents synapse with relay cells targeting the middle temporal area in the pulvinar and lateral geniculate nuclei. Front Neuroanat, 4, 8. https://doi.org/10.3389/neuro.05.008.2010

Warner, C. E., Kwan, W. C., & Bourne, J. A. (2012). The early maturation of visual cortical area mt is dependent on input from the retinorecipient medial portion of the inferior pulvinar. J Neurosci, 32(48), 17073–85. https://doi.org/10.1523/JNEUROSCI.3269-12.2012

Warner, C. E., Kwan, W. C., Wright, D., Johnston, L. A., Egan, G. F., & Bourne, J. A. (2015). Preservation of vision by the pulvinar following early-life primary visual cortex lesions. Curr Biol, 25(4), 424–34. https://doi.org/10.1016/j.cub.2014.12.028

Watanabe, T., Sasaki, Y., Shibata, K., & Kawato, M. (2017). Advances in fmri real-time neurofeedback. Trends Cogn Sci, 21(12), 997–1010. https://doi.org/10.1016/j.tics.2017.09.010

Watson, A. B., & Pelli, D. G. (1983). Quest: A bayesian adaptive psychometric method. Percept Psychophys, 33(2), 113–20. https://doi.org/10.3758/bf03202828

Watson, J. D., Myers, R., Frackowiak, R. S., Hajnal, J. V., Woods, R. P., Mazziotta, J. C., Shipp, S., & Zeki, S. (1993). Area v5 of the human brain: Evidence from a combined study using positron emission tomography and magnetic resonance imaging. Cereb Cortex, 3(2), 79–94.

Weber, J. T., Huerta, M. F., Kaas, J. H., & Harting, J. K. (1983). The projections of the lateral geniculate nucleus of the squirrel monkey: Studies of the interlaminar zones and the s layers. J Comp Neurol, 213(2), 135–45. https://doi.org/10.1002/cne.902130203

Weill-Chounlamountry, A., Poncet, F., Crop, S., Hesly, N., Mouton, A., Samri, D., Sarazin, M., & Pradat-Diehl, P. (2012). Physical medicine and rehabilitation multidisciplinary approach in a case of posterior cortical atrophy. Ann Phys Rehabil Med, 55(6), 430–9. https://doi.org/10.1016/j.rehab.2012.05.001

Weiskrantz, L. (1987). Residual vision in a scotoma. a follow-up study of 'form' discrimination. Brain, 110 (Pt 1), 77–92.

Weiskrantz, L. (1990). The ferrier lecture, 1989. outlooks for blindsight: Explicit methodologies for implicit processes. Proc R Soc Lond B Biol Sci, 239(1296), 247–78. https://doi.org/10.1098/rspb.1990.0016

Weiskrantz, L. (1996). Blindsight revisited. Curr Opin Neurobiol, 6(2), 215–20. https://doi.org/10.1016/s0959-4388(96)80075-4

Weiskrantz, L. (1998). Consciousness and commentaries. M.I.T. Press.

Weiskrantz, L., Warrington, E. K., Sanders, M. D., & Marshall, J. (1974). Visual capacity in the hemianopic field following a restricted occipital ablation. Brain, 97(4), 709–28.

Wessinger, C. M., Fendrich, R., Ptito, A., Villemure, J. G., & Gazzaniga, M. S. (1996). Residual vision with awareness in the field contralateral to a partial or complete functional hemispherectomy. Neuropsychologia, 34(11), 1129–37.

Wiesel, T. N., & Hubel, D. H. (1963). Effects of visual deprivation on morphology and physiology of cells in the cats lateral geniculate body. J Neurophysiol, 26, 978–93. https://doi.org/10.1152/jn.1963.26.6.978

Wiesel, T. N., & Hubel, D. H. (1965). Comparison of the effects of unilateral and bilateral eye closure on cortical unit responses in kittens. J Neurophysiol, 28(6), 1029–40. https://doi.org/10.1152/jn.1965.28.6.1029

Woolrich, M. W., Jbabdi, S., Patenaude, B., Chappell, M., Makni, S., Behrens, T., Beckmann, C., Jenkinson, M., & Smith, S. M. (2009). Bayesian analysis of neuroimaging data in fsl. Neuroimage, 45(1 Suppl), S173–86. https://doi.org/10.1016/j.neuroimage.2008.10.055

Worsley, K. J. (2001). Statistical analysis of activation images. Functional MRI, An introduction to methods, 14(1), 251–70.

Yabuta, N. H., Sawatari, A., & Callaway, E. M. (2001). Two functional channels from primary visual cortex to dorsal visual cortical areas. Science, 292(5515), 297–300. https://doi.org/10.1126/science.1057916

Yantis, S., Schwarzbach, J., Serences, J. T., Carlson, R. L., Steinmetz, M. A., Pekar, J. J., & Courtney, S. M. (2002). Transient neural activity in human parietal cortex during spatial attention shifts. Nat Neurosci, 5(10), 995–1002. https://doi.org/10.1038/nn921

Yarkoni, T. (2009). Big correlations in little studies: Inflated fmri correlations reflect low statistical power-commentary on vul et al. (2009). Perspect Psychol Sci, 4(3), 294–8. https://doi.org/10.1111/j.1745-6924.2009.01127.x

Yarkoni, T., Poldrack, R. A., Nichols, T. E., Van Essen, D. C., & Wager, T. D. (2011). Large-scale automated synthesis of human functional neuroimaging data. Nat Methods, 8(8), 665–70. https://doi.org/10.1038/nmeth.1635

Yokoi, I., & Komatsu, H. (2009). Relationship between neural responses and visual grouping in the monkey parietal cortex. J Neurosci, 29(42), 13210–21. https://doi.org/10.1523/JNEUROSCI.1995-09.2009

Yoshida, M., Hafed, Z. M., & Isa, T. (2017). Informative cues facilitate saccadic localization in blindsight monkeys. Front Syst Neurosci, 11, 5. https://doi.org/10.3389/fnsys.2017.00005

Yoshida, M., Takaura, K., Kato, R., Ikeda, T., & Isa, T. (2008). Striate cortical lesions affect deliberate decision and control of saccade: Implication for blindsight. J Neurosci, 28(42), 10517–30. https://doi.org/10.1523/JNEUROSCI.1973-08.2008

Yu, H. H., Atapour, N., Chaplin, T. A., Worthy, K. H., & Rosa, M. G. P. (2018). Robust visual responses and normal retinotopy in primate lateral geniculate nucleus following long-term lesions of striate cortex. J Neurosci, 38(16), 3955–3970. https://doi.org/10.1523/JNEUROSCI.0188-18.2018

Zanto, T. P., Rubens, M. T., Thangavel, A., & Gazzaley, A. (2011). Causal role of the prefrontal cortex in top-down modulation of visual processing and working memory. Nat Neurosci, 14(5), 656–61. https://doi.org/10.1038/nn.2773

Zatorre, R. (2018). Brenda milner and the origins of cognitive neuroscience. Current Biology Magazine, 28(11), 638–9. https://doi.org/DOI:10.1016/j.cub.2018.04.048

Zeki, S., & Ffytche, D. H. (1998). The riddoch syndrome: Insights into the neurobiology of conscious vision. Brain, 121 (Pt 1), 25–45. https://doi.org/10.1093/brain/121.1.25

Zeki, S., Watson, J. D., Lueck, C. J., Friston, K. J., Kennard, C., & Frackowiak, R. S. (1991). A direct demonstration of functional specialization in human visual cortex. J Neurosci, 11(3), 641–9. https://doi.org/10.1523/JNEUROSCI.11-03-00641.1991

Zeki, S. M. (1973). Colour coding in rhesus monkey prestriate cortex. Brain Res, 53(2), 422–7. https://doi.org/10.1016/0006-8993(73)90227-8

Zeki, S. M. (1974). Functional organization of a visual area in the posterior bank of the superior temporal sulcus of the rhesus monkey. J Physiol, 236(3), 549–73. https://doi.org/10.1113/jphysiol.1974.sp010452

Zeki, S. M. (1978a). Functional specialisation in the visual cortex of the rhesus monkey. Nature, 274(5670), 423–8.

Zhang, Y., Brady, M., & Smith, S. (2001). Segmentation of brain MR images through a hidden markov random field model and the expectation-maximization algorithm. IEEE Transactions on Medical Imaging, 20(1), 45–57. https://doi.org/10.1109/42.906424

Zihl, J., von Cramon, D., & Mai, N. (1983). Selective disturbance of movement vision after bilateral brain damage. Brain, 106 (Pt 2), 313–40. https://doi.org/10.1093/brain/106.2.313

Zihl, J., & Werth, R. (1984). Contributions to the study of "blindsight"–ii. the role of specific practice for saccadic localization in patients with postgeniculate visual field defects. Neuropsychologia, 22(1), 13–22.

Zuo, X. N., Xu, T., & Milham, M. P. (2019). Harnessing reliability for neuroscience research. Nat Hum Behav, 3(8), 768–771. https://doi.org/10.1038/s41562-019-0655-x

Appendix A

List of publications during PhD

Refereed Publications

(1) **MacLean, M.W.**, Hadid, V., Spreng, R.N., Lepore, F. (2023).Revealing robust neural correlates of conscious and unconscious visual processing: activation likelihood estimation meta-analyses. Neuroimage

(2) **(Co-first author)** Tran, A.*, **MacLean, M.W.***, Hadid, V.*, Nguyen, D.K., Lazzouni, L., Tremblay, J., Dehaes, M.**, Lepore, F.**. (2019). Neuronal mechanisms of motion detection underlying blindsight assessed by functional magnetic resonance imaging. Neuropsychologia

(3) Simon, M., Campbell, E., Genest, F., **MacLean, M.W.**, Champoux F. et Lepore, F. (2020). The Impact of Deafness on Brain Plasticity: A Systematic Review of the White and Grey Matter. Frontiers in Neuroscience

(4) Gau, R., Barilari, M., Rezk, M., Battal, C., Gurtubay, A., **MacLean, M.W.**, Falagiarda, F., Cerpelloni, F., Shahzad, I., Chouinard-Leclaire, C., Nunes, M., Caron-Guyon, J., & Collignon, O. (2022). bidSPM (2.1.0). Zenodo & GitHub

(5) **MacLean, M.W.**, Gau, R., Landry, C., Rezk, M., Nguyen, D.K., Collignon, O., Lepore, F. (In prep). Reorganization of cortical and subcortical motion-selective brain regions in cortical visual impairment.

(6) Hadid, V. **MacLean, M.W.**, Pascarella, A., Lajnef, T., Higgins, M.C., Grand-Maître, C., Nguyen, D.K., Jerbi, K., et Lepore, F. (In prep). Interhemispheric transfer of visual mismatch negativity: a marker of implicit visual processing.

Refereed Conference Publications/ Abstracts / Posters (5/20 selected)

(1) **MacLean, M.W.**, Hadid, V., Spreng, R.N., Lepore, F. (2022). Revealing robust neural correlates of conscious and unconscious visual proccessing: activation likelihood estimation meta-analyses. Vision Sciences Society Annual Meeting. Florida, USA, Journal of Vision

(2) **MacLean, M.W.**, Hadid, V., Lazzouni, L., Lepore, F. (2018). Using fMRI to Identify Neuronal Mechanisms of Motion Detection Underlying Blindsight. Vision Sciences Society Annual Meeting. Florida, USA, Journal of Vision

(3) Hadid, V., **MacLean, M.W.**, Dandrimont, J., Grand-Maître, C., Higgins, MC., Faghel-Soubeyrand, S., Lepore, F. (2023). Early processing of unattended emotional faces increases the brain response to attended emotional expressions: An SSVEP study. Proceedings Volume 12567, 18th International Symposium on Medical Information Processing and Analysis; 1256718, Proceedings Society of Photo-Optical Instrumentation Engineers (SPIE)

(4) **MacLean, M.W.**, Hadid, V., Lazzouni, L.,Nguyen, D.K., Lepore, F. (2018). Neuronal Mechanisms of Motion Detection Underlying Blindsight Assessed by Functional Magnetic Resonance Imaging. Society for Neurosciences Annual Meeting (SfN). San Diego, Californie, USA.

(5) **MacLean, M.W.**, Hadid, V., Lazzouni, L., Tran, A., Dehaes, M., Lepore, F. (2017). Imaging Blindsight: A study of motion detection and MRI. Canadian Association for Neurosciences 11th Annual Meeting (ACN-CAN), Montréal, Canada.